Dissertation der Fakultät für Biologie

der Ludwig-Maximilians-Universität München

Epigenetic Mechanisms Linking Psychological Stress and Aging-Related Disease

Max Planck Institut für Psychiatrie

Abteilung für Translationale Forschung in der Psychiatrie

und

Ludwig-Maximilians-Universität München

Fakultät für Biologie

Vorgelegt von

Anthony S. Zannas (legal: Antonios Zannas)

München, Deutschland

2017

Tag der Einreichung: 27.02.2017

Tag der mündlichen Prüfung: 09.10.2017

Erster Gutachter: PD Dr. rer. nat. habil. Carsten T. Wotjak

Zweiter Gutachter: Prof. Dr. rer. nat. Wolfgang Enard

Dritter Gutachter: Prof. Dr. rer. nat. Michael Boshart

Vierter Gutachter: PD Dr. rer. nat. Benedikt Grothe

Fünfter Gutachter: Prof. Dr. rer. nat. Elisabeth Weiß

Sechster Gutachter: PD Dr. rer. nat. Mathias V. Schmidt

Content **Page**

Abbreviations 4

List of Publications 6

Summary 7

Aims of the thesis 8

Overarching introduction 9

Paper I, Zannas et al., *Genome Biology* 2015; 16(1):266 21

Paper II, Gassen et al., *Science Signaling* 2015; 8(404):ra119 33

Manuscript I, Zannas et al., *Unpublished* 47

Overarching discussion 114

References 124

Acknowledgements 145

Curriculum Vitae 146

Eidesstattliche Erklärung 153

Declaration/Declaration of contribution as co-author 155

Abbreviations

%	percent
3'UTR	3 Prime Untranslated Region
AVP	arginine vasopressin gene
BDNF	Brain-Derived Neurotrophic Factor
CpG	cytosine-guanine dinucleotide
CRH	Corticotrophin Releasing Hormone
CTQ	Childhood Trauma Questionnaire
Delta-Age	Epigenetic age acceleration, the difference between DNA methylation-predicted and chronological age
DEX	Dexamethasone
DNA	Deoxyribonucleic acid
DNMT	DNA methyltransferase
FKBP5	FK506 binding protein 5 (gene and protein name)
FKBP51	FK506 binding protein 51 kDa (protein name)
GR	Glucocorticoid Receptor (protein name)
GRE	Glucocorticoid Response Element
HDAC	Histone deacetylase
HPA-axis	Hypothalamus-Pituitary-Adrenal axis
Hsp90	Heat shock protein 90
IKK-α	Nuclear factor Kappa-B Kinase subunit alpha

kb	kilobase
MDD	Major Depressive Disorder or Major Depression
MeCP2	MEthyl CpG binding Protein 2
miRNA	micro RNA
mRNA	messenger RNA
n	Number
NF-κB	nuclear factor kappa-light-chain-enhancer of activated B cells
NFAT	Nuclear Factor of Activated T-cells
NIK	NF-κB-Inducing Kinase
p	p-value
PBMC	Peripheral Blood MonoCytes
PTSD	Post-Traumatic Stress Disorder
RNA	Ribonucleic acid
SNP	Single Nucleotide Polymorphism
TET	Ten-Eleven Translocation enzymes
TSS	Transcription start site

List of Publications

The work presented in this cumulative thesis was conducted under the supervision of Elisabeth B. Binder MD, PhD at the Department for Translational Research in Psychiatry at the Max Planck Institute of Psychiatry in Munich, Germany. The thesis contains the following published articles:

Publication I:

Zannas AS, Arloth J, Carrillo-Roa T, Iurato S, Röh S, Ressler KJ, Nemeroff CB, Smith AK, Bradley B, Heim C, Lange JF, Brückl T, Ising M, Wray NR, Erhardt A, Binder EB, Mehta D. Lifetime stress accelerates epigenetic aging in an urban, African American cohort: relevance of glucocorticoid signaling. *Genome Biology* 2015; 16(1):266. doi: 10.1186/s13059-015-0828-5

Publication II:

Gassen NC, Fries GR, **Zannas AS**, Rüegg J, Hartmann J, Zschocke J, Hafner K, Pfaffeneder T, Zimmermann SN, Knop M, Weber F, Kloiber S, Lucae S, Chrousos GP, Carell T, Ising M, Binder EB, Schmidt MV, Rein T. Chaperoning epigenetics: FKBP51 regulates DNMT1 phosphorylation and activity, impacting BDNF and antidepressant action. *Science Signaling* 2015; 8(404):ra119. doi: 10.1126/scisignal.aac7695

Summary

Psychological stress has been associated with accelerated cellular aging and increased disease risk, but the underlying molecular mechanisms remain elusive. The overarching goal of this thesis is to examine epigenetic regulation as a novel mechanism linking stress-related phenotypes with aging-related diseases. To achieve this goal, the thesis examines large human cohorts, where genome-wide DNA methylation and gene expression have been measured in peripheral blood, and which have detailed information on stress-related phenotypes, including childhood and lifetime stress, major depression, and posttraumatic stress disorder. The epigenetic effects of stress-related phenotypes are examined both 1) at the systems level, using a genome-wide measure of epigenetic aging, and 2) selectively at the stress-responsive *FKBP5* gene. The results presented here show that stress-related phenotypes accelerate both epigenetic aging and aging-related demethylation of the *FKBP5* gene. By examining subjects exposed to glucocorticoid agonists, this work further illustrates that age-related DNA methylation sites may be susceptible to stress-induced dysregulation of glucocorticoid signaling. Furthermore, mechanistic dissection of these effects shows that the age- and stress-related epigenetic upregulation of *FKBP5* may be associated with functional effects on gene expression, alterations in biological pathways critical for immune function and epigenetic regulation, and heightened risk for aging-related disease. Overall, these findings provide molecular insights into the mechanisms through which stress-related phenotypes may contribute to disease risk.

Aims of the thesis

The first aim of this thesis is to investigate whether stress-related phenotypes accelerate epigenetic changes as life progresses both at the genome-wide level and at stress-responsive genetic loci in peripheral blood. As a genome-wide marker of epigenetic aging, this work examines the DNA methylation-based age predictor, "epigenetic clock." As a stress-responsive locus, it examines the gene encoding FK506 binding protein 51 (*FKBP5*), a co-chaperone and modulator of the glucocorticoid receptor complex.

The second aim of the thesis is to mechanistically dissect the functional consequences of age- and stress-related epigenetic changes, by examining how these changes influence genome-wide and *FKBP5* expression levels, and how changes in *FKBP5* expression impacts downstream biological pathways. This aim is achieved by combining genome-wide gene expression data from humans with experiments in relevant cellular models.

The third aim is to examine the relevance of these genomic effects on disease risk. This is achieved by examining how epigenetic and gene expression changes are associated with peripheral inflammation and cardiovascular disease phenotypes.

Overarching introduction

Psychological stress and aging-related disease

The increase in life expectancy over the last decades constitutes a major accomplishment of modern medicine, but it also results in an exponential rise in the number of older adults —which is predicted to more than double over the next two decades (Prevention, 2013; Statistics, 2012)— and a concomitant explosion in the prevalence of aging-related diseases, including cardiovascular disease, cancer, and dementia. Because these conditions are worldwide the leading causes of morbidity and mortality (Niccoli and Partridge, 2012), it is important to gain understanding into how modifiable factors may impact healthy aging and shape risk for aging-related diseases.

A well-documented risk factor for aging-related disease is psychological stress. Increased risk for aging-related diseases has been observed in individuals exposed to excessive and chronic stress (Chandola *et al*, 2006; Peavy *et al*, 2009; Powell *et al*, 2011; Powell *et al*, 2013; Rozanski *et al*, 1999; Zannas *et al*, 2012), in individuals experiencing traumatic events during sensitive developmental periods, such as during childhood (Danese and McEwen, 2012; Danese *et al*, 2008; Felitti *et al*, 1998), and in patients with stress-related psychiatric disorders, including major depression and posttraumatic stress disorder (Danese *et al*, 2008; Vaccarino *et al*, 2013). At the molecular level, studies show that stress can induce cellular aging as measured with telomere length. In particular, telomere shortening has been observed with a wide-range of stressors, including chronic caregiver stress (Epel *et al*, 2004; Litzelman *et al*, 2014), stress *in utero* and early life (Entringer *et al*, 2011; Entringer *et al*, 2013; Kananen *et al*, 2010; Savolainen *et al*, 2014), work stress (Ahola *et al*, 2012), and perceived stress (Parks *et al*, 2009; Puterman *et al*, 2010).

How could stress-related phenotypes increase risk for aging-related disease? A plausible mediator of this relationship could be the impact of stress on immune function and peripheral inflammation. This hypothesis is supported by studies showing heightened peripheral inflammation in association with childhood trauma (Danese *et al*, 2008; Danese *et al*, 2007), acculturative stress (Fang *et al*, 2014), and depressive syndromes (Danese *et al*, 2009; Danese *et al*, 2008). Because inflammation is a key process implicated in the pathogenesis of several aging-related diseases (Franceschi and Campisi, 2014; Howcroft *et al*, 2013) and immune functions are influenced by stress responses (Danese *et al*, 2012), these studies overall suggest that psychological stressors of certain type, timing, and duration could contribute to accelerated aging and aging-related disease phenotypes, potentially through their effects on immune function and peripheral inflammation. However, the underlying mechanisms and the cascade of molecular events linking stress and aging are poorly understood.

Epigenetic regulation through DNA methylation: a plausible mechanism linking stress and aging

Among plausible molecular processes that could mediate the impact of stress on complex phenotypes, it is relevant to consider epigenetic regulation. Epigenetics is a composite term derived from the Greek prefix "epi-," which means "over", and "genetics." In its modern use, epigenetics denotes the set of biological processes that regulate gene expression without influencing the underlying nucleotide sequence. The constantly growing repertoire of epigenetic processes includes various types of DNA methylation, posttranslational histone modifications, noncoding RNAs, and higher-order changes in chromatin conformation (Telese *et al*, 2013). Beyond their central role in mammalian development and cell differentiation, these processes collectively constitute a molecular interface, which can be shaped by environmental factors

(Telese *et al*, 2013), including stress exposure (Zannas and West, 2014), and can in turn contribute to regulation of genomic function and the expression of complex phenotypes, including diseases of the aging (Brunet and Berger, 2014). Consequently, epigenetic regulation represents a plausible mechanism to consider when examining the impact of stress exposure on aging-related disease phenotypes.

Despite the epigenome's ability to respond dynamically to environmental changes, a body of evidence in both humans and rodents shows that stress exposure across different life stages can result in lasting epigenetic modifications. More specifically, exposure to stress as early as *in utero* can induce profound changes in DNA methylation (Boersma *et al*, 2014; Cao-Lei *et al*, 2014; Dong *et al*, 2015; Mychasiuk *et al*, 2011; Palacios-Garcia *et al*, 2015; Palma-Gudiel *et al*, 2015; Schraut *et al*, 2014; Xu *et al*, 2014), histone modifications (Benoit *et al*, 2015; Winston *et al*, 2014), and changes in the expression of miRNAs (Monteleone *et al*, 2014; Zucchi *et al*, 2013). Likewise, stressors occurring during childhood and adolescence can induce lasting changes in DNA methylation (Anier *et al*, 2014; Doherty *et al*, 2016; Houtepen *et al*, 2016; Klengel *et al*, 2013; McGowan *et al*, 2009; Murgatroyd *et al*, 2009; Niwa *et al*, 2013; Ouellet-Morin *et al*, 2013; Perroud *et al*, 2011; Roth *et al*, 2009; Tyrka *et al*, 2012; Tyrka *et al*, 2015; Unternaehrer *et al*, 2012; van der Knaap *et al*, 2014, 2015; Weaver *et al*, 2004; Weaver *et al*, 2006), histone modifications (Kao *et al*, 2012), miRNA changes (Zhang *et al*, 2015), and alterations in DNA-binding of the methyl CpG binding protein 2 (MeCP2) (Murgatroyd *et al*, 2009). Lasting epigenetic changes have also been observed following stress exposure during adulthood, including DNA methylation changes (Alasaari *et al*, 2012; Elliott *et al*, 2010; Lam *et al*, 2012; Le Francois *et al*, 2015; Roth *et al*, 2011; Tran *et al*, 2013; Uchida *et al*, 2011; Ursini *et al*, 2011; Witzmann *et al*, 2012), histone modifications (Erburu *et al*, 2015; Nasca *et al*, 2015;

Renthal *et al*, 2007; Uchida *et al*, 2011), miRNA changes (Volk *et al*, 2016; Volk *et al*, 2014; Zhang *et al*, 2015), higher-order changes in chromatin conformation (Sun *et al*, 2015), and alterations in MeCP2 binding to DNA (Uchida *et al*, 2011). Notably, the epigenetic modifications associated with stress can, in many cases, last long after stressor exposure, potentially persisting throughout life and even across generations. This has been observed for several epigenetic modifications, including changes in DNA methylation, histone modifications, and miRNA changes (Dias and Ressler, 2014; Montagud-Romero *et al*, 2016; Rodgers *et al*, 2013; Rodgers *et al*, 2015; Yehuda *et al*, 2015).

Among epigenetic modifications associated with stress exposure, this thesis focuses on the role of DNA methylation that occurs at the 5' cytosine of cytosine-guanine dinucleotides (CpG), for simplicity denoted hereafter as DNA methylation. Following the advent of genome-wide methylation arrays, DNA methylation has become the most widely studied epigenetic modification in human cohorts. DNA methylation was initially considered a stable epigenetic change, but was subsequently shown to be a reversible process that responds dynamically to environmental factors. Increases in DNA methylation are mediated by DNA methyltransferases (DNMTs), whereas DNA methylation decreases are effected by enzymes involved in active demethylation, such as the TET family of 5-methylcytosine dioxygenases (Telese *et al*, 2013). Despite the dynamic nature of DNA methylation signatures, certain methylation markers can be stabilized during life and even across generations (Dias *et al*, 2014; Gassen *et al*, 2016; Yehuda *et al*, 2015), thereby exerting long-term influence on genomic function and potentially contributing to the development of complex phenotypes.

While these observations suggest that DNA methylation holds promise as biomarker of stress-related disease, an inherent limitation is that, like all epigenetic processes, DNA

methylation shows considerable cell and tissue specificity. Therefore, although some epigenetic signatures may show similar patterns across multiple tissues (Capra, 2015; Hannon *et al*, 2015; Horvath, 2013), changes in DNA methylation modifications should be examined, when feasible, in the tissue implicated in the disease phenotype under study. In the present thesis, this limitation is partly overcome by assessing DNA methylation changes in peripheral blood monocytes (PBMC), a tissue that plays central role in orchestrating immune responses and is highly relevant for examining the impact of stress on peripheral inflammation and aging-related disease phenotypes.

DNA methylation as biomarker of aging-related disease phenotypes

Aging is associated with widespread changes in DNA methylation (Bjornsson *et al*, 2008; Christensen *et al*, 2009; Hernandez *et al*, 2011; Heyn *et al*, 2012; Horvath, 2013; Horvath *et al*, 2012; Rakyan *et al*, 2010). The pattern of these changes shows substantial variability along the human lifespan. Advancing age is generally associated with increasing inter-individual variability in DNA methylation levels, and there is an overall increase in DNA methylation levels in early life with subsequent decline later in life (Hannum *et al*, 2013; Herbstman *et al*, 2013; Heyn *et al*, 2012; Li *et al*, 2010; Talens *et al*, 2012; Weidner *et al*, 2014). Despite these age-related changes in global methylation, the pattern of DNA methylation changes also varies across distinct sites. For example, methylation sites that are not located in CpG islands and those with high methylation levels tend to decrease with increasing age (Christensen *et al*, 2009; Heyn *et al*, 2012; Weidner *et al*, 2014), whereas methylation sites located in CpG islands and with low methylation levels tend to increase with advancing age (Heyn *et al*, 2012; Rakyan *et al*, 2010; Weidner *et al*, 2014). Age-related changes in DNA methylation have in most cases been

examined in peripheral blood (Bjornsson *et al*, 2008; Christensen *et al*, 2009; Florath *et al*, 2014; Heyn *et al*, 2012; Horvath, 2013; Horvath *et al*, 2012; Rakyan *et al*, 2010; Talens *et al*, 2012; Weidner *et al*, 2014), and studies suggest that they hold promise as biomarkers for aging research (Bell *et al*, 2012; Issa, 2014; Langevin *et al*, 2014; Poulsen *et al*, 2007). Furthermore, the role of DNA methylation as biomarker has been supported by studies showing that the DNA methylation changes observed in tissues implicated in aging-related diseases, such as cancer tissues and atherosclerotic arteries, show striking similarities with age-related methylation changes, including global decreases in methylation and CpG-island hypermethylation (Castillo-Diaz *et al*, 2010; Jones and Baylin, 2007). Beyond their potential role as biomarkers, age-related epigenetic changes have been further proposed to represent a hallmark of the aging process (Benayoun *et al*, 2015; Lopez-Otin *et al*, 2013).

Among potential DNA methylation-based biomarkers of aging, promise has been shown for the composite predictors of chronological age, which are calculated by integrating the methylation status of multiple CpGs across the genome that strongly correlate with age (Bocklandt *et al*, 2011; Florath *et al*, 2014; Hannum *et al*, 2013; Horvath, 2013; Koch and Wagner, 2011; Weidner *et al*, 2014). Among these DNA methylation-based age predictors, particular promise has been shown for the so-called "epigenetic clock," a predictor comprised of 353 CpGs (Horvath, 2013), which robustly correlates with chronological age across multiple human tissues. Despite the strong correlations between the DNA methylation (epigenetic clock)-predicted age and chronological age, some individuals show substantial differences between the two, and this difference (Delta-Age) has been proposed as a measure of accelerated epigenetic or biological aging (Horvath, 2013). Notably, since the introduction of this measure in aging research, accumulating evidence shows that accelerated epigenetic aging is associated with a

host of aging-related phenotypes, including physical and cognitive decline (Levine *et al*, 2015b; Marioni *et al*, 2015b; Wolf *et al*, 2015), cancer incidence and outcomes (Levine *et al*, 2015a; Perna *et al*, 2016; Zheng *et al*, 2016), frailty in the elderly (Breitling *et al*, 2016), osteoarthritis (Vidal-Bralo *et al*, 2016), Parkinson's disease (Horvath and Ritz, 2015), menopause (Levine *et al*, 2016), obesity (Horvath *et al*, 2014), cardiovascular disease (Perna *et al*, 2016), and all-cause mortality (Chen *et al*, 2016; Marioni *et al*, 2016; Marioni *et al*, 2015a; Perna *et al*, 2016).

Although these observations show that age-related DNA methylation changes are associated with disease phenotypes, the exact cascade of molecular events that drives these changes is elusive. Because age-related DNA methylation changes may result from a complex interplay among genetic and environmental factors (Fraga *et al*, 2005; Gronniger *et al*, 2010; Hannum *et al*, 2013; Horvath, 2013; Lu *et al*, 2016), stress exposure and stress-related phenotypes could contribute to these changes, accounting to an extent for the inter-individual variability in disease risk. The molecular mechanisms driving these changes may be distinct across different methylation sites; for example, senescence-associated transcription factors may be involved in sites where methylation rises (Hanzelmann *et al*, 2015), whereas downregulation of DNMT1 appears to play central role in sites where methylation declines with advancing age (Li *et al*, 2010). The following section discusses potential mechanisms through which psychological stress may drive epigenetic changes and, in particular, lasting changes in DNA methylation.

HPA axis and glucocorticoid signaling as molecular effectors of stress

Psychological stress triggers a set of behavioral, hormonal, neural, and molecular responses that can have profound effects on body tissues. A primary effector of the stress response, and the

focus of this thesis is the hypothalamic-pituitary-adrenal (HPA) axis. The HPA axis is set into motion by the hypothalamus, a brain region that secretes corticotropin-releasing hormone and arginine vasopressin, thereby signaling the anterior pituitary to secrete adrenocorticotropic hormone (ACTH) (Chrousos and Gold, 1992). ACTH in turn triggers adrenal release of glucocorticoids, cortisol in humans, in the periphery. Homeostatic regulation of the HPA axis is essential, and HPA dysregulation has been linked with increased risk for behavioral and somatic disease phenotypes in both humans and rodents (Barha *et al*, 2011; Bourke and Neigh, 2011; de Kloet *et al*, 2006; Heim *et al*, 2008; Jankord *et al*, 2011). Such dysregulation can occur upon exposure to stressors of certain duration, intensity, type, and timing (Tsigos and Chrousos, 2002); for example, chronic stress deregulates the circadian and ultradian rhythmicity of glucocorticoid secretion (Lightman, 2008). Consequently, dysregulated HPA axis and glucocorticoid secretion represent a prime mechanism for examining the molecular effects of stress on body tissues.

While glucocorticoids can have both genomic and nongenomic effects on target tissues (Uchoa *et al*, 2014), their genomic effects are to a large extent mediated by the glucocorticoid receptor (GR). The GR primarily functions as a ligand-dependent transcription factor that regulates gene transcription either through direct binding to conserved DNA sequences called glucocorticoid response elements (GRE) or through interactions with other transcription factors that can be GRE-dependent or -independent (Vockley *et al*, 2016). Beyond the rapid regulation of gene transcription, however, the genomic actions of glucocorticoids can also result in lasting epigenetic modifications. The most widely described epigenetic effect of glucocorticoids is the rapid demethylation, which can result in global methylation decreases (Bose *et al*, 2010; Bose *et al*, 2015), but most strikingly occurs within or near GREs (Klengel *et al*, 2013; Thomassin *et al*,

2001; Wiench *et al*, 2011a; Wiench *et al*, 2011b). Glucocorticoid-induced hypermethylation has also been observed, most notably in promoter CpGs (Niwa *et al*, 2013). The mechanisms underlying these effects are largely unknown; however, glucocorticoids have been shown to upregulate the Tet family of 5-methylcytosine dioxygenases (TET) (Bose *et al*, 2015; Sawamura *et al*, 2015), which actively demethylate DNA, and to downregulate the maintenance methyltransferase DNMT1 (Yang *et al*, 2012) and the methyltransferase DNMT3a (Bose *et al*, 2015). Besides changes in DNA methylation, glucocorticoids can also induce changes in histone methylation and acetylation, which can occur at sites of direct GR binding (Vockley *et al*, 2016), or through the interactions of the GR with other transcription factors and the consequent recruitment of histone modifiers to target genomic sites (Di Stefano *et al*, 2015; Zannas and Chrousos, 2015b). Glucocorticoids can also regulate several miRNAs (Dwivedi *et al*, 2015; Ko *et al*, 2015), and can induce chromatin remodeling, thereby changing accessibility of GR-binding sites to transcription factors (Vockley *et al*, 2016). Despite these observations, the mechanisms through which glucocorticoids modulate the epigenetic machinery are poorly understood.

An important conclusion drawn from studies to date is the potential of time-limited glucocorticoid exposure to exert long-lasting effects on the epigenome. This is supported by work in both cell lines and rodents showing that changes in DNA methylation can last long after cessation of glucocorticoid exposure (Bose *et al*, 2010; Bose *et al*, 2015; Lee *et al*, 2010; Niwa *et al*, 2013). These lasting effects are thought to represent a "molecular memory" that can influence subsequent responses to glucocorticoids, ultimately shaping genomic function and phenotypic expression (Klengel *et al*, 2013; Thomassin *et al*, 2001; Wiench *et al*, 2011a; Wiench *et al*, 2011b; Zannas *et al*, 2014). As discussed above, these principles parallel the observation that psychological stress, which dysregulates glucocorticoid secretion, can induce long-lasting

epigenetic modifications that can persist throughout life and even across generations (Dias *et al*, 2014; Gassen *et al*, 2016; Yehuda *et al*, 2015). Because epigenetic changes can influence genomic function and phenotypic expression, this work highlights that DNA methylation is an important mechanism that may underlie the pathogenesis of stress-related disease phenotypes.

FKBP5: a stress- and glucocorticoid-responsive immunophilin

As highlighted above, the lasting effects of stress on the epigenome are likely to occur at genomic sites that are targeted by the GR. Therefore, beyond examining the association of stress-related disease phenotypes with epigenetic markers derived from genome-wide approaches, such as the epigenetic clock, it is also relevant to determine how stress throughout life epigenetically regulates selective glucocorticoid-responsive loci. One such locus is the gene encoding FK506 binding protein 51 (FKBP5/FKBP51), which is the most robustly induced gene upon glucocorticoid exposure in peripheral blood (Menke *et al*, 2012). As suggested by its responsivity to glucocorticoids, upregulation of *FKBP5* can result from stress-induced DNA demethylation that occurs at CpGs within or near *FKBP5* GREs (Klengel *et al*, 2013; Lee *et al*, 2010; Lee *et al*, 2011). Consequently, a plausible hypothesis is that persistent stress or multiple stressors accumulating throughout life could lead to sustained epigenetic upregulation of *FKBP5*. Furthermore, it is plausible that FKBP5 could itself influence downstream components of the epigenetic machinery, mediating some of the effects of stress on the epigenome.

FKBP5 is a 51-kDa immunophilin that was originally named after its ability to bind the immunosuppressant drug FK506 (Wiederrecht *et al*, 1992), but it is best known for its ability to function as a co-chaperone and modulator of the glucocorticoid receptor complex (Zannas *et al*, 2016). More specifically, FKBP5 has been shown to exert intracellular negative feedback on GR

function, by delaying nuclear translocation and decreasing transcriptional activity of the GR (Wochnik *et al*, 2005). The ability of FKBP5 to modulate the GR complex stems from its function as a co-chaperone that interacts with and influences the folding of other members of the steroid receptor complex, most notably the heat shock protein 90 (Hsp90) and the P23 protein (Schiene-Fischer and Yu, 2001). The result of these molecular effects is that changes in FKBP5 levels can lead to altered GR sensitivity, an effect that in turn could have important implications for stress-related disease phenotypes.

In particular, a body of evidence shows that FKBP5 upregulation may be associated with a number of aberrant phenotypes, including aging-related disease phenotypes (Binder *et al*, 2008; Blair *et al*, 2013; Kim *et al*, 2012; Klengel *et al*, 2013; Pereira *et al*, 2014; Romano *et al*, 2004; Romano *et al*, 2010; Sinclair *et al*, 2013). The potential of FKBP5 upregulation to contribute to aberrant phenotypes could result from its downstream effects on diverse biological pathways (Zannas *et al*, 2016). Among processes influenced by FKBP5, studies in cells and mice have shown that it can influence immune pathways, including the NF-κB (nuclear factor kappa-light-chain-enhancer of activated B cells) and the calcineurin/NFAT (nuclear factor of activated T-cells) signaling pathways (Avellino *et al*, 2005; Baughman *et al*, 1995; Bouwmeester *et al*, 2004; Daudt and Yorio, 2011; Erlejman *et al*, 2014; Giordano *et al*, 2006; Kim *et al*, 2012; Li *et al*, 2002; Maiaru *et al*, 2016; Park *et al*, 2007; Romano *et al*, 2004; Romano *et al*, 2010; Romano *et al*, 2015; Srivastava *et al*, 2015; Weiwad *et al*, 2006). Because immune dysregulation is a potential process linking stress and disease risk, together these studies suggest that the impact of FKBP5 on immune pathways could be one molecular mechanism through which stress contributes to somatic phenotypes along the lifespan. However, this hypothesis has not been examined in living humans.

Zannas et al. Genome Biology (2015) 16:266
DOI 10.1186/s13059-015-0828-5

Genome Biology

RESEARCH Open Access

Lifetime stress accelerates epigenetic aging in an urban, African American cohort: relevance of glucocorticoid signaling

Anthony S. Zannas[1,2*], Janine Arloth[1,3], Tania Carrillo-Roa[1], Stella Iurato[1], Simone Röh[1], Kerry J. Ressler[4,5,6], Charles B. Nemeroff[7], Alicia K. Smith[4], Bekh Bradley[8,4], Christine Heim[9,13], Andreas Menke[10,11], Jennifer F. Lange[1], Tanja Brückl[1], Marcus Ising[11], Naomi R. Wray[12], Angelika Erhardt[1], Elisabeth B. Binder[1,4*] and Divya Mehta[12]

Abstract

Background: Chronic psychological stress is associated with accelerated aging and increased risk for aging-related diseases, but the underlying molecular mechanisms are unclear.

Results: We examined the effect of lifetime stressors on a DNA methylation-based age predictor, epigenetic clock. After controlling for blood cell-type composition and lifestyle parameters, cumulative lifetime stress, but not childhood maltreatment or current stress alone, predicted accelerated epigenetic aging in an urban, African American cohort (n = 392). This effect was primarily driven by personal life stressors, was more pronounced with advancing age, and was blunted in individuals with higher childhood abuse exposure. Hypothesizing that these epigenetic effects could be mediated by glucocorticoid signaling, we found that a high number (n = 85) of epigenetic clock CpG sites were located within glucocorticoid response elements. We further examined the functional effects of glucocorticoids on epigenetic clock CpGs in an independent sample with genome-wide DNA methylation (n = 124) and gene expression data (n = 297) before and after exposure to the glucocorticoid receptor agonist dexamethasone. Dexamethasone induced dynamic changes in methylation in 31.2 % (110/353) of these CpGs and transcription in 81.7 % (139/170) of genes neighboring epigenetic clock CpGs. Disease enrichment analysis of these dexamethasone-regulated genes showed enriched association for aging-related diseases, including coronary artery disease, arteriosclerosis, and leukemias.

Conclusions: Cumulative lifetime stress may accelerate epigenetic aging, an effect that could be driven by glucocorticoid-induced epigenetic changes. These findings contribute to our understanding of mechanisms linking chronic stress with accelerated aging and heightened disease risk.

Keywords: Aging, Aging-related disease, DNA methylation, Epigenetics, Gene expression, Glucocorticoids, Psychological stress

Background

The last decades have witnessed a dramatic increase in life expectancy. As a result, the number of older adults is predicted to more than double over the next two decades [1, 2]. While this increase in life expectancy is undoubtedly one of the biggest achievements of modern medicine, population aging also brings forth an unprecedented increase in aging-related diseases, including cardiovascular disease, cancer, and dementia [3]. Given that these conditions are currently the leading causes of morbidity and mortality, it is imperative to gain insights into factors that impact healthy aging and contribute to aging-related diseases.

An important risk factor for accelerated aging and aging-related diseases is psychological stress. Although stressors are ubiquitous in nature and necessary for survival [4], excessive and chronic stress has been associated with accelerated cellular aging [5, 6] and increased

* Correspondence: anthony_zannas@psych.mpg.de; binder@psych.mpg.de
Elisabeth B. Binder and Divya Mehta are joint senior authors on this work.
[1]Department of Translational Research in Psychiatry, Max Planck Institute of Psychiatry, Munich, Germany
Full list of author information is available at the end of the article

risk for aging-related disease phenotypes, including cardiovascular disease, immune dysregulation, and late-life neuropsychiatric disorders [7–12]. Furthermore, stressors occurring during sensitive developmental periods, such as childhood maltreatment, have been linked with later development of aging-related diseases [13–15]. Lastly, stress-related psychiatric disorders, including major depression and post-traumatic stress disorder (PTSD), are themselves risk factors for such diseases [15, 16]. Despite these observations, the molecular mechanisms linking psychological stress with accelerated aging and aging-related diseases remain largely unknown.

One plausible mechanism that may mediate the adverse effects of stress on the aging process is epigenetic regulation. Long-term epigenetic changes can be induced by environmental stimuli, including psychological stressors, and can shape complex phenotypes [17]. The most studied epigenetic modification in this context is DNA methylation. Stressors can induce lasting changes in DNA methylation [18, 19], an effect that is in part mediated by the genomic effects of glucocorticoids, a primary molecular effector of the stress response [20]. Glucocorticoids exert actions in essentially every body organ via activation of the glucocorticoid receptor (GR), a transcription factor that regulates gene expression by the binding of its homodimer to glucocorticoid response elements (GREs) in regulatory regions of target genes [21]. Beyond regulating gene transcription, GRE binding can locally induce lasting changes in DNA methylation, a form of molecular memory that shapes subsequent responses to glucocorticoids and stressors [17, 18, 22–24]. Therefore, it is plausible that stress and glucocorticoid exposure throughout the lifetime could impact cellular aging via cumulative effects on aging-related DNA methylation sites.

Aging and aging-related diseases are associated with profound changes in DNA methylation [25–31]. Recognizing the importance of DNA methylation in the aging process has led to recent development of several DNA methylation-based predictors of aging [27, 32–34]. Among these, a composite predictor comprised of 353 Cytosine-phosphate-Guanosine sites (CpGs) across the genome ('epigenetic clock') was shown to strongly correlate with chronological age across multiple tissues in humans [27], suggesting its usefulness as a biomarker in aging-related research. Using this predictor, accelerated epigenetic aging (Δ-age), defined as the difference between DNA methylation-predicted age (DNAM-age) and chronological age, has been associated with aging-related and other phenotypes, including cancer, obesity, cytomegalovirus infection, Down's syndrome, PTSD, physical and cognitive decline, all-cause mortality, and the presence of higher self-control and lower socioeconomic status [27, 35–41]. However, no studies have examined the relationship between this predictor and cumulative lifetime stress nor the potential molecular mechanisms underlying this relationship.

In the present study, we first show that cumulative lifetime stress, but not childhood or current stress alone, is associated with accelerated epigenetic aging in a cohort of highly traumatized African American individuals. Examining GR signaling as a potential mechanism underlying this effect, we identify that a high number of epigenetic clock CpGs are located within functional GREs and show dynamic methylation changes following GR activation by exposure to the GR agonist dexamethasone (DEX). Lastly, we show that genes neighboring these CpGs are dynamically regulated by DEX and that these DEX-regulated genes show enriched association for aging-related diseases. Taken together, our findings support a model of stress-induced acceleration of epigenetic aging, overall contributing to our understanding of mechanisms linking chronic stress with accelerated aging and heightened disease risk.

Results

Prediction of chronological age using the epigenetic clock

DNAM-age was calculated from peripheral blood from two independent samples, derived from the Grady Trauma Project (GTP) and the Max Planck Institute of Psychiatry (MPIP) cohorts using genome-wide Illumina HumanMethylation450 BeadChips (450 K), as previously described [27]. Given that the GTP primarily comprises (>90 %) African American participants, we excluded other ethnicities to minimize confounders. This resulted in a total of 393 participants with DNAM-age data. In contrast, the MPIP cohort consists only of Caucasian participants with a total of 124 participants with baseline DNAM-age data. The mean (SD, range) age was 41.33 years (12.85, range 18 to 77 years) for the GTP and 39.5 years (14.14, range 21 to 71 years) for the MPIP. The n (%) of female participants was 278 (70.7 %) for the GTP and 44 (35.5 %) for the MPIP. To validate the epigenetic clock predictor in our cohorts, we correlated DNAM-age with chronological age as previously described [27]. This correlation was strong for both the GTP ($r = 0.90$, $P < 2.2 \times 10^{-16}$) (Fig. 1a) and MPIP ($r = 0.94$, $P < 2.2 \times 10^{-16}$) cohorts (Fig. 1b) and proved robust and similar for both genders ($r = 0.89$ for male vs. $r = 0.90$ for female in the GTP; $r = 0.95$ for male vs. $r = 0.94$ for female in the MPIP).

Epigenetic age acceleration is associated with cumulative lifetime stress, but not childhood or current stress alone, in an urban, African American cohort

We then hypothesized that epigenetic age acceleration (Δ-age), calculated by subtracting the actual chronological

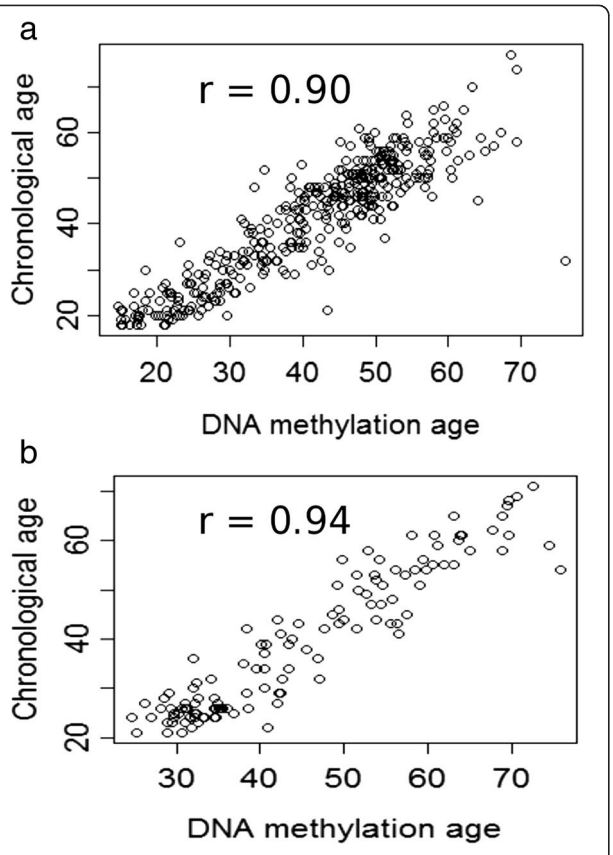

Fig. 1 Correlation between chronological age and age predicted by DNA methylation-based predicted age in two independent cohorts. **a** GTP cohort (n = 393). **b** MPIP cohort (n = 124)

age from DNAM-age [27], would be positively associated with exposure to life stress. This hypothesis was tested in the highly traumatized GTP cohort. The mean (SD, range) Δ-age in the GTP was −0.13 years (5.69, range −17.31 to 43.98 years). A total of 304 GTP participants had data on lifetime stressors assessed by the Stressful Events Questionnaire (SEQ) and 386 participants had data on childhood maltreatment assessed by the Childhood Trauma Questionnaire (CTQ). The individual items from the SEQ were summed to yield a total score of lifetime stress exposure (Life Stress), and a similar total score was generated for the CTQ (Child Stress). The SEQ additionally assesses stressor exposure over the last year, and these items were summed to yield a score of more recent stress exposure (Current Stress). Linear regression models controlling for sex and age showed that Life Stress was positively associated with Δ-age ($\beta = 0.24$, $SE = 0.08$, $P = 2.8 \times 10^{-3}$), and this effect remained significant after further controlling for Houseman blood cell counts and technical batch effects ($\beta = 0.18$, $SE = 0.08$, $P = 1.8 \times 10^{-2}$) (Fig. 2a), lifestyle parameters, including body mass index, smoking, alcohol, cocaine, marijuana, and heroin use ($\beta = 0.31$, $SE = 0.11$, $P = 7.4 \times 10^{-3}$), as well depressive symptomatology, psychiatric treatments, and genome-wide SNP-based principal components ($\beta = 0.28$, $SE = 0.13$, $P = 2.7 \times 10^{-2}$).

In secondary analyses, we examined whether the effect of lifetime stress on age acceleration depends on the type of stressor and other moderating variables. Based on previous work distinguishing between life events that affect the individual directly vs. life events that affect one's social network [42], we separately summed SEQ items assessing personal life events (Personal Life Stress) and items assessing network events (Network Life Stress). Δ-age showed a positive and significant association with Personal Life Stress ($\beta = 0.26$, $SE = 0.10$, $P = 8.7 \times 10^{-3}$) (Fig. 2b) and a positive but not significant association with Network Life Stress ($P = 1.1 \times 10^{-1}$) (Fig. 2c). No significant interactions were noted between Life Stress or Personal Life Stress and either sex or age. However, stratification of the GTP by a median split of age showed that the effect of Personal Life Stress on Δ-age was marginally stronger in older ($\beta = 0.33$, $SE = 0.17$, $P = 5.3 \times 10^{-2}$) (Fig. 2d) as compared to younger participants ($\beta = 0.15$, $SE = 0.14$, $P = 2.8 \times 10^{-1}$) (Fig. 2e). On the other hand, Δ-age was not associated with either CTQ score ($P = 4 \times 10^{-1}$) or Current Stress alone ($P = 1.3 \times 10^{-1}$). However, when participants were stratified based on the severity of childhood maltreatment, only individuals exposed to lower levels (none or mild) of sexual and physical childhood abuse (based on respective CTQ subscale scores) showed significant effects of Life Stress on Δ-age (Fig. 2f). This was not a consequence of differential stress exposure burden between the two groups, since, as expected, individuals exposed to higher levels of childhood abuse also had higher levels of Life Stress with a mean (SD) Life Stress of 12.32 (3.64) as compared to 10.01 (3.76) in individuals with lower levels of childhood abuse ($t_{299} = 5.38$, $P = 1.5 \times 10^{-7}$). Furthermore, the two strata showed similar correlations between DNAM-age and chronological age ($r = 0.91$ for higher vs. 0.92 for lower abuse, Fisher z score = 0.6, $P = 5.5 \times 10^{-1}$). Lastly, we found no association between Δ-age and current stress-related psychiatric phenotypes, including depressive ($P = 3.4 \times 10^{-1}$) and PTSD symptomatology ($P = 7.9 \times 10^{-1}$) in the GTP. In line with this finding, depression diagnosis was not associated with Δ-age in the MPIP cohort ($P = 2.3 \times 10^{-1}$, n = 72 controls vs. 52 depressed). Taken together, these findings show that cumulative lifetime stress, but not childhood trauma or current stress alone, is associated with accelerated epigenetic aging, an effect that is primarily driven by personal life events, may be more evident in advancing ages, and is blunted in participants exposed to high levels of childhood abuse.

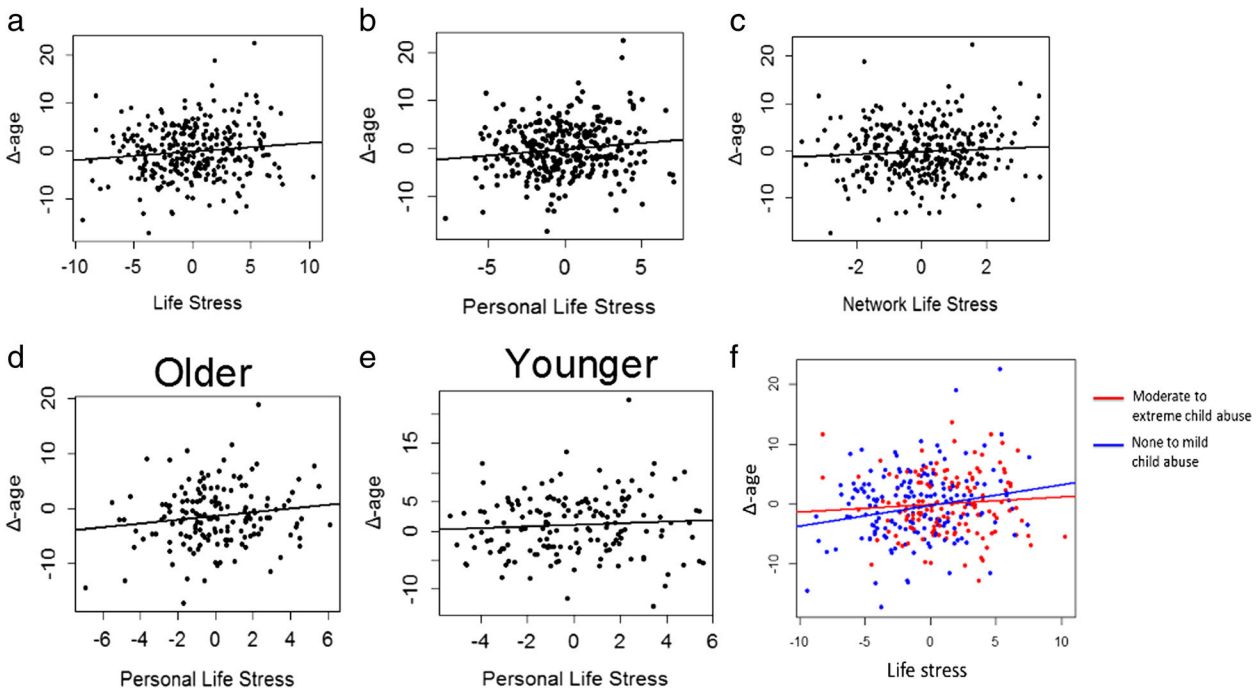

Fig. 2 Cumulative lifetime stress is associated with epigenetic age acceleration in a highly traumatized human cohort derived from the Grady Trauma Project. Epigenetic age acceleration (Δ-age) was calculated by subtracting chronological age from DNA methylation predicted age. Δ-age was regressed on cumulative lifetime stress (Life Stress) after adjusting for covariates (fitted stress measures are shown). **a** Life Stress was positively associated with epigenetic age acceleration (β = 0.18, SE = 0.08, $P = 1.8 \times 10^{-2}$), and this association remained significant after further controlling for lifestyle parameters, including body mass index, smoking, alcohol, cocaine, marijuana, and heroin use (β = 0.31, SE = 0.11, $P = 7.4 \times$ 10-3), as well depressive symptomatology, psychiatric treatments, and genome-wide SNP-based principal components (β = 0.28, SE = 0.13, $P = 2.7 \times 10^{-2}$). Statistically significant association was found for Personal Life Stress (β = 0. 26, SE = 0.10, $P = 8.7 \times 10^{-3}$) (**b**), whereas the effect of Network Life Stress was not significant ($P = 1.1 \times 10^{-1}$) (**c**). Age stratification by a median split showed that the effect of Personal Life Stress on Δ-age was stronger in older (β = 0.33, SE = 0.17, $P = 5.3 \times 10^{-2}$) (**d**), as compared to younger participants (β = 0.15, SE = 0.14, $P = 2.8 \times 10^{-1}$) (**e**). Stratification of the effect of cumulative life stress on epigenetic age acceleration based on the presence or not of moderate to severe physical or sexual child abuse showed that Life Stress was positively associated with Δ-age in participants with no or mild physical and sexual child abuse (β = 0.34, SE = 0.11, $P = 2.5 \times 10^{-3}$, n = 212) but not in those with moderate to extreme child abuse ($P = 3.9 \times 10^{-1}$, n = 174) (**f**)

Epigenetic clock CpGs and neighboring genes are regulated by GR activation and show enriched association with aging-related diseases

The effect of lifetime stress on epigenetic aging prompted us to examine susceptibility of individual epigenetic clock CpGs to glucocorticoids, a primary molecular effector of stress responses, as a potential mechanism underlying this association. To address this hypothesis, we first examined whether epigenetic clock CpGs show DNA methylation changes 3 h after oral exposure to a GR agonist (1.5 mg of DEX) in the independent MPIP cohort (n = 124). After correcting for multiple testing, 110 of the 353 CpGs showed statistically significant methylation changes (false discovery rate (FDR)-adjusted $P < 5 \times 10^{-2}$). Among the DEX-regulated CpGs, 98 (89 %) showed decrease in methylation, whereas 12 (11 %) showed increase in methylation (Additional file 1: Table S1). We next examined the effect of acute DEX exposure on the epigenetic clock by comparing DNAM-age at baseline vs. 3 h after DEX exposure (n = 124). There was no effect of DEX on DNA methylation-predicted age (baseline mean DNAM-age = 45.24 vs. post-DEX mean DNAM-age = 45.15, paired $t_{123} = 0.31$, $P = 7.6 \times 10^{-1}$).

Given that GR binding to GREs can exert changes in DNA methylation, we then examined whether epigenetic clock CpGs co-localize with GREs. Among the 353 epigenetic clock CpGs, 85 CpGs were located within GREs as defined by CHIP-Seq peaks in a lymphoblastoid cell line (LCL) (Additional file 1: Table S1). This CpG-GRE co-localization significantly differed from the one expected by chance as determined by randomly drawing 1,000 sets (n = 353 CpGs) of CpG sites from all CpGs present on the 450 K array (expected mean 48.8, SD 6.1, range 31 to 68, $p_{perm} < 1 \times 10^{-3}$) (Fig. 3a). Proximity to GREs was particularly observed for DEX-regulated CpGs (Fig. 3b), with 17 of these sites located right within GREs and 35 within 1 kb distance from GREs. Because the 353 CpGs were originally derived from the 21,369 (21 K) CpGs that overlap the 27 K and 450 K Illumina arrays [27], we next examined whether the epigenetic clock

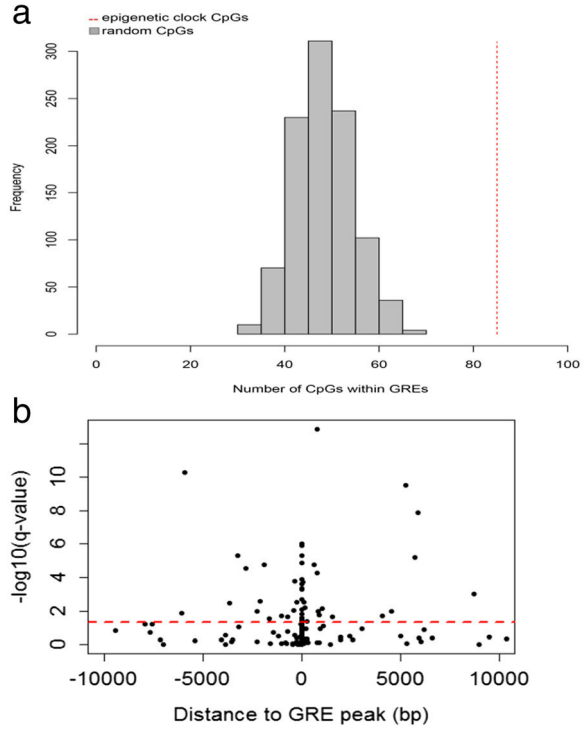

Fig. 3 Epigenetic clock CpGs co-localize with functional glucocorticoid response elements (GREs) and show methylation changes following GR activation. **a** Epigenetic clock CpGs co-localize with functional GREs. GRE peaks were derived from ENCODE *NR3C1* ChIP-seq data from lymphoblastoid cell lines. Among the 353 epigenetic clock CpGs, 85 CpG sites were noted to be located within GR ChIP-Seq peaks in a lymphoblastoid cell line (shown with the red dotted line) (Additional file 1: Table S1). This number significantly differed (p_{perm} <0.001) from the CpG-GRE overlap predicted by 1,000 randomly selected sets of CpGs covered by the 450 K array (mean 48.8, SD 6.14, range 31 to 68). **b** Epigenetic clock CpGs that are significantly regulated by DEX exposure are in proximity to GREs. GRE peaks were derived from ENCODE *NR3C1* ChIP-seq data from lymphoblastoid cell lines. Volcano plot was zoomed for +/− 10 kb distance around the GRE peaks. The dotted red line in the volcano plot represents the level of statistical significance ($P = 5 \times 10^{-2}$) after FDR correction for multiple comparisons. Further details on DEX-regulated CpGs are given in Additional file 1: Table S1

CpG-GRE co-localization differs from the one present in the 21 K background. Epigenetic clock CpG-GRE co-localization did not differ from the one expected by chance when randomly drawing 1,000 CpG sets (n = 353 CpGs) from the 21 K CpG sites (expected mean 3,094, SD 50.7, range 2,927–3,270, $p_{perm} = 9.7 \times 10^{-1}$). Given that this lack of enrichment could be the result of high CpG-GRE co-localization already present in the 21 K, as a last step we compared the co-localization present in the 21 K with the 450 K background and we noted significantly higher CpG-GRE co-localization in the 21 K as compared to the 450 K background ($p_{perm} < 1 \times 10^{-3}$). These findings suggest that the increased epigenetic clock CpG-GRE co-localization is a more general property of the 21 K CpGs used to develop the epigenetic clock. Yet the presence of a high number of epigenetic clock CpGs within functional GREs is in line with our hypothesis that these sites may be highly susceptible to GR activation.

We then assessed whether genes that have transcription start sites (TSS) in the proximity of epigenetic clock CpGs are also dynamically regulated by GR activation. For this purpose, we used peripheral blood genome-wide gene expression array data in the MPIP cohort to examine the DEX-induced changes in the expression of genes with transcription start sites (TSS) close to epigenetic clock CpGs based on the 450 K annotation from [43]. Using these criteria, we annotated 344 unique genes. Of these, 333 genes were present on the gene expression microarray and a total of 170 genes, corresponding to 220 epigenetic clock CpGs, were expressed above background in the MPIP cohort (Additional file 2: Table S2). Transcription of these genes was detected by 216 unique gene expression array probes. After FDR-based correction for multiple testing, 167 out of the 216 detected probes, corresponding to 139 unique genes (81.7 %), showed significant changes in gene expression following DEX exposure (FDR-adjusted *P* values <0.05) (Fig. 4).

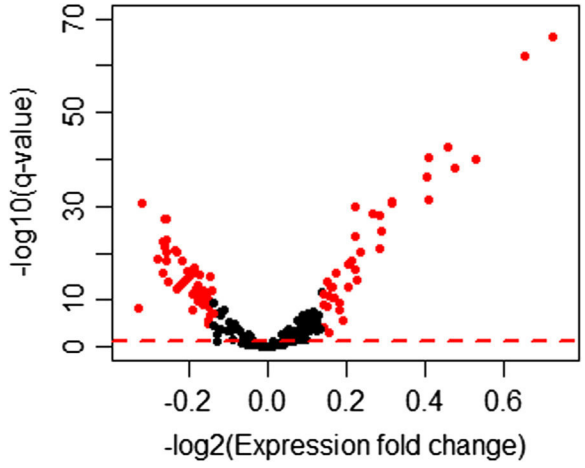

Fig. 4 Glucocorticoid receptor activation regulates the expression of genes with transcription start sites (TSS) near epigenetic clock CpGs. Gene TSS near epigenetic clock CpGs were identified based on the annotation from [43]. The volcano plot shows DEX-induced fold change in gene expression plotted against their corrected *P* values (q values). The dotted red line represents the corrected level of statistical significance ($q = 5 \times 10^{-2}$) after FDR correction for multiple comparisons. Among the 216 unique array probes, 167 probes, corresponding to 139 unique genes, showed significant changes in gene expression following DEX. Fifty-eight per cent of these probes (n = 97) showed upregulation and 42 % (n = 70) showed downregulation. The mean (SD, range) distance of each regulated gene TSS to the corresponding epigenetic clock CpGs was ±419.3 bp (336.65 bp, range 1 to 1,423 bp). Marked in red are the probes showing fold changes in gene expression >1.1. Further details are provided in Additional file 2: Table S2

Fifty-eight per cent of these probes (n = 97) showed upregulation and 42 % (n = 70) showed downregulation. The mean (SD, range) distance of each regulated gene TSS to the corresponding epigenetic clock CpGs was ±419.3 bp (336.65 bp, range 1 to 1,423 bp). To rule out potential bias derived from the 21 K background, we then asked whether genes neighboring epigenetic clock CpGs are more responsive to GR activation compared to genes neighboring the 21 K CpGs. A total of 5,443 unique genes, corresponding to 21,015 21 K CpGs, showed significant DEX-induced mRNA expression changes (FDR-adjusted P values $<5 \times 10^{-2}$). The number of DEX-regulated genes was significantly higher for the genes with TSS close to epigenetic clock CpGs as compared to 21 K CpGs (Fisher's exact test $P = 6.3 \times 10^{-5}$). Taken together, these data demonstrate enhanced responsivity of genes neighboring epigenetic clock CpGs to GR activation.

Lastly, we performed disease enrichment analysis in WebGestalt using the set of unique DEX-regulated genes (n = 139) as the input for the analysis and the genes expressed above background in our peripheral blood gene expression arrays as the reference set of genes. After FDR correction for multiple testing, this resulted in enriched association for aging-related diseases, including coronary artery disease, arteriosclerosis, and leukemias (FDR-adjusted P $<5 \times 10^{-2}$ each) (Additional file 3: Table S3).

Discussion

The present study sought to determine the effect of life stressors on epigenetic aging, as measured with the epigenetic clock [27] in peripheral blood samples. While previous studies found associations of the epigenetic clock with several phenotypes [27, 35–41], this is the first study to use this predictor in a highly traumatized cohort. As hypothesized, accelerated epigenetic aging was associated with cumulative lifetime stress burden. Given that epigenetic effects of the stress response can be mediated by GR signaling, we further examined the molecular basis of this association by annotating epigenetic clock CpG sites in relation to GREs and examining the impact of GR activation on these sites. We found that GREs co-localize with epigenetic clock CpGs and that glucocorticoid activation can induce dynamic methylation changes of these sites as well as changes in the expression of genes neighboring epigenetic clock CpGs. Taken together, these converging findings support a model of stress-induced accelerated epigenetic aging, plausibly mediated by the lasting effects of cumulative stressor exposure and aberrant glucocorticoid signaling on the epigenome.

Further examination of the relationship between life stress and epigenetic aging led us to several interesting observations. First, this relationship was apparent for cumulative stress exposure throughout the lifetime, whereas no significant association was found with childhood maltreatment or current stress alone. This finding is in accordance with a recent study observing no effect of childhood trauma on epigenetic aging in combat veterans [35] and suggests that cumulative stressors over the lifetime, rather than time-limited stressors either during childhood or adulthood, have a stronger or more lasting effect on epigenetic aging. Nonetheless, it is also possible that these null findings may be due to lack of power, the timing of DNA methylation assessments, or reversibility of epigenetic aging, possibilities that could be addressed by future longitudinal studies. Second, the effect of lifetime stress was driven by personal stressors – affecting the participant directly – rather than network stressors that occur to someone within the participant's network. This is congruent with previous studies showing that personal life events are more strongly correlated with genetic factors as compared to network events [44]. In line with the effects of lifetime vs. current stress, these effects were more pronounced in older individuals, suggesting cumulative epigenetic vulnerability in older individuals. Lastly, the epigenetic effects of lifetime stress were blunted in individuals with higher levels of childhood abuse. This finding could not be attributed to differences in the levels of lifetime stress, since individuals exposed to higher levels of childhood abuse also had higher levels of cumulative lifetime stress burden. Thus, it is possible that early trauma exposure triggers additional mechanisms of risk and resilience that may interfere with subsequent effects of stressors on epigenetic aging, a hypothesis that remains to be tested by future studies.

The effects of lifetime stress on epigenetic aging in peripheral blood are likely mediated by persistent neuroendocrine alterations induced by cumulative stress exposure. Stressors and glucocorticoids can drive persistent changes in the expression of glucocorticoid-responsive genes and concomitant changes in DNA methylation at CpGs located at or near GREs [17, 18, 22, 45]. Supporting this hypothesis, we noted that a high number of epigenetic clock CpG sites are located within functional GREs and show dynamic methylation changes following DEX exposure. Notably, most of these CpGs show DEX-induced decrease in methylation, whereas far fewer sites show increased methylation (98 vs. 12). This is in accordance with previous studies showing that activation of the GR results in local demethylation of CpGs in the proximity of a GRE [18, 22, 23] and that site-specific decreases in methylation have been implicated in aging-related phenotypes [46]. CpG demethylation has been proposed to be potentially mediated by at least two enzymatic processes, base excision repair and

oxidation [47, 48]. Examining the role of these processes may provide further insights into mechanisms of stress-induced epigenetic aging. Furthermore, an open question concerns the sequence of molecular events that determine whether some stress-induced DNA methylation changes become embedded and longlasting, while other changes are dynamic and reversible. Given the low dose and acute exposure to glucocorticoids in our study, additional experiments with different doses and more chronic *in vitro* or *in vivo* GR activation will be necessary to better elucidate this mechanism.

An important implication of our findings is the potential role of stress-induced epigenetic aging in health and disease. Increasing age and aging-related diseases have been associated with global and site-specific changes in DNA methylation [25–30, 39]. The age-related epigenetic clock CpGs co-localize with genes that show enrichment for cell growth and survival, organismal development, and cancer [27]. Furthermore, we show that DEX-regulated genes neighboring epigenetic clock CpGs show enriched association for aging-related diseases, including coronary artery disease, arteriosclerosis, and leukemias. These findings raise the possibility that lifetime stress may contribute to these diseases via its cumulative impact on epigenetic regulation of genes implicated in aging-related diseases.

The findings of the present study should be viewed in the context of its limitations. Although we observe an association between epigenetic age acceleration and lifetime stressors in the GTP cohort, the cross-sectional design of the study limits conclusions regarding the direction of causality. As discussed above, it is plausible that epigenetic aging of peripheral blood cells results from persistent alterations of the neuroendocrine but also immune milieu induced by repetitive stressor exposure. However, accelerated epigenetic aging might alternatively represent a vulnerability marker that predisposes individuals to expose themselves to stressful environments. It is also important to acknowledge that, while the high levels of traumatic events in the GTP make this cohort highly suitable for examining the effects of lifetime stress on the epigenome, they may also limit generalizability of these findings to other less traumatized cohorts. Moreover, the present study examined epigenetic aging in peripheral blood only. While this tissue is easily accessible and relevant for biomarker research, other tissues may be more susceptible to psychological stress and should be examined in the context of specific diseases. For example, disease-specific effects on the epigenetic clock have been demonstrated for liver tissue in the context of obesity [39]. Another limitation is the use of Chip-Seq data from lymphoblastoid cell lines to examine epigenetic clock CpG-GRE co-localization. This cell line represents the best available proxy for peripheral blood, the source tissue for our methylation data, but this approach may also be limited by the tissue specificity of functional GREs and the altered epigenetic landscapes of immortalized cell lines. Lastly, although we corrected for several confounders that might influence DNA methylation, such as sex, age, smoking, body mass index, substance abuse, current psychiatric symptoms and treatments, other factors not captured by our methods may have confounded the observed relationships. These limitations may be overcome in future studies by employing detailed prospective measurements of lifestyle factors, stressor exposure, DNA methylation, and incidence of stress-related phenotypes at different time points throughout the lifetime.

Conclusions

The present study provides evidence that cumulative life stress exposure is associated with accelerated epigenetic aging and that these effects may be mediated by glucocorticoid signaling. Our findings further suggest that DNA methylation-based age prediction in peripheral blood may be a useful molecular marker to incorporate in future studies examining the effects of life stress exposure. These findings offer novel insights into the molecular mechanisms linking psychological stress with diseases of the aging.

Methods

Clinical samples

The effect of lifetime stress on epigenetic aging was examined in the Grady Trauma Project (GTP), a large study conducted in Atlanta, Georgia, that investigates the role of genetic and environmental factors in shaping responses to stressful life events. The GTP includes more than 7,000 participants from a predominantly African American, urban population of low socioeconomic status [49, 50]. This population is characterized by high prevalence and severity of trauma over the lifetime and is thus particularly relevant for examining the effects of stressors on epigenetic markers. For this purpose, we used a subsample of GTP participants with genome-wide DNA methylation data. All participants provided written informed consent and all procedures were approved by the Institutional Review Boards of the Emory University School of Medicine and Grady Memorial Hospital (IRB00002114).

We examined glucocorticoid-induced methylation changes of epigenetic clock CpGs and responsivity of genes closest to these CpGs in 297 Caucasian participants recruited at the Max Planck Institute of Psychiatry (MPIP). Recruitment strategies and characterization of participants have been previously described [51, 52]. These consisted of 200 male (83 healthy probands and 117 inpatients with depressive disorders) and 97 female (48 healthy probands and 49 depressed) individuals. Baseline whole blood samples were obtained at 18:00 after 2 h

of fasting and abstention from coffee and physical activity (baseline). Participants then received 1.5 mg oral dexamethasone (DEX) and a second blood draw was performed at 21:00, 3 h after DEX ingestion (post-DEX). The study was approved by the local ethics committee (approval number: 318/00) and all individuals gave written informed consent. All experimental methods comply with the Helsinki Declaration.

Psychometric instruments

Childhood trauma was measured in the GTP with the Childhood Trauma Questionnaire (CTQ), a validated self-report questionnaire that assesses five types of maltreatment during childhood: sexual, physical, and emotional abuse, as well as emotional and physical neglect [53]. Scores for each type of maltreatment were derived from participant responses to questionnaire items and scores from all types were summed to yield a total CTQ score reflecting overall burden of childhood maltreatment. Moderate to extreme sexual abuse was defined by a cutoff score of 8 or above in the CTQ sexual abuse subscale, and moderate to extreme physical abuse was defined by a cutoff score of 10 or above in the physical abuse subscale as previously described [54].

Stressful lifetime events in the GTP were assessed with the Stressful Events Questionnaire (SEQ), a 39-item self-report instrument that has been described in detail [55]. The SEQ covers a wide range of stressor exposure, ranging from personal life events, such as divorce, unemployment, crime, and financial stressors, to network life events, such as knowing someone who was murdered. Participants report whether they have experienced these events either in the past year or at any time in their life. Although the SEQ assesses life event exposure throughout the lifetime, it does not include questions specific for childhood maltreatment. Life events are summed to yield a total score that reflects the number of stressors experienced over the last year (Current Stress) or cumulative number of stressors experienced throughout one's lifetime (Life Stress).

Participants underwent the Structured Clinical Interviews for DSM-IV defined psychiatric diagnoses. Given the observed relation between stress-related psychiatric disorders and accelerated cellular aging, we also examined major depression and PTSD as variables of interest. In the GTP, current depressive symptomatology was assessed with the 21-item validated Beck Depression Inventory (BDI) [56, 57] and current PTSD symptomatology was assessed with the validated 17-item PTSD Symptom Scale (PSS) [49, 58].

DNA methylation

Genomic DNA from the GTP cohort (n = 393) and the MPIP (n = 124) was extracted from whole blood using the Gentra Puregene Blood Kit (QIAGEN). DNA quality and quantity was assessed by NanoDrop 2000 Spectrophotometer (Thermo Scientific) and Quant-iT Picogreen (Invitrogen). Genomic DNA was bisulfite converted using the Zymo EZ-96 DNA Methylation Kit (Zymo Research) and DNA methylation levels were assessed for >480,000 CpG sites using the Illumina HumanMethylation450 BeadChip array. Hybridization and processing was performed according to manufacturer's instructions as previously described [59]. Quality control of methylation data, including intensity read outs, filtering (detection P value >0.01 in at least 75 % of the samples), cellular composition estimation, as well as beta and M-value calculation was done using the minfi Bioconductor R package version 1.10.2 [60].

For the GTP cohort, X chromosome, Y chromosome, and non-specific binding probes were removed [61]. We also excluded probes if single nucleotide polymorphisms (SNPs) were documented in the interval for which the Illumina probe is designed to hybridize. Given that the GTP cohort includes individuals from different ethnicities, we also removed probes if they were located close (10 bp from query site) to a SNP which had Minor Allele Frequency of ≥0.05, as reported in the 1,000 Genomes Project, for any of the populations represented in the samples. Technical batch effects were identified by inspecting the association of the first principal components of the methylation levels with plate, sentrix array, and position (row) and by further visual inspection of principal component plots using the shinyMethyl Bioconductor R package version 0.99.3 [62]. This procedure identified row and slide as technical batches. The raw methylation data and all related phenotypes for the GTP cohort have been deposited into NCBI GEO (GSE72680).

For the MPIP cohort, filtered beta values were reduced by eliminating any CpG sites/probes on sex chromosomes, as well as probes found to have SNPs at the CpG site itself or in the single-base extension site with a MAF ≥1 % in the 1,000 Genomes Project European population and/or non-specific binding probes according to [61]. Additionally, we performed a re-alignment of the array probe sequences using Bismark (doi: 10.1093/bioinformatics/btr167). This yielded a total of 425,883 CpG sites for further analysis. Using the same procedure for batch identification as above, we identified processing (experiment) date as technical batch in the MPIP. The data were then normalized with functional normalization [63], an extension of quantile normalization included in the minfi R package and batch-corrected using ComBat. The raw methylation data and all related phenotypes for the MPIP cohort have been deposited into NCBI GEO (GSE74414).

Gene expression

In the DEX-treated (MPIP) cohort (n = 297, including the 124 individuals used for the MPIP methylation analysis), both baseline and post-DEX whole blood RNA was collected using PAXgene Blood RNA Tubes (PreAnalytiX), processed as described previously [51, 52]. Samples had a mean RNA integrity number (RIN) of 8 ± 0.51 SD. Blood RNA was hybridized to Illumina HumanHT-12 v3 and v4 Expression BeadChips (Illumina, San Diego, CA, USA). Raw probe intensities were exported using Illumina's GenomeStudio and further statistical processing was carried out using R. All 29,075 probes present on both microarrays, excluding X and Y chromosomes as well as cross-hybridizing probes identified by using the Re-Annotator pipeline (http://dx.doi.org/10.1101/019596) were first filtered with an Illumina detection *P* value of 0.05 in at least 50 % of the samples, leaving 11,994 expressed probes for further analysis. Subsequently, each transcript was transformed and normalized through variance stabilization and normalization (VSN) [64]. Using the same procedure for batch identification as for the methylation data, we identified slide, amplification round, array version, and amplification plate column as technical batches. The data were then adjusted using ComBat [65] and have been deposited into NCBI GEO (GSE64930).

Statistical analyses

All statistical analyses were conducted in R version 3.1.0 (http://www.r-project.org/) [66]. Unless indicated otherwise, *P* values are nominal and two-tailed. All corrections for multiple testing were performed using the FDR method of Benjamini and Hochberg. The level of statistical significance was set a priori at 0.05 (5×10^{-2}).

DNA methylation-based age prediction was performed using the R code and statistical pipeline developed by Horvath [27]. This predictor was developed using 82 Illumina DNA methylation array datasets (n = 7,844) involving 51 healthy tissues and cell types [27]. The raw data were normalized using BMIQ normalization method [67] implemented in the Horvath DNA methylation-based age predictor R script [27]. Robustness and reproducibility of the epigenetic age predictor was tested using 40× technical replicates of an individual control sample, randomized across microarray chips and batches used to measure DNA methylation in the GTP cohort. The average epigenetic age (DNAM-age) of the control sample (true age = 32 years) was 32.64 (SD: 0.23) years with an average correlation $r = 0.97$ (0.001). Age acceleration (Δ-age) was defined (as previously) as the average difference between DNAM-age and chronological age. One GTP participant had extreme Δ-age (43.98 years), and using the Grubbs' test (http://graphpad.com/quickcalcs/grubbs2/) was noted to be the only outlier ($Z = 3.80$, $P < 5 \times 10^{-2}$). Although primary analyses were conducted without this outlier, inclusion of this individual did not substantially alter the reported results. Generalized linear regression models tested the relationship of Δ-age with stressors and stress-related phenotypes (GTP cohort). Because DNAM-age is calculated from raw beta values (before Combat correction for batches), technical batches identified for the GTP (row and slide) and the MPIP cohort (processing date) were tested as potential confounders in the respective regression models. In the GTP, models were further adjusted for age, sex, Houseman cell counts, body mass index, smoking, alcohol, current substance abuse, and the principal components from population stratification checks. In the MPIP, models were adjusted for gender, age, body mass index, and Houseman cell counts.

To determine if methylation signals or gene expression levels are significantly different before and after DEX stimulation in the MPIP cohort, likelihood ratio tests accounting for gender, age, body mass index, disease status, and estimated cell-type counts were applied to each CpG site (n = 353) and expression array probe (n = 11,994), respectively. DNA methylation and gene expression changes were corrected for multiple comparisons using FDR. The 353 epigenetic clock CpGs were annotated to a total of 344 genes. Among these, 170 genes were detected in peripheral blood by 216 gene expression array probes (163 genes were expressed below background and 11 genes were not covered by the gene expression arrays).

To account for population stratification due to discrepancies between self-reported and actual race in the GTP, we used genome-wide SNP data that were available for 382 participants. Of the 700 k SNPs present on the Omni Quad and Omni express arrays, 645,8315 autosomal SNPs were left after filtering with the following criteria: minor allele frequency of >1 %; Hardy-Weinberg equilibrium of 0.000001; and genotyping rate of >98 %. The samples were clustered to calculate rates of identity by descent (IBD). We then ran multidimensional scaling analysis on the IBD matrix using PLINK2 (https://www.cog-genomics.org/plink2) and plotted the first ten axes of variation against each other. No outliers were detected. The first two principal components were used as covariates in regression models to adjust for population stratification.

To identify whether epigenetic clock CpG sites are co-localized with GREs, we used ENCODE *NR3C1* ChIP-Seq data from lymphoblastoid cell lines (*accession: ENCSR904YPP*) for which no aligned tracks are currently available. Initial filtering was performed using FASTX Toolkit (v. 0.0.14, http://hannonlab.cshl.edu/fastx_toolkit/index.html) and Prinseq (v. 0.20.3) [68] to eliminate artefacts and low quality reads. Alignment on

hg19 was performed using BWA (v. 0.7.10) [69] allowing only uniquely mappable alignments with an alignment quality of above 20. Reads from both ChIP-Seq and both control libraries were pooled leading to 46,453,650 and 68,227,580 used reads, respectively. Peak-calling was carried out by MACS14 (v. 1.4.2) [70] using default settings, resulting in approximately 23,000 annotated signals. The average length of ChIP-Seq signal as defined by the peak calling was 746.3 bps (SD: 370.6). We generated 1,000 sets (n = 353 CpGs) of randomly drawn CpG sites (without replacement) from the set of all CpGs present on the 450 K BeadChip array (excluding X and Y chromosomes). For every set we counted the percentage of CpG sites within a GRE ChIP-Seq signal (+/− 0 bp). On this basis we constructed the null distribution and compared it to the observed percentage of clock CpG sites within a GRE ChIP-Seq signal to measure the enrichment statistics.

Disease enrichment analysis was performed using the WEB-based GEne SeT AnaLysis Toolkit (WebGestalt; http://bioinfo.vanderbilt.edu/webgestalt/) [71, 72]. This was performed by using as input the set of unique DEX-regulated genes neighboring epigenetic clock CpGs (n = 139) and as reference the set of genes expressed above background in our peripheral blood gene expression arrays. The minimum number of genes for the enrichment analysis was set at 5, the statistic performed was hypergeometric test, and results were corrected for multiple testing using FDR.

Additional files

Additional file 1: Table S1. Location of epigenetic clock CpGs in relation to the nearest glucocorticoid response element (as shown by within GR ChIP-Seq peaks in a lymphoblastoid cell line) and their methylation changes in response to the glucocorticoid receptor agonist dexamethasone. (DEX). (XLSX 68 kb)

Additional file 2: Table S2. Annotation of genes with transcription start sites (TSS) near epigenetic clock CpGs and their expression changes in response to DEX. Gene annotation was based on [43]. (XLSX 26 kb)

Additional file 3: Table S3. WebGestalt Disease enrichment analysis of the set of unique DEX-regulated genes (n = 139) with TSS near epigenetic clock CpGs. For the primary analysis, we used as reference the set of genes expressed above background in our peripheral blood gene expression arrays. This analysis was repeated using a more condensed background comprised only of the genes neighboring 21 K CpGs that showed DEX-induced mRNA expression changes (n = 5,443). While this post-hoc analysis yielded no statistically significant results after correction for multiple testing (*P* values presented in the last column), the top 10 diseases were very similar (with higher but nominally significant *P* values for the top three hits) with the analysis using the broader reference set of genes. (XLSX 10 kb)

Competing interests
The authors declare no competing interests.

Authors' contributions
ASZ, EBB, and DM conceived and designed the study. TCR, JA, and SI were involved in the DNA methylation analyses. JA, SR, and AM analyzed the DEX-treated sample. JA and SR performed the GRE enrichment analysis. KJR, AKS, BB, JFL, MI, TB, AE, CBH, and CH contributed the clinical samples. ASZ performed the statistical analyses with substantial input from JA, TCR, NRW, and DM. ASZ performed the disease enrichment analysis with input from JA, EBB, and DM. ASZ wrote the manuscript with input from EBB and DM. All authors read and approved the final manuscript.

Acknowledgements
This work was supported by a European Research Council starting grant (grant# 281338, GxE molmech) within the FP7 framework to E.B.B., a Marie-Sklodowska Curie fellowship (H2020 grant# 653240) to ASZ, a grant from the National Alliance for Research in Schizophrenia and Affective Disorders and a grant from the Behrens Weise Stiftung to EBB, a grant from the National Institute of Mental Health (MH071538) to KJR, a grant from the National Institute of Mental Health (MH58922) to CBN, a grant by the German Federal Ministry of Education and Research (BMBF) through the Integrated Network IntegraMent (Integrated Understanding of Causes and Mechanisms in Mental Disorders), under the auspices of the e:Med Programme (grant # 01ZX1314J to EB), and a grant from ERA-NET Neuron to AE. DM is supported by a grant from the National Health and Medical Research Council (1047956). CH is supported in part by Public Health Service Grant UL1 RR025008 from the Clinical and Translational Science Award program, the US National Institutes of Health, the National Center for Research Resources, and by a K Award (K01 MH073698–01, Neural Substrates of Depression Risk after Child Abuse). CBN is supported by the National Institute of Health, the American Psychiatric Publishing, Xhale, and Clintara; has been consulting for Xhale, Takeda, SK Pharma, Shire, Roche, Lilly, Allergan, Mitsubishi Tanabe Pharma Development America, Taisho Pharmaceutical Inc., Lundbeck, Prismic Pharmaceuticals, Clintara LLC, Total Pain Solutions (TPS); is a stockholder of Xhale, Celgene, Seattle Genetics, Abbvie, Titan Pharmaceuticals; is in the scientific advisory board of American Foundation for Suicide Prevention (AFSP), Brain and Behavior Research Foundation (BBRF) (formerly named National Alliance for Research on Schizophrenia and Depression [NARSAD]), Xhale, Anxiety Disorders Association of America (ADAA), Skyland Trail, Clintara LLC, RiverMend Health LLC; is in the board of directors of AFSP, Gratitude America, ADAA; and holds patents of Method and devices for transdermal delivery of lithium (US 6,375,990B1) and Method of assessing antidepressant drug therapy via transport inhibition of monoamine neurotransmitters by ex vivo assay (US 7,148,027B2).

Author details
[1]Department of Translational Research in Psychiatry, Max Planck Institute of Psychiatry, Munich, Germany. [2]Department of Psychiatry and Behavioral Sciences, Duke University Medical Center, Durham, NC, USA. [3]Institute of Computational Biology, Helmholtz Zentrum München, Neuherberg, Germany. [4]Department of Psychiatry and Behavioral Sciences, Emory University Medical School, Atlanta, GA, USA. [5]Howard Hughes Medical Institute, Chevy Chase, MD, USA. [6]Yerkes National Primate Research Center, Emory University, Atlanta, GA, USA. [7]Department of Psychiatry and Behavioral Sciences and the Center on Aging, University of Miami Miller School of Medicine, Miami, FL, USA. [8]Atlanta Veterans Affairs Medical Center, Decatur, GA, USA. [9]Institute of Medical Psychology, Charité Universitätsmedizin Berlin, Berlin, Germany. [10]Current Address: Department of Psychiatry, Psychosomatics, and Psychotherapy, University of Wuerzburg, Wuerzburg, Germany. [11]Max Planck Institute of Psychiatry, Munich, Germany. [12]The University of Queensland, Queensland Brain Institute, St Lucia Qld 4072, Australia. [13]Department of Biobehavioral Health, Pennsylvania State University, University Park, PA, USA.

Received: 20 July 2015 Accepted: 10 November 2015
Published online: 17 December 2015

References
1. Centers for Disease Control and Prevention. The State of Aging and Health in America 2013. Atlanta, GA: Centers for Disease Control and Prevention; 2013.
2. Office for National Statistics. National Population Projections, 2012-based Statistical Bulletin. Newport: Office for National Statistics; 2012.
3. Niccoli T, Partridge L. Ageing as a risk factor for disease. Curr Biol. 2012;22:R741–52.
4. Karatsoreos IN, McEwen BS. Psychobiological allostasis: resistance, resilience and vulnerability. Trends Cogn Sci. 2011;15:576–84.

5. Epel ES, Blackburn EH, Lin J, Dhabhar FS, Adler NE, Morrow JD, et al. Accelerated telomere shortening in response to life stress. Proc Natl Acad Sci U S A. 2004;101:17312–5.
6. Epel ES, Lin J, Wilhelm FH, Wolkowitz OM, Cawthon R, Adler NE, et al. Cell aging in relation to stress arousal and cardiovascular disease risk factors. Psychoneuroendocrinology. 2006;31:277–87.
7. Chandola T, Brunner E, Marmot M. Chronic stress at work and the metabolic syndrome: prospective study. BMJ. 2006;332:521–5.
8. Rozanski A, Blumenthal JA, Kaplan J. Impact of psychological factors on the pathogenesis of cardiovascular disease and implications for therapy. Circulation. 1999;99:2192–217.
9. Powell ND, Allen RG, Hufnagle AR, Sheridan JF, Bailey MT. Stressor-induced alterations of adaptive immunity to vaccination and viral pathogens. Immunol Allergy Clin North Am. 2011;31:69–79.
10. Powell ND, Tarr AJ, Sheridan JF. Psychosocial stress and inflammation in cancer. Brain Behav Immun. 2013;30(Suppl):S41–7.
11. Zannas AS, McQuoid DR, Steffens DC, Chrousos GP, Taylor WD. Stressful life events, perceived stress, and 12-month course of geriatric depression: direct effects and moderation by the 5-HTTLPR and COMT Val158Met polymorphisms. Stress. 2012;15:425–34.
12. Peavy GM, Salmon DP, Jacobson MW, Hervey A, Gamst AC, Wolfson T, et al. Effects of chronic stress on memory decline in cognitively normal and mildly impaired older adults. Am J Psychiatry. 2009;166:1384–91.
13. Danese A, McEwen BS. Adverse childhood experiences, allostasis, allostatic load, and age-related disease. Physiol Behav. 2012;106:29–39.
14. Felitti VJ, Anda RF, Nordenberg D, Williamson DF, Spitz AM, Edwards V, et al. Relationship of childhood abuse and household dysfunction to many of the leading causes of death in adults. The Adverse Childhood Experiences (ACE) Study. Am J Prev Med. 1998;14:245–58.
15. Danese A, Moffitt TE, Pariante CM, Ambler A, Poulton R, Caspi A. Elevated inflammation levels in depressed adults with a history of childhood maltreatment. Arch Gen Psychiatry. 2008;65:409–15.
16. Vaccarino V, Goldberg J, Rooks C, Shah AJ, Veledar E, Faber TL, et al. Post-traumatic stress disorder and incidence of coronary heart disease: a twin study. J Am Coll Cardiol. 2013;62:970–8.
17. Zannas AS, West AE. Epigenetics and the regulation of stress vulnerability and resilience. Neuroscience. 2014;264:157–70.
18. Klengel T, Mehta D, Anacker C, Rex-Haffner M, Pruessner JC, Pariante CM, et al. Allele-specific FKBP5 DNA demethylation mediates gene-childhood trauma interactions. Nat Neurosci. 2013;16:33–41.
19. Weaver IC, Cervoni N, Champagne FA, D'Alessio AC, Sharma S, Seckl JR, et al. Epigenetic programming by maternal behavior. Nat Neurosci. 2004;7:847–54.
20. Chrousos GP, Gold PW. The concepts of stress and stress system disorders. Overview of physical and behavioral homeostasis. JAMA. 1992;267:1244–52.
21. Bamberger CM, Schulte HM, Chrousos GP. Molecular determinants of glucocorticoid receptor function and tissue sensitivity to glucocorticoids. Endocr Rev. 1996;17:245–61.
22. Thomassin H, Flavin M, Espinas ML, Grange T. Glucocorticoid-induced DNA demethylation and gene memory during development. EMBO J. 2001;20:1974–83.
23. Wiench M, John S, Baek S, Johnson TA, Sung MH, Escobar T, et al. DNA methylation status predicts cell type-specific enhancer activity. EMBO J. 2011;30:3028–39.
24. Wiench M, Miranda TB, Hager GL. Control of nuclear receptor function by local chromatin structure. FEBS J. 2011;278:2211–30.
25. Heyn H, Li N, Ferreira HJ, Moran S, Pisano DG, Gomez A, et al. Distinct DNA methylomes of newborns and centenarians. Proc Natl Acad Sci U S A. 2012;109:10522–7.
26. Bjornsson HT, Sigurdsson MI, Fallin MD, Irizarry RA, Aspelund T, Cui H, et al. Intra-individual change over time in DNA methylation with familial clustering. JAMA. 2008;299:2877–83.
27. Horvath S. DNA methylation age of human tissues and cell types. Genome Biol. 2013;14:R115.
28. Christensen BC, Houseman EA, Marsit CJ, Zheng S, Wrensch MR, Wiemels JL, et al. Aging and environmental exposures alter tissue-specific DNA methylation dependent upon CpG island context. PLoS Genet. 2009;5:e1000602.
29. Hernandez DG, Nalls MA, Gibbs JR, Arepalli S, van der Brug M, Chong S, et al. Distinct DNA methylation changes highly correlated with chronological age in the human brain. Hum Mol Genet. 2011;20:1164–72.
30. Rakyan VK, Down TA, Maslau S, Andrew T, Yang TP, Beyan H, et al. Human aging-associated DNA hypermethylation occurs preferentially at bivalent chromatin domains. Genome Res. 2010;20:434–9.
31. Horvath S, Zhang Y, Langfelder P, Kahn RS, Boks MP, van Eijk K, et al. Aging effects on DNA methylation modules in human brain and blood tissue. Genome Biol. 2012;13:R97.
32. Hannum G, Guinney J, Zhao L, Zhang L, Hughes G, Sadda S, et al. Genome-wide methylation profiles reveal quantitative views of human aging rates. Mol Cell. 2013;49:359–67.
33. Weidner CI, Lin Q, Koch CM, Eisele L, Beier F, Ziegler P, et al. Aging of blood can be tracked by DNA methylation changes at just three CpG sites. Genome Biol. 2014;15:R24.
34. Bocklandt S, Lin W, Sehl ME, Sanchez FJ, Sinsheimer JS, Horvath S, et al. Epigenetic predictor of age. PLoS One. 2011;6:e14821.
35. Boks MP, Mierlo HC, Rutten BP, Radstake TR, De Witte L, Geuze E, et al. Longitudinal changes of telomere length and epigenetic age related to traumatic stress and post-traumatic stress disorder. Psychoneuroendocrinology. 2015;51:506–12.
36. Marioni RE, Shah S, McRae AF, Chen BH, Colicino E, Harris SE, et al. DNA methylation age of blood predicts all-cause mortality in later life. Genome Biol. 2015;16:25.
37. Marioni RE, Shah S, McRae AF, Ritchie SJ, Muniz-Terrera G, Harris SE, et al. The epigenetic clock is correlated with physical and cognitive fitness in the Lothian Birth Cohort 1936. Int J Epidemiol. 2015;44:1388–96.
38. Horvath S, Garagnani P, Bacalini MG, Pirazzini C, Salvioli S, Gentilini D, et al. Accelerated epigenetic aging in Down syndrome. Aging Cell. 2015;14:491–5.
39. Horvath S, Erhart W, Brosch M, Ammerpohl O, von Schonfels W, Ahrens M, et al. Obesity accelerates epigenetic aging of human liver. Proc Natl Acad Sci U S A. 2014;111:15538–43.
40. Miller GE, Yu T, Chen E, Brody GH. Self-control forecasts better psychosocial outcomes but faster epigenetic aging in low-SES youth. Proc Natl Acad Sci U S A. 2015;112:10325–30.
41. Kananen L, Nevalainen T, Jylhava J, Marttila S, Hervonen A, Jylha M, et al. Cytomegalovirus infection accelerates epigenetic aging. Exp Gerontol. 2015;72:227–9.
42. Kendler KS, Karkowski LM, Prescott CA. Causal relationship between stressful life events and the onset of major depression. Am J Psychiatry. 1999;156:837–41.
43. Price ME, Cotton AM, Lam LL, Farre P, Emberly E, Brown CJ, et al. Additional annotation enhances potential for biologically-relevant analysis of the Illumina Infinium HumanMethylation450 BeadChip array. Epigenetics Chromatin. 2013;6:4.
44. Bolinskey PK, Neale MC, Jacobson KC, Prescott CA, Kendler KS. Sources of individual differences in stressful life event exposure in male and female twins. Twin Res. 2004;7:33–8.
45. Lee RS, Tamashiro KL, Yang X, Purcell RH, Harvey A, Willour VL, et al. Chronic corticosterone exposure increases expression and decreases deoxyribonucleic acid methylation of Fkbp5 in mice. Endocrinology. 2010;151:4332–43.
46. Vandiver AR, Irizarry RA, Hansen KD, Garza LA, Runarsson A, Li X, et al. Age and sun exposure-related widespread genomic blocks of hypomethylation in nonmalignant skin. Genome Biol. 2015;16:80.
47. Niehrs C, Schafer A. Active DNA demethylation by Gadd45 and DNA repair. Trends Cell Biol. 2012;22:220–7.
48. Pastor WA, Aravind L, Rao A. TETonic shift: biological roles of TET proteins in DNA demethylation and transcription. Nat Rev Mol Cell Biol. 2013;14:341–56.
49. Binder EB, Bradley RG, Liu W, Epstein MP, Deveau TC, Mercer KB, et al. Association of FKBP5 polymorphisms and childhood abuse with risk of posttraumatic stress disorder symptoms in adults. JAMA. 2008;299:1291–305.
50. Gillespie CF, Bradley B, Mercer K, Smith AK, Conneely K, Gapen M, et al. Trauma exposure and stress-related disorders in inner city primary care patients. Gen Hosp Psychiatry. 2009;31:505–14.
51. Menke A, Arloth J, Putz B, Weber P, Klengel T, Mehta D, et al. Dexamethasone stimulated gene expression in peripheral blood is a sensitive marker for glucocorticoid receptor resistance in depressed patients. Neuropsychopharmacology. 2012;37:1455–64.
52. Arloth J, Bogdan R, Weber P, Frishman G, Menke A, Wagner KV, et al. Genetic differences in the immediate transcriptome response to stress predict risk-related brain function and psychiatric disorders. Neuron. 2015;86:1189–202.

53. Bernstein DP, Stein JA, Newcomb MD, Walker E, Pogge D, Ahluvalia T, et al. Development and validation of a brief screening version of the Childhood Trauma Questionnaire. Child Abuse Negl. 2003;27:169–90.
54. DiLillo D, Fortier MA, Hayes SA, Trask E, Perry AR, Messman-Moore T, et al. Retrospective assessment of childhood sexual and physical abuse: a comparison of scaled and behaviorally specific approaches. Assessment. 2006;13:297–312.
55. Smith AK, Conneely KN, Kilaru V, Mercer KB, Weiss TE, Bradley B, et al. Differential immune system DNA methylation and cytokine regulation in post-traumatic stress disorder. Am J Med Genet B Neuropsychiatr Genet. 2011;156B:700–8.
56. Beck AT, Steer RA, Garbin MG. Psychometric Properties of the Beck Depression Inventory - 25 Years of Evaluation. Clinical Psychology Review. 1988;8:77–100.
57. Beck AT, Ward CH, Mendelson M, Mock J, Erbaugh J. An inventory for measuring depression. Arch Gen Psychiatry. 1961;4:561–71.
58. Coffey SF, Dansky BS, Falsetti SA, Saladin ME, Brady KT. Screening for PTSD in a substance abuse sample: psychometric properties of a modified version of the PTSD Symptom Scale Self-Report. Posttraumatic stress disorder. J Trauma Stress. 1998;11:393–9.
59. Mehta D, Klengel T, Conneely KN, Smith AK, Altmann A, Pace TW, et al. Childhood maltreatment is associated with distinct genomic and epigenetic profiles in posttraumatic stress disorder. Proc Natl Acad Sci U S A. 2013;110:8302–7.
60. Aryee MJ, Jaffe AE, Corrada-Bravo H, Ladd-Acosta C, Feinberg AP, Hansen KD, et al. Minfi: a flexible and comprehensive Bioconductor package for the analysis of Infinium DNA methylation microarrays. Bioinformatics. 2014;30:1363–9.
61. Chen YA, Lemire M, Choufani S, Butcher DT, Grafodatskaya D, Zanke BW, et al. Discovery of cross-reactive probes and polymorphic CpGs in the Illumina Infinium HumanMethylation450 microarray. Epigenetics. 2013;8:203–9.
62. Fortin JP, Fertig E, Hansen K. shinyMethyl: interactive quality control of Illumina 450k DNA methylation arrays in R. F1000Res. 2014;3:175.
63. Fortin JP, Labbe A, Lemire M, Zanke BW, Hudson TJ, Fertig EJ, et al. Functional normalization of 450 k methylation array data improves replication in large cancer studies. Genome Biol. 2014;15:503.
64. Lin SM, Du P, Huber W, Kibbe WA. Model-based variance-stabilizing transformation for Illumina microarray data. Nucleic Acids Res. 2008;36:e11.
65. Johnson WE, Li C, Rabinovic A. Adjusting batch effects in microarray expression data using empirical Bayes methods. Biostatistics. 2007;8:118–27.
66. R Development Core Team. A Language and Environment for Statistical Computing. Vienna: R Foundation for Statistical Computing; 2014.
67. Teschendorff AE, Marabita F, Lechner M, Bartlett T, Tegner J, Gomez-Cabrero D, et al. A beta-mixture quantile normalization method for correcting probe design bias in Illumina Infinium 450 k DNA methylation data. Bioinformatics. 2013;29:189–96.
68. Schmieder R, Edwards R. Quality control and preprocessing of metagenomic datasets. Bioinformatics. 2011;27:863–4.
69. Li H, Durbin R. Fast and accurate short read alignment with Burrows-Wheeler transform. Bioinformatics. 2009;25:1754–60.
70. Zhang Y, Liu T, Meyer CA, Eeckhoute J, Johnson DS, Bernstein BE, et al. Model-based analysis of ChIP-Seq (MACS). Genome Biol. 2008;9:R137.
71. Wang J, Duncan D, Shi Z, Zhang B. WEB-based GEne SeT AnaLysis Toolkit (WebGestalt): update 2013. Nucleic Acids Res. 2013;41:W77–83.
72. Zhang B, Kirov S, Snoddy J. WebGestalt: an integrated system for exploring gene sets in various biological contexts. Nucleic Acids Res. 2005;33:W741–8.

NEUROSCIENCE

Chaperoning epigenetics: FKBP51 decreases the activity of DNMT1 and mediates epigenetic effects of the antidepressant paroxetine

Nils C. Gassen,[1*†] Gabriel R. Fries,[1,2†] Anthony S. Zannas,[1,3] Jakob Hartmann,[4] Jürgen Zschocke,[1] Kathrin Hafner,[1] Tania Carrillo-Roa,[1] Jessica Steinbacher,[5] S. Nicole Preißinger,[1] Lianne Hoeijmakers,[4] Matthias Knop,[6] Frank Weber,[6] Stefan Kloiber,[6] Susanne Lucae,[6] George P. Chrousos,[7] Thomas Carell,[5] Marcus Ising,[6] Elisabeth B. Binder,[1,8] Mathias V. Schmidt,[4] Joëlle Rüegg,[9] Theo Rein[1*]

Epigenetic processes, such as DNA methylation, and molecular chaperones, including FK506-binding protein 51 (FKBP51), are independently implicated in stress-related mental disorders and antidepressant drug action. FKBP51 associates with cyclin-dependent kinase 5 (CDK5), which is one of several kinases that phosphorylates and activates DNA methyltransferase 1 (DNMT1). We searched for a functional link between FKBP51 (encoded by *FKBP5*) and DNMT1 in cells from mice and humans, including those from depressed patients, and found that FKBP51 competed with its close homolog FKBP52 for association with CDK5. In human embryonic kidney (HEK) 293 cells, expression of FKBP51 displaced FKBP52 from CDK5, decreased the interaction of CDK5 with DNMT1, reduced the phosphorylation and enzymatic activity of DNMT1, and diminished global DNA methylation. In mouse embryonic fibroblasts and primary mouse astrocytes, FKBP51 mediated several effects of paroxetine, namely, decreased the protein-protein interactions of DNMT1 with CDK5 and FKBP52, reduced phosphorylation of DNMT1, and decreased the methylation and increased the expression of the gene encoding brain-derived neurotrophic factor (*Bdnf*). In human peripheral blood cells, *FKBP5* expression inversely correlated with both global and *BDNF* methylation. Peripheral blood cells isolated from depressed patients that were then treated ex vivo with paroxetine revealed that the abundance of BDNF positively correlated and phosphorylated DNMT1 inversely correlated with that of FKBP51 in cells and with clinical treatment success in patients, supporting the relevance of this FKBP51-directed pathway that prevents epigenetic suppression of gene expression.

INTRODUCTION

Environmental factors and their influence on gene expression are recognized as key players in several psychiatric diseases, including major depressive disorder (MDD) (*1*–*3*). Although yet unclear, it is proposed that these environmental effects are mediated by epigenetic changes, such as methylation and demethylation of DNA and posttranslational modifications of histones. Such epigenetic marks control the accessibility of transcriptional machinery to the DNA and are responsive to both environmental stressors and to genetic variations. Whereas histone modifications occur at various sites and involve the action of various enzymes, DNA methylation is largely confined to CpG dinucleotides in the mammalian genome and is executed by DNA methyltransferases (DNMTs) (*4*), which comprise a family of proteins with three subtypes that exhibit different specificities and functions: DNMT1, DNMT3a, and DNMT3b (*5*).

Epigenetic mechanisms are considered not only crucial in shaping the phenotype of complex psychiatric disorders but also important for the response to certain medications (*6*–*9*). For instance, some antidepressants can reduce DNMT1 activity (*10*), the major DNMT ensuring the maintenance DNA methylation during S phase that has also been implicated in de novo methylation (*11*, *12*); this effect of antidepressants appears to be partly due to the reduction of the amounts of the histone methyltransferase G9a (*13*). Furthermore, DNMT inhibitors applied either systemically or locally in the hippocampus induce antidepressant-like effects in mice, which are accompanied by increased expression of the gene encoding brain-derived neurotrophic factor (BDNF) (*14*). Epigenetic regulation of BDNF is implicated in the development and treatment of psychiatric diseases in several studies (*9*, *15*–*17*).

The activity of DNMT1 is modulated by several interacting proteins and by posttranslational modifications (*18*, *19*), including phosphorylation (*20*–*22*). Among the phosphorylated sites of DNMT1 is Ser^{154}, which is targeted by cyclin-dependent kinases (CDKs), such as CDK5, and increases DNMT1 activity (*23*). Thus, several mechanisms might be considered for the antidepressant-induced effects on DNMT1.

Psychological stress and trauma are consistently associated with MDD (*1*). The glucocorticoid receptor (GR) is integral to the stress response and is controlled by a complex of chaperones and cochaperones (*24*). The

[1]Department of Translational Research in Psychiatry, Max Planck Institute of Psychiatry, 80804 Munich, Germany. [2]Department of Psychiatry and Behavioral Sciences, University of Texas Health Science Center, Houston, TX 77054, USA. [3]Department of Psychiatry and Behavioral Sciences, Duke University Medical Center, Durham, NC 27710, USA. [4]Department of Stress Neurobiology and Neurogenetics, Max Planck Institute of Psychiatry, 80804 Munich, Germany. [5]Department of Organic Chemistry, Faculty of Chemistry and Pharmacy, Ludwig Maximilians University, 81377 Munich, Germany. [6]Department of Clinical Research, Max Planck Institute of Psychiatry, 80804 Munich, Germany. [7]First Department of Pediatrics, University of Athens Medical School, Athens 11527, Greece. [8]Department of Psychiatry and Behavioral Sciences, Emory University, Atlanta, GA 30329, USA. [9]Department of Clinical Neuroscience, Center for Molecular Medicine, Karolinska Institutet, 171 76 Stockholm, Sweden and Swedish Toxicology Science Research Center, Swetox, 151 36 Södertälje, Sweden.
*Corresponding author. E-mail: ncgassen@psych.mpg.de (N.C.G.); theorein@psych.mpg.de (T.R.)
†First co-authors.

cochaperones FK506-binding protein 51 (FKBP51) and FKBP52 are major determinants of GR activity by competing with each other for access to the GR-chaperone heterocomplex and by exerting opposing effects on GR function with FKBP52-promoting and FKBP51-inhibiting GR activity (*25*–*27*). Conversely, FKBP51 abundance increases after GR activation (*28*–*30*). Notably, FKBP51 has been linked genetically to the response to antidepressants, and enhanced abundance of FKBP51 is associated with improved treatment response (*31*–*36*). In addition, FKBP51 and FKBP52 interact with several proteins including CDK5 (*36*, *37*). Therefore, we aimed to explore potential mechanisms by which the stress-related cochaperones FKBP51 and FKBP52 modulate DNMT1 phosphorylation and activity and whether this might contribute to the clinical response to antidepressant treatment in patients with MDD.

RESULTS

FKBP51 and FKBP52 were differentially associated with DNMT1 and modulate its phosphorylation and activity

Previously, we found that CDK5 formed a protein complex with FKBP51 or FKBP52 (*36*). Because CDK5 has been reported to regulate DNMT1 by phosphorylation at Ser^{154} (*23*), we investigated whether FKBP51 and FKBP52 modulate CDK5's action on DNMT1. We initially tested for associations between CDK5 and DNMT1 with ectopic FLAG-tagged FKBP51 or FKBP52 in human embryonic kidney (HEK) 293 cells by co-immunoprecipitation. Both FKBP51 and FKBP52 were associated with CDK5 (Fig. 1A), consistent with our previous results (*36*); however, only FKBP52 was associated with DNMT1 (Fig. 1B). Coexpressing both FKBPs revealed that they compete with each other for binding to CDK5 (Fig. 1C). Notably, coexpression of FKBP51 also reduced the interaction between FKBP52 and DNMT1 (Fig. 1C).

Because FKBP51 and FKBP52 are cochaperones of heat shock protein 90 (Hsp90) (*25*) and Hsp90 interacts with both CDK5 and DNMT1 (*38*, *39*), we explored the possibility that Hsp90 function might be important for complex assembly. We exposed HEK293 cells to increasing concentrations of 17-AAG, an Hsp90 inhibitor and geldanamycin derivative, immunoprecipitated CDK5, and probed for the interaction with Hsp90 and DNMT1. There was no significant effect

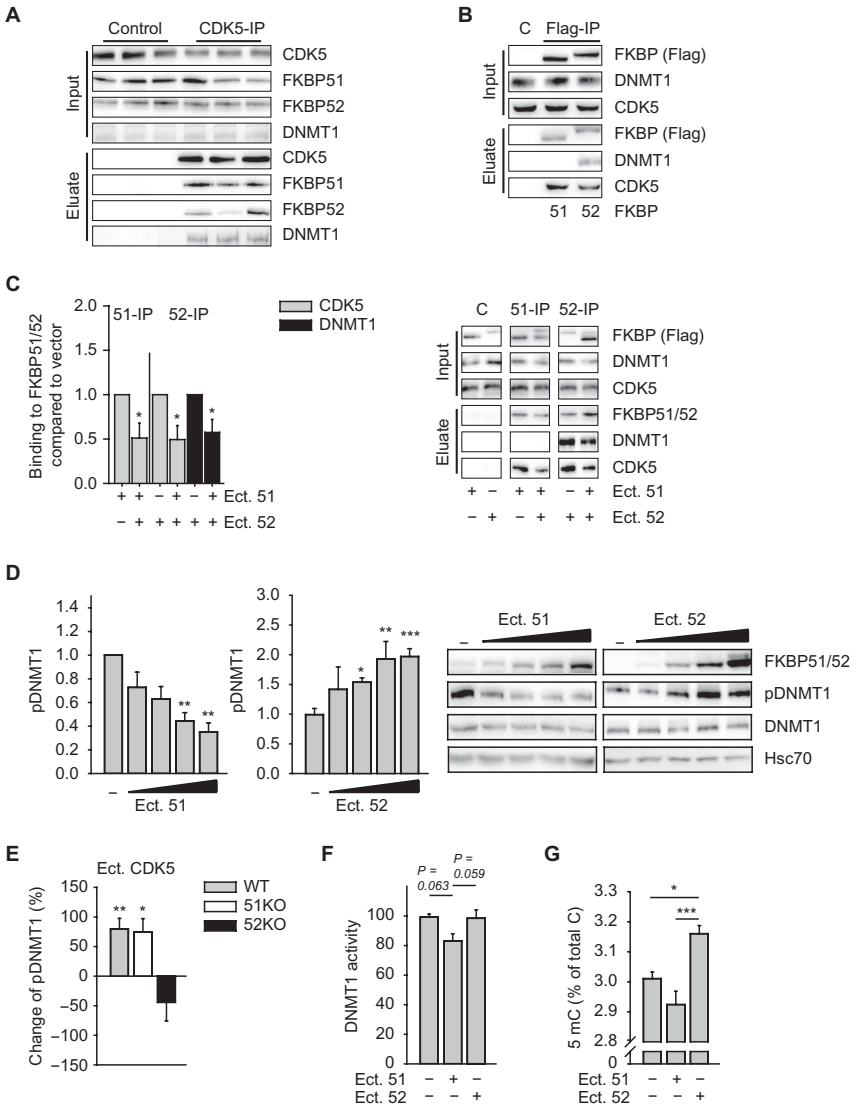

Fig. 1. FKBP51 and FKBP52 differentially affect CDK5-dependent phosphorylation and activity of DNMT1. (**A**) Immunoprecipitation (IP) for CDK5 followed by Western blotting in lysates from HEK293 cells transfected with FKBP51 or FKBP52. Control: without primary antibody [immunoglobulin G (IgG) control in fig. S1A]. (**B** and **C**) Immunoprecipitation for the FLAG tag (B) or FKBP51 or FKBP52 (C) followed by Western blotting in lysates from HEK293 cells transfected with FLAG-tagged FKBP51, FKBP52, or both, as indicated. C, control [vector-transfected cells (B) or without primary antibody (C) (IgG control in fig. S1A)]. Blots are representative of three independent experiments. Ect., ectopic expression. Graph (C) displays the association of FKBP51 (51-IP) or FKBP52 (52-IP) to CDK5 or DNMT1 in the dual transfected samples relative to the singly transfected samples. Data are means + SEM of three independent experiments. (**D**) Western blotting for DNMT1 and phosphorylated (p) DNMT1 (at Ser^{154}) in primary rat astrocytes transfected with FKBP51 or FKBP52. Amount of phosphorylated DNMT1 was calculated relative to that of total DNMT1; this was then calculated relative to that in the control vector sample (–), arbitrarily set to 1. Data are mean + SEM of three to six independent experiments. (**E**) Quantification of Western blotting analysis of the phosphorylation of DNMT1 (corrected for total DNMT1) in wild-type (WT), *Fkbp51* knockout (51KO), or *Fkbp52* knockout (52KO) MEFs transfected with CDK5 relative to vector-transfected cells. Data are means + SEM of three independent experiments. Representative blot is shown in fig. S2B; full blots for (D) and (E) are shown in data file S1. (**F** and **G**) DNMT1 enzymatic activity in total nuclear lysates from primary astrocytes (F) and cytosine methylation (percent of total cytosine) assessed by mass spectrometry in isolated total DNA from primary rat astrocytes transfected with FKBP51 or FKBP52 or a control vector. 5mC, 5-methylcytosine. Data are means + SEM of three independent experiments each performed with two (F) or three (G) technical replicates. $^{*}P < 0.05$, $^{**}P < 0.01$. Statistical details in tables S2 and S3.

of Hsp90 inhibition on complex assembly of CDK5 and DNMT1 (fig. S1, A to D, and data file S1).

In addition to DNMT1, which typically maintains DNA methylation, DNMT3a and DNMT3b also shape the methylome as de novo methyltransferases (*5*). Coimmunoprecipitation revealed an association between FKBP52 and DNMT3a but not DNMT3b, whereas FKBP51 associated with none (fig. S1, E and F).

Considering the reported effects of CDK5 on DNMT1, we analyzed the phosphorylation of DNMT1 at Ser^{154} upon overexpression of FKBP51 or FKBP52 in HEK293 cells or primary rat astrocytes. Overexpressing FKBP51 significantly lowered the phosphorylation of DNMT1, whereas overexpressing FKBP52 increased it (Fig. 1D, data file S1, and fig. S2A). Because phosphorylation of Ser^{154} is important for DNMT1 activity (*23*), this suggests that FKBP52 promotes whereas FKBP51 inhibits DNMT1 activity. To check for the relevance of the FKBPs on CDK5-induced DNMT1 Ser^{154} phosphorylation, we overexpressed CDK5 in wild-type, 51KO, and 52KO mouse embryonic fibroblasts (MEFs) and monitored DNMT1 phosphorylation. CDK5 overexpression did not change the phosphorylation of DNMT1 in 52KO MEFs (as opposed to wild-type cells), whereas a marked increase in phosphorylation of DNMT1 was evident in wild-type and 51KO MEFs (Fig. 1E, data file S1, and fig. S2B).

To determine whether the FKBP51/52-dependent changes in phosphorylation of DNMT1 go along with changes in DNMT1 activity, we transfected primary rat astrocytes with plasmids expressing FKBP51 or FKBP52 and determined the enzymatic DNA methylation activity in total cell lysates. There was a trend toward lower methylase activity in FKBP51-transfected cells than in FKBP52-transfected cells (Fig. 1F). Analysis of the content of total methylated cytosines in genomic DNA revealed significantly lower DNA methylation in FKBP51-transfected than in FKBP52-transfected cells (Fig. 1G). There was no difference in hydroxymethylation (fig. S2C).

To further shed light on the possible mechanism involved in the FKBP-directed regulation of DNMT1 activity by CDK5, we analyzed the association of the CDK5 regulatory proteins p25, p35, and p39 (*40*) in the human neuroblastoma cell line SKNMC. Although all three proteins were detected in protein lysates, only the CDK5 activator p35 associated with DNMT1 (Fig. 2A), indicating that active CDK5 is recruited to DNMT1. Ectopic expression of FKBP52 enhanced the association of p35 with DNMT1, whereas ectopic expression of FKBP51 did not (Fig. 2, A and B, and data file S2). There was no significant change in the association of DNMT1 with CDK5 (Fig. 2C).

FKBP51 has been suggested to facilitate the dephosphorylation of tau, depending on its peptidylprolylisomerase (PPIase) activity (*41*). To test the relevance of PPIase activity in the regulation of DNMT1 phosphorylation, we expressed increasing amounts of a PPIase-deficient mutant of FKBP51 (*25*, *42*) in HEK293 cells. PPIase-deficient FKBP51 exerted similar effects on phosphorylation of DNMT1 as the nonmutated FKBP51 (Fig. 2D and data file S2).

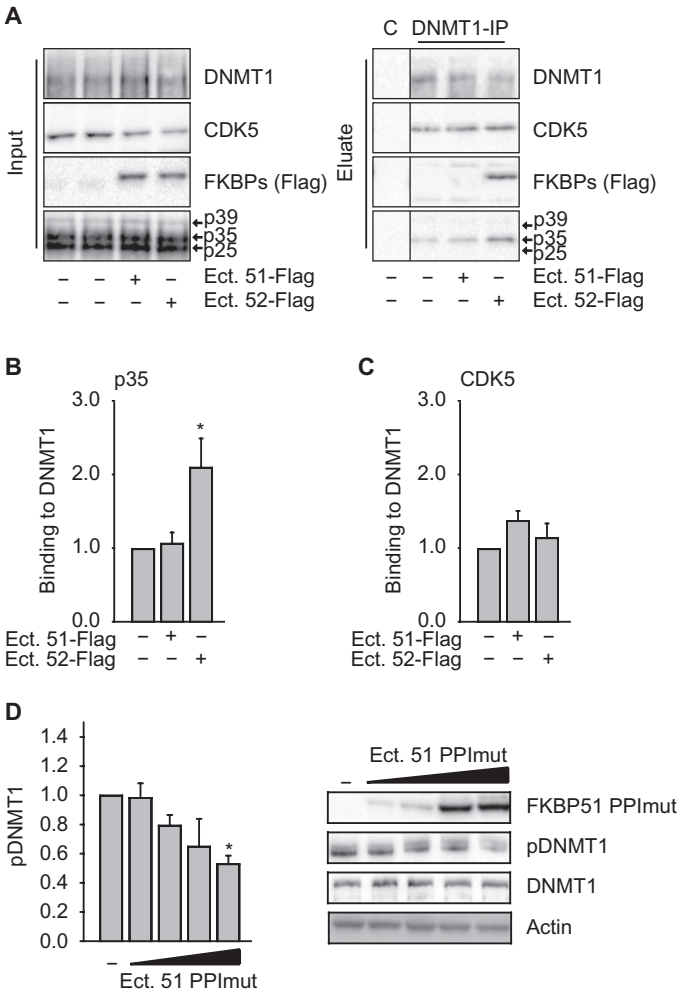

Fig. 2. FKBP51 does not change the interaction of DNMT1 with the CDK5 activator protein p35 and acts independently of its PPIase activity on the phosphorylation of DNMT1. (**A** to **C**) Immunoprecipitation for DNMT1 followed by Western blotting as indicated (A) and quantification of DNMT1-p35 (B) and DNMT1-CDK5 (C) interaction in SKNMC cells transfected with FLAG-tagged FKBP51 or FKBP52 or vector control (indicated by "-" in both lanes). IgG control in fig. S1A. (**D**) Western blotting as indicated in HEK293 cells transfected with PPIase-deficient mutant FKBP51 (F67D/D68V: 51 PPImut). Phosphorylated DNMT1 was calculated against total DNMT1, relative to that in the control vector sample (–), arbitrarily set to 1. Data are means ± SEM from three independent experiments.*$P < 0.05$. Statistical details in table S2. Full blots for (B) and (D) are shown in data file S2.

Modulation of DNMT1 phosphorylation and activity by paroxetine depend on FKBP51

On the basis of previous evidence of an inhibitory effect of paroxetine on DNMT1 (*13*), we sought to assess whether the antidepressant action on DNMT1 involves DNMT1 phosphorylation or its association with CDK5, FKBP51, and FKBP52. First, we tested whether paroxetine affects the association between the FKBPs and CDK5 in HEK293 cells. We found that treatment with paroxetine increased the association between FKBP51 and CDK5 and reduced the interaction between FKBP52 and CDK5 (Fig. 3A, fig. S3, and data file S1). There was no significant effect on the interaction between FKBP52 and DNMT1.

We next checked for the effects of paroxetine on phosphorylation of DNMT1 in primary astrocytes and found that it decreased phosphorylation of DNMT1 in a dose-dependent manner (Fig. 3B). Furthermore, we found evidence that the antidepressant-induced reduction in phosphorylation of DNMT1 requires the presence of FKBP51 because paroxetine decreased phosphorylation of DNMT1 in primary astrocytes from wild-type mice but not in primary astrocytes from 51KO mice (Fig. 3C and data file S3). Similar results were obtained in wild-type and 51KO MEFs (Fig. 3D, fig. S4A, and data file S3). Likewise, paroxetine reduced DNMT1 enzymatic activity in wild-type but not in 51KO MEFs (Fig. 3E and data file S3). To test whether these results can be translated to the action of paroxetine in an established animal model, we determined phosphorylation of DNMT1 in mice that were acutely or chronically treated with

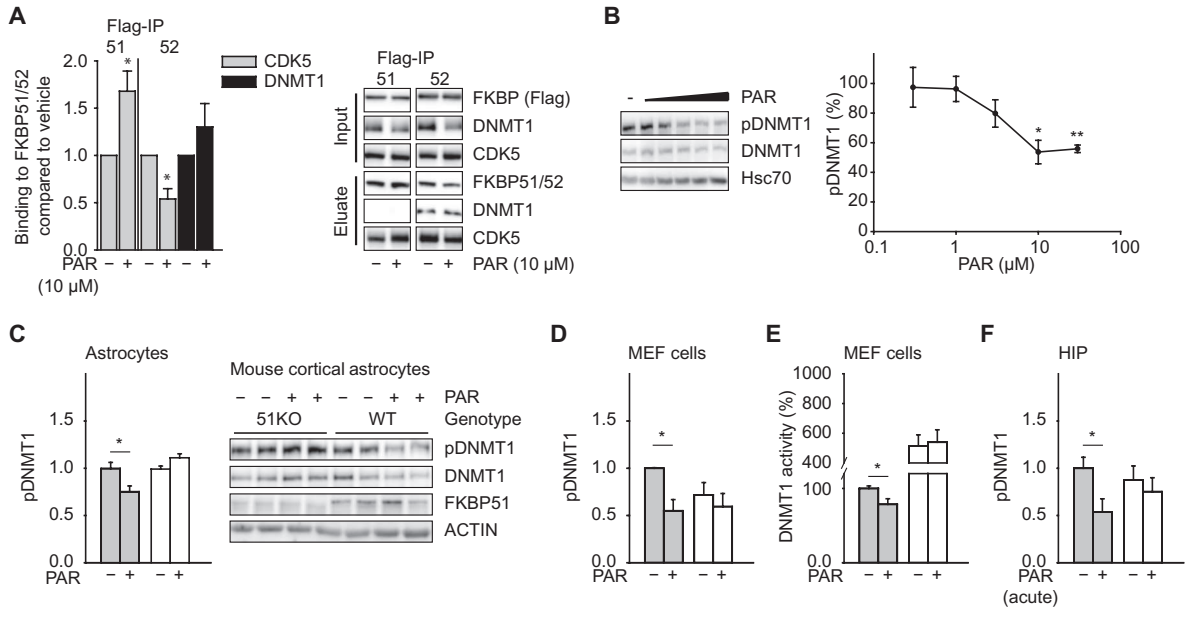

Fig. 3. The effect of paroxetine on DNMT1 is linked to FKBP51. (**A**) Immunoprecipitation for the FLAG tag followed by Western blotting for CDK5 in HEK cells transfected with FLAG-tagged FKBP51 or FKBP52 and treated with paroxetine (PAR, 10 μM) or vehicle for 72 hours. Data from paroxetine-treated samples are presented relative to that in vehicle-treated samples, set to 1. IgG control in fig. S1A. (**B**) Western blotting for phosphorylated DNMT1 relative to total DNMT1 in primary cortical rat astrocytes treated with increasing concentrations of paroxetine or vehicle (–). Data are means ± SEM from three experiments. (**C**) Western blotting in lysates from WT (gray bars) or 51KO (white bars) primary murine astrocytes treated with paroxetine or vehicle (–). Data are means ± SEM of three experiments, each performed in duplicate. (**D** and **E**) Quantification of the abundance of phosphorylated DNMT1 relative to total DNMT determined by Western blotting (D) and enzymatic DNMT1 activity (E) in WT (gray bars) or 51KO (white bars) MEFs treated with paroxetine or vehicle (–). Data are means + SEM of three (D) or four (E) independent experiments performed in technical duplicates. (**F** to **H**) Abundance of phosphorylated relative to total DNMT1 in the prefrontal cortex (PFC) and hippocampus (HIP) of 51KO mice (white bars) and WT mice (gray bars) treated with paroxetine or vehicle in an acute (45 min) (F and G) or chronic (21 days) (H) regimen (*33*). Data are means + SEM of 8 to 10 animals. $^{*}P < 0.05$, $^{**}P < 0.01$. Statistical details are in tables S2 and S3. Full blots for (C) and (F) to (H) are shown in data file S3.

paroxetine (45-min or 21-days treatment duration, respectively). Tissue was available from previous experiments that documented that the behavioral effect of paroxetine was absent in mice lacking FKBP51 (*33*). Acute and chronic treatment with paroxetine led to reduced phosphorylation of DNMT1, both in the hippocampus and in the prefrontal cortex, only in the presence of FKBP51 (Fig. 3, F to H; fig. S4, B to D; and data file S3).

We also investigated the effects of the tricyclic antidepressant amitriptyline on phosphorylation of DNMT1. In MEFs, there was no significant effect of amitriptyline (fig. S5A). In wild-type mice previously treated with amitriptyline (*33*), a reduction in phosphorylation of DNMT1 was observed in the prefrontal cortex but not in the hippocampus (fig. S5, B and C). This effect of amitriptyline was abolished in 51KO mice (fig. S5C). To also test another neuropharmacologically active substance, we analyzed protein extracts from mice that had been treated with the neuroleptic haloperidol (*33*). Haloperidol displayed no significant effect on phosphorylation of DNMT1 in the hippocampus and slightly enhanced phosphorylation of DNMT1 in the prefrontal cortex (fig. S5, D to G), contrasting the effects of the antidepressants paroxetine and amitriptyline.

FKBP51- and paroxetine-modulated DNMT1 activity correlates with *Bdnf* promoter methylation and expression in mice

In addition to the effects of FKBP51 and paroxetine on global DNA methylation through their action on DNMT1, we analyzed possible local consequences at *Bdnf*, the gene encoding BDNF, as a locus relevant to neuropsychiatry. *Bdnf* features different epigenetically controlled promoters that give rise to multiple isoforms at the mRNA level with different untranslated exons at the 5′ end spliced to a common protein-coding exon at the 3′ end (*43*, *44*). To date, the *Bdnf* promoter of exon IV (called promoter IV) is one of the best characterized (*9*, *45*, *46*). The expression of promoter IV is representative of *Bdnf* expression in the brain and also reflects the changes induced by neuronal activity and antidepressants (*16*, *17*, *47*, *48*). Therefore, we analyzed the methylation of promoter IV in the brain of wild-type and 51KO mice that had been treated with paroxetine for 45 min (*33*). In these animals, paroxetine induced the demethylation of *Bdnf* at promoter IV in the prefrontal cortex of wild-type but not 51KO mice (Fig. 4A and table S1). The extent of demethylation varied between 10 and 40 percentage points, depending on the CpG site.

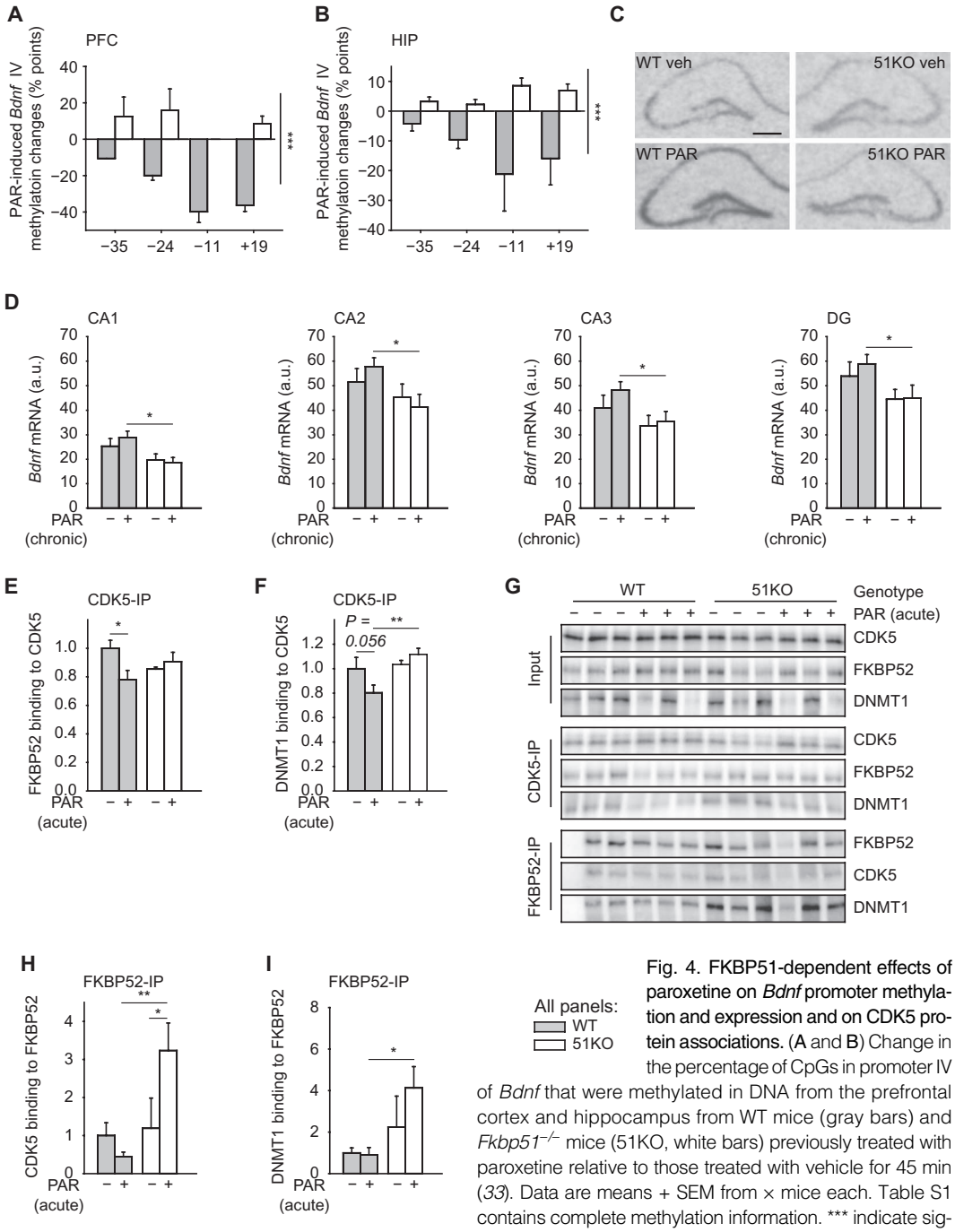

Fig. 4. FKBP51-dependent effects of paroxetine on *Bdnf* promoter methylation and expression and on CDK5 protein associations. (**A** and **B**) Change in the percentage of CpGs in promoter IV of *Bdnf* that were methylated in DNA from the prefrontal cortex and hippocampus from WT mice (gray bars) and *Fkbp51*$^{-/-}$ mice (51KO, white bars) previously treated with paroxetine relative to those treated with vehicle for 45 min (*33*). Data are means + SEM from × mice each. Table S1 contains complete methylation information. *** indicate significant overall genotype effects. (**C** and **D**) *Bdnf* expression assessed by in situ hybridization shown in the dorsal hippocampus (C) and quantified in hippocampal sections from WT and 51KO mice treated with paroxetine for 21 days (chronic) or vehicle (–) (*33*). Scale bar, 500 μm. a.u., arbitrary units; DG, dentate gyrus. (**E** to **I**) Protein binding to CDK5 (E and F) or FKBP52 (H and I) in brain extracts from WT and 51KO mice that had been treated with paroxetine for 45 min (*33*). Western blot representing three animals for each condition and treatment shown in (G). IgG control in fig. S1A. Data are means + SEM from 9 to 10 animals for each condition or treatment. Data from WT mice treated with vehicle were set to 1. *$P < 0.05$, **$P < 0.01$, ***$P < 0.001$. Statistical details in tables S2 and S3.

paroxetine (table S1). Less pronounced effects were observed in the hippocampus, but there was still a significant genotype effect (Fig. 4B and table S1). In addition, we analyzed the promoter of exon I, but no significant changes in DNA methylation were observed (table S1). We also analyzed the effect of amitriptyline on the methylation of *Bdnf* at the exon IV promoter in the hippocampus and in the prefrontal cortex of wild-type and 51KO mice, but there was no significant change in methylation (fig. S6).

To assess changes in the transcription of *Bdnf*, we performed in situ hybridization in brain slices from wild-type and 51KO mice that had previously been treated with paroxetine or vehicle for 21 days (*33*). In all subregions of the hippocampal formation, we observed a similar pattern: the amount of *Bdnf* mRNA was significantly higher in wild-type mice treated with paroxetine than it was in 51KO mice treated with paroxetine (Fig. 4, C and D).

These data are in line with the hypothesis that FKBP51-dependent reduction of DNMT1 activity by paroxetine, also indicated by the decrease of phosphorylation of DNMT1 (Fig. 3, F to H, and fig. S4, B to D), leads to demethylation and activation of the *Bdnf* gene. To evaluate whether FKBP51 mediates the effects of paroxetine on CDK5 and FKBP52 complexes in mice, we performed CDK5 and FKBP52 immunoprecipitation in brain extracts from wild-type and 51KO mice that had been treated with paroxetine for 45 min (*33*). Paroxetine changed the association of CDK5 with FKBP52 and with DNMT1 in wild-type but not 51KO mice (Fig. 4, E to G). This is consistent with the inhibitory effect of paroxetine on FKBP52-CDK5 association we observed in cells (Fig. 3A). When we precipitated FKBP52, the association with CDK5 or DNMT1 in the presence of paroxetine was greater in 51KO than in wild-type mice (Fig. 4, G to I). Thus, FKBP51 mediates the impact of paroxetine on protein associations.

In 51KO mice, there was some increase in DNA methylation upon paroxetine treatment, but this change was not statistically significant (Fig. 4A and table S1). There was no significant genotype effect in the absence of

Cellular and clinical treatment responses support the physiological relevance of FKBP51-dependent effects of paroxetine on DNMT1 and BDNF

To translate the findings obtained from cellular and animal studies to humans, we made use of the whole-blood DNA methylation and RNA data available from the Grady Trauma Project, an ongoing study examining the role of genetic and environmental factors that predict stress responses (*49*, *50*). The expression of *FKBP5* (the gene encoding FKBP51) was negatively correlated with the average global DNA methylation, as measured by 450K arrays ($r = -0.127$, $P = 0.015$, $n = 365$), and with the average amount of *BDNF* methylation found over the entire *BDNF* locus (total of 79 CpGs), as well as with the average methylation of CpGs located near the transcription start sites of exon I (33 CpGs) and exon IV (31 CpGs) of the gene (Fig. 5, A and B, and fig. S7).

To test protein correlations, we first analyzed the phosphorylation of DNMT1 and FKBP51 in peripheral blood mononuclear cells (PBMCs) from healthy individuals. We observed that the amounts of FKBP51 and phosphorylated DNMT1 were inversely correlated, in line with a negative effect of FKBP51 on the phosphorylation of DNMT1 (Fig. 5C). We also checked for the effects of paroxetine on the same cells by treating PBMCs ex vivo with paroxetine or vehicle for 48 hours. In PBMCs, the concentration used for paroxetine was chosen to match therapeutic concentrations in the serum according to the consensus guidelines for therapeutic drug monitoring in psychiatry (*51*). We found that higher amounts of FKBP51 were significantly associated with smaller paroxetine-induced changes in phosphorylation of DNMT1 (Fig. 5D), further corroborating the notion that FKBP51 modulates the effects of paroxetine on DNMT1 phosphorylation.

Because FKBP51 abundance is increased upon stress (*28*–*30*), we explored the possibility that stress-induced glucocorticoids change pDNMT through increasing the amount of FKBP51. PBMCs were isolated from 21 healthy individuals before and after oral intake of dexamethasone, a synthetic corticosteroid that selectively activates GR. In response to dexamethasone, we observed a negative correlation between the change in the phosphorylation of DNMT1 and the change in FKBP51 abundance: after dexamethasone treatment, increased abundance of FKBP51 was correlated with decreased phosphorylation of DNMT1 (Fig. 5E), consistent with the role of FKBP51 as mediator of stress-induced dephosphorylation of DNMT1.

Because higher protein amounts of FKBP51 in PBMCs were associated with better clinical treatment outcome in depressed patients (*33*), we hypothesized that phosphorylation of DNMT1 might also be linked to treatment response. Therefore, we determined the level of phosphorylation of DNMT1 in PBMCs from 40 patients of the Munich Antidepressant Response Signature (MARS) (*52*) project before and after 6 weeks of psychopharmacological treatment (with various antidepressants by doctor's choice). The change of phosphorylation of DNMT1 showed a negative correlation with the clinical treatment response [presented as the reduction in the Hamilton Depression Rating Scale (HDRS) from beginning of treatment to 6 weeks later] (Fig. 6A). Similarly, when we collected PBMCs from the patients at the time of admission to the clinic and treated the cells with paroxetine ex vivo, the cellular response (a decrease) in the phosphorylation of DNMT1 also negatively correlated with patients' (increased) reduction in HDRS (Fig. 6B). The change in the phosphorylation of DNMT1 observed in PBMCs in response to paroxetine ex vivo and the change in the phosphorylation of DNMT1 observed in patients after clinical treatment were well correlated (Fig. 6C). Overall, nonresponders tended to exhibit an increase in the phosphorylation of DNMT1 after 6 weeks of clinical treatment or after paroxetine treatment of their PBMCs ex vivo (fig. S8, A and B). When determining BDNF abundance, we found that the increase in BDNF secreted from PBMCs cultured and treated with paroxetine ex vivo significantly correlated with the abundance of FKBP51 (Fig. 6D). Likewise, the change in BDNF concentration in the serum of patients 6 weeks after clinical treatment also positively correlated with the abundance of FKBP51 in their blood cells collected at the beginning of treatment (Fig. 6E). Furthermore, the BDNF response in PBMCs cultured with paroxetine ex vivo positively correlated with the clinical treatment outcome observed in patients (Fig. 6F). A trend toward positive correlation was also observed for the change of BDNF in the serum and the clinical treatment outcome after 6 weeks (Fig. 6G). Together, these results support the physiological and clinical relevance of FKBP51 in inhibiting DNMT1 activation and promoting *BDNF* expression in modulating the action of antidepressants.

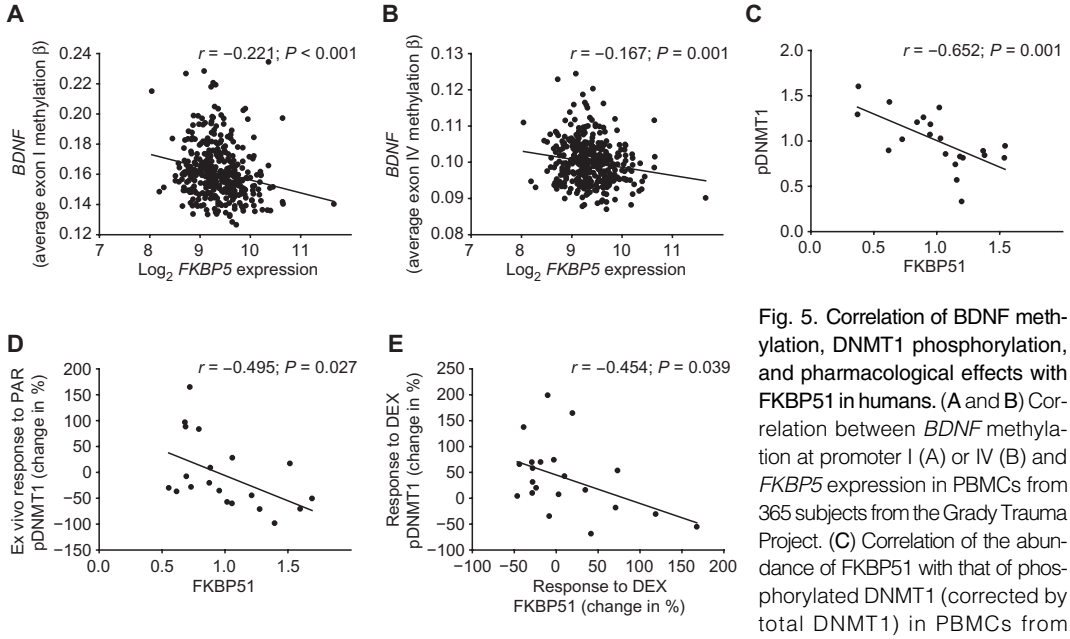

Fig. 5. Correlation of BDNF methylation, DNMT1 phosphorylation, and pharmacological effects with FKBP51 in humans. (A and B) Correlation between *BDNF* methylation at promoter I (A) or IV (B) and *FKBP5* expression in PBMCs from 365 subjects from the Grady Trauma Project. (C) Correlation of the abundance of FKBP51 with that of phosphorylated DNMT1 (corrected by total DNMT1) in PBMCs from healthy individuals ($n = 21$). (D) Correlation of FKBP51 abundance with the change in pDNMT1 abundance after ex vivo paroxetine exposure (48 hours, relative to vehicle) in PBMCs from healthy individuals ($n = 20$). (E) Correlation of the change in the phosphorylation of DNMT1 with that of FKBP51 in PBMCS isolated from healthy individuals that received dexamethasone (DEX, 1.5 mg, 6 hours; $n = 21$). Data were analyzed by Pearson correlation (A and B) or partial correlation corrected for age and gender (C to E).

DISCUSSION

Adaptation to stressful life events is a fundamental physiological process that involves several mechanisms, including epigenetic programming (*24*, *53*, *54*). Gene

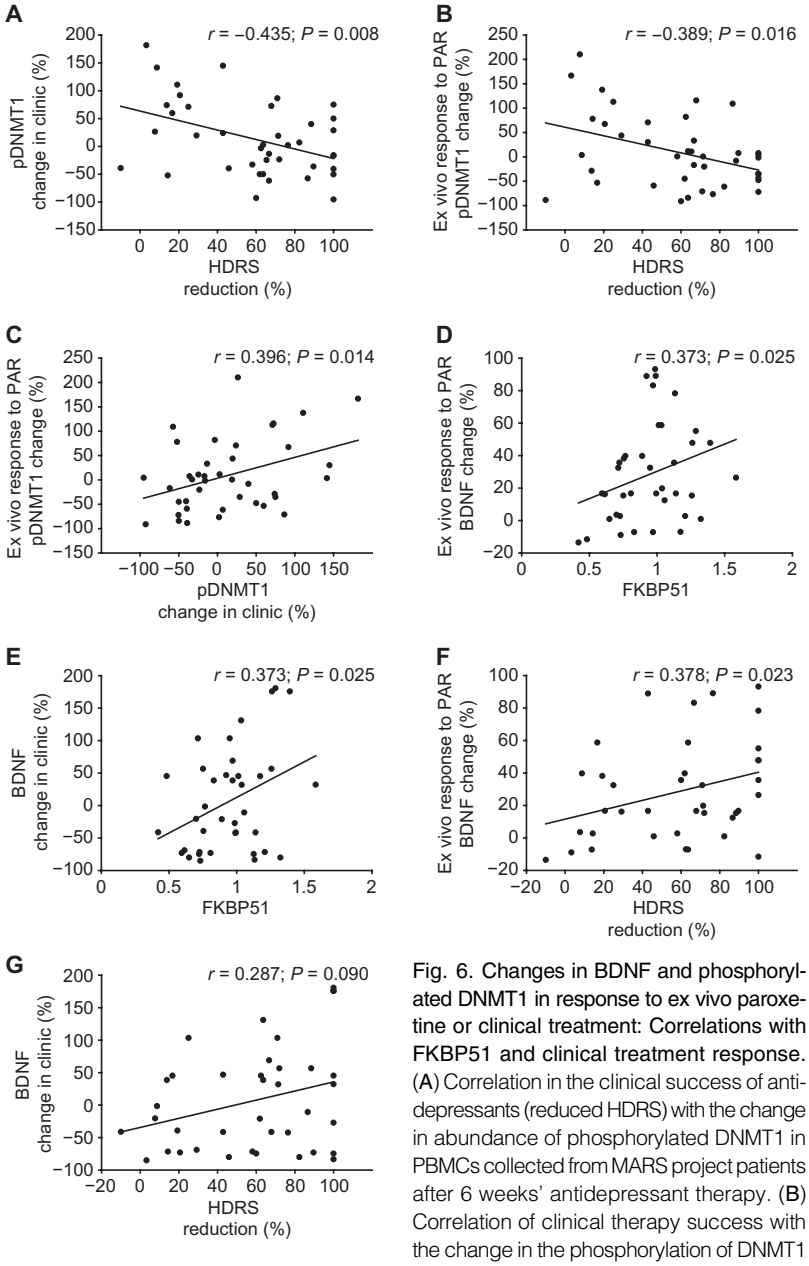

Fig. 6. Changes in BDNF and phosphorylated DNMT1 in response to ex vivo paroxetine or clinical treatment: Correlations with FKBP51 and clinical treatment response. (**A**) Correlation in the clinical success of antidepressants (reduced HDRS) with the change in abundance of phosphorylated DNMT1 in PBMCs collected from MARS project patients after 6 weeks' antidepressant therapy. (**B**) Correlation of clinical therapy success with the change in the phosphorylation of DNMT1 in respective patients' PBMCs isolated before therapy and treated ex vivo with paroxetine. (**C**) Correlation of the change in the phosphorylation of DNMT1 in PBMCs isolated from patients after clinical therapy [as described in (A)] with that in respective patients' PBMCs isolated before therapy and treated ex vivo with paroxetine. (**D** and **E**) Correlation of the abundance of FKBP51 with that of BDNF in PBMCs either (D) isolated before therapy and treated ex vivo with paroxetine or (E) isolated after clinical therapy [as described in (A)]. (**F** and **G**) Correlation of the clinical success of antidepressants (reduced HDRS) with that of BDNF in PBMCs either (F) isolated before therapy and treated ex vivo with paroxetine or (G) isolated after clinical therapy [as described in (A)]. Protein abundance was assessed in cell extracts by Western blotting. The abundance of phosphorylated DNMT1 was normalized to total DNMT1. Data were analyzed by Pearson correlation coefficient corrected for age and gender.

programming through the GR is evident from several reports (*55*). The established paradigm is that GR binds to chromatin targets and interacts with the epigenetic machinery at these sites, thereby changing local epigenetic marks. Our study adds another twist to GR-mediated epigenetic programming by delineating a new route: we found that the GR-enhanced cochaperone FKBP51 suppresses the activity of the epigenetic enzyme DNMT1 by impairing its formation of a heterocomplex with CDK5. Our data suggest that FKBP51 displaces FKBP52 from CDK5, thereby preventing the subsequent interaction with and phosphorylation of DNMT1 at Ser^{154}, causing reduced activity of DNMT1 and decreased DNA methylation in the genome, including at the *Bdnf* gene. This displacement favoring FKBP51 chaperoning is promoted by paroxetine and possibly other antidepressants (Fig. 7).

Part of the translational aspect of this study uses PBMCs cultivated and treated ex vivo. Although signal transduction in peripheral cells ex vivo may not reliably replicate molecular activity in brain cells, the proteins involved in this study are present in multiple cell types and appear to have similar functional interactions in human PBMCs as they did in mouse brain tissue and astrocytes. Furthermore, our correlation analyses indicated that examining the effects on the activation of DNMT1 in patient PBMCs ex vivo may serve as a biomarker to predict the clinical response to antidepressants.

The data reported here support the notion that the role of chaperones in the management of stress reactivity extends beyond protein homeostasis to the genome and epigenome. For example, several landmark studies from the Lindquist laboratory document the role of Hsp90 in the evolution of heritable new traits in several organisms (*56*–*60*). The new traits shaped not only the phenotype but also the responsiveness to diverse drugs.

Our finding of the association of the chaperone FKBP51 with CDK5 in the regulation of DNMT1 adds insight into the molecular and physiological functions of FKBP51, which appears to be a versatile protein. In addition to its role as a potent inhibitor of GR (*25*–*27*), FKBP51 regulates other steroid receptors and associates with and regulates the kinase AKT through the recruitment of PH domain and leucine-rich repeat protein phosphatases (PHLPPs), with implications for cancer treatment (*61*). FKBP51 also forms protein complexes with Beclin1, AKT, and PHLPPs in the regulation of autophagy and affects tau stability, microtubule polymerization, neurite outgrowth, glycogen synthase kinase 3β (GSK3β) signaling, aging, and nuclear factor κB (NFκB) signaling in immune processes (*26*, *33*, *36*, *41*, *62*–*64*). Similar to the divergent effects of FKBP51 and FKBP52 on CDK5, the two highly homologous FKBPs are reported to exert opposite effects on several other cellular processes (*64*). Even though both FKBPs feature a well-described enzymatic activity [peptidylprolyl isomerization (*65*)], it appears that they rather function as protein scaffolds to promote various and at least partially differing protein complexes, such as what we observed regarding their interaction with CDK5.

Several functions of FKBP51 appear to contribute to its role in the cellular and organismal response to antidepressants (*31*–*35*). Originally, because of its effect on GR signaling (*25*), FKBP51 was included as candidate in the first gene association study in depression (*31*). Since then, cellular, animal, and clinical data suggest that the role of FKBP51 in regulating GSK3β, AKT, and autophagy signaling mediate antidepressant effects (*33*, *36*). GSK3β and AKT decrease or increase, respectively, DNMT1 protein abundance (*66*). In our data set, we found no evidence that the presence

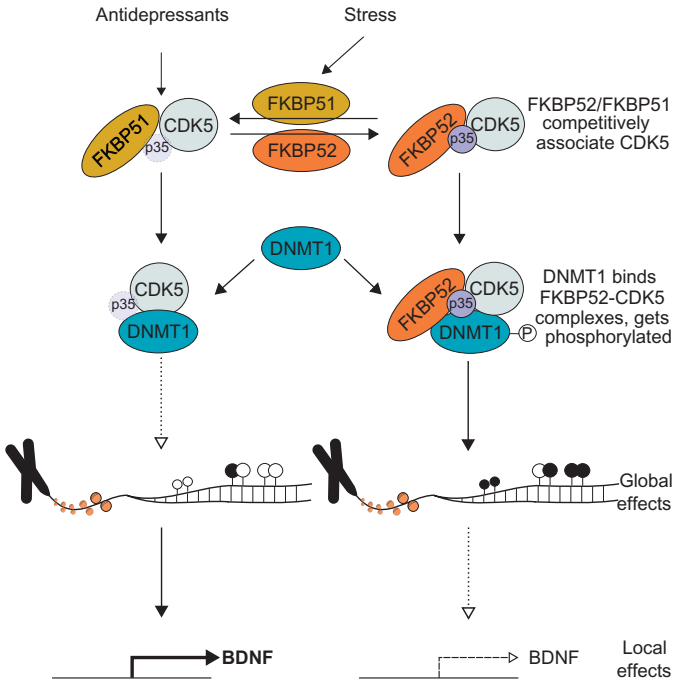

Fig. 7. Model of antidepressant effects on global and local epigenetic marks mediated through FKBP51-regulated suppression of DNMT1 activity. Schematic summarizing of our findings. FKBP51 competes with FKBP52 for binding to CDK5 and its activator p35. Because DNMT1 preferentially associates with FKBP52-CDK5-p35 complexes, DNMT1 displays higher phosphorylation and activity in the presence of high FKBP52 abundance but not when FKBP51 dominates the CDK5-p35 complexes. This causes differences in global DNA methylation and *BDNF* promoter methylation and expression. The stress-enhanced protein FKBP51 may thus mediate the impact of stress on epigenetic programming. Furthermore, this pathway is targeted by paroxetine and possibly other antidepressants to swap chaperone binding to CDK5, which may mediate the clinical response in patients with depression.

of FKBP51 alters the overall abundance of DNMT1, possibly because FKBP51 inhibits both AKT and GSK3β (*33*, *36*, *61*). Although we suggest that the specific suppression of DNMT1 phosphorylation is mediated through the interaction of FKBP51 with CDK5, given the potential for multiple kinases being affected by FKBP51 (*37*), we cannot yet exclude the possibility that kinases other than CDK5 contribute to this mechanism.

The present and several additional studies portray FKBP51 as "reactivity protein" in the sense that it shapes the responsiveness to stress and drug treatment (*33*, *36*, *61*, *67*, *68*). Part of this conclusion extends from experiments with 51KO mice. Deletion of genes often goes along with compensatory mechanisms that are evoked by the organism throughout development. The effect of *FKBP5* deletion is not always detectable in the absence of a stimulus (*33*, *36*, *67*, *68*); in our study, a difference in phosphorylation of DNMT1 between brains from wild-type and those from 51KO animals was only evident after treatment with paroxetine. Thus, it appears that possible compensatory changes in response to gene deletion do not compromise the effects evoked by challenges later in life.

It is tempting to speculate about the possibility to target (enhance) FKBP51 or downstream processes for the treatment of depression or other stress-related diseases. However, we would like to point out that due to the multifactorial actions of FKBP51, more studies are necessary to dissect which functions of FKBP51 are important and how it might be possible to specifically affect a subset of these functions when targeting FKBP51 directly rather than by targeting downstream processes. A promising FKBP51-targeting compound has been presented recently (*69*). This compound is designed as inhibitor of the peptidylprolyl isomerase activity but because this activity appears dispensable for many functions of FKBP51, it is not clear yet which of the molecular actions of FKBP51 are influenced in which direction. Because the gene encoding FKBP51 has also been suggested as a risk factor for psychiatric disorders (*31*, *49*, *70*), timing of pharmacological FKBP51 targeting will likely be important. Moreover, if one limits the ability of FKBP51 to reduce GR function, more FKBP51 might be produced because of an ultrashort feedback loop (*28*, *30*, *71*). Alternatively, our study also supports the consideration of DNMT1 inhibitors for drug development in depression (*14*, *48*).

MATERIALS AND METHODS

Cells

HEK293 cells [American Type Culture Collection (ATCC), CRL-1573], SKNMC cells (gift from C. Behl, University of Mainz, Germany), and MEFs (gift from M. Cox, University of Texas at El Paso) were maintained in Dulbecco's modified Eagle's medium (DMEM; Gibco) supplemented with 10% fetal calf serum (FCS) and 100 U/ml penicillin and streptomycin, respectively. Enriched astroglial cultures were prepared from postnatal day–1 Sprague-Dawley rat pups (Charles River) or wild-type and 51KO mice and were handled as described previously (*72*).

Transfection of astrocytes and MEF cells

Detached MEFs or cortical astrocytes (2×10^6) were resuspended in 100 μl of transfection buffer [50 mM Hepes (pH 7.3), 90 mM NaCl, 5 mM KCl, and 0.15 mM $CaCl_2$] (*73*). Up to 5 μg of plasmid DNA expressing the respective construct was added to the cell suspension, and electroporation was carried out using the Amaxa Nucleofactor system (Lonza). Cells were replated at a density of $10^5 \times cm^{-2}$ and further processed for Western blot analysis or assessment of DNMT1 activity.

Plasmids

The constructs expressing FLAG-tagged FKBP51, PPIase-deficient FKBP51 (F67D/D68V) or FKBP52, and hemagglutinin-tagged CDK5 have been described previously (*25*, *74*). The plasmids pcDNA3/Myc-DNMT3A and pcDNA3/Myc-DNMT3B1 were from Addgene (#35521 and #35522).

Coimmunoprecipitation

Coimmunoprecipitations (CoIPs) of FLAG-tagged FKBP51/52 or endogenous CDK5, FKBP51, and FKBP52 were performed in HEK293 cells essentially as described previously (*26*). Briefly, 5×10^6 cells were electroporated with 5 μg of the respective expression plasmids using a GenePulser (Bio-Rad) at 350 V/700 μF in 400 μl of electroporation buffer [50 mM K_2HPO_4/KH_2PO_4, 20 mM KAc (pH 7.35), and 25 mM $MgSO_4$]. After 3 days of cultivation in DMEM/10% FCS, cells were lysed in CoIP buffer [20 mM tris-HCl (pH 8.0), 100 mM NaCl, 1 mM EDTA, and 0.5% Igepal complemented with protease inhibitor cocktail (Sigma)] for 20 min at 4°C with constant mixing. In the case of precipitating endogenous proteins from brain lysates, the tissue was homogenized and lysed in the same buffer. The lysates were cleared by centrifugation, and the protein concentration was determined and adjusted (brain lysates, $1\ \mu g \times \mu l^{-1}$; cell lysates, $1.2\ \mu g \times \mu l^{-1}$); 1 ml of lysate was incubated with 2.5 μg of FLAG, FKBP51, FKBP52, or CDK5 antibody overnight at 4°C with constant mixing. Subsequently, 20 μl of bovine serum albumin–blocked protein G Dynabeads (Invitrogen, 100-03D) were added to the lysate-antibody mix followed by

a 3-hour incubation at 4°C. Beads were washed three times with PBS, and bound proteins were eluted with 100 µl of 1 × FLAG peptide solution (100 to 200 µg × ml^{-1}, Sigma F3290) in PBS for 30 min at 4°C. In case of precipitation of endogenous proteins, elution was performed by adding 60 µl of Laemmli sample buffer and by incubation at 95 °C for 5 min. Five to fifteen micrograms of the input lysates or 2.5 to 5 µl of the immunoprecipitates were separated by SDS–polyacrylamide gel electrophoresis (PAGE) and analyzed by Western blotting. When quantifying coimmunoprecipitated proteins, their signals were normalized to input protein and to precipitated interactor protein.

Western blot analysis

Western blot analysis was conducted as previously described (*13*). Briefly, protein extracts were obtained by lysing cells in 62.5 mM tris, 2% SDS, and 10% sucrose, supplemented with protease (Sigma, P2714) and phosphatase (Roche, 04906837001) inhibitor cocktail, followed by sonication of samples and heating at 95°C for 5 min. Proteins were separated by SDS-PAGE and electrotransferred onto nitrocellulose membranes. Blots were placed in tris-buffered saline (TBS) supplemented with 0.05% Tween (Sigma, P2287) and 5% nonfat milk for 1 hour at room temperature, followed by an incubation with the primary antibody (diluted in TBS/0.05% Tween) overnight at 4°C. Primary antibodies recognizing the following epitopes or proteins were used: FLAG (1:7000; Rockland, 600-401-383), FKBP51 (1:1000; Bethyl, A301-430A), FKBP52 (1:2000; Bethyl, A301-427A), actin (1:5000; Santa Cruz Biotechnology, sc-1616), DNMT1 (1:1000; Imgenex, IMG-261A), CDK5 (1:1000; Cell Signaling Technology, #2506), p25 and p35 (1:1000; Cell Signaling Technology, #2680), p39 (1:1000; Cell Signaling Technology, #3275), myc (1:1000; Sigma-Aldrich, C3956), and Hsc70 (heat-shock cognate 70; 1:2000; Santa Cruz Biotechnology, sc-7298). Subsequently, blots were washed and probed with the respective horseradish peroxidase–conjugated secondary antibody for 1 hour at room temperature. Enhanced chemiluminesence detection reagent (Millipore) was applied to visualize the immunoreactive bands at ChemiDoc MP (Millipore). In the figures, bands corresponding to the respective proteins are displayed. Full lane blots corresponding to Figs. 1 to 3 and figs. S1 and S3 are shown in data files S1 to S3.

In situ hybridization

Mouse tissue was available from experiments described previously (*33*). Frozen brains were coronally sectioned in a cryostat microtome at 18 µm and kept at −80°C. In situ hybridization using a ^{35}S uridine triphosphate–labeled ribonucleotide probe for BDNF (forward primer: 5′-GCGGCAGATAAAAAGACTGC and reverse primer: 5′-AAGTTGTGCGCAAATGACTG; size, 495 bp) was performed as described previously (*75*). The slides were exposed to Kodak BioMax magnetic resonance films (Eastman Kodak Co.) and developed. Autoradiographs were digitized, and expression was determined by optical densitometry using the freely available National Institutes of Health (NIH) ImageJ software. The mean of two unilateral measurements (dorsal hippocampal subregions: CA1, CA2, CA3, and dentate gyrus) was calculated for each animal, subtracting the background signal of a nearby structure not expressing the gene of interest from the measurements.

Determination of BDNF

BDNF was quantified in the serum using the commercially available enzyme-linked immunosorbent assay (ELISA) kit human BDNF DuoSet, (R&D Systems, #DY248).

Subjects and preparation of human PBMCs

Human PBMCs were collected from 21 healthy male volunteers (average age was 25.8 ± 2.7 years) for analysis of protein-protein correlations (Fig. 5C). The same volunteers received 1.5 mg of dexamethasone (orally), and protein expression changes in PBMCs were determined 6 hours later (Fig. 5E). PBMCs from another group of volunteers (20 men, average age of 34.8 ± 6.9 years) were collected for ex vivo cultivation and determination of paroxetine effects (Fig. 5D). In addition, PBMCs were collected before and after antidepressant treatment from 40 patients participating in the MARS study (*52*) and diagnosed with depression according to the diagnostic criteria of Diagnostic and Statistical Manual of Mental Disorders, 4th Edition (DSM-IV; 23 women and 17 men, average age of 48.85 ± 14.7 years).

MARS is an open-label trial investigating outcome predictors for antidepressant treatment. The type of treatment was chosen according to the attending doctor's choice and in agreement with the patients. Dosage was adjusted and monitored according to plasma medication concentrations. Treatment outcome was weekly evaluated with the 21 items version of the HDRS. Fasting venous blood samples were collected through venipuncture on admission and after 6 weeks of antidepressant treatment. Samples were diluted with PBS, carefully loaded on Biocoll solution (BioChrom AG, L6113) and centrifuged at 800*g* for 20 min. PBMCs were enriched by selecting the interphase of the Biocoll gradient, followed by washing two times with ice-cold PBS. Cells were then resuspended in RPMI and plated at 4 × $10^5/cm^2$. After recovery for 6 hours, cells were treated with either 365 nM paroxetine or vehicle. This concentration has been chosen to match therapeutic concentrations in the serum according to the consensus guidelines for therapeutic drug monitoring in psychiatry (*51*). Patients and healthy subjects gave informed written consent, and the study was approved by the ethics committee of the Ludwig Maximilians University in Munich, Germany.

Global methylation analysis

Total cytosine methylation and hydroxymethylation in genomic DNA from rat astrocytes was determined by quantitative LC/UV-ESI-MS/MS analysis of digested DNA samples as described previously (*76*).

Gene expression and DNA methylation profiling in subjects from the Grady Trauma Project

Whole-blood samples were obtained from 365 subjects from the Grady Trauma Project. The Grady Trauma Project is an ongoing study that includes more than 6000 subjects from a highly traumatized, urban population of low socioeconomic status and examines the role of genetic and environmental factors on stress responses (*49*, *50*). All subjects provided written informed consent, and all procedures were approved by the Institutional Review Boards of the Emory University School of Medicine and Grady Memorial Hospital.

To assess DNA methylation, whole-blood genomic DNA was extracted using the Gentra Puregene Blood Kit (Qiagen). DNA quantity and quality were assessed by Quant-iT PicoGreen (Invitrogen) and NanoDrop 2000 Spectrophotometer (Thermo Scientific). Subsequently, DNA was bisulfite-converted with the Zymo EZ-96 DNA Methylation Kit (Zymo Research), and DNA methylation was assessed with Illumina HumanMethylation450 BeadChip (450K) arrays. Hybridization and processing was performed as previously described (*77*). Quality control of methylation data, including intensity readouts, normalization, and cellular composition estimation, was carried out using the minfi Bioconductor R package version 1.10.2 (*78*). Failed probes were excluded on the basis of a detection of *P* value greater than 0.01 in at least 75% of the samples ($n = 233$ probes). We also removed probes in X or Y chromosome and nonspecific binding probes (*79*) if single nucleotide polymorphisms (SNPs) were documented in the interval for which the Illumina probe is designed to hybridize or if they were located close (10 bp from query site) to SNPs reported in the 1000 Genomes Project to have minor allele frequency ≥ 0.05 (*80*). Data were normalized

with functional normalization included in the minfi R package (*81*). Batch effects were identified after inspection of principal component analysis using the shinyMethyl Bioconductor R package version 0.99.39 and removed using COMBAT (*82*). As previously recommended (*83*), we used *M* values to perform the statistical analyses involving DNA methylation and β methylation values to visualize the relationships with gene expression.

To assess gene expression, whole-blood RNA was collected with PAXgene Blood RNA Tubes (PreAnalytiX) and processed as previously described (*84*). Blood RNA was then hybridized to Illumina HumanHT-12 version 3 and version 4 Expression BeadChips (Illumina). Gene expression was measured using the Illumina HumanHT-12 version 3 Expression BeadChip Kit (Illumina). Raw microarray scan files were exported with the Illumina BeadStudio program 13 and were analyzed with R (www.R-project.org). Using Illumina internal controls, microarray data were transformed and normalized through variance stabilizing normalization (*85*). Potential confounding as a result of batch effects was corrected using an empirical Bayes method (*82*). Data reproducibility was confirmed with six pairs of technical replicates (average Pearson correlation = 0.996). The raw array data for the Grady study have been deposited to Gene Expression Omnibus (GEO) both for gene expression (GSE58137) and DNA methylation (GSE72680).

DNMT1 activity assay

DNMT1 activity was measured as previously described (*13*), with the modification that astrocytes were also transfected with FKBP51, FKBP52, or vector plasmids 3 days before cell harvesting.

Bdnf promoter methylation analysis

The methylation status of *Bdnf* promoters I and IV in mouse brain was analyzed by bisulfite pyrosequencing. Briefly, total DNA was isolated from specific brain regions using NucleoSpin Tissue (Macherey-Nagel), according to the manufacturer's instructions. After quantification, about 300 ng of DNA were bisulfite-converted using the EZ DNA Methylation Kit (Zymo Research), and bisulfite-converted DNA samples were used as templates for polymerase chain reactions (PCRs) amplifying promoters I and IV of the *Bdnf* gene. Primers used for the bisulfite PCR and pyrosequencing are provided in table S4. Pyrosequencing primers were designed with the MethMarker software and carried out on a PSQ96 (Pyrosequencing) using PyroMark Gold Q96 reagents (Qiagen) according to the manufacturer's recommendations.

Statistical analysis

Statistical analyses were performed with SigmaPlot 13.0 and SPSS 18. Student's *t* tests or Mann-Whitney tests were applied to compare two groups, whereas one- or two-way analysis of variance (ANOVA) were performed for comparisons between three or more groups, followed by Bonferroni, Tukey's, or Duncan's post hoc test, as appropriate. Correlations between variables were analyzed using the Pearson correlation coefficient. Treatment outcome in the patient sample was determined as percent reduction of the HDRS rating scores between admission and after 6 weeks of antidepressant treatment. In case of an early discharge from the hospital (after at least 2 weeks of antidepressant treatment), missing HDRS scores were estimated using nonlinear regression with sex, age, and previous HDRS scores as predictor variables. *P* values lower than 0.05 were considered statistically significant.

Ethics statement

All experiments were carried out in the animal facilities of the Max Planck Institute of Psychiatry in Munich, Germany. The experiments were carried out in accordance with the European Communities' Council Directive 86/609/EEC. All efforts were made to minimize animal suffering during the experiments. The protocols were approved by the committee for the Care and Use of Laboratory Animals of the Government of Upper Bavaria, Germany. Approval for the MARS project was received by the ethics committee in charge (submission no. 318/00, ethics committee of the Medical Faculty at the Ludwig Maximilians University, Munich, Germany), and participants gave oral and written consent before study inclusion.

SUPPLEMENTARY MATERIALS

www.sciencesignaling.org/cgi/content/full/8/404/ra119/DC1

Fig. S1. DNMT protein interaction analysis.
Fig. S2. FKBP51 and FKBP52 differentially affect the phosphorylation and activity of DNMT1.
Fig. S3. Paroxetine promotes FKBP51 binding to CDK5.
Fig. S4. FKBP51 shapes the effect of paroxetine on DNMT1.
Fig. S5. The effect of amitriptyline and haloperidol on the phosphorylation of DNMT1.
Fig. S6. The effect of amitriptyline on *Bdnf* promoter IV methylation.
Fig. S7. DNA methylation of *Bdnf* inversely correlates with the abundance of *FKBP5* mRNA.
Fig. S8. Cellular and clinical change in the abundance of phosphorylated DNMT1 in PBMCs in response to antidepressants.
Table S1. Pyrosequencing results of *Bdnf* promoter methylation analyses in wild-type and 51KO mice.
Table S2. Statistical details of ANOVA analysis by figure panel.
Table S3. Statistical details of Student's *t* test or Mann-Whitney analysis by figure panel.
Table S4. Primers for bisulfite PCR and pyrosequencing.
Data file S1. Blot collections for Fig. 1 and figs. S1 and S3.
Data file S2. Blot collections for Fig. 2.
Data file S3. Blot collections for Fig. 3

REFERENCES AND NOTES

1. T. Klengel, E. B. Binder, Gene-environment interactions in major depressive disorder. *Can. J. Psychiatry* **58**, 76–83 (2013).
2. F. J. Raabe, D. Spengler, Epigenetic risk factors in PTSD and depression. *Front. Psychiatry* **4**, 80 (2013).
3. E. J. Nestler, Epigenetic mechanisms of depression. *JAMA Psychiatry* **71**, 454–456 (2014).
4. S. L. Berger, The complex language of chromatin regulation during transcription. *Nature* **447**, 407–412 (2007).
5. R. Z. Jurkowska, T. P. Jurkowski, A. Jeltsch, Structure and function of mammalian DNA methyltransferases. *Chembiochem* **12**, 206–222 (2011).
6. T. Klengel, E. B. Binder, Gene × environment interactions in the prediction of response to antidepressant treatment. *Int. J. Neuropsychopharmacol.* **16**, 701–711 (2013).
7. V. Vialou, J. Feng, A. J. Robison, E. J. Nestler, Epigenetic mechanisms of depression and antidepressant action. *Annu. Rev. Pharmacol. Toxicol.* **53**, 59–87 (2013).
8. A. Menke, E. B. Binder, Epigenetic alterations in depression and antidepressant treatment. *Dialogues Clin. Neurosci.* **16**, 395–404 (2014).
9. N. M. Tsankova, O. Berton, W. Renthal, A. Kumar, R. L. Neve, E. J. Nestler, Sustained hippocampal chromatin regulation in a mouse model of depression and antidepressant action. *Nat. Neurosci.* **9**, 519–525 (2006).
10. T. Perisic, N. Zimmermann, T. Kirmeier, M. Asmus, F. Tuorto, M. Uhr, F. Holsboer, T. Rein, J. Zschocke, Valproate and amitriptyline exert common and divergent influences on global and gene promoter-specific chromatin modifications in rat primary astrocytes. *Neuropsychopharmacology* **35**, 792–805 (2010).
11. M. Fatemi, A. Hermann, H. Gowher, A. Jeltsch, Dnmt3a and Dnmt1 functionally cooperate during de novo methylation of DNA. *Eur. J. Biochem.* **269**, 4981–4984 (2002).
12. M. G. Goll, T.H. Bestor, Eukaryotic cytosine methyltransferases. *Annu. Rev. Biochem.* **74**, 481–514 (2005).
13. N. Zimmermann, J. Zschocke, T. Perisic, S. Yu, F. Holsboer, T. Rein, Antidepressants inhibit DNA methyltransferase 1 through reducing G9a levels. *Biochem. J.* **448**, 93–102 (2012).
14. A. J. Sales, C. Biojone, M. S. Terceti, F. S. Guimarães, M. V. M. Gomes, S. R. L. Joca, Antidepressant-like effect induced by systemic and intra-hippocampal administration of DNA methylation inhibitors. *Br. J. Pharmacol.* **164**, 1711–1721 (2011).
15. A. Tadić, L. Müller-Engling, K. F. Schlicht, A. Kotsiari, N. Dreimüller, A. Kleimann, S. Bleich, K. Lieb, H. Frieling, Methylation of the promoter of brain-derived neurotrophic factor exon IV and antidepressant response in major depression. *Mol. Psychiatry* **19**, 281–283 (2014).
16. Y. Dwivedi, H. S. Rizavi, G. N. Pandey, Antidepressants reverse corticosterone-mediated decrease in brain-derived neurotrophic factor expression: Differential regulation of specific exons by antidepressants and corticosterone. *Neuroscience* **139**, 1017–1029 (2006).

17. B. G. Dias, S. B. Banerjee, R. S. Duman, V. A. Vaidya, Differential regulation of Brain Derived Neurotrophic Factor transcripts by antidepressant treatments in the adult rat brain. *Neuropharmacology* **45**, 553–563 (2003).
18. W. Qin, H. Leonhardt, G. Pichler, Regulation of DNA methyltransferase 1 by interactions and modifications. *Nucleus* **2**, 392–402 (2011).
19. S. Kar, M. Deb, D. Sengupta, A. Shilpi, S. Parbin, J. Torrisani, S. Pradhan, S. Patra, An insight into the various regulatory mechanisms modulating human DNA methyltransferase 1 stability and function. *Epigenetics* **7**, 994–1007 (2012).
20. J. F. Glickman, J. G. Pavlovich, N. O. Reich, Peptide mapping of the murine DNA methyltransferase reveals a major phosphorylation site and the start of translation. *J. Biol. Chem.* **272**, 17851–17857 (1997).
21. R. Goyal, P. Rathert, H. Laser, H. Gowher, A. Jeltsch, Phosphorylation of serine-515 activates the Mammalian maintenance methyltransferase Dnmt1. *Epigenetics* **2**, 155–160 (2007).
22. G. Lavoie, P.-O. Estève, N. B. Laulan, S. Pradhan, Y. St-Pierre, PKC isoforms interact with and phosphorylate DNMT1. *BMC Biol.* **9**, 31 (2011).
23. G. Lavoie, Y. St-Pierre, Phosphorylation of human DNMT1: Implication of cyclin-dependent kinases. *Biochem. Biophys. Res. Commun.* **409**, 187–192 (2011).
24. E. R. de Kloet, M. Joëls, F. Holsboer, Stress and the brain: From adaptation to disease. *Nat. Rev. Neurosci.* **6**, 463–475 (2005).
25. G. M. Wochnik, J. Rüegg, G. A. Abel, U. Schmidt, F. Holsboer, T. Rein, FK506-binding proteins 51 and 52 differentially regulate dynein interaction and nuclear translocation of the glucocorticoid receptor in mammalian cells. *J. Biol. Chem.* **280**, 4609–4616 (2005).
26. J.-P. Schülke, G. M. Wochnik, I. Lang-Rollin, N. C. Gassen, R. T. Knapp, B. Berning, A. Yassouridis, T. Rein, Differential impact of tetratricopeptide repeat proteins on the steroid hormone receptors. *PLOS One* **5**, e11717 (2010).
27. D. L. Riggs, P. J. Roberts, S. C. Chirillo, J. Cheung-Flynn, V. Prapapanich, T. Ratajczak, R. Gaber, D. Picard, D. F. Smith, The Hsp90-binding peptidylprolyl isomerase FKBP52 potentiates glucocorticoid signaling in vivo. *EMBO J.* **22**, 1158–1167 (2003).
28. T. R. Hubler, J. G. Scammell, Intronic hormone response elements mediate regulation of *FKBP5* by progestins and glucocorticoids. *Cell Stress Chaperones* **9**, 243–252 (2004).
29. R. S. Lee, K. L. K. Tamashiro, X. Yang, R. H. Purcell, A. Harvey, V. L. Willour, Y. Huo, M. Rongione, G. S. Wand, J. B. Potash, Chronic corticosterone exposure increases expression and decreases deoxyribonucleic acid methylation of *Fkbp5* in mice. *Endocrinology* **151**, 4332–4343 (2010).
30. V. Paakinaho, H. Makkonen, T. Jääskeläinen, J. J. Palvimo, Glucocorticoid receptor activates poised *FKBP51* locus through long-distance interactions. *Mol. Endocrinol.* **24**, 511–525 (2010).
31. E. B. Binder, D. Salyakina, P. Lichtner, G. M. Wochnik, M. Ising, B. Pütz, S. Papiol, S. Seaman, S. Lucae, M. A. Kohli, T. Nickel, H. E. Künzel, B. Fuchs, M. Majer, A. Pfennig, N. Kern, J. Brunner, S. Modell, T. Baghai, T. Deiml, P. Zill, B. Bondy, R. Rupprecht, T. Messer, O. Köhnlein, H. Dabitz, T. Brückl, N. Müller, H. Pfister, R. Lieb, J. C. Mueller, E. Lõhmussaar, T. M. Strom, T. Bettecken, T. Meitinger, M. Uhr, T. Rein, F. Holsboer, B. Muller-Myhsok, Polymorphisms in *FKBP5* are associated with increased recurrence of depressive episodes and rapid response to antidepressant treatment. *Nat. Genet.* **36**, 1319–1325 (2004).
32. M. Lekman, G. Laje, D. Charney, A. J. Rush, A. F. Wilson, A. J. Sorant, R. Lipsky, S. R. Wisniewski, H. Manji, F. J. McMahon, S. Paddock, The *FKBP5*-gene in depression and treatment response—an association study in the Sequenced Treatment Alternatives to Relieve Depression (STAR*D) Cohort. *Biol. Psychiatry* **63**, 1103–1110 (2008).
33. N. C. Gassen, J. Hartmann, J. Zschocke, J. Stepan, K. Hafner, A. Zellner, T. Kirmeier, L. Kollmannsberger, K. V. Wagner, N. Dedic, G. Balsevich, J. M. Deussing, S. Kloiber, S. Lucae, F. Holsboer, M. Eder, M. Uhr, M. Ising, M. V. Schmidt, T. Rein, Association of FKBP51 with priming of autophagy pathways and mediation of antidepressant treatment response: Evidence in cells, mice, and humans. *PLOS Med.* **11**, e1001755 (2014).
34. G. Laje, R. H. Perlis, A. J. Rush, F. J. McMahon, Pharmacogenetics studies in STAR*D: Strengths, limitations, and results. *Psychiatr. Serv.* **60**, 1446–1457 (2009).
35. Y.-F. Zou, F. Wang, X.-L. Feng, W.-F. Li, J.-H. Tao, F.-M. Pan, F. Huang, H. Su, Meta-analysis of FKBP5 gene polymorphisms association with treatment response in patients with mood disorders. *Neurosci. Lett.* **484**, 56–61 (2010).
36. N. C. Gassen, J. Hartmann, A. S. Zannas, A. Kretzschmar, J. Zschocke, G. Maccarrone, K. Hafner, A. Zellner, L. Kollmannsberger, K. V. Wagner, D. Mehta, S. Kloiber, C. W. Turck, S. Lucae, G. P. Chrousos, F. Holsboer, E. B. Binder, M. Ising, M. V. Schmidt, T. Rein, FKBP51 inhibits GSK3β and augments the effects of distinct psychotropic medications. *Mol. Psychiatry* 10.1038/mp.2015.38 (2015).
37. M. Taipale, G. Tucker, J. Peng, I. Krykbaeva, Z. Y. Lin, B. Larsen, H. Choi, B. Berger, A. C. Gingras, S. Lindquist, A quantitative chaperone interaction network reveals the architecture of cellular protein homeostasis pathways. *Cell* **158**, 434–448 (2014).
38. Q. Zhou, A. T. Agoston, P. Atadja, W. G. Nelson, N. E. Davidson, Inhibition of histone deacetylases promotes ubiquitin-dependent proteasomal degradation of DNA methyltransferase 1 in human breast cancer cells. *Mol. Cancer Res.* **6**, 873–883 (2008).
39. W. Luo, F. Dou, A. Rodina, S. Chip, J. Kim, Q. Zhao, K. Moulick, J. Aguirre, N. Wu, P. Greengard, G. Chiosis, Roles of heat-shock protein 90 in maintaining and facilitating the neurodegenerative phenotype in tauopathies. *Proc. Natl. Acad. Sci. U.S.A.* **104**, 9511–9516 (2007).
40. J. P. Lopes, P. Agostinho, Cdk5: Multitasking between physiological and pathological conditions. *Prog. Neurobiol.* **94**, 49–63 (2011).
41. U. K. Jinwal, J. Koren III, S. I. Borysov, A. B. Schmid, J. F. Abisambra, L. J. Blair, A. G. Johnson, J. R. Johnson, C. L. Shults, J. C. O'Leary III, Y. Jin, J. Buchner, M. B. Cox, C. A. Dickey, The Hsp90 cochaperone, FKBP51, increases Tau stability and polymerizes microtubules. *J. Neurosci.* **30**, 591–599 (2010).
42. R. L. Barent, S. C. Nair, D. C. Carr, Y. Ruan, R. A. Rimerman, J. Fulton, Y. Zhang, D. F. Smith, Analysis of FKBP51/FKBP52 chimeras and mutants for Hsp90 binding and association with progesterone receptor complexes 79. *Mol. Endocrinol.* **12**, 342–354 (1998).
43. T. Aid, A. Kazantseva, M. Piirsoo, K. Palm, T. Timmusk, Mouse and rat *BDNF* gene structure and expression revisited. *J. Neurosci. Res.* **85**, 525–535 (2007).
44. F. Boulle, D. L. van den Hove, S. B. Jakob, B. P. Rutten, M. Hamon, J. van Os, K.-P. Lesch, L. Lanfumey, H. W. Steinbusch, G. Kenis, Epigenetic regulation of the BDNF gene: Implications for psychiatric disorders. *Mol. Psychiatry* **17**, 584–596 (2012).
45. K. Martinowich, D. Hattori, H. Wu, S. Fouse, F. He, Y. Hu, G. Fan, Y. E. Sun, DNA methylation-related chromatin remodeling in activity-dependent *BDNF* gene regulation. *Science* **302**, 890–893 (2003).
46. F. D. Lubin, T. L. Roth, J. D. Sweatt, Epigenetic regulation of *bdnf* gene transcription in the consolidation of fear memory. *J. Neurosci.* **28**, 10576–10586 (2008).
47. A. E. West, W. G. Chen, M. B. Dalva, R. E. Dolmetsch, J. M. Kornhauser, A. J. Shaywitz, M. A. Takasu, X. Tao, M. E. Greenberg, Calcium regulation of neuronal gene expression. *Proc. Natl. Acad. Sci. U.S.A.* **98**, 11024–11031 (2001).
48. Y. Wei, P. A. Melas, G. Wegener, A. A. Mathé, C. Lavebratt, Antidepressant-like effect of sodium butyrate is associated with an increase in TET1 and in 5-hydroxymethylation levels in the *Bdnf* gene. *Int. J. Neuropsychopharmacol.* **18**, pyu032 (2014).
49. E. B. Binder, R. G. Bradley, W. Liu, M. P. Epstein, T. C. Deveau, K. B. Mercer, Y. Tang, C. F. Gillespie, C. M. Heim, C. B. Nemeroff, A. C. Schwartz, J. F. Cubells, K. J. Ressler, Association of *FKBP5* polymorphisms and childhood abuse with risk of posttraumatic stress disorder symptoms in adults. *JAMA* **299**, 1291–1305 (2008).
50. C. F. Gillespie, B. Bradley, K. Mercer, A. K. Smith, K. Conneely, M. Gapen, T. Weiss, A. C. Schwartz, J. F. Cubells, K. J. Ressler, Trauma exposure and stress-related disorders in inner city primary care patients. *Gen. Hosp. Psychiatry* **31**, 505–514 (2009).
51. C. Hiemke, P. Baumann, N. Bergemann, A. Conca, O. Dietmaier, K. Egberts, M. Fric, M. Gerlach, C. Greiner, G. Gründer, E. Haen, U. Havemann-Reinecke, S. E. Jaquenoud, H. Kirchherr, G. Laux, U. C. Lutz, T. Messer, M. J. Müller, B. Pfuhlmann, B. Rambeck, P. Riederer, B. Schoppek, J. Stingl, M. Uhr, S. Ulrich, R. Waschgler, G. Zernig, AGNP Consensus Guidelines for Therapeutic Drug Monitoring in Psychiatry: Update 2011. *Pharmacopsychiatry* **44**, 195–235 (2011).
52. J. M. Hennings, T. Owashi, E. B. Binder, S. Horstmann, A. Menke, S. Kloiber, T. Dose, B. Wollweber, D. Spieler, T. Messer, R. Lutz, H. Künzel, T. Bierner, T. Pollmächer, H. Pfister, T. Nickel, A. Sonntag, M. Uhr, M. Ising, F. Holsboer, S. Lucae, Clinical characteristics and treatment outcome in a representative sample of depressed inpatients–Findings from the Munich Antidepressant Response Signature (MARS) project. *J. Psychiatr. Res.* **43**, 215–229 (2009).
53. A. Harris, J. Seckl, Glucocorticoids, prenatal stress and the programming of disease. *Horm. Behav.* **59**, 279–289 (2011).
54. N. Provençal, E. B. Binder, The effects of early life stress on the epigenome: From the womb to adulthood and even before. *Exp. Neurol.* **268**, 10–20 (2015).
55. V. G. Moisiadis, S. G. Matthews, Glucocorticoids and fetal programming part 2: Mechanisms. *Nat. Rev. Endocrinol.* **10**, 403–411 (2014).
56. L. E. Cowen, S. Lindquist, Hsp90 potentiates the rapid evolution of new traits: Drug resistance in diverse fungi. *Science* **309**, 2185–2189 (2005).
57. N. Rohner, D. F. Jarosz, J. E. Kowalko, M. Yoshizawa, W. R. Jeffery, R. L. Borowsky, S. Lindquist, C. J. Tabin, Cryptic variation in morphological evolution: HSP90 as a capacitor for loss of eyes in cavefish. *Science* **342**, 1372–1375 (2013).
58. L. Whitesell, S. Santagata, M. L. Mendillo, N. U. Lin, D. A. Proia, S. Lindquist, HSP90 empowers evolution of resistance to hormonal therapy in human breast cancer models. *Proc. Natl. Acad. Sci. U.S.A.* **111**, 18297–18302 (2014).
59. D. F. Jarosz, S. Lindquist, Hsp90 and environmental stress transform the adaptive value of natural genetic variation. *Science* **330**, 1820–1824 (2010).
60. S. L. Rutherford, S. Lindquist, Hsp90 as a capacitor for morphological evolution. *Nature* **396**, 336–342 (1998).
61. H. Pei, L. Li, B. L. Fridley, G. D. Jenkins, K. R. Kalari, W. Lingle, G. Petersen, Z. Lou, L. Wang, FKBP51 affects cancer cell response to chemotherapy by negatively regulating Akt. *Cancer Cell* **16**, 259–266 (2009).
62. J. C. O'Leary III, S. Dharia, L. J. Blair, S. Brady, A. G. Johnson, M. Peters, J. Cheung-Flynn, M. B. Cox, G. de Erausquin, E. J. Weeber, U. K. Jinwal, C. A. Dickey, A new anti-depressive strategy for the elderly: Ablation of FKBP5/FKBP51. *PLOS One* **6**, e24840 (2011).
63. H. R. Quintá, D. Maschi, C. Gomez-Sanchez, G. Piwien-Pilipuk, M. D. Galigniana, Subcellular rearrangement of hsp90-binding immunophilins accompanies neuronal differentiation and neurite outgrowth. *J. Neurochem.* **115**, 716–734 (2010).

64. C. L. Storer, C. A. Dickey, M. D. Galigniana, T. Rein, M. B. Cox, FKBP51 and FKBP52 in signaling and disease. *Trends Endocrinol. Metab.* **22**, 481–490 (2011).
65. F. Pirkl, J. Buchner, Functional analysis of the hsp90-associated human peptidyl prolyl *cis*/*trans* isomerases FKBP51, FKBP52 and cyp40. *J. Mol. Biol.* **308**, 795–806 (2001).
66. L. Sun, H. Zhao, Z. Xu, Q. Liu, Y. Liang, L. Wang, X. Cai, L. Zhang, L. Hu, G. Wang, X. Zha, Phosphatidylinositol 3-kinase/protein kinase B pathway stabilizes DNA methyltransferase I protein and maintains DNA methylation. *Cell. Signal.* **19**, 2255–2263 (2007).
67. J. Hartmann, K. V. Wagner, C. Liebl, S. H. Scharf, X.-D. Wang, M. Wolf, F. Hausch, T. Rein, U. Schmidt, C. Touma, J. Cheung-Flynn, M. B. Cox, D. F. Smith, F. Holsboer, M. B. Müller, M. V. Schmidt, The involvement of FK506-binding protein 51 (FKBP5) in the behavioral and neuroendocrine effects of chronic social defeat stress. *Neuropharmacology* **62**, 332–339 (2012).
68. C. Touma, N. C. Gassen, L. Herrmann, J. Cheung-Flynn, D. R. Büll, I. A. Ionescu, J.-M. Heinzmann, A. Knapman, A. Siebertz, A.-M. Depping, J. Hartmann, F. Hausch, M. V. Schmidt, F. Holsboer, M. Ising, M. B. Cox, U. Schmidt, T. Rein, FK506 binding protein 5 shapes stress responsiveness: Modulation of neuroendocrine reactivity and coping behavior. *Biol. Psychiatry* **70**, 928–936 (2011).
69. S. Gaali, A. Kirschner, S. Cuboni, J. Hartmann, C. Kozany, G. Balsevich, C. Namendorf, P. Fernandez-Vizarra, C. Sippel, A. S. Zannas, R. Draenert, E. B. Binder, O. F. Almeida, G. Rühter, M. Uhr, M. V. Schmidt, C. Touma, A. Bracher, F. Hausch, Selective inhibitors of the FK506-binding protein 51 by induced fit. *Nat. Chem. Biol.* **11**, 33–37 (2014).
70. A. Roy, E. Gorodetsky, Q. Yuan, D. Goldman, M.-A. Enoch, Interaction of *FKBP5*, a stress-related gene, with childhood trauma increases the risk for attempting suicide. *Neuropsychopharmacology* **35**, 1674–1683 (2010).
71. T. Klengel, D. Mehta, C. Anacker, M. Rex-Haffner, J. C. Pruessner, C. M. Pariante, T. W. Pace, K. B. Mercer, H. S. Mayberg, B. Bradley, C. B. Nemeroff, F. Holsboer, C. M. Heim, K. J. Ressler, T. Rein, E. B. Binder, Allele-specific *FKBP5* DNA demethylation mediates gene–childhood trauma interactions. *Nat. Neurosci.* **16**, 33–41 (2013).
72. B. Franke, M. Figiel, J. Engele, CNS glia are targets for GDNF and neurturin. *Histochem. Cell Biol.* **110**, 595–601 (1998).
73. B. G. Schumann, P. Jutzi, I. Roditi, Genome-wide RNAi screens in bloodstream form trypanosomes identify drug transporters . *Mol. Biochem. Parasitol.* **175**, 91–94 (2011).
74. S. van den Heuvel, E. Harlow, Distinct roles for cyclin-dependent kinases in cell cycle control. *Science* **262**, 2050–2054 (1993).
75. M. V. Schmidt, V. Sterlemann, K. Ganea, C. Liebl, S. Alam, D. Harbich, M. Greetfeld, M. Uhr, F. Holsboer, M. B. Müller, Persistent neuroendocrine and behavioral effects of a novel, etiologically relevant mouse paradigm for chronic social stress during adolescence. *Psychoneuroendocrinology* **32**, 417–429 (2007).
76. T. Pfaffeneder, F. Spada, M. Wagner, C. Brandmayr, S. K. Laube, D. Eisen, M. Truss, J. Steinbacher, B. Hackner, O. Kotljarova, D. Schuermann, S. Michalakis, O. Kosmatchev, S. Schiesser, B. Steigenberger, N. Raddaoui, G. Kashiwazaki, U. Müller, C. G. Spruijt, M. Vermeulen, H. Leonhardt, P. Schär, M. Müller, T. Carell, Tet oxidizes thymine to 5-hydroxymethyluracil in mouse embryonic stem cell DNA. *Nat. Chem. Biol.* **10**, 574–581 (2014).
77. D. Mehta, T. Klengel, K. N. Conneely, A. K. Smith, A. Altmann, T. W. Pace, M. Rex-Haffner, A. Loeschner, M. Gonik, K. B. Mercer, B. Bradley, B. Müller-Myhsok, K. J. Ressler, E. B. Binder, Childhood maltreatment is associated with distinct genomic and epigenetic profiles in posttraumatic stress disorder. *Proc. Natl. Acad. Sci. U.S.A.* **110**, 8302–8307 (2013).
78. M. J. Aryee, A. E. Jaffe, H. Corrada-Bravo, C. Ladd-Acosta, A. P. Feinberg, K. D. Hansen, R. A. Irizarry, Minfi: A flexible and comprehensive Bioconductor package for the analysis of Infinium DNA methylation microarrays. *Bioinformatics* **30**, 1363–1369 (2014).
79. E. M. Price, A. M. Cotton, L. L. Lam, P. Farré, E. Emberly, C. J. Brown, W. P. Robinson, M. S. Kobor, Additional annotation enhances potential for biologically-relevant analysis of the Illumina Infinium HumanMethylation450 BeadChip array. *Epigenetics Chromatin* **6**, 4 (2013).
80. Y.-A. Chen, M. Lemire, S. Choufani, D. T. Butcher, D. Grafodatskaya, B. W. Zanke, S. Gallinger, T. J. Hudson, R. Weksberg, Discovery of cross-reactive probes and polymorphic CpGs in the Illumina Infinium HumanMethylation450 microarray. *Epigenetics* **8**, 203–209 (2013).
81. J.-P. Fortin, A. Labbe, M. Lemire, B. W. Zanke, T. J. Hudson, E. J. Fertig, C. M. Greenwood, K. D. Hansen, Functional normalization of 450k methylation array data improves replication in large cancer studies. *Genome Biol.* **15**, 503 (2014).
82. W. E. Johnson, C. Li, A. Rabinovic, Adjusting batch effects in microarray expression data using empirical Bayes methods. *Biostatistics* **8**, 118–127 (2007).
83. W. Huber, A. von Heydebreck, H. Sültmann, A. Poustka, M. Vingron, Variance stabilization applied to microarray data calibration and to the quantification of differential expression. *Bioinformatics* **18**, S96–S104 (2002).
84. P. Du, X. Zhang, C.-C. Huang, N. Jafari, W. A. Kibbe, L. Hou, S. M. Lin, Comparison of Beta-value and M-value methods for quantifying methylation levels by microarray analysis. *BMC* Bioinformatics **11**, 587 (2010).
85. A. Menke, J. Arloth, B. Pütz, P. Weber, T. Klengel, D. Mehta, M. Gonik, M. Rex-Haffner, J. Rubel, M. Uhr, S. Lucae, J. M. Deussing, B. Müller-Myhsok, F. Holsboer, E. B. Binder, Dexamethasone stimulated gene expression in peripheral blood is a sensitive marker for glucocorticoid receptor resistance in depressed patients. *Neuropsychopharmacology* **37**, 1455–1464 (2012).

Acknowledgments: We are indebted to J. Hornung for performing the BDNF ELISA analysis. We also thank C. Behl (University of Mainz, Germany) and M. Cox (University of Texas at El Paso) for providing us with SKNMC cells and MEFs, respectively. **Funding:** N.C.G. was supported in part by a European Research Council (ERC) starting grant to E.B.B. [Framework Programme 7 grant no. 281338 (GxE-MOLMECH)]. A.S.Z. was supported in part by ERC starting grant 281338 and in part by a Marie-Sklodowska Curie fellowship (H2020 grant #653240). J.R. credits funding from the Swiss National Science Foundation (PZ00P3_126319) and from the Swedish Research Council Formas. G.P.C. was supported by the National and Kapodistrian University of Athens. **Author contributions:** N.C.G. and G.R.F. performed biochemical and molecular biology experiments and contributed to the study design and manuscript preparation; A.S.Z. performed the correlation analysis in the Grady sample and performed the statistical analyses; J.H. provided animal tissue and performed the in situ hybridization assays; J.Z. contributed to the study design; K.H. performed molecular biology and cell culture experiments; T.C.-R. and M.I. performed the statistical analyses; J.S. performed the global methylation analysis; S.N.P. contributed to the DNMT1 activity assay; L.H. contributed to the in situ hybridization assays; M.K. and F.W. provided the BDNF ELISA kit; S.K. and S.L. contributed to the organization of the MARS sample; G.P.C. contributed to manuscript preparation; T.C. performed the global DNA methylation assays; E.B.B. contributed to organizing the Grady sample collection; M.V.S. provided animal tissue; J.R. performed the bisulfite sequencing, primer design, and pyrosequencing; T.R. contributed to the study design and manuscript preparation. **Competing interests:** The authors declare they have no competing interests. **Data and materials availability:** The raw array data for the Grady study have been deposited to Gene Expression Omnibus, both for gene expression (GSE58137) and DNA methylation (GSE72680).

Submitted 10 June 2015
Accepted 6 November 2015
Final Publication 24 November 2015
10.1126/scisignal.aac7695
Citation: N. C. Gassen, G. R. Fries, A. S. Zannas, J. Hartmann, J. Zschocke, K. Hafner, T. Carrillo-Roa, J. Steinbacher, S. N. Preißinger, L. Hoeijmakers, M. Knop, F. Weber, S. Kloiber, S. Lucae, G. P. Chrousos, T. Carell, M. Ising, E. B. Binder, M. V. Schmidt, J. Rüegg, T. Rein, Chaperoning epigenetics: FKBP51 decreases the activity of DNMT1 and mediates epigenetic effects of the antidepressant paroxetine. *Sci. Signal.* **8**, ra119 (2015).

Chaperoning epigenetics: FKBP51 decreases the activity of DNMT1 and mediates epigenetic effects of the antidepressant paroxetine

Nils C. Gassen, Gabriel R. Fries, Anthony S. Zannas, Jakob Hartmann, Jürgen Zschocke, Kathrin Hafner, Tania Carrillo-Roa, Jessica Steinbacher, S. Nicole Preißinger, Lianne Hoeijmakers, Matthias Knop, Frank Weber, Stefan Kloiber, Susanne Lucae, George P. Chrousos, Thomas Carell, Marcus Ising, Elisabeth B. Binder, Mathias V. Schmidt, Joëlle Rüegg and Theo Rein

(November 24, 2015)
Science Signaling **8** (404), ra119. [doi: 10.1126/scisignal.aac7695]

Stress-responsive FKBP5 is epigenetically upregulated by age and stress-related phenotypes and contributes to NF-κB-driven inflammation and cardiovascular risk

Anthony S. Zannas[1,2,*], Nils C. Gassen[1], Meiwen Jia[1], Jens Baumert[3], Kathrin Hafner[1], Maik Ködel[1], Andreas Haehle[4], Stella Iurato[1], Tania Carrillo-Roa[1], Rebecca T. Emeny[5,3], Jari Lahti[6], Katri Räikkönen[6], Rebecca Waldenberger[3,7], Simone Wahl[3,7], Sonja Kunze[3,7], Susanne Lucae[1], Bekh Bradley[9,8], Christian Gieger[3,7], Felix Hausch[4], Alicia K. Smith[8], Kerry J. Ressler[8,10,11], Karl-Heinz Ladwig[3], Bertram Müller-Myhsok[1], Theo Rein[1], Elisabeth B. Binder[1,8,*]

[1] Department of Translational Research in Psychiatry, Max Planck Institute of Psychiatry, Munich, Germany
[2] Department of Psychiatry and Behavioral Sciences, Duke University Medical Center, Durham, NC, USA
[3] Institute of Epidemiology II, Helmholtz Zentrum München - German Research Centre for Environmental Health, Neuherberg, Germany
[4] Technical University, Darmstadt, Germany
[5] Geisel School of Medicine at Dartmouth, Lebanon, NH, USA
[6] Institute of Behavioural Sciences, University of Helsinki, Helsinki
[7] Research Unit of Molecular Epidemiology, Helmholtz Zentrum München - German Research Centre for Environmental Health, Neuherberg, Germany
[8] Department of Psychiatry and Behavioral Sciences, Emory University Medical School, Atlanta, GA, USA
[9] Atlanta Veterans Affairs Medical Center, Decatur, GA, USA
[10] Division of Depression & Anxiety Disorders, McLean Hospital, Belmont, Massachusetts 02478, USA
[11] Department of Psychiatry, Harvard Medical School, Boston, Massachusetts 02478, USA

***** Correspondence should be addressed to ASZ (anthony_zannas@psych.mpg.de) or EBB (binder@psych.mpg.de)

ABSTRACT

Aging and stress-related phenotypes are associated with heightened inflammation and disease risk, but the underlying molecular mechanisms are unknown. We examined the role in these relations of the stress-responsive immunophilin FKBP5. In four independent human cohorts (total n=2,818), increasing age consistently decreased *FKBP5* methylation at select CpGs, and this age-related demethylation was accelerated by depressive symptoms and childhood trauma and was associated with *FKBP5* upregulation in human peripheral blood. *FKBP5* upregulation was associated with proinflammatory cellular and gene expression profiles and with extensive changes in NF-κB-related genes. In accordance, *FKBP5* overexpression in immune cells promoted chemokine secretion, and it strengthened the interactions of regulatory kinases of NF-κB, but not in the presence of FKBP5 antagonists. Notably, the same age-and stress-related CpGs associated with *FKBP5* upregulation were also demethylated in subjects with myocardial infarction. These findings identify FKBP5 as mediator of stress-driven peripheral inflammation and potential contributor to stress-related cardiovascular risk.

INTRODUCTION

Aging is characterized by a progressive decline in functioning and a gradual increase in disease risk[1], yet individuals of the same age exhibit substantial variability in their risk for developing age-related diseases. Among prevalent risk factors for disease risk, studies support the role of psychosocial stress and stress-related phenotypes, most notably chronic stress and childhood trauma[2-7], as well as major depressive disorder (MDD) and posttraumatic stress disorder (PTSD)[8-10]. Studies further suggest that aging and stress-related phenotypes may synergistically influence disease risk by contributing to peripheral inflammation[8,11-15], but the underlying molecular mechanisms are not well understood.

The effects of stress on inflammation and disease risk could be mediated by stress-responsive molecules able to modulate immune function. A relevant molecule to examine in this context is the immunophilin FK506-binding protein 51 (FKBP51/FKBP5), a co-chaperone that is acutely induced by stress and glucocorticoid exposure and influences several biological pathways, including immune pathways in both cells and mice[16-31]. Interestingly, FKBP5 is not only upregulated by stress, but also in the aging brain[32,33] and in a number of age-related disease phenotypes[24,26,27,32,34]. However, whether age also regulates *FKBP5* in peripheral blood remains unknown. Moreover, given that *FKBP5* can be regulated by stress-induced epigenetic effects[35-38], a plausible hypothesis is that stressors accumulating along the lifespan could lead to a lasting epigenetic upregulation of FKBP5 that may contribute to peripheral inflammation and disease risk.

Here we address these questions using both human cohorts and cellular models. In living humans, increasing age and stress-related phenotypes interact to epigenetically upregulate *FKBP5* in peripheral blood, an effect that contributes to a proinflammatory blood cell composition and gene expression profile and altered NF-κB (nuclear factor kappa-light-chain-enhancer of activated B cells) expression network. In immune cells, FKBP5 overexpression promotes chemokine secretion through physical interactions with key

regulators of the NF- κB pathway, whereas these effects can be prevented by concomitant treatment with FKBP5 antagonists. Notably, the same age-and stress-related epigenetic signatures associated with *FKBP5* upregulation are also observed in subjects with history of myocardial infarction, a condition associated with inflammatory states. These findings provide molecular insights into the mechanisms through which stress-related phenotypes contribute to peripheral inflammation and cardiovascular risk.

RESULTS

FKBP5 methylation decreases along the lifespan at select CpGs

Epigenetic changes occur at susceptible genomic sites throughout life largely as a result of environmental factors[39]. This so-called "epigenetic drift" may account for interindividual variability in genomic function and disease risk[40]. To identify *FKBP5* sites that may be particularly susceptible to environmental factors, including stress exposure along the lifespan, we first examined how *FKBP5* methylation changes with increasing age using Illumina HumanMethylation450 BeadChip array (450K) data from the Grady Trauma Project (GTP; n=393), the Cooperative Health Research in the Region of Augsburg (KORA; n=1,727), and the Max Planck Institute of Psychiatry cohort (MPIP; n=538) (for demographics see **Supplementary Table 1**). These analyses included all available cytosine-guanine dinucleotides (CpGs) covered by the 450K that are located within or in close proximity (10kb upstream or downstream) to the *FKBP5* locus. After controlling for confounders (see Methods) and FDR correction for multiple comparisons, two CpGs (cg20813374 and cg00130530) were consistently and robustly demethylated with age across all cohorts (FDR $q<0.05$; **Supplementary Table 2**). Based on previous annotation of the 450K array[41], the two age-regulated sites are located in close proximity to each other within non-island genomic regions close to the *FKBP5* transcription start site (TSS) (-461bp for cg20813374 and -483bp

for cg00130530; **Supplementary Table 2**). The two CpGs showed significant pairwise correlations across cohorts (GTP: r = 0.83, $p<2.2 \times 10^{-16}$; KORA: r = 0.61, $p<2.2 \times 10^{-16}$; MPIP r = 0.37, $p<2.2 \times 10^{-16}$). The adjusted effect of age on average methylation of the two age-regulated CpGs for all cohorts is depicted on **Fig. 1a**.

Childhood trauma and depressive phenotypes accelerate demethylation of the age-regulated *FKBP5* CpGs

Given that stress exposure can induce demethylation of *FKBP5*[30,35], it is plausible that higher burden of stress or psychopathology across the lifespan could accelerate demethylation of the age-regulated *FKBP5* CpGs. To address this hypothesis, we examined the interactive effects between age and stress-related phenotypes on the age-regulated CpGs. After adjusting for all covariates (see Methods), depressive symptoms significantly accelerated age-related demethylation of *FKBP5* in the GTP, KORA, and MPIP (total n=2,250, meta-analysis interaction $p=3 \times 10^{-2}$; **Fig. 1b**) In contrast, we observed no significant acceleration by childhood maltreatment, lifetime stress, or PTSD in the GTP, where these phenotypes were available. Because MDD has been shown to influence disease profiles by interacting with childhood trauma[8], we further examined whether the effect of depression on age-related *FKBP5* demethylation is moderated by childhood trauma severity as measured with the childhood trauma questionnaire (CTQ) in the GTP. This stratified analysis yielded a significant age-depression interaction in the higher-CTQ (interaction $p=4.6 \times 10^{-2}$) but not the lower-CTQ group (interaction $p=3.3 \times 10^{-1}$). Lastly, to examine whether exposure to a severe and prolonged childhood stressor is sufficient to induce lasting demethylation of the age-regulated CpGs, we compared subjects that underwent prolonged early childhood separation from their parents with sex- and age-matched nonseparated controls in the Helsinki Birth Cohort Study (HBCS; n=160, for demographics see **Supplementary Table 1**). Separation was associated with demethylation of the age-regulated CpGs ($p=7.4 \times 10^{-3}$; **Fig. 1c**).

Together, these findings suggest that childhood trauma and depressive phenotypes synergize to accelerate age-related demethylation of *FKBP5*.

Aging and stress-related phenotypes epigenetically upregulate *FKBP5* in peripheral blood

Changes in DNA methylation can shape gene expression, eventually contributing to cellular function and phenotypic expression[42-44]. To examine whether age-related changes in *FKBP5* methylation influence *FKBP5* expression levels, we used *FKBP5* mRNA data measured in the GTP cohort with Illumina HumanHT-12 v3 and v4 Expression BeadChip arrays (n=355). After controlling for confounders (see Methods), *FKBP5* expression negatively correlated with methylation of the age-regulated sites ($p=1.6 \times 10^{-2}$; **Fig. 2a**). Given that *FKBP5* mRNA is robustly induced by glucocorticoids[30,45], we next examined whether age-related *FKBP5* demethylation moderates the effect of cortisol on *FKBP5* expression. After confirming a strong positive association between cortisol and *FKBP5* levels ($p=2.3 \times 10^{-9}$), we found that the cortisol-*FKBP5* relationship was stronger at lower as compared to higher methylation levels (interaction $p=1.4 \times 10^{-3}$)**,** as well as in older as compared to younger subjects (interaction $p=2.4 \times 10^{-5}$) **(Fig. 2b)**. Furthermore, depressive symptoms strengthened the cortisol-*FKBP5* relationship but only in the high-CTQ group (interaction $p = 7.3 \times 10^{-5}$) **(Figure 2c)**. Overall, these findings indicate that increasing age interacts with stress-related phenotypes to epigenetically upregulate *FKBP5*.

FKBP5 upregulation promotes NF-κB-driven peripheral inflammation and chemotaxis

FKBP5 upregulation has been previously linked with the development of aberrant phenotypes, an effect that may be driven by alterations in distinct biological pathways[24-27,32,34,46,47]. To examine the genome-wide functional implications of *FKBP5* in peripheral

blood, we correlated the *FKBP5* expression levels with all genes in the GTP (n=355). After FDR correction for multiple comparisons, *FKBP5* showed significant correlation (FDR-adjusted $p<0.05$) with a total of 3,275 genes (**Supplementary Table 3**). Using these genes as input and the unique array genes expressed above background (except *FKBP5*) as the reference set of genes (9,538 genes), we then performed disease association analysis in WebGestalt. By far the strongest enrichment was observed for inflammation and was conferred by a total of 123 inflammation-related genes (FDR-adjusted $p=9.2 \times 10^{-6}$; **Fig. 3a**; **Supplementary Table 3**). Notably, *FKBP5* showed strong positive associations with a host of proinflammatory genes, such as interleukin and toll-like receptors. To examine whether this proinflammatory profile may be explained by changes in peripheral blood composition, we correlated *FKBP5* expression levels with blood cell proportions. Higher *FKBP5* levels correlated with increased granulocyte to lymphocyte (G/L) ratio ($p=8.3 \times 10^{-9}$; (**Supplementary Fig. 1**), suggesting that *FKBP5* upregulation is associated with enhanced chemotaxis of proinflammatory cells. To test this hypothesis, we overexpressed FKBP5 in Jurkat T cells (≈3.2-fold induction; **Fig. 3b**) and tested their potential to secrete interleukin-8 (IL-8), a major chemokine that promotes granulocyte chemotaxis and peripheral inflammation. FKBP5 overexpression nearly doubled secretion of IL-8 upon immune stimulation ($p=4.4 \times 10^{-7}$; **Fig. 3c**).

To examine whether the proinflammatory effect of FKBP5 may be driven by distinct transcription factors, we then performed transcription factor target analysis in the GTP using the same input and reference gene sets (3,275/9,538). The strongest enrichment was observed for NF-κB (FDR-adjusted adjusted $p=4.8 \times 10^{-3}$; **Figure 3a**; **Supplementary Table 3**), a master immune regulator that can be influenced by FKBP5[20,26]. To experimentally confirm that FKBP5 upregulation promotes NF-κB signaling in immune cells, we performed dual-luciferase reporter assays comparing NF-κB activity between Jurkat cells overexpressing FKBP5 and cells expressing control vector. FKBP5 overexpression resulted in increased NF-

κB activity following immune stimulation **(Fig. 3d)**. Taken together, these findings indicate that FKBP5 upregulation in peripheral blood promotes peripheral inflammation through effects on NF-κB signaling. Therefore, our further analyses sought to better characterize the mechanisms via which FKBP5 impacts the NF-κB pathway.

FKBP5 expression changes are associated with extensive alterations in the NF-κB co-expression network

To determine the effect of FKBP5 on NF-κB signaling, we used gene expression data in the GTP (n=355) to calculate the pairwise correlations between genes encoding molecules that directly interact along the NF-κB pathway, and we adjusted each pairwise correlation for the expression levels of all other partners in the pathway. These partial pairwise correlations were then compared between subjects with higher and those with lower *FKBP5* expression levels (see Methods). As shown arithmetically in **Supplementary Table 4** and schematically in **Fig. 3e**, several partial pairwise correlations significantly differed between the two groups. The strongest effect was noted for the *MAP3K14-CHUK* pair ($r_{low\ FKBP5} = 0.13$ vs. $r_{high\ FKBP5} = -0.28$, $p = 1.9 \times 10^{-3}$), and this effect remained robust after controlling for sex, age, cortisol, and blood cell proportions ($p=7.1 \times 10^{-3}$), indicating that the effects of *FKBP5* on NF-κB signaling are independent of changes in cortisol levels or blood cell composition.

FKBP5 upregulation promotes NF-κB signaling by strengthening the interaction of key regulatory kinases, whereas these effects are prevented by FKBP5 antagonists

Because FKBP5 acts as a molecular co-chaperone, its effects on NF-κB signaling could result from physical interactions of this co-chaperone with regulators of the NF-κB pathway. Intriguingly, *MAP3K14* and *CHUK,* the gene pair most profoundly influenced by changes in *FKBP5* levels (**Fig. 3e)**, encode respectively the NF-kappa-B-inducing kinase (NIK) and the

antagonist of nuclear factor kappa-B kinase subunit alpha (IKK-α), two key regulatory kinases of the non-canonical NF-κB pathway. Specifically, NIK interacts with and phosphorylates IKKα at serine 176 (pIKKα^{S176}), and this phosphorylation event activates IKKα and facilitates NF-κB signaling[48,49].

To examine whether FKBP5 modulates the NIK-IKKα interaction complex, we performed a series of co-immunoprecipitation experiments in human Jurkat cell lines and peripheral blood monocytes (PBMC). These experiments showed an interaction of FKBP5 with both NIK and IKKα and an interaction between NIK and IKKα (**Fig. 4a**). We then examined whether FKBP5 upregulation can strengthen the FKBP5-NIK-IKKα interaction, by stimulating both cell types with the glucocorticoid receptor agonist (DEX), which robustly induces FKBP5 expression[45,47,50]. After confirming the induction (≈2.2-fold) of FKBP5 by DEX (**Fig. 4a**), we found that DEX treatment significantly increased the physical interaction among FKBP5, NIK, and IKKα in both Jurkat cells and PBMC, whereas this enhancement was abolished by concomitant treatment with the recently developed, selective FKBP5 antagonist SAFit1[51] in both cell types (**Fig. 4a,b**). These effects were accompanied by an increase in the functional phosphorylation of IKKα at serine 176 (pIKKα^{S176}), whereas pIKKα^{S176} induction was abolished by treatment with SAFit1 (**Fig. 4c**). The effect on pIKKα^{S176} was recapitulated by FKBP5 overexpression in Jurkat cells (**Fig. 4d**). Furthermore, FKBP5 overexpression nearly doubled NF-κB activity in Jurkat cells, whereas this effect was again prevented by concomitant treatment with SAFit1 **(Fig. 4e)**. These findings support a model whereby FKBP5 upregulation promotes NIK-IKKα interaction, pIKKα^{S176}, and NF-κB signaling, whereas these effects are prevented by concomitant treatment with selective FKBP5 antagonists (**Fig. 4f**).

Age-related *FKBP5* demethylation is associated with history of myocardial infarction

Besides the potential role of DNA methylation in the causality of disease states, recent studies suggest that methylation signatures, including those at stress-responsive loci, may hold promise as biomarkers for disease phenotypes[40,52,53]. Specifically, the converging findings presented above —indicating that demethylation of the age-regulated CpGs upregulates *FKBP5*, which in turn promotes peripheral inflammation— prompted us to ask whether demethylation of the same CpGs is also associated with inflammation-related disease. Inflammatory markers in peripheral blood, and in particular, IL-8 secretion and the G/L ratio shown here to increase with *FKBP5* upregulation, have been linked with increased risk for cardiovascular disease, most notably acute coronary syndromes[54-57]. To examine whether lower methylation of the age-regulated *FKBP5* CpGs is associated with acute cardiovascular risk, we used data on self-reported history of myocardial infarction (MI) that were available in the KORA and the MPIP. After controlling for potential confounders (see Methods), methylation of the age-regulated sites was significantly lower in individuals with positive history for MI in both cohorts (KORA: $p = 4.4 \times 10^{-2}$; MPIP: $p = 3.1 \times 10^{-2}$; **Fig. 5**).

DISCUSSION

Psychosocial stress and related phenotypes are prevalent throughout life and may confer risk for several disease phenotypes, including cardiovascular disease. While the underlying molecular mechanisms are not well understood, stress-related phenotypes have been associated with peripheral inflammation[8,11-13,15], a process that contributes to vascular pathology and disease risk[54-57]. Among potential mediators of stress-driven inflammation, the present study examined the role of the stress-responsive immunophilin FKBP5. Our findings support a model whereby aging and stress-related phenotypes interact to epigenetically upregulate *FKBP5*, an effect that promotes NF-κB-driven peripheral inflammation (**Fig. 6**). Mechanistically, the effects of FKBP5 upregulation on immune function may be in part

mediated by its physical interactions with key regulatory kinases of the NF-κB pathway that are amenable to treatment with FKBP5 antagonists. Importantly, the same age-and stress-related epigenetic signatures associated with *FKBP5* upregulation are also observed in subjects with history of myocardial infarction, suggesting their relevance for heightened cardiovascular risk.

The present study shows that *FKBP5* methylation is influenced by a complex interplay among increasing age, childhood trauma, and depressive symptoms (**Fig. 1**). Focusing on age-regulated *FKBP5* CpGs as potential sites of stress-induced epigenetic drift, we found that depressive symptoms accelerate demethylation of the age-regulated sites. By contrast, childhood trauma exerted both direct effects, as observed in subjects with prolonged early life separation, and indirect effects, as seen by its ability to moderate the effect of depression on age-regulated CpGs. While the cross-sectional nature of these analyses does not allow safe causal inferences, our findings extend previous studies supporting the cumulative impact of lifetime stress on the methylome and the potential of childhood trauma to moderate the epigenetic effects of subsequent adult stressors[52,58]. Notably, both childhood trauma and depressive symptoms led to decreases in *FKBP5* methylation; this is consistent with studies showing that *FKBP5* and other stress-responsive sites undergo demethylation upon stress and glucocorticoid exposure[35,38,52,59]. Together these findings provide novel insights, but also raise intriguing questions, into the mechanisms through which stressful experiences of different types, timing, and duration may interact to induce and stabilize changes in methylation of stress-responsive CpGs along the lifespan.

The effect of aging and stress-related phenotypes on *FKBP5* methylation is in turn associated with a modest increase in *FKBP5* expression and robust strengthening of the cortisol-*FKBP5* relationship in peripheral blood (**Fig. 2**). These findings suggest that older individuals with higher stress burden are likely to show exaggerated *FKBP5* levels in peripheral blood both at baseline and, most notably, upon stress exposure, when blood cortisol

rises. While in many cases dynamic FKBP5 responses favor adaptations to organismal and cellular stress[60-63], FKBP5 upregulation has also been linked with the development of aberrant phenotypes[24-27,32,34,46,47]. The phenotypic outcome may depend on the context of stress exposure and the pleiotropic effects of FKBP5 on downstream biological pathways[30,62,64,65].

In the present study, converging evidence in both living humans and immune cells shows that FKBP5 upregulation contributes to peripheral inflammation by promoting NF-κB signaling and secretion of the NF-κB target IL-8[66] (**Fig. 3**). The FKBP5-driven secretion of IL-8 in Jurkat T cells extends a previous study showing that FKBP5 downregulation suppresses NF-κB-mediated production of IL-8 in melanoma cells[29]. In turn, the proinflammatory effect of FKBP5 we observe in peripheral blood may in part be explained by the IL-8-mediated recruitment of granulocytes in peripheral blood[67], a possibility supported by the positive association we observe between *FKBP5* levels and the G/L ratio (**Supplementary Fig. 3**). Higher G/L ratio and IL-8 levels are associated with heightened cardiovascular risk and mortality[54-56], and because *FKBP5* is the most robustly induced gene by glucocorticoids in human blood[45], older inidividuals with higher levels of stress exposure —who have epigenetic upregulation of *FKBP5*— may be more prone to stress-induced peripheral inflammation and vascular pathology. This pathogenic cascade could explain the association we observe between *FKBP5* demethylation and history of MI (**Fig. 5**) and provides molecular insights into previous associations of stress-related phenotypes with heightened inflammation and cardiovascular risk[2,3,6,7,9,10].

Although FKBP5 has been previously shown to influence various players of the NF-κB pathway, to our knowledge this is the first study to uncover the interaction of FKBP5 with NIK and the functional modulation of the NIK-IKKα interaction upon FKBP5 upregulation and glucocorticoid exposure (**Fig. 4**). The FKBP5-mediated induction of NF-κB activity, which we observe here, is in accordance with the majority of previous studies showing that downregulation of FKBP5 inhibits NF-κB signaling[19-21,23,24,26-29,31], though opposite effects

have been reported in select cell lines[22]. We also show for the first time the effect of FKBP5 on NF-κB signaling in Jurkat T cells and PBMC, both relevant cellular models of peripheral inflammation. Strikingly, the FKBP5-driven induction of NF-κB can be prevented with concomitant use of FKBP5 antagonists (SAFit1). By contrast, as shown both here and in a previous study[51], SAFit1 has no effects on immune function under baseline FKBP5 levels, suggesting that FKBP5 antagonists could prevent the undesirable effects of stress only if targeted at immune systems with upregulated FKBP5.

In conclusion, the present study shows that the immunophilin FKBP5 mediates stress-driven peripheral inflammation, potentially contributing to stress-related cardiovascular risk. While the impact of stress on disease risk is undoubtedly mediated by multiple molecules —each having pleitropic effects on downstream pathways— the present study exemplifies how examining relevant molecules, by using converging evidence from both human cohorts and cellular models, can provide insights into how stress-related phenotypes could shape disease risk at the molecular level.

Figure 1. Childhood trauma and depressive phenotypes accelerate age-related demethylation of *FKBP5*. **(a)** Methylation decreases at age-regulated *FKBP5* CpGs along the lifespan (GTP: β_{age} = -0.0045, p = 8 x 10^{-8}; KORA: β_{age} = - 0.0055, p < 2 x 10^{-16}; MPIP: β_{age} = -0.0066, p = 2.1 x 10^{-8}; total n = 2,818). **(b)** Depressive phenotypes accelerate age-related *FKBP5* demethylation (GTP: β_{age} for moderate/severe depression = -0.0075 vs. β_{age} for no/mild depression = -0.0032; KORA: β_{age} for moderate/severe depression = -0.0063 vs. β_{age} for no/mild depression = -0.0047; MPIP: β_{age} for depressed = -0.0078 vs. β_{age} for non-depressed = -0.0047; total n = 2,250, meta-analysis interaction p = 3 x 10^{-2}, heterogeneity p = 2.8 x 10-1). **(c)** Early life separation is associated with demethylation of the age-regulated *FKBP5* CpGs in the HBCS ($\beta_{separation}$ = -0.0932, mean DNA methylation difference = 1.4%, p=7.4 x 10^{-3}). In all panels, the average methylation of the two age-regulated CpGs (cg20813374 and cg00130530) is depicted. The age-regulated CpGs were determined after examining all 450K-covered CpGs within or in close proximity (10kb upstream or downstream) to the *FKBP5* locus (**Supplementary Table 2**). All coefficients and p values are derived from models using M-values for DNA methylation and after correcting for covariates (see Methods). ** p < 10^{-2}. GTP, Grady Trauma Project; HBCS, Helsinki Birth Cohort Study; KORA, Cooperative Health Research in the Region of Augsburg F4 community study; MPIP, Max Planck Institute of Psychiatry case/control study.

Figure 2. Aging and stress-related phenotypes epigenetically upregulate *FKBP5* in peripheral blood in the Grady Trauma Project (n = 355). **(a)** *FKBP5* expression levels are negatively associated with average methylation of the age-regulated sites (β = -0.3835, p=1.6 x 10^{-2}). **(b)** The cortisol-*FKBP5* relationship is stronger at lower methylation levels of the age-regulated CpGs (interaction p=1.4 x 10^{-3}, $\beta_{cortisol}$ for lower methylation = 0.0299 vs. $\beta_{cortisol}$ for higher methylation = 0.0069) and in older ages (interaction p=2.4 x 10^{-5}, $\beta_{cortisol}$ for older subjects = 0.0376 vs. $\beta_{cortisol}$ for younger subjects = 0.0075). **(c)** Depressive symptoms strengthen the cortisol-D*FKBP5* relationship only in subjects with higher levels of childhood trauma (higher-CTQ group: interaction p=7.3 x 10^{-5}; lower-CTQ group: interaction p=1.4 x 10^{-1}). For all stratified analyses, we performed median splits of the respective continuous variables. All coefficients and p values are derived from models using M-values for DNA methylation and after correcting for covariates (see Methods). CTQ, Childhood Trauma Questionnaire.

Figure 3. *FKBP5* upregulation promotes NF-κB-driven peripheral inflammation. **(a)** *FKBP5*-related genes in peripheral blood show enrichment for inflammation-related genes and NF-κB gene targets. Disease association and transcription factor target analyses were performed using genome-wide gene expression data in the Grady Trauma Project (GTP; n = 355). The number of genes for each analysis is shown in parentheses. Statistical details are provided in **Supplementary Table 3**. **(b)** Control experiment confirming FKBP5 overexpression in Jurkat T cells transfected with FKBP51-FLAG *vs.* cells transfected with the control vector. **(c)** FKBP5 overexpression nearly doubles IL-8 secretion by stimulated Jurkat T cells. The bar graph depicts IL-8 secretion in stimulated cell supernatants measured with ELISA from two independent experiments (n = 8 per condition). For each experiment, fold ratios of IL-8 secretion were calculated relative to stimulated cells expressing the control vector. IL-8 was undetectable in non-stimulated cells (not shown). **(d)** FKBP5 overexpression increases NF-κB activity in stimulated Jurkat T cells. The bar graph depicts NF-κB reporter activity in stimulated cells measured with dual-luciferase reporter assays from three independent experiments (n = 9 per condition). For each experiment, fold ratios of NF-κB activity were calculated relative to non-stimulated cells expressing the control vector. **(e)** *FKBP5* expression changes are associated with extensive alterations in the NF-κB co-expression network in the GTP (n = 355). Stratification in higher- and lower-*FKBP5* expression groups was performed by a median split of *FKBP5* expression levels. The circles depict all genes encoding molecular partners of the NF-κB pathway. Pairwise correlations (blue lines) have been corrected for expression levels of all other genes in the pathway. Continuous lines show positive and dotted lines negative correlations. The thickness of each line corresponds to correlation strength for each pair. The gene pair with the most robust difference in correlation between the two groups (*CHUK-MAP3K14*) is highlighted in orange. Statistical details are provided in **Supplementary Table 4**. ** $p < 10^{-2}$; *** $p < 10^{-3}$.

Figure 4. FKBP5 upregulation promotes NF-κB signaling by strengthening the interaction of key regulatory kinases, whereas these effects are prevented by FKBP5 antagonists. **(a)** Immunoprecipitation (IP) for either FKBP5 or NIK followed by Western blotting in lysates from Jurkat T cells or peripheral blood monocytes (PBMC) treated with dexamethasone (DEX) and/or selective FKBP5 antagonists (SAFit1). Control: without primary antibody (IgG). **(b)** Quantifications of respective IPs, overall showing DEX-induced increase in FKBP5-NIK-IKKα interactions, which is prevented by concomitant treatment with SAFit1 (n = 3 biological replicates per condition). **(c** and **d)** Western blotting in Jurkat and PBMC lysates, overall showing increase in the functional phosphorylation of IKKα at serine 176 (pIKKα) by DEX treatment (c) and FKBP5 overexpression (d), both of which are prevented by SAFit1 treatment (n = 3-4 per condition). **(e)** FKBP5 overexpression increases NF-κB activity in stimulated Jurkat T cells, whereas this increase is prevented by concomitant treatment with SAFit1. The bar graph depicts NF-κB reporter activity measured with dual-luciferase reporter assays from three independent experiments (n = 9 per condition). For each experiment, fold ratios of NF-κB activity were calculated by comparison to cells expressing the control vector. **(e)** Scheme summarizing the model supported by the IP and Western data. FKBP5 upregulation, which can be induced by DEX, strengthens the NIK-IKKα interaction, thereby inducing pIKKα and NF-κB signaling. These effects on NF-κB signaling are prevented by concomitant treatment with SAFit. All statistical comparisons were performed with two-way ANOVAs, and significant two-way interactions were followed by Bonferroni-corrected pairwise comparisons. * $p < 5 \times 10^{-2}$; ** $p < 10^{-2}$; *** $p < 10^{-3}$, significant pairwise comparisons.

Figure 5. Age-related *FKBP5* demethylation is associated with history of myocardial infarction. KORA: N = 1,648 subjects without *vs*. 62 with history of MI, $p = 4.4 \times 10^{-2}$, mean DNA methylation difference = 1.8%; MPIP: N = 310 subjects without *vs*. 8 with history of MI, $p = 3.1 \times 10^{-2}$, mean DNA methylation difference = 4.8%. All p values are derived from models using M-values for DNA methylation and after correcting for covariates (see Methods).

Figure 6. Conceptual scheme summarizing the model supported by the study's findings. Aging, childhood trauma, and depressive symptoms interact to demethylate FKBP5 at select CpGs located 483 bp (cg00130530) and 461bp (cg20813374) upstream from the transcription start site (TSS). These effects derepress *FKBP5* responses in peripheral blood upon stress and/or cortisol exposure. FKBP5 upregulation promotes NF-κB signaling, whereas this effect is prevented by concomitant treatment with FKBP5 antagonists. Disinhibited FKBP5 responses may lead to enhanced chemotaxis of proinflammatory cells and peripheral inflammation, potentially contributing to stress-related cardiovascular risk.

Supplementary Figure 1. Correlation between FKBP5 expression levels and the granulocyte to lymphocyte ratio, a marker of proinflammation that predicts heightened cardiovascular risk[54]. The reported p value is after controlling for covariates (see Methods).

ACKNOWLEDGEMENTS

This work was supported by a Marie-Sklodowska Curie fellowship (H2020 grant# 653240) to ASZ, a grant from the National Institute of Mental Health (MH071538) to KJR, as well as a European Research Council starting grant (grant# 281338, GxE molmech) within the FP7 framework, a grant from the National Alliance for Research in Schizophrenia and Affective Disorders, a grant from the Behrens Weise Stiftung, and a grant by the German Federal Ministry of Education and Research (BMBF) through the Integrated Network IntegraMent (Integrated Understanding of Causes and Mechanisms in Mental Disorders), under the auspices of the e:Med Programme (grant # 01ZX1314J), to EBB.

COMPETING FINANCIAL INTERESTS

The authors declare no competing financial interests.

AUTHOR CONTRIBUTIONS

ASZ and EBB conceived and designed the study. ASZ, JB, TCR, SI, RW, SW, SK, and AKS were involved in the DNA methylation analyses. ASZ, KH, and NCG designed and performed the protein experiments. ASZ and MK designed and performed the ELISA experiments. ASZ designed and performed the reporter gene assays with input from AH and FH. ASZ, MJ, and BM-M designed and performed the pathway analyses. JL, KR, SL, BB, CG, KJR, KHL, and EBB were involved in data collection. ASZ performed all the statistical analyses. ASZ wrote the manuscript with input from EBB. All authors read and approved the final manuscript.

REFERENCES

1. Niccoli, T. & Partridge, L. Ageing as a risk factor for disease. *Current biology : CB* **22**, R741-752 (2012).
2. Chandola, T., Brunner, E. & Marmot, M. Chronic stress at work and the metabolic syndrome: prospective study. *Bmj* **332**, 521-525 (2006).
3. Rozanski, A., Blumenthal, J.A. & Kaplan, J. Impact of psychological factors on the pathogenesis of cardiovascular disease and implications for therapy. *Circulation* **99**, 2192-2217 (1999).
4. Zannas, A.S., McQuoid, D.R., Steffens, D.C., Chrousos, G.P. & Taylor, W.D. Stressful life events, perceived stress, and 12-month course of geriatric depression: direct effects and moderation by the 5-HTTLPR and COMT Val158Met polymorphisms. *Stress* **15**, 425-434 (2012).
5. Peavy, G.M.*, et al.* Effects of chronic stress on memory decline in cognitively normal and mildly impaired older adults. *The American journal of psychiatry* **166**, 1384-1391 (2009).
6. Danese, A. & McEwen, B.S. Adverse childhood experiences, allostasis, allostatic load, and age-related disease. *Physiology & behavior* **106**, 29-39 (2012).
7. Felitti, V.J.*, et al.* Relationship of childhood abuse and household dysfunction to many of the leading causes of death in adults. The Adverse Childhood Experiences (ACE) Study. *American journal of preventive medicine* **14**, 245-258 (1998).
8. Danese, A.*, et al.* Elevated inflammation levels in depressed adults with a history of childhood maltreatment. *Archives of general psychiatry* **65**, 409-415 (2008).
9. Vaccarino, V.*, et al.* Post-traumatic stress disorder and incidence of coronary heart disease: a twin study. *Journal of the American College of Cardiology* **62**, 970-978 (2013).
10. Ruo, B.*, et al.* Depressive symptoms and health-related quality of life: the Heart and Soul Study. *JAMA : the journal of the American Medical Association* **290**, 215-221 (2003).
11. Danese, A., Pariante, C.M., Caspi, A., Taylor, A. & Poulton, R. Childhood maltreatment predicts adult inflammation in a life-course study. *Proceedings of the National Academy of Sciences of the United States of America* **104**, 1319-1324 (2007).
12. Fang, C.Y., Ross, E.A., Pathak, H.B., Godwin, A.K. & Tseng, M. Acculturative stress and inflammation among Chinese immigrant women. *Psychosomatic medicine* **76**, 320-326 (2014).
13. Elovainio, M.*, et al.* Depressive symptoms and C-reactive protein: the Cardiovascular Risk in Young Finns Study. *Psychological medicine* **36**, 797-805 (2006).
14. Franceschi, C. & Campisi, J. Chronic inflammation (inflammaging) and its potential contribution to age-associated diseases. *The journals of gerontology. Series A, Biological sciences and medical sciences* **69 Suppl 1**, S4-9 (2014).
15. Danese, A.*, et al.* Adverse childhood experiences and adult risk factors for age-related disease: depression, inflammation, and clustering of metabolic risk markers. *Archives of pediatrics & adolescent medicine* **163**, 1135-1143 (2009).
16. Baughman, G., Wiederrecht, G.J., Campbell, N.F., Martin, M.M. & Bourgeois, S. FKBP51, a novel T-cell-specific immunophilin capable of calcineurin inhibition. *Molecular and cellular biology* **15**, 4395-4402 (1995).
17. Li, T.K., Baksh, S., Cristillo, A.D. & Bierer, B.E. Calcium- and FK506-independent interaction between the immunophilin FKBP51 and calcineurin. *Journal of cellular biochemistry* **84**, 460-471 (2002).
18. Weiwad, M.*, et al.* Comparative analysis of calcineurin inhibition by complexes of immunosuppressive drugs with human FK506 binding proteins. *Biochemistry* **45**, 15776-15784 (2006).
19. Avellino, R.*, et al.* Rapamycin stimulates apoptosis of childhood acute lymphoblastic leukemia cells. *Blood* **106**, 1400-1406 (2005).

20. Bouwmeester, T.*, et al.* A physical and functional map of the human TNF-alpha/NF-kappa B signal transduction pathway. *Nature cell biology* **6**, 97-105 (2004).
21. Daudt, D.R. & Yorio, T. FKBP51 protects 661w cell culture from staurosporine-induced apoptosis. *Molecular vision* **17**, 1172-1181 (2011).
22. Erlejman, A.G.*, et al.* NF-kappaB transcriptional activity is modulated by FK506-binding proteins FKBP51 and FKBP52: a role for peptidyl-prolyl isomerase activity. *The Journal of biological chemistry* **289**, 26263-26276 (2014).
23. Giordano, A.*, et al.* Rapamycin antagonizes NF-kappaB nuclear translocation activated by TNF-alpha in primary vascular smooth muscle cells and enhances apoptosis. *American journal of physiology. Heart and circulatory physiology* **290**, H2459-2465 (2006).
24. Kim, Y.S.*, et al.* Functional changes in myeloid-derived suppressor cells (MDSCs) during tumor growth: FKBP51 contributes to the regulation of the immunosuppressive function of MDSCs. *Journal of immunology (Baltimore, Md. : 1950)* **188**, 4226-4234 (2012).
25. Maiaru, M.*, et al.* The stress regulator FKBP51 drives chronic pain by modulating spinal glucocorticoid signaling. *Science translational medicine* **8**, 325ra319 (2016).
26. Romano, M.F.*, et al.* Rapamycin inhibits doxorubicin-induced NF-kappaB/Rel nuclear activity and enhances the apoptosis of melanoma cells. *European journal of cancer (Oxford, England : 1990)* **40**, 2829-2836 (2004).
27. Romano, S.*, et al.* Role of FK506-binding protein 51 in the control of apoptosis of irradiated melanoma cells. *Cell death and differentiation* **17**, 145-157 (2010).
28. Romano, S.*, et al.* FKBP51 employs both scaffold and isomerase functions to promote NF-kappaB activation in melanoma. *Nucleic acids research* **43**, 6983-6993 (2015).
29. Srivastava, S.K.*, et al.* Interleukin-8 is a key mediator of FKBP51-induced melanoma growth, angiogenesis and metastasis. *British journal of cancer* **112**, 1772-1781 (2015).
30. Zannas, A.S., Wiechmann, T., Gassen, N.C. & Binder, E.B. Gene-Stress-Epigenetic Regulation of FKBP5: Clinical and Translational Implications. *Neuropsychopharmacology : official publication of the American College of Neuropsychopharmacology* **41**, 261-274 (2016).
31. Park, J.*, et al.* Glucocorticoids modulate NF-kappaB-dependent gene expression by up-regulating FKBP51 expression in Newcastle disease virus-infected chickens. *Molecular and cellular endocrinology* **278**, 7-17 (2007).
32. Blair, L.J.*, et al.* Accelerated neurodegeneration through chaperone-mediated oligomerization of tau. *The Journal of clinical investigation* **123**, 4158-4169 (2013).
33. Jinwal, U.K.*, et al.* The Hsp90 cochaperone, FKBP51, increases Tau stability and polymerizes microtubules. *The Journal of neuroscience : the official journal of the Society for Neuroscience* **30**, 591-599 (2010).
34. Pereira, M.J.*, et al.* FKBP5 expression in human adipose tissue increases following dexamethasone exposure and is associated with insulin resistance. *Metabolism: clinical and experimental* **63**, 1198-1208 (2014).
35. Klengel, T.*, et al.* Allele-specific FKBP5 DNA demethylation mediates gene-childhood trauma interactions. *Nature neuroscience* **16**, 33-41 (2013).
36. Lee, R.S.*, et al.* Chronic corticosterone exposure increases expression and decreases deoxyribonucleic acid methylation of Fkbp5 in mice. *Endocrinology* **151**, 4332-4343 (2010).
37. Lee, R.S.*, et al.* A measure of glucocorticoid load provided by DNA methylation of Fkbp5 in mice. *Psychopharmacology* **218**, 303-312 (2011).
38. Wiench, M.*, et al.* DNA methylation status predicts cell type-specific enhancer activity. *The EMBO journal* **30**, 3028-3039 (2011).
39. Tan, Q.*, et al.* Epigenetic drift in the aging genome: a ten-year follow-up in an elderly twin cohort. *International journal of epidemiology* **45**, 1146-1158 (2016).
40. Gassen, N.C., Chrousos, G.P., Binder, E.B. & Zannas, A.S. Life stress, glucocorticoid signaling, and the aging epigenome: Implications for aging-related diseases. *Neurosci Biobehav Rev* (2016).

41. Price, M.E.*, et al.* Additional annotation enhances potential for biologically-relevant analysis of the Illumina Infinium HumanMethylation450 BeadChip array. *Epigenetics & chromatin* **6**, 4 (2013).
42. Irvine, R.A., Lin, I.G. & Hsieh, C.L. DNA methylation has a local effect on transcription and histone acetylation. *Molecular and cellular biology* **22**, 6689-6696 (2002).
43. Sun, Z.*, et al.* Integrated analysis of gene expression, CpG island methylation, and gene copy number in breast cancer cells by deep sequencing. *PloS one* **6**, e17490 (2011).
44. Zannas, A.S. & West, A.E. Epigenetics and the regulation of stress vulnerability and resilience. *Neuroscience* **264**, 157-170 (2014).
45. Menke, A.*, et al.* Dexamethasone stimulated gene expression in peripheral blood is a sensitive marker for glucocorticoid receptor resistance in depressed patients. *Neuropsychopharmacology : official publication of the American College of Neuropsychopharmacology* **37**, 1455-1464 (2012).
46. Sabbagh, J.J.*, et al.* Age-associated epigenetic upregulation of the FKBP5 gene selectively impairs stress resiliency. *PloS one* **9**, e107241 (2014).
47. Zannas, A.S., Wiechmann, T., Gassen, N.C. & Binder, E.B. Gene-Stress-Epigenetic Regulation of FKBP5: Clinical and Translational Implications. *Neuropsychopharmacology : official publication of the American College of Neuropsychopharmacology* (2015).
48. Ling, L., Cao, Z. & Goeddel, D.V. NF-kappaB-inducing kinase activates IKK-alpha by phosphorylation of Ser-176. *Proceedings of the National Academy of Sciences of the United States of America* **95**, 3792-3797 (1998).
49. Oeckinghaus, A. & Ghosh, S. The NF-kappaB family of transcription factors and its regulation. *Cold Spring Harbor perspectives in biology* **1**, a000034 (2009).
50. Zannas, A.S. & Binder, E.B. Gene-environment interactions at the FKBP5 locus: sensitive periods, mechanisms and pleiotropism. *Genes, brain, and behavior* (2013).
51. Gaali, S.*, et al.* Selective inhibitors of the FK506-binding protein 51 by induced fit. **11**, 33-37 (2015).
52. Zannas, A.S.*, et al.* Lifetime stress accelerates epigenetic aging in an urban, African American cohort: relevance of glucocorticoid signaling. *Genome biology* **16**, 266 (2015).
53. Horvath, S. DNA methylation age of human tissues and cell types. *Genome biology* **14**, R115 (2013).
54. Bhat, T.*, et al.* Neutrophil to lymphocyte ratio and cardiovascular diseases: a review. *Expert review of cardiovascular therapy* **11**, 55-59 (2013).
55. Boekholdt, S.M.*, et al.* IL-8 plasma concentrations and the risk of future coronary artery disease in apparently healthy men and women: the EPIC-Norfolk prospective population study. *Arteriosclerosis, thrombosis, and vascular biology* **24**, 1503-1508 (2004).
56. Cavusoglu, E.*, et al.* Elevated baseline plasma IL-8 levels are an independent predictor of long-term all-cause mortality in patients with acute coronary syndrome. *Atherosclerosis* **242**, 589-594 (2015).
57. Zhang, X.*, et al.* Interleukin-8 gene polymorphism is associated with acute coronary syndrome in the Chinese Han population. *Cytokine* **56**, 188-191 (2011).
58. Ursini, G.*, et al.* Stress-related methylation of the catechol-O-methyltransferase Val 158 allele predicts human prefrontal cognition and activity. *The Journal of neuroscience : the official journal of the Society for Neuroscience* **31**, 6692-6698 (2011).
59. Thomassin, H., Flavin, M., Espinas, M.L. & Grange, T. Glucocorticoid-induced DNA demethylation and gene memory during development. *The EMBO journal* **20**, 1974-1983 (2001).
60. Gassen, N.C., Hartmann J, Zannas AS, Zschocke J, Maccarrone G, Hafner K, Zellner A, Wagner KV, Mehta D, Kloiber S, Turck CW, Lucae S, Chrousos GP, Holsboer F, Binder EB, Ising M, Schmidt MV, Rein T. FKBP51 inhibits GSK3β and augments the effects of distinct psychotropic medications. *Molecular psychiatry* **In press**(2015).

61. Gassen, N.C.*, et al.* Association of FKBP51 with priming of autophagy pathways and mediation of antidepressant treatment response: evidence in cells, mice, and humans. *PLoS medicine* **11**, e1001755 (2014).
62. Binder, E.B.*, et al.* Polymorphisms in FKBP5 are associated with increased recurrence of depressive episodes and rapid response to antidepressant treatment. *Nature genetics* **36**, 1319-1325 (2004).
63. Gassen, N.C.*, et al.* Chaperoning epigenetics: FKBP51 decreases the activity of DNMT1 and mediates epigenetic effects of the antidepressant paroxetine. *Sci Signal* **8**, ra119 (2015).
64. Touma, C.*, et al.* FK506 binding protein 5 shapes stress responsiveness: modulation of neuroendocrine reactivity and coping behavior. *Biological psychiatry* **70**, 928-936 (2011).
65. Hartmann, J.*, et al.* The involvement of FK506-binding protein 51 (FKBP5) in the behavioral and neuroendocrine effects of chronic social defeat stress. *Neuropharmacology* **62**, 332-339 (2012).
66. Roebuck, K.A. Regulation of interleukin-8 gene expression. *Journal of interferon & cytokine research : the official journal of the International Society for Interferon and Cytokine Research* **19**, 429-438 (1999).
67. Kobayashi, Y. The role of chemokines in neutrophil biology. *Frontiers in bioscience : a journal and virtual library* **13**, 2400-2407 (2008).

Figure 1

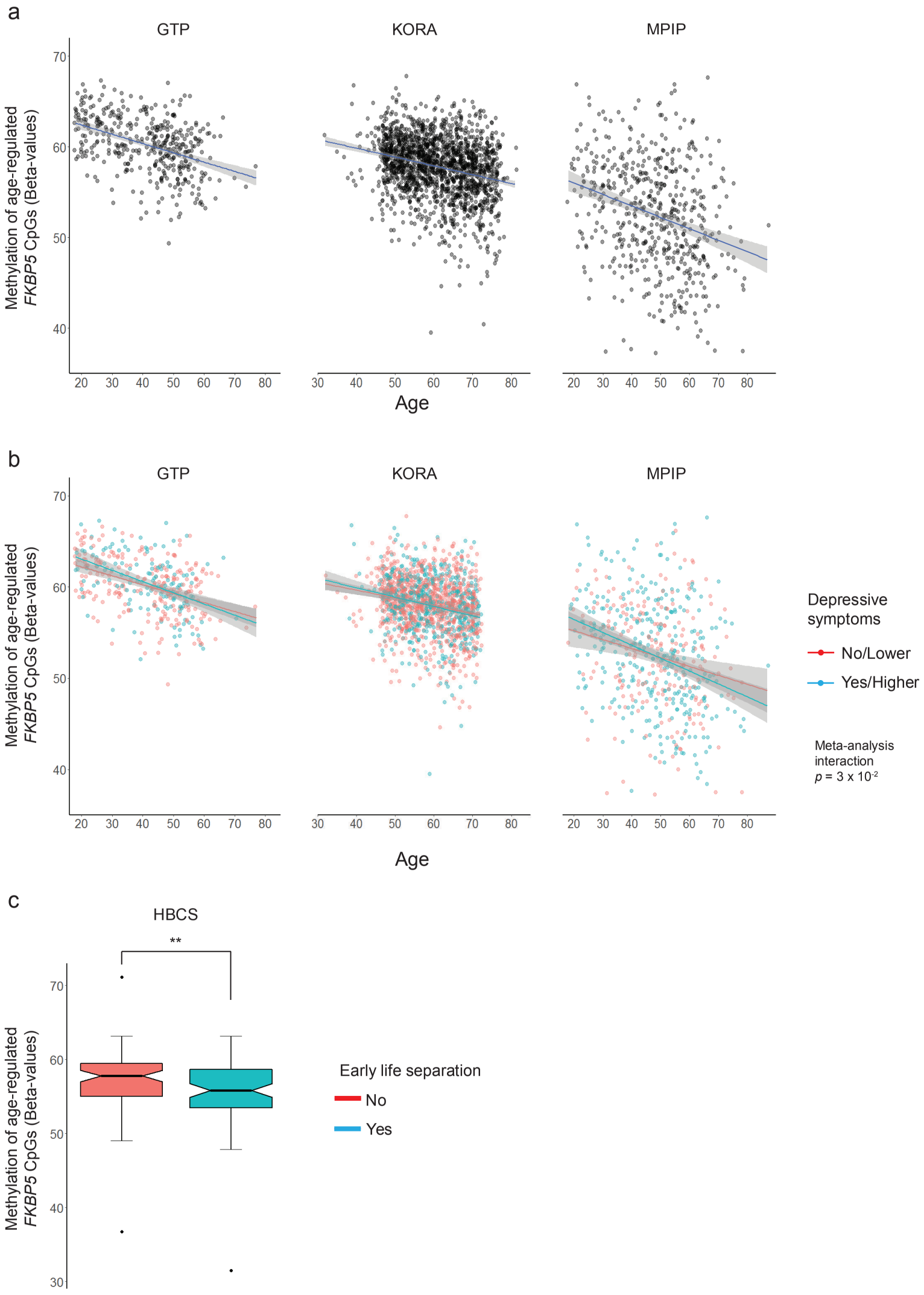
a
GTP
KORA
MPIP
Methylation of age-regulated FKBP5 CpGs (Beta-values)
70
60
50
40
20 30 40 50 60 70 80
30 40 50 60 70 80
Age
b
GTP
KORA
MPIP
Methylation of age-regulated FKBP5 CpGs (Beta-values)
Age
Depressive symptoms
No/Lower
Yes/Higher
Meta-analysis interaction
p = 3 x 10-2
c
HBCS
**
Methylation of age-regulated FKBP5 CpGs (Beta-values)
70
60
50
40
30
Early life separation
No
Yes

Figure 2

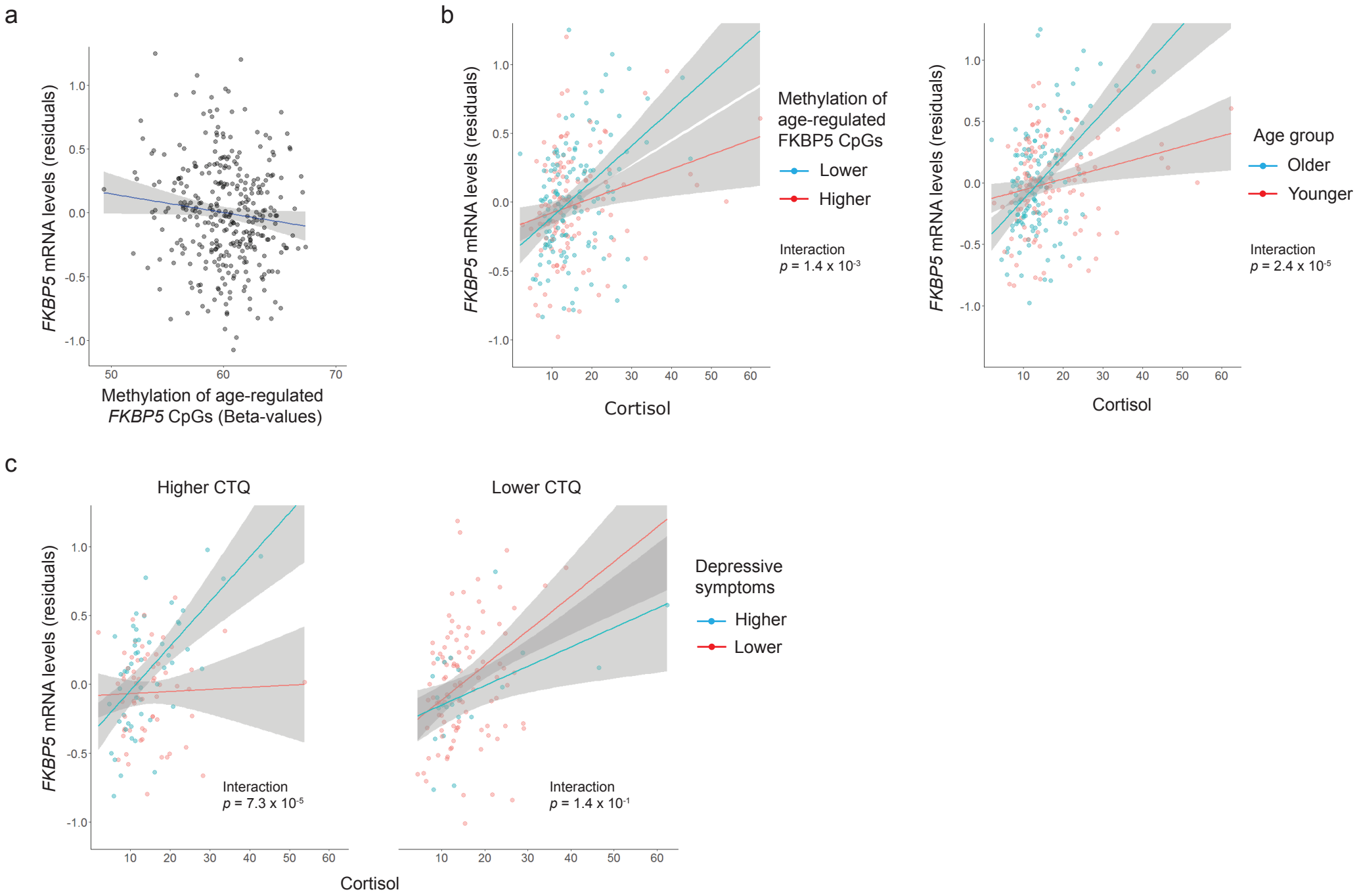
a
FKBP5 mRNA levels (residuals)
Methylation of age-regulated FKBP5 CpGs (Beta-values)
b
FKBP5 mRNA levels (residuals)
Cortisol
Methylation of age-regulated FKBP5 CpGs
Lower
Higher
Interaction p = 1.4 x 10-3
FKBP5 mRNA levels (residuals)
Cortisol
Age group
Older
Younger
Interaction p = 2.4 x 10-5
c
Higher CTQ
Lower CTQ
FKBP5 mRNA levels (residuals)
Interaction p = 7.3 x 10-5
Interaction p = 1.4 x 10-1
Cortisol
Depressive symptoms
Higher
Lower

Figure 3

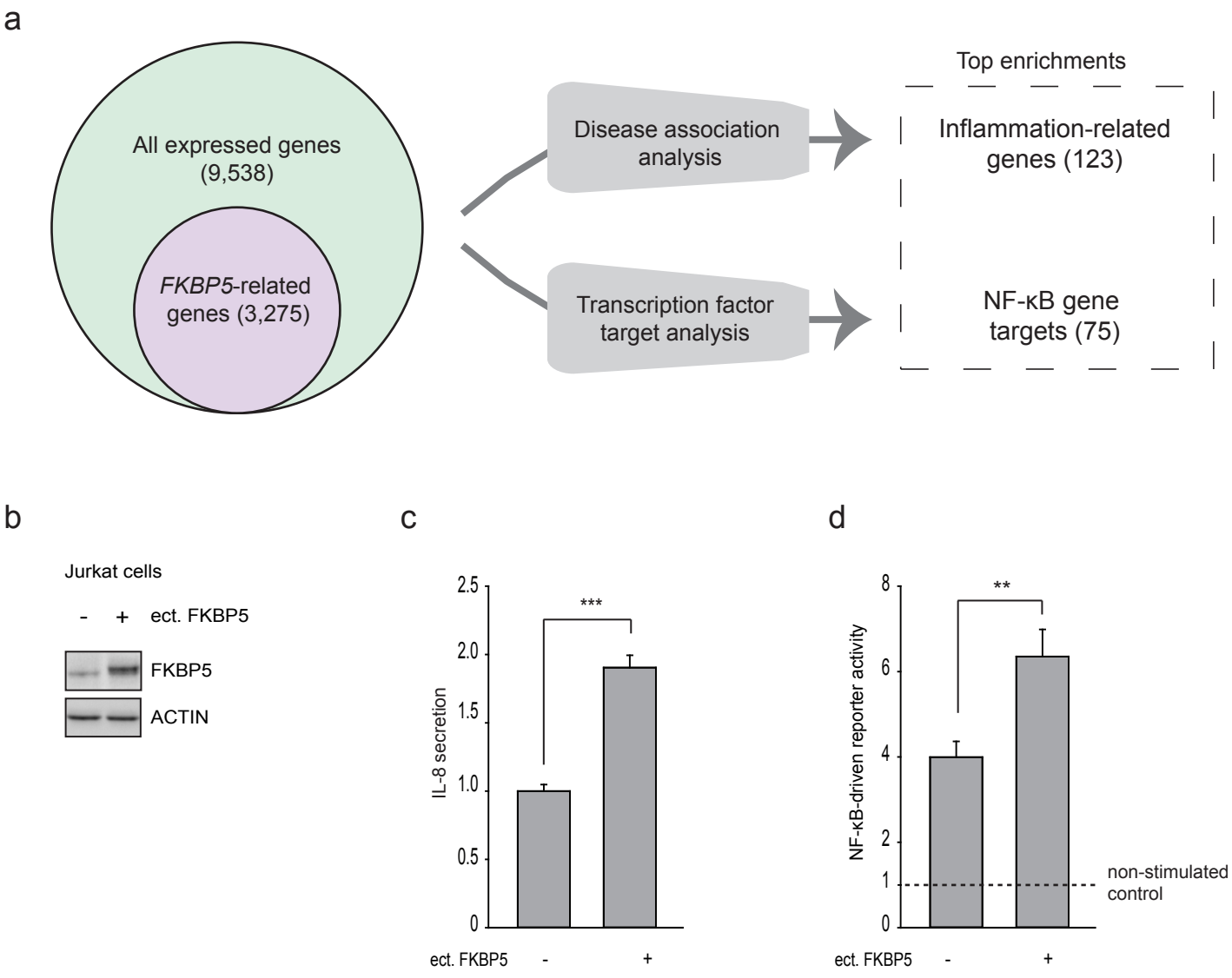
a
All expressed genes (9,538)
FKBP5-related genes (3,275)
Disease association analysis
Transcription factor target analysis
Top enrichments
Inflammation-related genes (123)
NF-κB gene targets (75)
b
Jurkat cells
- + ect. FKBP5
FKBP5
ACTIN
c
IL-8 secretion
2.5
2.0
1.5
1.0
0.5
0
***
ect. FKBP5 - +
d
NF-κB-driven reporter activity
8
6
4
2
1
0
**
non-stimulated control
ect. FKBP5 - +
e
Higher FKBP5 expression levels
Lower FKBP5 expression levels
CD40LG
TRIM25
TNFRSF13C
CD40
DDX58
RELB
TLR4
CD14
TNFSF13B
TICAM1
MYD88
TRAF6
IRAK4
TAB1
TAB3
IRAK1
RIPK1
BCL2
BCL2A1
NFKB2
TRADD
MAP3K7
TAB2
BIRC3
BCL2L1
DADD45B
TNFRSF1A
BIRC2
CXCL8
NFKL
RELA
CHUK
MAP3K14
TRAF5
TNFSF14
IL1B
TNF
LTBR
CFLAR
PTGS2
IKBKB
LTA
TRAF1
TNFAIP3
NFKBIA
BTK
LTB
CSNK2A3
CSNK2A2
IKBKG
CSNK2A1
CSNK2B
PLCG2
SYK
LAT
CARD11
ZAP70
PLCG1
PRKCQ
PRKCB

Figure 4

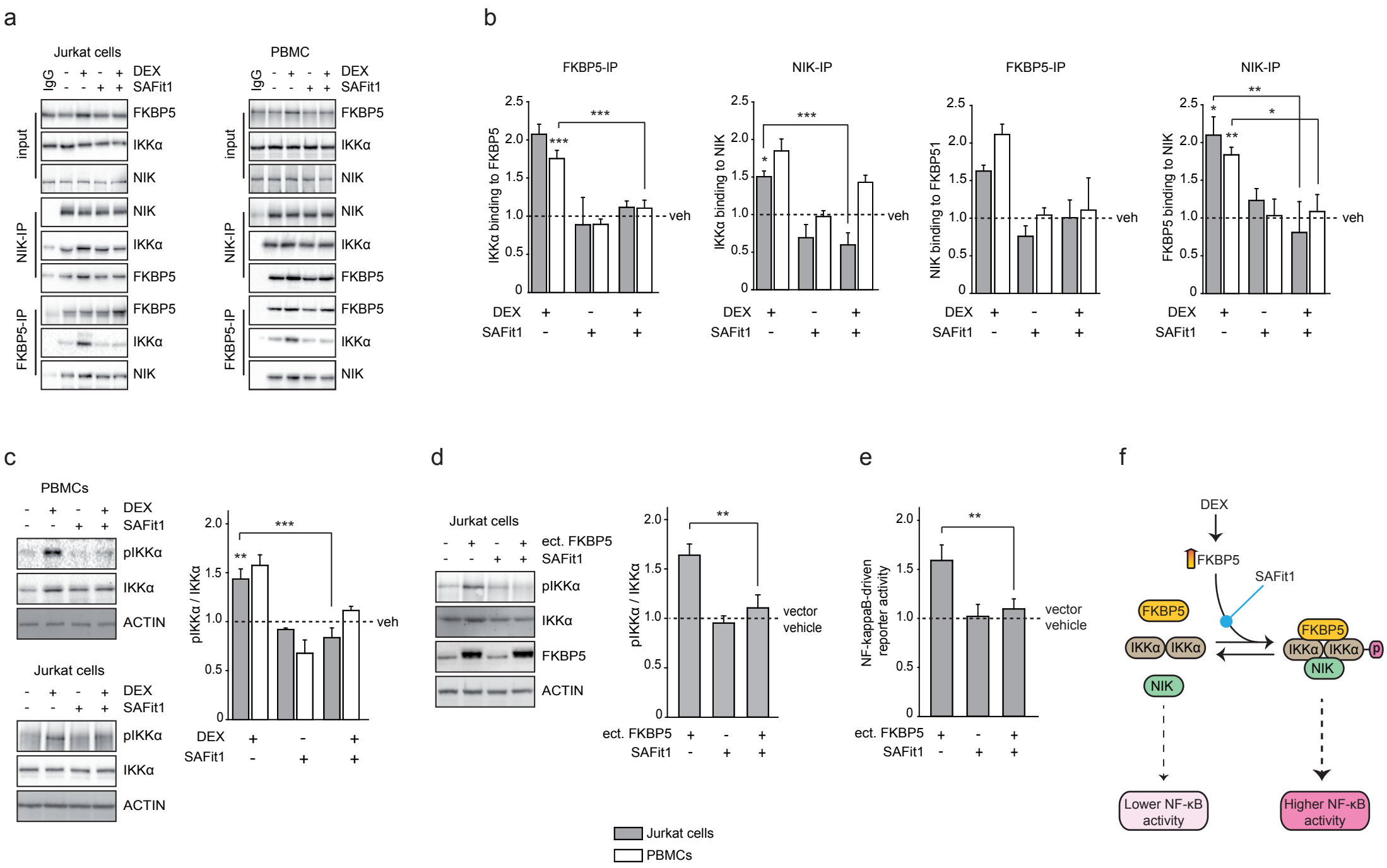
a
Jurkat cells
PBMC
IgG
DEX
SAFit1
input
NIK-IP
FKBP5-IP
FKBP5
IKKα
NIK
b
FKBP5-IP
NIK-IP
IKKα binding to FKBP5
IKKα binding to NIK
NIK binding to FKBP51
FKBP5 binding to NIK
veh
c
PBMCs
Jurkat cells
pIKKα
IKKα
ACTIN
pIKKα / IKKα
d
ect. FKBP5
vector
vehicle
e
NF-kappaB-driven reporter activity
f
DEX
FKBP5
SAFit1
IKKα
NIK
p
Lower NF-κB activity
Higher NF-κB activity
Jurkat cells
PBMCs

Figure 5

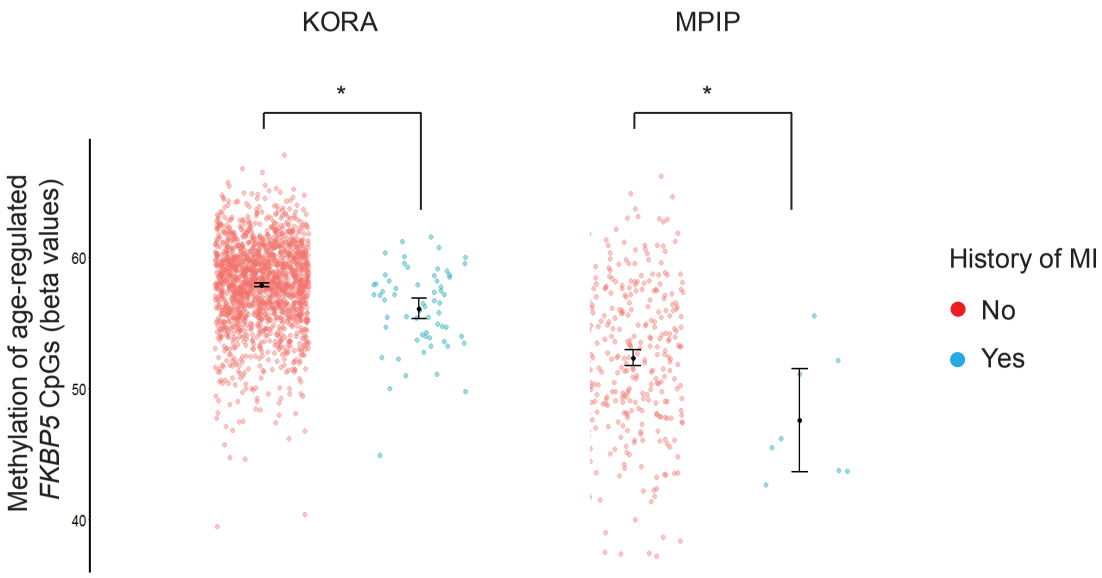
KORA
MPIP
*
*
Methylation of age-regulated
FKBP5 CpGs (beta values)
60
50
40
History of MI
No
Yes

Figure 6

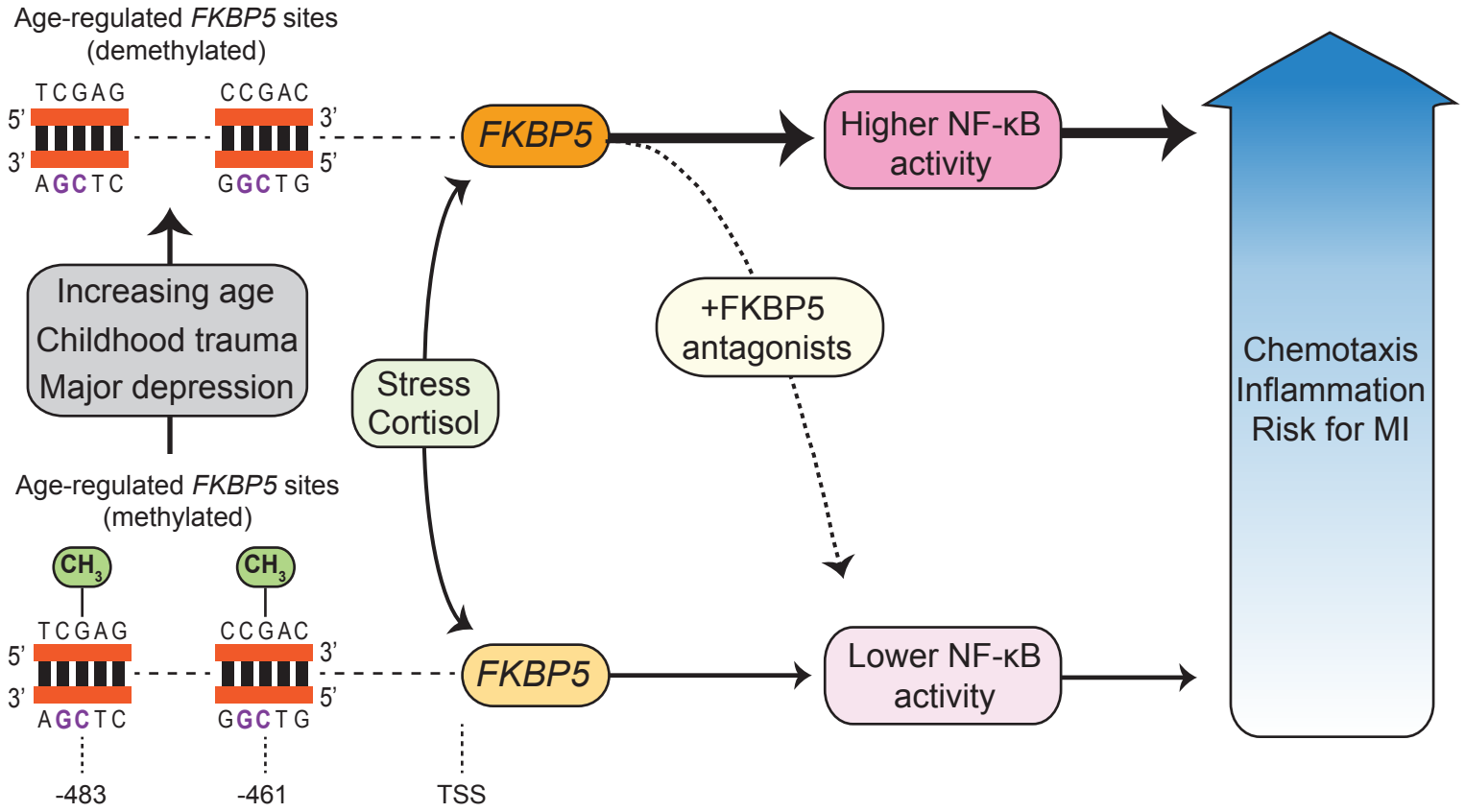
Age-regulated *FKBP5* sites
(demethylated)
TCGAG
CCGAC
5'
3'
3'
5'
AGCTC
GGCTG
Increasing age
Childhood trauma
Major depression
Age-regulated *FKBP5* sites
(methylated)
CH3
CH3
TCGAG
CCGAC
5'
3'
3'
5'
AGCTC
GGCTG
-483
-461
TSS
Stress
Cortisol
FKBP5
FKBP5
Higher NF-κB
activity
Lower NF-κB
activity
+FKBP5
antagonists
Chemotaxis
Inflammation
Risk for MI

Supplementary Table 1. Demographics and characteristics of study cohorts

	Grady (n=411)	**KORA** (n=1,727)	**MPIP** (n=538)	**HBCS** (n=160)
Age, mean, range (SD)	41.4, 18-77 (13)	61, 32-81 (8.9)	47.7, 18-87 (13.4)	63.5, 58-69 (2.8)
Sex, n (%)				
Male	119 (29)	845 (48.9)	229 (42.6)	160 (100)
Female	292 (71)	882 (51.1)	309 (57.4)	NA
Race, n (%)				
AA	411 (100)	NA	NA	NA
Caucasian	NA	1,727 (100)	538 (100)	160 (100)
Other	NA	NA	NA	NA
CTQ, mean (SD)	42.6 (18.3)	NA	NA	NA
Severity of depressive symptoms (BDI), n (%)				
Low	250 (64.6)	NA	NA	NA
High	137 (35.4)	NA	NA	NA
Depressed mood/exhaustion (DEEX), n (%)				
Low	NA	957 (65.2)	NA	NA
High	NA	510 (34.8)	NA	NA

Depressed cases/controls, n (%)				
Nondepressed	NA	NA	209 (39.1)	NA
Depressed	NA	NA	325 (60.9)	NA
Early separation, n (%)				
Separated	NA	NA	NA	80 (50)
Nonseparated	NA	NA	NA	80 (50)
Available 450K data, n	393	1,727	538	160
Available gene expression data, n	355	NA	NA	NA

Supplementary Table 2

name	#bin	chrom	chromStart	chromEnd	score	strand	thickStart
cg20813374	857	chr6	35657180	35657181	120	-	35657180
cg00130530	857	chr6	35657202	35657203	114	-	35657202
cg18357736	857	chr6	35705548	35705549	134	+	35705548
cg23873288	857	chr6	35705850	35705851	477	+	35705850
cg25114611	857	chr6	35696870	35696871	521	-	35696870
cg13719443	857	chr6	35700381	35700382	142	+	35700381
cg19014730	856	chr6	35635984	35635985	648	+	35635984
cg25994725	857	chr6	35703435	35703436	572	-	35703435
cg14642437	857	chr6	35652521	35652522	920	-	35652521
cg03591753	857	chr6	35659140	35659141	736	+	35659140
cg07944278	857	chr6	35699424	35699425	51	+	35699424
cg14284211	856	chr6	35570223	35570224	332	+	35570223
cg17085721	856	chr6	35645341	35645342	910	-	35645341
cg05741161	857	chr6	35699498	35699499	71	+	35699498
cg07061368	856	chr6	35631735	35631736	847	+	35631735
cg21626086	857	chr6	35704928	35704929	764	-	35704928
cg00610228	857	chr6	35695933	35695934	79	+	35695933
cg07485685	857	chr6	35696060	35696061	32	+	35696060
cg00862770	857	chr6	35655763	35655764	41	+	35655763
cg06937024	857	chr6	35695489	35695490	33	-	35695489
cg08915438	857	chr6	35697759	35697760	741	-	35697759
cg10913456	857	chr6	35656589	35656590	15	+	35656589
cg22211300	857	chr6	35704822	35704823	795	-	35704822
cg26868354	857	chr6	35699951	35699952	52	+	35699951
cg01294490	857	chr6	35656905	35656906	93	+	35656905
cg01321308	857	chr6	35704223	35704224	64	+	35704223
cg02665568	856	chr6	35544467	35544468	846	+	35544467
cg10780318	857	chr6	35704148	35704149	77	+	35704148
cg16052510	856	chr6	35603143	35603144	812	-	35603143
cg19226017	857	chr6	35697184	35697185	839	+	35697184
cg07633853	856	chr6	35569471	35569472	433	-	35569471
cg18726036	856	chr6	35543610	35543611	937	-	35543610
cg03546163	857	chr6	35654363	35654364	724	-	35654363
cg23416081	857	chr6	35693572	35693573	621	+	35693572
cg08586216	856	chr6	35612351	35612352	908	-	35612351
cg08636224	857	chr6	35657921	35657922	881	-	35657921
cg00140191	857	chr6	35656242	35656243	37	-	35656242
cg11845071	857	chr6	35695859	35695860	17	-	35695859
cg06087101	856	chr6	35551932	35551933	85	-	35551932
cg07843056	857	chr6	35656847	35656848	11	+	35656847
cg10300814	856	chr6	35565116	35565117	897	-	35565116
cg15929276	857	chr6	35687456	35687457	112	+	35687456
cg16012111	857	chr6	35656757	35656758	63	+	35656757
cg17030679	857	chr6	35696299	35696300	92	+	35696299
cg00052684	857	chr6	35694245	35694246	665	-	35694245

		Effects of age in the Grady				Effects of age in the KORA		
thickEnd	itemRgb	Coefficient	t value	p value	q value	Coefficient	t value	p value
35657181	0,0,205	-0.0054607	-6.11751	3.22E-09	1.42E-07	-0.00736	-12.6943	2.37E-35
35657203	0,0,205	-0.0038199	-4.08717	5.72E-05	1.26E-03	-0.00407	-6.64303	4.12E-11
35705549	0,0,205	-0.0029015	-3.60401	0.000371	0.005444	-0.00492	-5.6474	1.9E-08
35705851	128,0,128	-0.0029819	-3.05615	0.00246	0.02706	-0.00054	-0.74372	0.457148
35696871	128,0,128	-0.0021073	-2.77685	0.005862	0.051584	-0.00298	-5.43903	6.13E-08
35700382	0,0,205	-0.0024314	-2.63532	0.008878	0.065103	-0.00147	-2.56969	0.010263
35635985	255,127,0	-0.0033178	-2.5419	0.011568	0.072716	-0.00197	-1.50514	0.132473
35703436	128,0,128	-0.0021795	-2.46129	0.014451	0.079483	-0.00319	-3.01026	0.002648
35652522	255,127,0	-0.002673	-2.13716	0.033458	0.163571	-0.00154	-1.25236	0.210612
35659141	255,127,0	0.00117248	1.859871	0.06396	0.23452	0.000417	1.258235	0.208479
35699425	0,0,205	0.00307827	1.934743	0.054036	0.23452	0.006041	1.203135	0.22909
35570224	128,0,128	-0.0018162	-1.89744	0.058805	0.23452	-0.00168	-1.54423	0.122719
35645342	255,127,0	-0.001863	-1.79788	0.07328	0.248025	-0.00141	-1.00029	0.317315
35699499	0,0,205	-0.001172	-1.59164	0.112603	0.309658	-0.00017	-0.23048	0.81775
35631736	255,127,0	-0.0020621	-1.6114	0.108227	0.309658	-0.00435	-2.79372	0.005269
35704929	255,127,0	0.00129673	1.59924	0.110903	0.309658	-0.00033	-0.50164	0.615984
35695934	0,0,205	-0.0016398	-1.48257	0.139322	0.360597	0.001211	1.207049	0.22758
35696061	0,0,205	-0.0023459	-1.39365	0.164537	0.402202	-0.00331	-0.36892	0.712232
35655764	0,0,205	0.00121426	1.243536	0.214718	0.43187	0.00051	0.249271	0.803181
35695490	0,0,205	0.00320536	1.240233	0.215935	0.43187	-0.01218	-1.38721	0.165559
35697760	255,127,0	0.00186397	1.304645	0.193093	0.43187	-0.00102	-1.14243	0.253436
35656590	0,0,205	0.00271904	1.251844	0.211679	0.43187	0.004101	0.499023	0.617828
35704823	255,127,0	-0.0008445	-1.18181	0.238291	0.442686	-0.00101	-1.85953	0.063123
35699952	0,0,205	0.00084856	1.173837	0.241465	0.442686	0.0001	0.118814	0.905437
35656906	0,0,205	0.0010166	0.88074	0.37922	0.564982	0.000324	0.260912	0.794192
35704224	0,0,205	0.00061148	0.873269	0.38327	0.564982	-0.0005	-0.6469	0.51778
35544468	255,127,0	0.00110126	0.898657	0.369613	0.564982	-0.00089	-0.62598	0.531411
35704149	0,0,205	0.00077473	0.869699	0.385215	0.564982	0.000589	0.614234	0.539143
35603144	255,127,0	0.0015079	0.949422	0.343231	0.564982	-5.4E-05	-0.02958	0.976409
35697185	255,127,0	-0.0009848	-0.96894	0.333416	0.564982	0.00047	0.498083	0.61849
35569472	128,0,128	-0.0015421	-0.84451	0.399109	0.566477	0.010183	0.986322	0.324385
35543611	255,127,0	0.00100256	0.704214	0.481889	0.662597	-0.00219	-1.92149	0.054836
35654364	255,127,0	0.00124224	0.655363	0.512776	0.682124	-0.00398	-2.33511	0.019671
35693573	255,127,0	-0.0006283	-0.63324	0.527095	0.682124	-0.00169	-3.05802	0.002263
35612352	255,127,0	-0.0005937	-0.52724	0.59845	0.752337	0.00194	1.424833	0.154388
35657922	255,127,0	-0.0004224	-0.45937	0.64633	0.789958	0.0007	0.637144	0.524116
35656243	0,0,205	-0.0005857	-0.28974	0.772231	0.918329	-9.6E-05	-0.01242	0.990089
35695860	0,0,205	-0.0005065	-0.24204	0.808931	0.936657	-0.00549	-0.64994	0.515816
35551933	0,0,205	-1.65E-04	-0.07142	0.943114	0.969369	-0.00341	-2.72711	0.006454
35656848	0,0,205	-0.0001648	-0.03843	0.969369	0.969369	0.003979	0.435325	0.663383
35565117	255,127,0	-4.929E-05	-0.04863	0.961246	0.969369	-0.00152	-1.22509	0.220712
35687457	0,0,205	7.1538E-05	0.046326	0.963083	0.969369	-0.01368	-2.68774	0.007267
35656758	0,0,205	9.83E-05	0.095616	0.923894	0.969369	0.001839	1.452296	0.146603
35696300	0,0,205	1.41E-04	0.125257	0.900411	0.969369	-0.00128	-1.18822	0.234911
35694246	255,127,0	NA	NA	NA	NA	-0.00219	-1.88701	0.059334

Effects of age in the MPIP

q value	Coefficient	t value	p value	q value
1.06E-33	-0.008486326	-5.53062	5.11E-08	2.25E-06
9.28E-10	-0.005942286	-3.72754	0.000215	0.004731
2.85E-07	-0.0051099	-2.84359	0.00464	0.06435
0.709367	-0.000407146	-0.37192	0.710106	0.867907
6.9E-07	-0.003383814	-2.6931	0.007312	0.06435
0.046182	-0.003167353	-1.84487	0.065637	0.320892
0.37258	-0.001988293	-2.03017	0.042859	0.253446
0.019863	-0.001638524	-1.48727	0.137562	0.413116
0.422841	0.000207793	0.140263	0.888508	0.961746
0.422841	-0.001077513	-1.46904	0.142441	0.413116
0.422841	-7.77383E-05	-0.09972	0.920609	0.961746
0.368158	-0.003335117	-1.73301	0.0837	0.368282
0.521333	-5.4397E-05	-0.04799	0.961746	0.961746
0.87616	-0.000906078	-1.05628	0.291343	0.522004
0.033872	-0.000396566	-0.33158	0.74034	0.874458
0.752218	0.000434503	0.444536	0.656844	0.835057
0.422841	0.001132291	0.938634	0.348364	0.567704
0.821806	-0.001161764	-1.52611	0.127603	0.413116
0.87616	-0.000921469	-0.9548	0.340133	0.567704
0.392114	-0.00029627	-0.48165	0.630263	0.835057
0.438639	-0.00419694	-2.75134	0.006147	0.06435
0.752218	-0.001854449	-2.21668	0.027086	0.198633
0.202896	1.54E-04	0.178993	0.858015	0.961746
0.94755	-0.001766213	-1.99954	0.046081	0.253446
0.87616	-0.001616459	-1.37737	0.169002	0.413116
0.713572	-0.001390459	-1.31479	0.189174	0.438087
0.713572	0.001236426	1.055134	0.291865	0.522004
0.713572	-0.0018522	-1.51217	0.131112	0.413116
0.990089	0.001901819	1.044839	0.296593	0.522004
0.752218	0.001205412	0.897713	0.369763	0.57174
0.521333	0.000623096	0.437394	0.662011	0.835057
0.202896	0.001431617	1.08716	0.277481	0.522004
0.080473	7.88E-05	0.103827	0.917347	0.961746
0.019863	-0.001448144	-0.82473	0.409911	0.601203
0.38597	0.001096196	1.420029	0.156211	0.413116
0.713572	0.000743784	0.884529	0.376828	0.57174
0.990089	-5.69E-05	-0.07066	0.943699	0.961746
0.713572	0.000208683	0.311941	0.755213	0.874458
0.036306	-0.001256067	-0.79467	0.427178	0.606317
0.785585	-0.001377381	-1.42132	0.155835	0.413116
0.422841	0.001143342	1.164145	0.244911	0.515902
0.036337	-0.001611337	-1.40639	0.160219	0.413116
0.38597	0.000516412	0.434306	0.66425	0.835057
0.422841	-0.00139674	-1.1609	0.246226	0.515902
0.202896	NA	NA	NA	NA

Disease	Number of Genes
Inflammation	123
Bacterial Infections	56
Necrosis	106
Hydrops Fetalis	21
Hyperpigmentation	18
Gram-Negative Bacterial Infections	39
Common Cold	63
Respiratory Tract Infections	64
Melanosis	15
Bronchial Diseases	57

Supplementary Table 3

Statistics for significant diseases

C=235;O=123;E=80.73;R=1.52;rawP=7.57e-09;adjP=9.21e-06
C=97;O=56;E=33.32;R=1.68;rawP=1.87e-06;adjP=0.0011
C=216;O=106;E=74.20;R=1.43;rawP=4.61e-06;adjP=0.0015
C=27;O=21;E=9.28;R=2.26;rawP=4.80e-06;adjP=0.0015
C=22;O=18;E=7.56;R=2.38;rawP=6.59e-06;adjP=0.0016
C=64;O=39;E=21.99;R=1.77;rawP=1.18e-05;adjP=0.0024
C=120;O=63;E=41.22;R=1.53;rawP=3.02e-05;adjP=0.0053
C=123;O=64;E=42.26;R=1.51;rawP=3.77e-05;adjP=0.0057
C=20;O=15;E=6.87;R=2.18;rawP=0.0002;adjP=0.0221
C=112;O=57;E=38.48;R=1.48;rawP=0.0002;adjP=0.0221

Inflammation-related genes

Gene Symbol	beta coefficient	nominal p value	fdr-adjust p value
MMP9	0.684081518	3.09E-10	2.53E-09
IL1R2	0.566654243	3.13E-27	1.28E-25
CEBPD	0.480668435	1.45E-22	3.76E-21
IL18R1	0.464453217	3.61E-28	2.22E-26
DUSP1	0.449429137	1.61E-18	2.48E-17
ORM1	0.445917893	1.73E-07	6.67E-07
NAMPT	0.435025537	1.08E-08	5.77E-08
IL13RA1	0.41581729	7.87E-18	9.68E-17
IRAK3	0.407098117	1.53E-22	3.76E-21
TLR8	0.388715476	2.17E-16	2.43E-15
TLR2	0.387400934	2.90E-29	3.56E-27
TLR4	0.384626067	4.95E-20	1.02E-18
FPR2	0.377356641	2.21E-08	1.09E-07
TLR5	0.367479198	1.16E-09	8.37E-09
CD163	0.335881522	5.67E-19	9.96E-18
FPR1	0.314000143	1.86E-08	9.51E-08
ITGAM	0.312357016	1.08E-14	1.02E-13
CXCR1	0.310259131	1.37E-07	5.43E-07
ALOX5	0.307999903	4.41E-10	3.39E-09
ALOX5AP	0.297385187	8.46E-09	4.96E-08
S100A12	0.278909351	0.001670509	0.002389217
ADM	0.260029478	0.000641148	0.001065693
TREM1	0.248663489	2.55E-06	7.83E-06
TNFAIP6	0.248610967	0.00257583	0.003481616
ENTPD1	0.245420827	1.42E-15	1.45E-14
LY96	0.239005748	1.90E-05	3.95E-05
CXCL16	0.237317236	8.65E-07	2.95E-06
CEBPB	0.230763623	3.00E-08	1.42E-07
NFKBIA	0.228992201	3.23E-09	1.98E-08
FCGR2A	0.215407732	7.19E-06	1.85E-05
CXCR2	0.211012085	0.001068554	0.001602832
RETN	0.21058321	0.01586697	0.016400314
MYD88	0.208259258	6.46E-08	2.74E-07
NLRP12	0.205071809	1.08E-08	5.77E-08
IL4R	0.20291588	8.88E-05	0.000170727
TNFRSF1A	0.202417641	4.37E-06	1.19E-05
IL1RN	0.198768135	0.00040592	0.000713259
IL6ST	0.198412828	1.40E-06	4.41E-06
IL17RA	0.197957216	3.17E-06	9.28E-06
IL10RB	0.196049234	1.44E-10	1.26E-09
SELL	0.195994519	9.25E-05	0.000175105
C5AR1	0.195238456	0.000205723	0.000377671
CASP1	0.188119209	1.14E-07	4.68E-07
ZFP36	0.183934196	2.93E-06	8.80E-06
SERPINA1	0.179503315	7.22E-06	1.85E-05
TNFSF13B	0.177445234	0.000825575	0.001288621
HSPA1B	0.176420869	5.39E-06	1.44E-05
TIMP1	0.172673927	0.000822678	0.001288621

TLR6	0.168820362	1.01E-06	3.26E-06
PLAUR	0.166612685	1.65E-05	3.55E-05
CD14	0.16611474	0.000276697	0.000493243
CHUK	0.165667344	7.70E-18	9.68E-17
MAPK14	0.164727678	2.18E-09	1.49E-08
OSM	0.164574234	1.23E-05	2.81E-05
NOD2	0.161685042	0.003678409	0.004435729
LTB4R	0.159007204	5.90E-07	2.13E-06
STAT3	0.155460508	4.60E-07	1.72E-06
SELPLG	0.149165939	0.000445034	0.000770974
BCL10	0.148776514	5.46E-08	2.40E-07
CARD8	0.144871565	1.60E-05	3.52E-05
IL6R	0.14012784	0.002147151	0.00293444
PTAFR	0.136092322	0.001921332	0.002716366
IRAK4	0.134877814	2.98E-09	1.93E-08
NFKB1	0.134014828	3.29E-06	9.43E-06
IKBKG	0.130383236	2.85E-05	5.76E-05
ANXA1	0.130203007	0.000827651	0.001288621
PECAM1	0.129501877	0.000892952	0.001372914
F2RL1	0.123314772	0.007587343	0.008407596
NFKBIZ	0.120023326	0.00470153	0.005507506
IRF1	0.11964364	0.012863897	0.013640167
CCR2	0.116629854	9.69E-06	2.29E-05
RCAN1	0.112483772	8.89E-07	2.96E-06
HPSE	0.111383491	0.000244685	0.000442593
SOCS3	0.109583073	0.004550887	0.005382299
ADIPOR2	0.109271796	8.70E-06	2.14E-05
NLRP3	0.104785425	0.000609514	0.001041253
CARD16	0.10350658	1.83E-05	3.88E-05
PIK3CD	0.090833315	0.007494019	0.008379675
PTPN2	0.088722727	0.000702432	0.001151988
TRAF3IP2	0.086542869	0.002961432	0.003695784
TNFAIP3	0.080100771	0.003144102	0.003828956
IL1RAP	0.07949029	0.002828537	0.003626765
HIF1A	0.072219718	0.005202065	0.005979944
TNFAIP8L2	0.061064562	0.002745426	0.003592419
ADORA2B	0.059095047	0.005495082	0.006258287
ADAM17	0.052399583	0.010995964	0.011969059
MAP3K7	0.044048652	0.017079787	0.017079787
TRAF6	0.032325573	0.004846396	0.005623648
MAP3K14	-0.05296715	0.00137599	0.002009456
IL23A	-0.059042421	0.014300211	0.014906152
CCL3	-0.064408626	0.002912586	0.00369328
TNF	-0.064552552	0.011243983	0.012131666
ALOX15	-0.067813122	0.013582075	0.014278592
MAZ	-0.069654198	0.002974655	0.003695784
SFTPD	-0.071748494	0.003825975	0.004568883
IL12RB1	-0.072193083	0.002006878	0.002805068
KLF2	-0.075626476	0.010628397	0.011672258
P2RX7	-0.077772639	0.002830646	0.003626765

PPARD	-0.081043617	1.94E-05	3.97E-05
SIGIRR	-0.082236908	0.002705693	0.003578497
ADORA2A	-0.082809198	0.003124957	0.003828956
IFNG	-0.084841981	0.016847177	0.016985269
BPIFA1	-0.087435574	0.001181906	0.001751499
CD40	-0.089015821	0.000813221	0.001288621
F2R	-0.10420127	4.40E-05	8.58E-05
PLA2G2D	-0.107836381	0.012033862	0.012871
NOD1	-0.108542087	8.53E-06	2.14E-05
TRPA1	-0.124820033	1.45E-05	3.23E-05
CCR6	-0.128247976	3.54E-08	1.61E-07
LTB	-0.137537799	0.000981616	0.001490603
CCL5	-0.138819059	0.016415155	0.01668648
IL18	-0.146424229	0.001388648	0.002009456
IL10	-0.146441153	0.005654359	0.006380607
ACP5	-0.153268287	0.002616126	0.003497646
IL10RA	-0.153655151	1.18E-05	2.74E-05
ICAM2	-0.16220602	7.34E-07	2.58E-06
IL2RB	-0.164932166	0.002072265	0.002863917
CX3CR1	-0.175684408	0.000102118	0.00019031
PPBP	-0.182534847	0.016142107	0.01654566
BDKRB1	-0.198525938	3.04E-05	6.04E-05
IL32	-0.200554941	9.41E-06	2.27E-05
TMSB4X	-0.215714048	3.61E-06	1.01E-05
CLC	-0.326173416	0.00062178	0.001047657

Transcription Factor Target	Number of Genes
hsa_V$NFKB_C	75
hsa_GGGTGGRR_V$PAX4_03	271
hsa_V$PAX4_03	63
hsa_TGACAGNY_V$MEIS1_01	180
hsa_V$ARNT_02	80
hsa_TGANTCA_V$AP1_C	225
hsa_V$AP1FJ_Q2	65
hsa_TTGTTT_V$FOXO4_01	388
hsa_V$MEIS1_01	57
hsa_TAAYNRNNTCC_UNKNOWN	39

Statistics for significant diseases

C=144;O=75;E=49.47;R=1.52;rawP=8.01e-06;adjP=0.0048
C=663;O=271;E=227.77;R=1.19;rawP=0.0002;adjP=0.0242
C=126;O=63;E=43.29;R=1.46;rawP=0.0002;adjP=0.0242
C=421;O=180;E=144.63;R=1.24;rawP=0.0002;adjP=0.0242
C=168;O=80;E=57.71;R=1.39;rawP=0.0002;adjP=0.0242
C=548;O=225;E=188.26;R=1.20;rawP=0.0004;adjP=0.0330
C=135;O=65;E=46.38;R=1.40;rawP=0.0006;adjP=0.0330
C=994;O=388;E=341.48;R=1.14;rawP=0.0006;adjP=0.0330
C=115;O=57;E=39.51;R=1.44;rawP=0.0005;adjP=0.0330
C=72;O=39;E=24.73;R=1.58;rawP=0.0004;adjP=0.0330

NFKB-related genes

Gene Symbol	beta coefficient	nominal p value	fdr-adjust p value
IL18R1	0.464453217	3.61E-28	2.71E-26
XPO6	0.31937061	5.27E-12	1.97E-10
FOS	0.309348885	6.87E-10	1.29E-08
NFKBIA	0.228992201	3.23E-09	4.84E-08
IL1RN	0.198768135	0.00040592	0.000951375
RHOG	0.174148362	2.05E-05	0.000102744
BCKDK	0.164503562	2.27E-08	2.84E-07
RGL1	0.15799469	8.34E-07	7.05E-06
BCL3	0.157650167	0.000420445	0.000955556
MAP3K8	0.143443863	9.92E-06	6.20E-05
RIN2	0.140793936	1.22E-05	6.55E-05
RAB10	0.140437973	5.44E-07	5.83E-06
LIX1L	0.137800467	2.95E-11	7.37E-10
PRKCD	0.132297165	0.000213285	0.000620286
NUP153	0.122550194	3.73E-06	2.73E-05
IRF1	0.11964364	0.012863897	0.014399885
GNA13	0.116993805	0.000176122	0.00055038
ZNF217	0.114337331	0.001154151	0.00227793
FUT7	0.107951233	0.000227155	0.000630985
LASP1	0.107016238	0.000215032	0.000620286
DNAJA1	0.1011257	0.000329587	0.000852381
RHOA	0.100231568	0.001987826	0.00355243
ARPC5	0.098642419	0.016273109	0.016636982
ANKHD1	0.0966872	1.12E-05	6.49E-05
GADD45B	0.094541587	0.002246107	0.003917629
TMEM88	0.084289459	0.005124534	0.007686802
MOB3C	0.084221031	0.006517674	0.009170021
STX4	0.082604922	0.000402966	0.000951375
GPBP1	0.07356536	0.001583382	0.00296884
ALG6	0.07299218	0.003255373	0.005425621
RAP2C	0.069993847	0.012310945	0.014204937
SIN3A	0.069732275	0.006840859	0.009170021
ZNF800	0.069441522	0.008683582	0.011038451
PPP2R5E	0.069021879	0.009020497	0.011275622
C4orf32	0.065644833	0.012670533	0.014398333
PPP3CA	0.065085653	0.000616222	0.001359313
LRRFIP2	0.06373689	0.001038262	0.002104586
ANKHD1-EIF4EBP3	0.063436005	0.00338456	0.005518304
PTPRJ	0.062773732	0.016974057	0.016974057
INO80D	0.051455996	0.015256939	0.015892645
CHD4	-0.053163141	0.010308622	0.012272169
CD70	-0.055732558	0.005684573	0.008359667
SLC6A12	-0.056007442	0.008258504	0.0106791
IL23A	-0.059042421	0.014300211	0.015321655
CDC37	-0.067234867	0.009917246	0.012193335
SOCS2	-0.068121343	0.006846949	0.009170021
SCAF4	-0.069577897	0.007237649	0.009523222
HOXB6	-0.071973212	0.00026763	0.000716866

PCBP4	-0.076440886	0.000350769	0.000876923
IER5	-0.076592766	0.003978347	0.006348427
PFN1	-0.077142455	0.00471044	0.007360063
HCFC1	-0.084139618	0.006316696	0.00911062
CD40	-0.089015821	0.000813221	0.001742616
TRIB2	-0.091235744	0.010177571	0.012272169
TCTA	-0.096277567	4.61E-05	0.000181955
ENO3	-0.099501559	0.001989361	0.00355243
BCL11A	-0.10263154	5.91E-05	0.000221766
MLLT6	-0.102666422	0.004889854	0.00748447
EIF5A	-0.106031141	0.013549929	0.014728183
CD74	-0.109894237	0.013447025	0.014728183
DDR1	-0.11265689	0.006743331	0.009170021
PURG	-0.113044219	6.60E-05	0.000225083
CD247	-0.117294609	0.014686657	0.015514074
SYMPK	-0.121091293	4.01E-06	2.73E-05
SPTB	-0.12718435	0.010716518	0.01255842
RALGDS	-0.130466343	0.001254976	0.002413415
LTB	-0.137537799	0.000981616	0.002045034
CCL5	-0.138819059	0.016415155	0.016636982
CXCR5	-0.140963751	3.05E-05	0.000127286
BDNF	-0.167787053	0.000121264	0.000395428
GDPD5	-0.177416693	8.46E-07	7.05E-06
PTMS	-0.182125073	6.35E-05	0.000225083
FAM117A	-0.21360573	2.88E-05	0.000127205
RANBP10	-0.25049502	2.43E-05	0.000113672
BCL2L1	-0.272543632	0.002935254	0.005003273

Supplementary Table 4

gene1	gene2	Partial correlation in lower FKBP5 group
MAP3K14	CHUK	0.132436629
TRAF5	TAB3	-0.110467438
TNFSF14	LTBR	0.071238297
RELA	PTGS2	0.179752297
TLR4	TICAM1	-0.092933208
MYD88	TAB1	-0.146650236
PRKCB	CARD11	0.04715756
TRAF6	TAB1	0.177279293
IRAK4	TAB3	-0.12829314
BTK	CHUK	0.137688847
MAP3K14	TAB2	-0.060587472
RIPK1	MAP3K7	0.11824212
ZAP70	LAT	-0.079190985
NFKB1	BCL2	0.11910841
RELA	BIRC3	-0.242890674
PRKCQ	CARD11	0.044708189
CD40	TRAF6	0.174198063
RELA	IL1B	0.161272883
BTK	IKBKB	0.108360452
TNFRSF1A	TRADD	0.070085264
TRADD	TAB2	0.019197261
TRAF5	MAP3K14	0.043723895
BIRC3	RIPK1	-0.016049575
LTBR	TRAF5	-0.012855229
BIRC2	RIPK1	0.022034958
LAT	PLCG1	0.255379888
IRAK1	TAB1	0.070563226
IRAK1	TAB2	-0.145736375
CSNK2B	NFKBIA	0.133486117
RIPK1	TAB2	0.017519098
RIPK1	TAB3	0.025294604
TRAF5	TAB1	-0.180974135
DDX58	TRAF6	0.056179678
TRADD	TAB3	0.025808766
RELA	BCL2	0.235036324
NFKB1	NFKBIA	0.235863281
NFKBIA	NFKB1	0.235863281
NFKB1	IL1B	0.231656702
RELB	TNFSF13B	0.119999885
MAP3K7	IKBKB	0.170053728
NFKB1	TRAF1	-0.062980105
CSNK2A1	NFKBIA	-0.063627755

RIPK1	TAB1	0.184068978
NFKB1	GADD45B	-0.129871096
NFKB1	CFLAR	0.133751003
TRIM25	DDX58	0.172814544
CHUK	NFKB2	0.13045199
NFKB2	TNFSF13B	0.066157861
RELA	BIRC2	-0.091272133
NFKB1	BCL2L1	0.238463855
CD14	TLR4	0.169720956
IRAK4	TAB2	-0.073391111
MYD88	TAB2	0.018096715
TRAF6	TAB3	0.065013758
NFKB1	TNFAIP3	-0.10940864
RELA	TRAF1	-0.008309294
IRAK4	MAP3K7	0.160351607
NFKB1	BIRC2	0.004745478
TNFRSF1A	TRAF5	0.015645208
MYD88	IRAK4	0.102080512
TNFRSF1A	RIPK1	0.153632996
TRAF6	TAB2	0.009191737
LTB	LTBR	-0.139841382
SYK	BTK	0.170704222
TNF	TNFRSF1A	-0.114509548
TRAF5	TAB2	0.197906574
CD40LG	CD40	-0.140908404
MAP3K14	TAB1	-0.025226161
RELA	NFKB2	0.09715396
TRAF5	MAP3K7	0.120597931
BTK	IKBKG	0.036876583
RELA	TNF	-0.096476824
TRAF6	MAP3K14	0.012714424
NFKB1	BCL2A1	0.077533938
MYD88	TRAF6	0.076802967
BTK	PLCG2	-0.005180287
NFKBIA	RELA	0.084011194
RELA	NFKBIA	0.084011194
TRAF6	MAP3K7	0.027560944
NFKB1	NFKB2	0.051904974
IRAK1	MAP3K7	0.106635656
IRAK1	TAB3	0.00525706
RELA	BCL2A1	-0.009474199
NFKB1	TNF	-0.106668698
RELA	GADD45B	0.032493649
RELA	BCL2L1	-0.067685043

RELA	CXCL8	0.042867685
TRADD	TAB1	0.003033641
TNFSF13B	TNFRSF13C	-0.105947084
RELA	TNFAIP3	0.004822892
TICAM1	RIPK1	-0.078743797
CSNK2A3	NFKBIA	-0.182557122
MAP3K14	MAP3K7	-0.135832519
TLR4	MYD88	0.089085064
MYD88	TAB3	-0.075184545
IKBKB	NFKBIA	0.096968983
CSNK2A2	NFKBIA	-0.085464184
NFKB1	CXCL8	-0.064135883
TRADD	MAP3K7	-0.019213748
NFKB1	BIRC3	-0.045010747
TICAM1	TRAF6	-0.073616907
IRAK4	TAB1	-0.044424501
MYD88	IRAK1	0.029573907
LTA	LTBR	-0.040120183
NFKB1	PTGS2	-0.041918814
MYD88	MAP3K7	0.098745902
MAP3K14	TAB3	0.05488285

Partial correlation in higher FKBP5 group	Difference in partial correlations	p value
-0.275039094	0.407475723	0.0019
0.215465481	0.325932919	0.0052
-0.263448577	0.334686873	0.0087
-0.138725032	0.318477329	0.013
0.219816225	0.312749433	0.0174
0.150640471	0.297290708	0.018
-0.227360317	0.274517877	0.0288
-0.090086652	0.267365945	0.0413
0.159453376	0.287746516	0.0445
-0.179678413	0.317367259	0.0448
0.206314426	0.266901898	0.0494
-0.174900151	0.29314227	0.0742
0.150136714	0.229327699	0.0763
-0.11194658	0.231054989	0.0906
-0.030933939	0.211956735	0.101
0.257787533	0.213079344	0.112
-0.038803568	0.213001631	0.1161
-0.035543278	0.196816161	0.1162
-0.07361192	0.181972372	0.123
-0.134659342	0.204744607	0.1348
-0.176427818	0.195625079	0.1436
-0.133503135	0.177227029	0.1495
0.155588014	0.171637589	0.1689
0.148269488	0.161124717	0.1704
-0.154848979	0.176883937	0.1751
0.079319001	0.176060887	0.1752
0.249470693	0.178907466	0.1765
0.020342585	0.16607896	0.1887
-0.036126981	0.169613098	0.1991
-0.146279139	0.163798237	0.2323
0.181969645	0.156675041	0.2328
-0.039008143	0.141965992	0.2491
-0.09437496	0.150554639	0.2609
-0.128932058	0.154740823	0.2872
0.10017325	0.134863074	0.2896
0.08532022	0.150543061	0.3003
0.08532022	0.150543061	0.3003
0.102885706	0.128770996	0.3025
-0.024058581	0.144058466	0.3074
0.031594807	0.138458921	0.3264
0.067811925	0.130792031	0.327
-0.191080621	0.127452866	0.3435

0.067329816	0.116739162	0.3438
-0.006591367	0.123279729	0.3499
0.022250933	0.11150007	0.3905
0.290044984	0.117230439	0.3954
0.015204604	0.115247386	0.4148
0.181851065	0.115693204	0.4278
0.020460433	0.111732566	0.448
0.137483437	0.100980418	0.4597
0.077197478	0.092523478	0.4648
0.023978195	0.097369306	0.4696
0.107905721	0.089809006	0.4708
-0.026282954	0.091296711	0.4834
-0.196088904	0.086680264	0.4919
-0.107052161	0.098742867	0.497
0.247797795	0.087446188	0.5034
-0.088008843	0.092754321	0.5065
-0.069916498	0.085561705	0.5199
0.009217704	0.092862807	0.5204
0.232811824	0.079178828	0.5249
0.100608514	0.091416777	0.5277
-0.216819943	0.076978561	0.5507
0.253581313	0.08287709	0.5542
-0.034546864	0.079962684	0.5551
0.12036681	0.077539763	0.5553
-0.067513557	0.073394847	0.5584
0.05326085	0.07848701	0.5633
0.020799048	0.076354911	0.5695
0.049468462	0.071129469	0.5862
-0.031544552	0.068421134	0.5918
-0.036959744	0.05951708	0.6144
0.081924394	0.069209969	0.6159
0.013676504	0.063857434	0.6185
0.012109466	0.064693501	0.619
0.062166899	0.067347186	0.6226
0.012426088	0.071585106	0.6243
0.012426088	0.071585106	0.6243
0.093991947	0.066431003	0.6323
-0.007986131	0.059891104	0.6568
0.163953875	0.057318219	0.6569
-0.049217185	0.054474246	0.6731
0.038777601	0.0482518	0.703
-0.055543558	0.05112514	0.713
-0.00930505	0.041798699	0.7252
-0.112784033	0.04509899	0.7312

3.95E-05	0.042828161	0.7543
0.039041318	0.036007677	0.7701
-0.073167739	0.032779345	0.7976
0.036951641	0.032128749	0.7986
-0.044849528	0.033894269	0.8152
-0.159187905	0.023369217	0.861
-0.159003692	0.023171173	0.8635
0.109486869	0.020401804	0.8643
-0.051061591	0.024122954	0.8715
0.075885199	0.021083784	0.8788
-0.065618486	0.019845698	0.8906
-0.046133461	0.018002422	0.8907
-0.004067677	0.01514607	0.9015
-0.054324929	0.009314182	0.9505
-0.08159261	0.007975702	0.9522
-0.05021406	0.005789559	0.9632
0.023987969	0.005585939	0.9653
-0.034888229	0.005231954	0.9688
-0.046329746	0.004410933	0.9717
0.101716168	0.002970266	0.9815
0.057744665	0.002861815	0.9841

Supplementary Figure 1

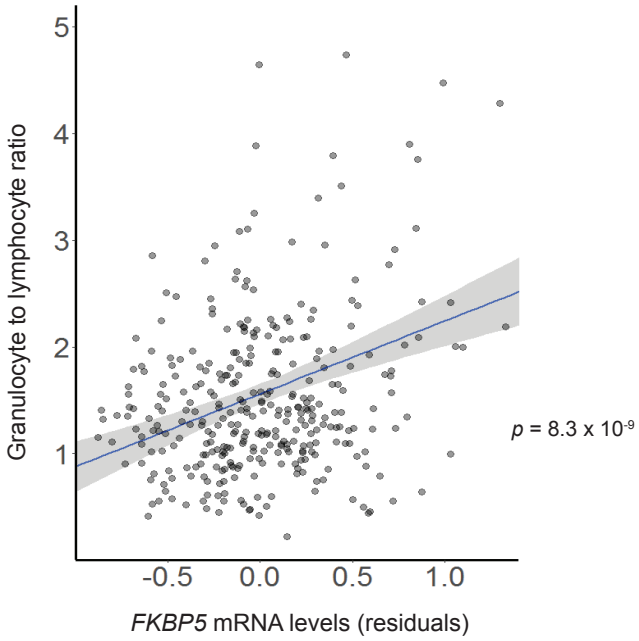

METHODS

Human cohorts and measures

The demographics for all participating cohorts and relevant variables are provided in **Supplementary Table 1**.

The first cohort, which served as discovery cohort for most of our analyses, was derived from the Grady Trauma Project (GTP), a large study conducted in Atlanta, Georgia that investigates the role of genetic and environmental factors in shaping stress responses. Participants predominantly come from an African American, urban population of low socioeconomic status(Binder *et al*, 2008; Gillespie *et al*, 2009). This population is characterized by high prevalence and severity of psychosocial stress exposure and is thereby particularly relevant for examining the impact of stress-related phenotypes on genomic regulation. All African American subjects with available *FKBP5* DNA methylation and/or genome-wide gene expression data were included in the analyses. Stress-related phenotypes of interest included depressive symptoms measured by the Beck Depression Inventory (BDI)(Beck *et al*, 1988; Beck *et al*, 1961), post-traumatic stress disorder symptomatology assessed with the validated 17-item PTSD Symptom Scale(Binder *et al*, 2008; Coffey *et al*, 1998), lifetime stressful events determined with the Stressful Events Questionnaire(Smith *et al*, 2011), and childhood trauma measured with the Childhood Trauma Questionnaire (CTQ)(Bernstein *et al*, 2003). Based on a standard BDI cutoff score(Beck *et al*, 1988), subjects were categorized as having high (total BDI score $\geq$ 19) or low levels (total BDI score < 19) of depressive symptoms. Lifetime abuse of substances, including tobacco, alcohol, cannabis, and heroin was assessed with the Kreek-McHugh-Schluger-Kellogg scale(Kellogg *et al*, 2003). Morning serum cortisol was measured as described previously with a commercial radioimmunoassay kit (Diagnostic Systems

Laboratories, Webster, TX, USA)(Kaminsky *et al*, 2015). All participants provided written informed consent and all procedures were approved by the Institutional Review Boards of the Emory University School of Medicine and Grady Memorial Hospital (IRB00002114).

The second cohort was derived from the KORA (Cooperative Health Research in the Region of Augsburg) F4 study, a follow-up study of the fourth KORA survey (S4) conducted in 1999—2001. Subjects were recruited from the city of Augsburg and two adjacent counties in the south of Germany(Holle *et al*, 2005), and DNA methylation was measured in a study subset. Depressive symptoms were assessed with the DEpression and EXhaustion subscale (DEEX scale) of the von Zerrssen symptom checklist(Ladwig *et al*, 2004). Based on a previously defined DEEX cutoff(Hafner *et al*, 2011), subjects were categorized as having high (total BDI score ≥ 11) or low levels (total DEEX score < 11) of depressive symptoms. Smoking was defined as current smoker, occasional smoker, former smoker, or never smoker. History of diagnosed myocardial infarction (MI) was determined using a self-reported questionnaire. The study has been conducted according to the principles expressed in the Declaration of Helsinki. Written informed consent has been given by each participant. All study protocols were reviewed and approved by the local ethical committee (Bayerische Landesärztekammer).

The third cohort comprised of Caucasian depressed and control subjects that were recruited at the Max Planck Institute of Psychiatry (MPIP). Recruitment strategies and characterization of case/control subjects have been previously described(Heck *et al*, 2009; Kohli *et al*, 2011; Lucae *et al*, 2006). Briefly, subjects were screened either with the Schedule for Clinical Assessment in Neuropsychiatry or the Composite International Diagnostic Screener, and diagnosis of major depression was ascertained according to the Diagnostic and Statistical Manual of Mental Disorders (DSM) IV criteria. Self-reported history of physician-diagnosed myocardial

infarction was documented upon enrollment in the study. Written informed consent was obtained from all subjects, and the study was approved by the ethics committee of the Ludwig-Maximilians-University in Munich.

The impact of severe early life stress on *FKBP5* methylation was examined in a subset of the Helsinki Birth Cohort Study (HBCS)(Barker *et al*, 2005). The HBCS has detailed information on the separation of Finnish children from their parents, which occurred during World War II and was documented by the Finnish National Archives registry between 1939 and 1946. The subset with available DNA methylation data includes separated and non-separated (control) males. In the separated subjects group, the mean age at separation was 4.7 years (SD, 2.4 years) and the mean length of separation 1.7 years (SD, 1 year). Based on self-report, subjects were categorized as never smokers, former smokers, occasional smokers, and active smokers. The HBCS was carried out in accordance with the Declaration of Helsinki, and the study protocol was approved by the Institutional Review Board of the National Public Health Institute. Written informed consent was obtained from all participants.

DNA methylation arrays

Genomic DNA from the GTP cohort, the MPIP, and the HBCS was extracted from whole blood using the Gentra Puregene Blood Kit (QIAGEN). DNA quality and quantity was assessed by NanoDrop 2000 Spectrophotometer (Thermo Scientific) and Quant-iT Picogreen (Invitrogen). Genomic DNA was bisulfite converted using the Zymo EZ-96 DNA Methylation Kit (Zymo Research) and DNA methylation levels were assessed for >480,000 CpG sites using the Illumina HumanMethylation450 BeadChip array. Hybridization and processing was performed according

to manufacturer's instructions as previously described(Mehta *et al*, 2013). Quality control of methylation data, including intensity read outs, filtering (detection P value >0.01 in >50% of the samples), cellular composition estimation, as well as beta and M-value calculation was done using the minfi Bioconductor R package version 1.10.2(Aryee *et al*, 2014). We excluded X chromosome, Y chromosome, and non-specific binding probes(Chen *et al*, 2013), as well as probes if single nucleotide polymorphisms (SNPs) were documented in the interval for which the Illumina probe is designed to hybridize. Given that the GTP cohort includes individuals from different ethnicities, we also removed probes if they were located close (10 bp from query site) to a SNP which had Minor Allele Frequency of ≥0.05, as reported in the 1,000 Genomes Project, for any of the populations represented in the samples. MPIP and HBCS data were normalized with functional normalization (FunNorm)(Fortin *et al*, 2014b), an extension of quantile normalization included in the R package *minfi*. Technical batch effects were identified by inspecting the association of the first principal components of the methylation levels with possible technical batches and by further visual inspection of principal component plots using the shinyMethyl Bioconductor R package version 0.99.3(Fortin *et al*, 2014a). This procedure identified array column in HBCS, 96-well plate and 96-well plate position in the MPIP as technical batches. The raw methylation data for the GTP cohort have been deposited into NCBI GEO (GSE72680).

For the KORA study, genomic DNA (1 µg) from 1814 samples was bisulfite converted using the EZ-96 DNA Methylation Kit (Zymo Research, Orange, CA, USA) according to the manufacturer's protocol, with the incubation conditions recommended for the Illumina Infinium Methylation Assay. Raw methylation data were generated by BeadArray Reader and extracted by GenomeStudio (version 2011.1) with methylation module (version 1.9.0). Data were

preprocessed using R version 3.0.1 (http://www.r-project.org/)(Team, 2014). Probes with signals from less than three functional beads and probes with a detection p-value > 0.01 were defined as low-confidence probes. As probe binding might be affected by single nucleotide polymorphisms (SNPs) in the binding area, CpG sites (CpGs) in close proximity (50bp) to SNPs with a minor allele frequency of at least 5% were excluded from the dataset. Color bias adjustment using smooth quantile normalization method as well as background level correction based on negative-control probes present on the Infinium HumanMethylation BeadChip was performed for each chip using the R package lumi (version 2.12.0)(Du *et al*, 2008). Beta values corresponding to low-confidence probes were then set to missing, and samples as well as CpGs were subjected to a 95% detection rate threshold, where samples and CpGs with more than 5% low-confidence probes were removed from the analysis. Finally, beta-mixture quantile normalization (BMIQ) was applied to correct the shift in the distribution of the beta values of the InfI and InfII probes(Teschendorff *et al*, 2013). BMIQ was done using the R package wateRmelon (version 1.0.3)(Pidsley *et al*, 2013).

DNA methylation analyses included 45 cytosine-guanine dinucleotides (CpGs) covered by the 450K that are located within or in close proximity (10kb upstream or downstream) to the *FKBP5* locus. All 45 CpGs were measured in the KORA, whereas one CpG (cg00052684) did not pass quality control in the other cohorts. All statistics involving DNA methylation are conducted and reported using M values, whereas Beta-values are used for figures and DNA methylation differences as a more intuitive measure of effect size. In all cohorts, DNA methylation data were used to calculate blood cell proportions as previously described(Houseman *et al*, 2012).

Gene expression arrays

Genome-wide gene expression data were measured in 355 African American subjects from the GTP. Whole blood RNA was collected, processed, and hybridized to Illumina HumanHT-12 v3 and v4 Expression BeadChips (Illumina, San Diego, CA, USA) as previously described(Mehta *et al*, 2013; Menke *et al*, 2012). The raw microarray scan files were exported using the Illumina Beadstudio program 13 and further analyzed in R (www.R-project.org). Microarray data were transformed and normalized via the variance stabilizing normalization with the use of Illumina internal controls(Huber *et al*, 2002). Empirical Bayes method was used to control for potential confounding as a result of batch effects(Johnson *et al*, 2007). Six pairs of technical replicates were used to confirm data reproducibility (average Pearson correlation 0.996). The raw gene expression array data for the GTP study have been deposited to GEO (GSE58137).

Population stratification

To control for potential confounding by population stratification, we used genome-wide SNP data. In the GTP, of the 700 k SNPs present on the Omni Quad and Omni express arrays, 645,8315 autosomal SNPs were left after filtering with the following criteria: minor allele frequency of >1 %; Hardy-Weinberg equilibrium of 0.000001; and genotyping rate of >98 %. The MPIP cohort was genotyped using the Illumina 300k, 610k and Omni express arrays. For each chip array, quality control was performed separately following the same quality control protocol like in GTP. After QC, we used the overlap of 168,138 SNPs across all chip types. The samples were clustered to calculate rates of identity by descent (IBD). We then ran multidimensional scaling analysis on the IBD matrix using PLINK2 (https://www.cog-

genomics.org/plink2) and plotted the first ten axes of variation against each other. No outliers were detected. The first two principal components were used as covariates in regression models to adjust for population stratification.

Pathway analyses

FKBP5 mRNA levels were correlated with the expression of all genes detected above background in peripheral blood in the GTP. Using the set of FDR-corrected genes correlating with *FKBP5* (n = 3,275) as input and the set of genes expressed above background (n = 9,538) as reference, we then performed disease association and transcription factor target analysis using the WEB-based GEne SeT AnaLysis Toolkit (WebGestalt; http://bioinfo.vanderbilt.edu/webgestalt/)(Wang *et al*, 2013; Zhang *et al*, 2005). This was performed with a hypergeometric test, whereby the minimum number of genes for the enrichment analysis was set at 5. Both analyses were FDR-corrected for multiple testing.

For the NF-κB co-expression network analyses, the list of NF-κB-related genes was acquired from the KEGG Pathway Database (http://www.genome.jp/dbget-bin/www_bget?pathway:hsa04064). Using the gene expression array data in the GTP, the pairwise correlation coefficients between gene pairs encoding molecules that directly interact along the NF-κB pathway were calculated and adjusted for the expression levels of all other pathway partners using the R package GeneNet(Schafer and Strimmer, 2005). These partial pairwise correlations were then compared between subjects with higher and those with lower *FKBP5* expression as defined by a median split of *FKBP5* mRNA levels. To test whether there is

a significant change of each gene pair between the two groups, the *FKBP5* high/low group assignments for each pair were permuted 10,000 times across samples.

Cell culture

Cell culture experiments were conducted in peripheral blood monocytes (PBMC) or Jurkat cell lines (ATCC, TIB-152), a frequently used human T-cell leukemia cell line that allows efficient and reproducible transfection with expression vectors. For PBMC isolation, the whole blood of healthy volunteers was collected via venipuncture, diluted with PBS, carefully loaded on Biocoll solution (BioChrom, L6113), and centrifuged at 800 g for 20 min without brake. PBMC were enriched by selecting the interphase of the Biocoll gradient and were then washed two times with ice-cold PBS and resuspended in medium. Both cell types were maintained in RPMI (Gibco) supplemented with 10% FCS and 100 units/ml penicillin and streptomycin. For all treatments, cells were left after seeding to rest overnight and the next day were incubated overnight with vehicle (0.05% DMSO), 100 nM DEX (Sigma, D4902), and/or 100 nM SAFit1. FKBP5 overexpression in Jurkat cells was performed using a previously described FKBP51-FLAG(Wochnik *et al*, 2005).

Western Blot Analysis

Protein extracts were obtained by lysing cells in 62.5 mM Tris, 2% SDS, and 10% sucrose, supplemented with protease (Sigma, P2714) and phosphatase (Roche, 04906837001) inhibitors. Samples were sonicated and heated at 95°C for 5 min. Proteins were separated by SDS-PAGE

and electro-transferred onto nitrocellulose membranes. Blots were placed in Tris-buffered saline, supplemented with 0.05% Tween (Sigma, P2287) and 5% non-fat milk for 1 h at room temperature and then incubated with primary antibody (diluted in TBS/0.05% Tween) overnight at 4°C. The following primary antibodies were used: FLAG (1:7,000, Rockland, 600-401-383), FKBP5 (1:1,000, Bethyl, A301-430A; 1:1000, Cell Signaling, #8245), IKKα (1:1000, Cell Signaling, # 2682), pIKKα^{S176} (1:1000, Cell Signaling, #2078), NIK (1:1000, Cell Signaling, #4994), and Actin (1:5,000, Santa Cruz, sc-1616). Subsequently, the blots were washed and probed with the respective horseradish-peroxidase or fluorophore-conjugated secondary antibody for 2 h at room temperature. The immuno-reactive bands were visualized either by using ECL detection reagent (Millipore, WBKL0500) or directly by excitation of the respective fluorophore. Recording of the band intensities was performed with the ChemiDoc MP system from Bio-Rad.

Co-immunoprecipitation experiments (CoIPs)

CoIPs of endogenous or FLAG-tagged FKBP5 with endogenous IKKα and NIK were performed in Jurkat cells and PBMC using previously described methods(Gassen *et al*, 2014). 5 x 10^6 cells were electroporated with 2 µg of the respective expression plasmids using the Amaxa Nucleofector Device and the Cell Line Nucleofector Kit V (Lonza, Basel, Switzerland). After 3 days of cultivation in medium, cells were lysed in CoIP buffer containing 20 mM Tris-HCl (pH 8.0), 100 mM NaCl, 1 mM EDTA, and 0.5% Igepal, complemented with protease inhibitor cocktail. This was followed by incubation on an overhead shaker for 20 min at 4°C. The lysate was cleared by centrifugation, the protein concentration was determined, and 1.2 mg of lysate was incubated with 2.5 µg of FLAG antibody overnight at 4°C. 20 µl of BSA-blocked Protein G

Dynabeads (Invitrogen, 100-03D) were added to the lysate-antibody mix, followed by 3 h of incubation at 4°C. The beads were washed three times with PBS, and protein-antibody complexes were eluted with 100 µl of 1 x FLAG-peptide solution (Sigma, 100–200 µg/ml, F3290) in CoIP buffer for 30 min at 4°C. 5–15 µg of the cell lysates or 2.5 µl of the immunoprecipitates was separated by SDS-PAGE.

Quantification of Protein Data

All protein data were normalized to Actin, which was detected on the same blot in the same lane (multiplexing). In the case of IKKα phosphorylation and to rule out confounding by changes in total IKKα levels, we normalized pIKKα by calculating its ratio to total IKKα. We obtained indistinguishable results when normalizing pIKKα to Actin.

Dual-luciferase reporter gene assays

1 x 10^6 Jurkat cells were transfected with NF- κB luciferase reporter (1µg, Promega, E8491) and Renilla control plasmids (300ng, Promega, E6921), as well as with either FKBP5-FLAG (1µg) or control vector (pRK5; 1µg), using the Amaxa Nucleofector Device. Immediately after transfection, cells were seeded on 96-well plates at a density of 20,000 cells/well and were left to rest overnight. On the next day, cells were incubated for 2 hours with SAFit1 or vehicle and were then stimulated overnight with Phorbol-12-myristate-13-acetate (PMA; 25ng/ml, Sigma, P1585) and ionomycin (375ng/ml, Sigma, I0634). Cells were then lysed in lysis buffer (Promega, E1941) and stored in -80°C until the plate was read with the TriStar² S LB 942

microplate reader (Berthold, Bad Wildbad, Germany) following a previously described protocol(Hampf and Gossen, 2006). To control for differences in transfection efficiency, the NF-κB-driven reporter gene activity was calculated as the ratio of Photinus to Renilla luciferase signals.

Enzyme-linked immunosorbent assay (ELISA) for human interleukin-8 (IL-8)

1 x 10^6 Jurkat cells were transfected with either FKBP5-FLAG (1µg) or control vector (1µg), were seeded in 24-well plates at a density of 500,000 cells/well and, after overnight rest, were stimulated with PMA (25ng/ml) and ionomycin (375ng/ml). Supernatants were collected the next day, cleared by centrifugation at 125g, and stored at -80°C until IL-8 measurement with ELISA, which was performed with a commercially available kit (Merck Millipore, EZHIL8).

Statistical analysis

All statistical analyses involving DNA methylation used M-values, which have shown superior statistical performance as compared to Beta-values(Du *et al*, 2010). To average the methylation levels of the two age-regulated *FKBP5* CpGs, we calculated the mean of the respective Beta-values and then transformed each mean to the corresponding M-values as previously described(Du *et al*, 2010). All p values reporting the statistical significance of DNA methylation analyses originate from tests using M values; however, to more intuitively depict methylation results, all figures show Beta-values for DNA methylation.

Linear regression models examined the effect of age and stress-related phenotypes on DNA methylation, while including as covariates all the potential confounders that were available in the respective cohorts. Covariates used in each cohort were as follows: age, sex, blood cell proportions, the first two genome-wide SNP-based principal components, smoking status, and substance use in the GTP; age, sex, blood cell proportions, smoking status, and the first two genome-wide SNP-based principal components in the KORA; age, sex, case/control status, blood cell proportions, and the first two genome-wide SNP-based principal components in the MPIP; and age, smoking status, and blood cell proportions in the HBCS. Linear regression models examining *FKBP5* expression as the dependent variable of interest in the GTP included as covariates age, sex, the first two SNP-based principal components, and blood cell proportions. These models tested methylation of the age-regulated *FKBP5* CpGs (M-values), age, stress-related phenotypes, and cortisol as the independent variables of interest. Lastly, linear regression models examined the association of history for MI with lower methylation of the age-regulated CpGs, while controlling for age, sex, and smoking status in the KORA, and while controlling for age and sex in the MPIP. For stratified analyses in the GTP, we performed median splits of the respective continuous variables. This was performed for methylation levels of the age-regulated *FKBP5* CpGs to distinguish subjects with higher vs. lower methylation, for CTQ scores to stratify individuals in high- vs. low-trauma groups, for chronological age to stratify younger vs. older individuals, and for *FKBP5* mRNA levels to distinguish subjects with higher vs. lower *FKBP5* expression. All p values reporting the statistical significance of regression models are after correction for relevant covariates as described above.

Experimental data were tested using student's t-test when comparing two groups and with two-way analysis of variance (ANOVA) when examining two factors of interest. Significant

interactions between factors in the two-way ANOVA were followed with Bonferroni-corrected pairwise comparisons.

Experimental data were analyzed in Sigma Plot version 13.0. All other statistical tests were performed in R version 3.1.0 (http://www.r-project.org/)(Team, 2014). The level of statistical significance was set a priori at 0.05 (5×10^{-2}). All reported p values are two-tailed and nominal, unless corrected for multiple testing as indicated and reported in the manuscript.

REFERENCES

1. Binder, E.B.*, et al.* Association of FKBP5 polymorphisms and childhood abuse with risk of posttraumatic stress disorder symptoms in adults. *JAMA : the journal of the American Medical Association* **299**, 1291-1305 (2008).

2. Gillespie, C.F.*, et al.* Trauma exposure and stress-related disorders in inner city primary care patients. *General hospital psychiatry* **31**, 505-514 (2009).

3. Beck, A.T., Steer, R.A. & Garbin, M.G. Psychometric Properties of the Beck Depression Inventory - 25 Years of Evaluation. *Clin Psychol Rev* **8**, 77-100 (1988).

4. Beck, A.T., Ward, C.H., Mendelson, M., Mock, J. & Erbaugh, J. An inventory for measuring depression. *Archives of general psychiatry* **4**, 561-571 (1961).

5. Coffey, S.F., Dansky, B.S., Falsetti, S.A., Saladin, M.E. & Brady, K.T. Screening for PTSD in a substance abuse sample: psychometric properties of a modified version of the PTSD Symptom Scale Self-Report. Posttraumatic stress disorder. *Journal of traumatic stress* **11**, 393-399 (1998).

6. Smith, A.K.*, et al.* Differential immune system DNA methylation and cytokine regulation in post-traumatic stress disorder. *American journal of medical genetics. Part B, Neuropsychiatric genetics : the official publication of the International Society of Psychiatric Genetics* **156B**, 700-708 (2011).

7. Bernstein, D.P.*, et al.* Development and validation of a brief screening version of the Childhood Trauma Questionnaire. *Child abuse & neglect* **27**, 169-190 (2003).

8. Kellogg, S.H.*, et al.* The Kreek-McHugh-Schluger-Kellogg scale: a new, rapid method for quantifying substance abuse and its possible applications. *Drug and alcohol dependence* **69**, 137-150 (2003).

9. Kaminsky, Z.*, et al.* Epigenetic and genetic variation at SKA2 predict suicidal behavior and post-traumatic stress disorder. *Translational psychiatry* **5**, e627 (2015).

10. Holle, R., Happich, M., Lowel, H. & Wichmann, H.E. KORA--a research platform for population based health research. *Gesundheitswesen (Bundesverband der Arzte des Offentlichen Gesundheitsdienstes (Germany))* **67 Suppl 1**, S19-25 (2005).

11. Ladwig, K.H., Marten-Mittag, B., Baumert, J., Lowel, H. & Doring, A. Case-finding for depressive and exhausted mood in the general population: reliability and validity of a symptom-driven diagnostic scale. Results from the prospective MONICA/KORA Augsburg Study. *Annals of epidemiology* **14**, 332-338 (2004).

12. Hafner, S.*, et al.* Association between social isolation and inflammatory markers in depressed and non-depressed individuals: results from the MONICA/KORA study. *Brain, behavior, and immunity* **25**, 1701-1707 (2011).

13. Heck, A.*, et al.* Investigation of 17 candidate genes for personality traits confirms effects of the HTR2A gene on novelty seeking. *Genes, brain, and behavior* **8**, 464-472 (2009).

14. Kohli, M.A.*, et al.* The neuronal transporter gene SLC6A15 confers risk to major depression. *Neuron* **70**, 252-265 (2011).

15. Lucae, S.*, et al.* P2RX7, a gene coding for a purinergic ligand-gated ion channel, is associated with major depressive disorder. *Human molecular genetics* **15**, 2438-2445 (2006).

16. Barker, D.J., Osmond, C., Forsen, T.J., Kajantie, E. & Eriksson, J.G. Trajectories of growth among children who have coronary events as adults. *The New England journal of medicine* **353**, 1802-1809 (2005).

17. Mehta, D.*, et al.* Childhood maltreatment is associated with distinct genomic and epigenetic profiles in posttraumatic stress disorder. *Proceedings of the National Academy of Sciences of the United States of America* **110**, 8302-8307 (2013).

18. Aryee, M.J.*, et al.* Minfi: a flexible and comprehensive Bioconductor package for the analysis of Infinium DNA methylation microarrays. *Bioinformatics* **30**, 1363-1369 (2014).

19. Chen, Y.A.*, et al.* Discovery of cross-reactive probes and polymorphic CpGs in the Illumina Infinium HumanMethylation450 microarray. *Epigenetics : official journal of the DNA Methylation Society* **8**, 203-209 (2013).

20. Fortin, J.P.*, et al.* Functional normalization of 450k methylation array data improves replication in large cancer studies. *Genome biology* **15**, 503 (2014).

21. Fortin, J.P., Fertig, E. & Hansen, K. shinyMethyl: interactive quality control of Illumina 450k DNA methylation arrays in R. *F1000Research* **3**, 175 (2014).

22. Team, R.C. A Language and Environment for Statistical Computing. *R Foundation for Statistical Computing, Vienna, Austria* (2014).

23. Du, P., Kibbe, W.A. & Lin, S.M. lumi: a pipeline for processing Illumina microarray. *Bioinformatics* **24**, 1547-1548 (2008).

24. Teschendorff, A.E.*, et al.* A beta-mixture quantile normalization method for correcting probe design bias in Illumina Infinium 450 k DNA methylation data. *Bioinformatics* **29**, 189-196 (2013).

25. Pidsley, R.*, et al.* A data-driven approach to preprocessing Illumina 450K methylation array data. *BMC genomics* **14**, 293 (2013).

26. Houseman, E.A.*, et al.* DNA methylation arrays as surrogate measures of cell mixture distribution. *BMC bioinformatics* **13**, 86 (2012).

27. Menke, A.*, et al.* Dexamethasone stimulated gene expression in peripheral blood is a sensitive marker for glucocorticoid receptor resistance in depressed patients. *Neuropsychopharmacology : official publication of the American College of Neuropsychopharmacology* **37**, 1455-1464 (2012).

28. Huber, W., von Heydebreck, A., Sultmann, H., Poustka, A. & Vingron, M. Variance stabilization applied to microarray data calibration and to the quantification of differential expression. *Bioinformatics* **18 Suppl 1**, S96-104 (2002).

29. Johnson, W.E., Li, C. & Rabinovic, A. Adjusting batch effects in microarray expression data using empirical Bayes methods. *Biostatistics (Oxford, England)* **8**, 118-127 (2007).

30. Wang, J., Duncan, D., Shi, Z. & Zhang, B. WEB-based GEne SeT AnaLysis Toolkit (WebGestalt): update 2013. *Nucleic acids research* **41**, W77-83 (2013).

31. Zhang, B., Kirov, S. & Snoddy, J. WebGestalt: an integrated system for exploring gene sets in various biological contexts. *Nucleic acids research* **33**, W741-748 (2005).

32. Schafer, J. & Strimmer, K. An empirical Bayes approach to inferring large-scale gene association networks. *Bioinformatics* **21**, 754-764 (2005).

33. Wochnik, G.M.*, et al.* FK506-binding proteins 51 and 52 differentially regulate dynein interaction and nuclear translocation of the glucocorticoid receptor in mammalian cells. *The Journal of biological chemistry* **280**, 4609-4616 (2005).

34. Gassen, N.C.*, et al.* Association of FKBP51 with priming of autophagy pathways and mediation of antidepressant treatment response: evidence in cells, mice, and humans. *PLoS medicine* **11**, e1001755 (2014).

35. Hampf, M. & Gossen, M. A protocol for combined Photinus and Renilla luciferase quantification compatible with protein assays. *Analytical biochemistry* **356**, 94-99 (2006).

36. Du, P.*, et al.* Comparison of Beta-value and M-value methods for quantifying methylation levels by microarray analysis. *BMC bioinformatics* **11**, 587 (2010).

Overarching discussion

Psychological stress is associated with accelerated cellular aging and increased risk for diseases of the aging, but the underlying molecular mechanisms are poorly understood. The present work examined large human cohorts with genome-wide DNA methylation and gene expression data from peripheral blood, as well as with detailed information on stress-related phenotypes, including childhood and lifetime stress, major depression, and posttraumatic stress disorder. The converging findings presented here show that higher stress burden throughout life accelerates the epigenetic impact of advancing age both at the systems level and at selective, stress-responsive sites, as exemplified by the *FKBP5* gene. Furthermore, by examining subjects exposed to glucocorticoid agonists, this work shows that age-related DNA methylation sites are susceptible to alterations in glucocorticoid signaling, which are frequently observed in stress-related phenotypes. By mechanistically dissecting the potential downstream effects of stress-induced epigenetic changes, the thesis illustrates that the age- and stress-related epigenetic upregulation of *FKBP5* may be associated with functional effects on gene expression, alterations in biological pathways critical for immune function and epigenetic regulation, and heightened risk for aging-related disease. These findings and their implications are discussed in more detail in the following sections.

Higher stress burden accelerates the epigenetic effects of advancing age

The work presented in this thesis shows that stress-related phenotypes accelerate the epigenetic changes that occur with advancing age. This was shown for the impact of cumulative lifetime stressors on epigenetic aging and for the effects of severe childhood trauma and depressive

phenotypes on the stress-responsive *FKBP5* locus (Zannas *et al*, 2015a). Interestingly, lifetime stressful experiences had no effect on *FKBP5* methylation and depressive symptoms did not influence epigenetic aging, overall suggesting that different stress-related phenotypes may influence different susceptibility sites across the epigenome. In both cases, childhood trauma moderated the subsequent impact of stress-related phenotypes. This moderation resulted in blunting of the epigenetic age acceleration associated with cumulative stress, but accentuation of the *FKBP5* demethylation associated with childhood trauma and depression. Together these findings indicate that repetitive stressors may interact in complex ways, which either enhance or attenuate sensitivity of the epigenome depending on the context and type of subsequent stress exposure. Such development-specific effects are concordant with previous observations that childhood trauma specifically influences glucocorticoid-sensitive CpGs of the *FKBP5* locus (Klengel *et al*, 2013). Moreover, the impact of lifetime stress on epigenetic aging became more apparent in older ages, suggesting that the epigenome becomes more sensitive to the "wear and tear" effects of stress as age advances. An intriguing possibility explaining this finding is that stressors synergize with other environmental factors and with the aging process itself to impact the aging epigenome (Gassen *et al*, 2016), possibly through converging effects at distinct components of the epigenetic machinery.

Glucocorticoid signaling as mediator of stress-induced effects on the aging epigenome

As discussed above, glucocorticoids could mediate the lasting effects of stress on the epigenome. In particular, stress-induced changes in DNA methylation are more likely to occur at susceptible CpGs, such as the ones located at or near GREs (Bose *et al*, 2010; Bose *et al*, 2015; Klengel *et al*, 2013; Thomassin *et al*, 2001; Wiench *et al*, 2011a; Wiench *et al*, 2011b; Yang *et al*, 2012).

Supporting the relevance of glucocorticoid signaling for the effects of stress on epigenetic aging, a large number of epigenetic clock CpGs (85 out of 353) were found to be located within functional GREs (Zannas *et al*, 2015a). Furthermore, in individuals exposed to the glucocorticoid receptor agonist dexamethasone (DEX), about one third of epigenetic clock CpGs (110 out of 353) showed dynamic methylation changes, and more than 80% of the genes neighboring these CpGs underwent rapid changes in their expression levels. These findings show that the age-regulated methylation sites that comprise the epigenetic clock are susceptible to glucocorticoids, thereby indicating that the effects of stress on epigenetic aging could be mediated by stress-induced alterations in HPA axis regulation and glucocorticoid signaling, which may have lasting consequences on the methylation status of susceptible CpGs.

Demethylation is more likely than hypermethylation at age- and stress-regulated CpGs

A striking observation concerning both the CpGs that comprise the epigenetic clock and the age-regulated sites of the *FKBP5* locus is that the majority of these sites undergo demethylation in response to stress-related phenotypes and glucocorticoid exposure (Zannas *et al*, 2015a). This is in line with previous studies showing that stress-responsive sites, especially ones located at or near GREs, are likely to undergo demethylation upon glucocorticoid exposure (Bose *et al*, 2010; Bose *et al*, 2015; Klengel *et al*, 2013; Thomassin *et al*, 2001; Wiench *et al*, 2011a; Wiench *et al*, 2011b; Yang *et al*, 2012). By contrast, no *FKBP5* CpGs and a minority of epigenetic clock CpGs (12 out of 110) underwent hypermethylation upon glucocorticoid exposure (Zannas *et al*, 2015a), suggesting that differential mechanisms may underlie the effects of stress on these sites. The hyper- or hypo-methylating effects of stress could also depend on the specific developmental and genomic context. For instance, *in utero* stress exposure has been shown to induce both DNMT1

and TET1 in specific tissues (Benoit *et al*, 2015; Dong *et al*, 2015), indicating that certain stressful environments could simultaneously promote methylation and demethylation processes, thereby promoting a milieu of dynamic methylation changes that are in turn stabilized at select genomic regions through yet unknown mechanisms.

FKBP5 as modulator of downstream epigenetic mechanisms

Previous studies show that FKBP5 is a versatile protein that can influence diverse biological pathways (Avellino *et al*, 2005; Baughman *et al*, 1995; Bouwmeester *et al*, 2004; Daudt *et al*, 2011; Erlejman *et al*, 2014; Gassen *et al*, 2014; Gassen, 2015; Giordano *et al*, 2006; Kim *et al*, 2012; Li *et al*, 2002; Maiaru *et al*, 2016; Park *et al*, 2007; Romano *et al*, 2004; Romano *et al*, 2010; Romano *et al*, 2015; Srivastava *et al*, 2015; Weiwad *et al*, 2006; Zannas *et al*, 2016). The work presented here expands the landscape of FKBP5-interacting pathways, by identifying the functional impact of FKBP5 on DNMT1, the methyltransferase that plays key roles in maintaining DNA methylation (Telese *et al*, 2013). More specifically, FKBP5 was shown to inhibit the activity of DNMT1 (Gassen *et al*, 2015), thereby decreasing methylation levels of the promoter of the gene that encodes the brain-derived neurotrophic factor (BDNF). Because FKBP5 is robustly induced by stress and mediates the effects of stress and glucocorticoids on downstream pathways, these findings suggest that FKBP5-mediated inhibition of DNMT1 could underlie the previously observed stress- and glucocorticoid-induced loss of DNA methylation (Bose *et al*, 2010; Bose *et al*, 2015; Klengel *et al*, 2013; Thomassin *et al*, 2001; Wiench *et al*, 2011a; Wiench *et al*, 2011b; Yang *et al*, 2012; Zannas *et al*, 2015a). Interestingly, *DNMT1* is downregulated with aging and upon glucocorticoid exposure (Li *et al*, 2010; Yang *et al*, 2012), whereas *FKBP5* is epigenetically upregulated by aging and stress-related phenotypes. Taken

together, these findings suggest that FKBP5 and DNMT1 form a feed-forward mechanism that could initiate and propagate the effects of stress on the aging epigenome.

FKBP5 contributes to NF-κB-driven peripheral inflammation

Unpublished work presented here (Zannas *et al*, unpublished) also shows that, in both humans and cells, FKBP5 promotes peripheral inflammation and secretion of the proinflammatory chemokine IL-8 (Roebuck, 1999). This is the first work to examine how upregulation of FKBP5 influences IL-8 secretion by immune cells, and it builds on a previous study showing that downregulation of FKBP5 suppresses IL-8 production in other cell types (Srivastava *et al*, 2015). The FKBP5-mediated increase in IL-8 suggests that the proinflammatory effect of FKBP5 could in part be explained by the IL-8-driven recruitment of granulocytes in peripheral blood (Kobayashi, 2008). Supporting this possibility, *FKBP5* mRNA positively correlated with the granulocyte to lymphocyte (G/L) ratio, suggesting that FKBP5 upregulation in peripheral blood is overall associated with a shift towards a proinflammatory blood cell composition. Because *FKBP5* is the gene that is most robustly induced by glucocorticoids in human blood (Menke *et al*, 2012), individuals with epigenetic upregulation of *FKBP5*, such as older adults with higher levels of depressive symptoms and trauma exposure, could be more vulnerable to developing stress-induced inflammation.

Several lines of evidence further suggested that the effects of FKBP5 on peripheral inflammation are driven by the NF-κB signaling pathway. Following an unbiased approach that used genome-wide gene expression data in human peripheral blood, the work presented here identified strong enrichment for NF-κB-related genes and profound changes in the NF-κB-coexpression network (Zannas *et al*, unpublished). Furthermore, mechanistic dissection of the

NF-κB pathway in both peripheral blood monocytes (PBMC) and Jurkat T cells identified a novel interaction between FKBP5 and the NF-κB-inducing kinase (NIK). This effect strengthened the interaction between NIK and the NF-κB kinase subunit alpha (IKKα), promoting functional phosphorylation of IKKα at serine 176 and facilitating NF-κB activity. These findings extend previous studies showing that downregulation of FKBP5 inhibits NF-κB activity (Avellino *et al*, 2005; Bouwmeester *et al*, 2004; Daudt *et al*, 2011; Giordano *et al*, 2006; Kim *et al*, 2012; Park *et al*, 2007; Romano *et al*, 2004; Romano *et al*, 2010; Romano *et al*, 2015; Srivastava *et al*, 2015). Intriguingly, the induction of NF-κB conferred by FKBP5 upregulation was abolished when cells were concomitantly treated with FKBP5 antagonists (SAFit1). By contrast, as shown both here and in a previous study (Gaali *et al*, 2015), SAFit1 does not influence immune function under baseline FKBP5 levels. Therefore, it is likely that FKBP5 antagonists could prevent some undesirable effects of stress on immune regulation, especially when targeted at individuals with upregulated FKBP5.

Implications for aging-related disease phenotypes

The findings presented in this thesis could have important implications for the pathogenesis of aging-related diseases, most notably cardiovascular disease. First, the DEX-regulated genes with TSS near epigenetic clock CpGs showed enriched association for aging-related disease phenotypes, coronary artery disease, arteriosclerosis, and leukemias (Zannas *et al*, 2015a). Second, demethylation of the age regulated *FKBP5* CpGs, a signature of stress-related phenotypes, was associated with previous history of myocardial infarction in two independent cohorts (Zannas *et al*, unpublished). Third, higher G/L ratio and IL-8 levels, both of which were associated with *FKBP5* upregulation (Zannas *et al*, unpublished), have been shown to predict

heightened cardiovascular risk and mortality (Bhat *et al*, 2013; Boekholdt *et al*, 2004; Cavusoglu *et al*, 2015). Taken together, these findings provide molecular insights into previous associations of stress-related phenotypes with heightened inflammation and cardiovascular risk (Chandola *et al*, 2006; Danese *et al*, 2012; Danese *et al*, 2009; Danese *et al*, 2008; Danese *et al*, 2007; Felitti *et al*, 1998; Rozanski *et al*, 1999; Ruo *et al*, 2003; Vaccarino *et al*, 2013).

Concluding remark

In conclusion, the findings of this cumulative thesis support a model whereby exposure to stress and stress-related phenotypes may have lasting effects on the aging epigenome. These effects can in turn dysregulate molecular effectors of stress and downstream biological pathways, potentially contributing to risk for the development of aging-related disease. These findings are schematically summarized below in **Scheme**.

Beyond providing molecular insights into the mechanisms through which psychological stress contributes to disease risk, these findings could also have future implications for the prevention and treatment of stress-related diseases. In particular, although stress-induced epigenetic changes can be long-lasting and persistent, they may also be reversible. Such reversibility has been supported, for example, by studies in rodents showing that methyl-donor supplementation can reverse the DNA methylation changes and negative behavioral outcomes conferred by early life stress (Roth *et al*, 2009; Weaver *et al*, 2005). Potential reversibility has been also demonstrated for stress-related epigenetic aging (Brody *et al*, 2016a; Brody *et al*, 2016b; Zannas, 2016). Nevertheless, stress-induced epigenetic signatures occur in a tissue-specific manner and are in many cases essential for successful adaptation to stressful environments (Russo *et al*, 2012; Zannas *et al*, 2014). Therefore, an important task for future

research will be to determine which stress-related epigenetic signatures may serve as disease biomarkers and the circumstances and tissues in which the modulation of these signatures may be indicated and feasible.

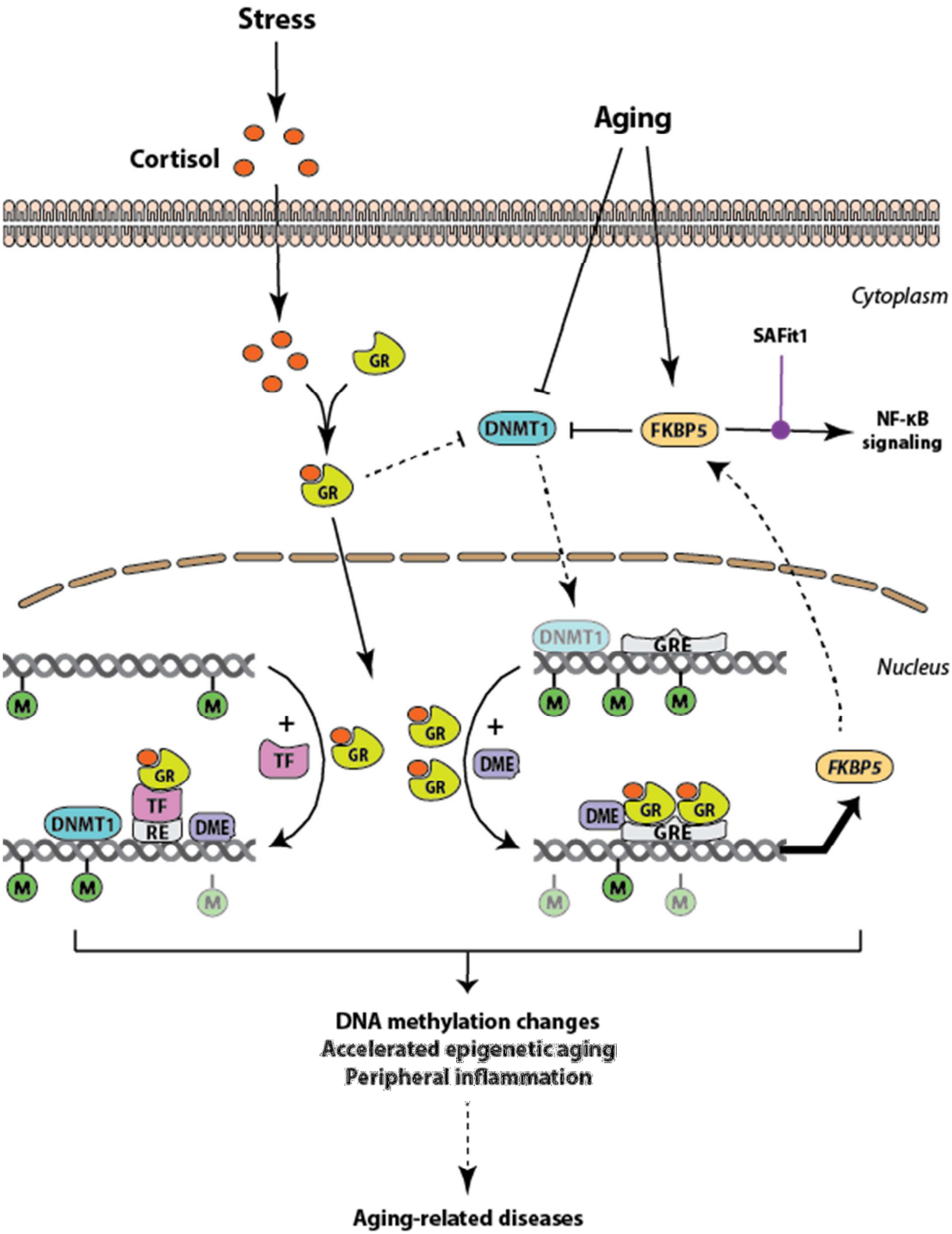
Stress
Cortisol
Aging
Cytoplasm
GR
SAFit1
DNMT1
FKBP5
NF-κB signaling
GR
Nucleus
DNMT1
GRE
M
M
M
+
TF
GR
GR
GR
+
DME
FKBP5
GR
TF
RE
DME
DNMT1
DME
GR
GR
GRE
M
M
M
M
M
M
DNA methylation changes
Accelerated epigenetic aging
Peripheral inflammation
Aging-related diseases

Scheme. Simplified scheme summarizing the molecular (DNA methylation) interplay between psychological stress and aging. Stress triggers adrenal release of cortisol, which enters the cells and activates the ligand-dependent transcription factor, glucocorticoid receptor (GR). The activated GR then shuttles into the nucleus and can induce DNA methylation changes either by direct binding to glucocorticoid response elements (GRE) or, presumably, by tethering via other transcription factors (TF), which can bind to their respective response elements (RE). GR-induced demethylation upregulates, among other gene targets, the stress-responsive *FKBP5* gene. FKBP5 is a versatile co-chaperone protein that influences multiple biological pathways. As shown in the present thesis, FKBP5 inhibits the activity of the maintenance DNA methyltransferase DNMT1, thereby forming a feed-forward mechanism that can propagate stress-induced demethylation. This is further accentuated with advancing age, which downregulates DNMT1 and upregulates FKBP5. Importantly, upregulated FKBP5 also facilitates NF-κB signaling, an effect that in cells is prevented by treatment with FKBP5 antagonists (SAFit1). Overall, these effects lead to widespread DNA methylation changes, accelerated epigenetic aging, and heightened peripheral inflammation, potentially contributing to increased risk for aging-related diseases.

References

Ahola K, Siren I, Kivimaki M, Ripatti S, Aromaa A, Lonnqvist J*, et al* (2012). Work-related exhaustion and telomere length: a population-based study. *PloS one* **7**(7): e40186.

Alasaari JS, Lagus M, Ollila HM, Toivola A, Kivimaki M, Vahtera J*, et al* (2012). Environmental stress affects DNA methylation of a CpG rich promoter region of serotonin transporter gene in a nurse cohort. *PloS one* **7**(9): e45813.

Anier K, Malinovskaja K, Pruus K, Aonurm-Helm A, Zharkovsky A, Kalda A (2014). Maternal separation is associated with DNA methylation and behavioural changes in adult rats. *European neuropsychopharmacology : the journal of the European College of Neuropsychopharmacology* **24**(3): 459-468.

Aryee MJ, Jaffe AE, Corrada-Bravo H, Ladd-Acosta C, Feinberg AP, Hansen KD*, et al* (2014). Minfi: a flexible and comprehensive Bioconductor package for the analysis of Infinium DNA methylation microarrays. *Bioinformatics* **30**(10): 1363-1369.

Avellino R, Romano S, Parasole R, Bisogni R, Lamberti A, Poggi V*, et al* (2005). Rapamycin stimulates apoptosis of childhood acute lymphoblastic leukemia cells. *Blood* **106**(4): 1400-1406.

Barha CK, Brummelte S, Lieblich SE, Galea LA (2011). Chronic restraint stress in adolescence differentially influences hypothalamic-pituitary-adrenal axis function and adult hippocampal neurogenesis in male and female rats. *Hippocampus* **21**(11): 1216-1227.

Barker DJ, Osmond C, Forsen TJ, Kajantie E, Eriksson JG (2005). Trajectories of growth among children who have coronary events as adults. *The New England journal of medicine* **353**(17): 1802-1809.

Baughman G, Wiederrecht GJ, Campbell NF, Martin MM, Bourgeois S (1995). FKBP51, a novel T-cell-specific immunophilin capable of calcineurin inhibition. *Molecular and cellular biology* **15**(8): 4395-4402.

Beck AT, Steer RA, Garbin MG (1988). Psychometric Properties of the Beck Depression Inventory - 25 Years of Evaluation. *Clin Psychol Rev* **8**(1): 77-100.

Beck AT, Ward CH, Mendelson M, Mock J, Erbaugh J (1961). An inventory for measuring depression. *Archives of general psychiatry* **4**: 561-571.

Bell JT, Tsai PC, Yang TP, Pidsley R, Nisbet J, Glass D*, et al* (2012). Epigenome-wide scans identify differentially methylated regions for age and age-related phenotypes in a healthy ageing population. *PLoS genetics* **8**(4): e1002629.

Benayoun BA, Pollina EA, Brunet A (2015). Epigenetic regulation of ageing: linking environmental inputs to genomic stability. *Nat Rev Mol Cell Biol* **16**(10): 593-610.

Benoit JD, Rakic P, Frick KM (2015). Prenatal stress induces spatial memory deficits and epigenetic changes in the hippocampus indicative of heterochromatin formation and reduced gene expression. *Behavioural brain research* **281**: 1-8.

Bernstein DP, Stein JA, Newcomb MD, Walker E, Pogge D, Ahluvalia T*, et al* (2003). Development and validation of a brief screening version of the Childhood Trauma Questionnaire. *Child abuse & neglect* **27**(2): 169-190.

Bhat T, Teli S, Rijal J, Bhat H, Raza M, Khoueiry G*, et al* (2013). Neutrophil to lymphocyte ratio and cardiovascular diseases: a review. *Expert review of cardiovascular therapy* **11**(1): 55-59.

Binder EB, Bradley RG, Liu W, Epstein MP, Deveau TC, Mercer KB*, et al* (2008). Association of FKBP5 polymorphisms and childhood abuse with risk of posttraumatic stress disorder symptoms in adults. *JAMA : the journal of the American Medical Association* **299**(11): 1291-1305.

Bjornsson HT, Sigurdsson MI, Fallin MD, Irizarry RA, Aspelund T, Cui H*, et al* (2008). Intra-individual change over time in DNA methylation with familial clustering. *JAMA : the journal of the American Medical Association* **299**(24): 2877-2883.

Blair LJ, Nordhues BA, Hill SE, Scaglione KM, O'Leary JC, 3rd, Fontaine SN*, et al* (2013). Accelerated neurodegeneration through chaperone-mediated oligomerization of tau. *The Journal of clinical investigation* **123**(10): 4158-4169.

Bocklandt S, Lin W, Sehl ME, Sanchez FJ, Sinsheimer JS, Horvath S*, et al* (2011). Epigenetic predictor of age. *PloS one* **6**(6): e14821.

Boekholdt SM, Peters RJ, Hack CE, Day NE, Luben R, Bingham SA*, et al* (2004). IL-8 plasma concentrations and the risk of future coronary artery disease in apparently healthy men and women: the EPIC-Norfolk prospective population study. *Arteriosclerosis, thrombosis, and vascular biology* **24**(8): 1503-1508.

Boersma GJ, Lee RS, Cordner ZA, Ewald ER, Purcell RH, Moghadam AA*, et al* (2014). Prenatal stress decreases Bdnf expression and increases methylation of Bdnf exon IV in rats. *Epigenetics : official journal of the DNA Methylation Society* **9**(3): 437-447.

Bose R, Moors M, Tofighi R, Cascante A, Hermanson O, Ceccatelli S (2010). Glucocorticoids induce long-lasting effects in neural stem cells resulting in senescence-related alterations. *Cell death & disease* **1**: e92.

Bose R, Spulber S, Kilian P, Heldring N, Lonnerberg P, Johnsson A*, et al* (2015). Tet3 mediates stable glucocorticoid-induced alterations in DNA methylation and Dnmt3a/Dkk1 expression in neural progenitors. *Cell death & disease* **6**: e1793.

Bourke CH, Neigh GN (2011). Behavioral effects of chronic adolescent stress are sustained and sexually dimorphic. *Hormones and behavior* **60**(1): 112-120.

Bouwmeester T, Bauch A, Ruffner H, Angrand PO, Bergamini G, Croughton K*, et al* (2004). A physical and functional map of the human TNF-alpha/NF-kappa B signal transduction pathway. *Nature cell biology* **6**(2): 97-105.

Breitling LP, Saum KU, Perna L, Schottker B, Holleczek B, Brenner H (2016). Frailty is associated with the epigenetic clock but not with telomere length in a German cohort. *Clinical epigenetics* **8**: 21.

Brody GH, Miller GE, Yu T, Beach SR, Chen E (2016a). Supportive Family Environments Ameliorate the Link Between Racial Discrimination and Epigenetic Aging: A Replication Across Two Longitudinal Cohorts. *Psychological science* **27**(4): 530-541.

Brody GH, Yu T, Chen E, Beach SR, Miller GE (2016b). Family-centered prevention ameliorates the longitudinal association between risky family processes and epigenetic aging. *J Child Psychol Psychiatry* **57**(5): 566-574.

Brunet A, Berger SL (2014). Epigenetics of aging and aging-related disease. *The journals of gerontology Series A, Biological sciences and medical sciences* **69 Suppl 1**: S17-20.

Cao-Lei L, Massart R, Suderman MJ, Machnes Z, Elgbeili G, Laplante DP*, et al* (2014). DNA methylation signatures triggered by prenatal maternal stress exposure to a natural disaster: Project Ice Storm. *PloS one* **9**(9): e107653.

Capra JA (2015). Extrapolating histone marks across developmental stages, tissues, and species: an enhancer prediction case study. *BMC genomics* **16**: 104.

Castillo-Diaz SA, Garay-Sevilla ME, Hernandez-Gonzalez MA, Solis-Martinez MO, Zaina S (2010). Extensive demethylation of normally hypermethylated CpG islands occurs in human atherosclerotic arteries. *International journal of molecular medicine* **26**(5): 691-700.

Cavusoglu E, Marmur JD, Yanamadala S, Chopra V, Hegde S, Nazli A*, et al* (2015). Elevated baseline plasma IL-8 levels are an independent predictor of long-term all-cause mortality in patients with acute coronary syndrome. *Atherosclerosis* **242**(2): 589-594.

Chandola T, Brunner E, Marmot M (2006). Chronic stress at work and the metabolic syndrome: prospective study. *Bmj* **332**(7540): 521-525.

Chen BH, Marioni RE, Colicino E, Peters MJ, Ward-Caviness CK, Tsai PC*, et al* (2016). DNA methylation-based measures of biological age: meta-analysis predicting time to death. *Aging* **8**(9): 1844-1865.

Chen YA, Lemire M, Choufani S, Butcher DT, Grafodatskaya D, Zanke BW*, et al* (2013). Discovery of cross-reactive probes and polymorphic CpGs in the Illumina Infinium HumanMethylation450 microarray. *Epigenetics : official journal of the DNA Methylation Society* **8**(2): 203-209.

Christensen BC, Houseman EA, Marsit CJ, Zheng S, Wrensch MR, Wiemels JL*, et al* (2009). Aging and environmental exposures alter tissue-specific DNA methylation dependent upon CpG island context. *PLoS genetics* **5**(8): e1000602.

Chrousos GP, Gold PW (1992). The concepts of stress and stress system disorders. Overview of physical and behavioral homeostasis. *JAMA : the journal of the American Medical Association* **267**(9): 1244-1252.

Coffey SF, Dansky BS, Falsetti SA, Saladin ME, Brady KT (1998). Screening for PTSD in a substance abuse sample: psychometric properties of a modified version of the PTSD Symptom Scale Self-Report. Posttraumatic stress disorder. *Journal of traumatic stress* **11**(2): 393-399.

Danese A, McEwen BS (2012). Adverse childhood experiences, allostasis, allostatic load, and age-related disease. *Physiology & behavior* **106**(1): 29-39.

Danese A, Moffitt TE, Harrington H, Milne BJ, Polanczyk G, Pariante CM*, et al* (2009). Adverse childhood experiences and adult risk factors for age-related disease: depression, inflammation, and clustering of metabolic risk markers. *Archives of pediatrics & adolescent medicine* **163**(12): 1135-1143.

Danese A, Moffitt TE, Pariante CM, Ambler A, Poulton R, Caspi A (2008). Elevated inflammation levels in depressed adults with a history of childhood maltreatment. *Archives of general psychiatry* **65**(4): 409-415.

Danese A, Pariante CM, Caspi A, Taylor A, Poulton R (2007). Childhood maltreatment predicts adult inflammation in a life-course study. *Proceedings of the National Academy of Sciences of the United States of America* **104**(4): 1319-1324.

Daudt DR, Yorio T (2011). FKBP51 protects 661w cell culture from staurosporine-induced apoptosis. *Molecular vision* **17**: 1172-1181.

de Kloet CS, Vermetten E, Geuze E, Kavelaars A, Heijnen CJ, Westenberg HG (2006). Assessment of HPA-axis function in posttraumatic stress disorder: pharmacological and non-pharmacological challenge tests, a review. *Journal of psychiatric research* **40**(6): 550-567.

Di Stefano V, Wang B, Parobchak N, Roche N, Rosen T (2015). RelB/p52-mediated NF-kappaB signaling alters histone acetylation to increase the abundance of corticotropin-releasing hormone in human placenta. *Sci Signal* **8**(391): ra85.

Dias BG, Ressler KJ (2014). Parental olfactory experience influences behavior and neural structure in subsequent generations. *Nature neuroscience* **17**(1): 89-96.

Doherty TS, Forster A, Roth TL (2016). Global and gene-specific DNA methylation alterations in the adolescent amygdala and hippocampus in an animal model of caregiver maltreatment. *Behavioural brain research* **298**(Pt A): 55-61.

Dong E, Dzitoyeva SG, Matrisciano F, Tueting P, Grayson DR, Guidotti A (2015). Brain-derived neurotrophic factor epigenetic modifications associated with schizophrenia-like phenotype induced by prenatal stress in mice. *Biological psychiatry* **77**(6): 589-596.

Du P, Kibbe WA, Lin SM (2008). lumi: a pipeline for processing Illumina microarray. *Bioinformatics* **24**(13): 1547-1548.

Du P, Zhang X, Huang CC, Jafari N, Kibbe WA, Hou L*, et al* (2010). Comparison of Beta-value and M-value methods for quantifying methylation levels by microarray analysis. *BMC bioinformatics* **11**: 587.

Dwivedi Y, Roy B, Lugli G, Rizavi H, Zhang H, Smalheiser NR (2015). Chronic corticosterone-mediated dysregulation of microRNA network in prefrontal cortex of rats: relevance to depression pathophysiology. *Translational psychiatry* **5**: e682.

Elliott E, Ezra-Nevo G, Regev L, Neufeld-Cohen A, Chen A (2010). Resilience to social stress coincides with functional DNA methylation of the Crf gene in adult mice. *Nature neuroscience* **13**(11): 1351-1353.

Entringer S, Epel ES, Kumsta R, Lin J, Hellhammer DH, Blackburn EH*, et al* (2011). Stress exposure in intrauterine life is associated with shorter telomere length in young adulthood. *Proceedings of the National Academy of Sciences of the United States of America* **108**(33): E513-518.

Entringer S, Epel ES, Lin J, Buss C, Shahbaba B, Blackburn EH*, et al* (2013). Maternal psychosocial stress during pregnancy is associated with newborn leukocyte telomere length. *American journal of obstetrics and gynecology* **208**(2): 134.e131-137.

Epel ES, Blackburn EH, Lin J, Dhabhar FS, Adler NE, Morrow JD*, et al* (2004). Accelerated telomere shortening in response to life stress. *Proceedings of the National Academy of Sciences of the United States of America* **101**(49): 17312-17315.

Erburu M, Munoz-Cobo I, Dominguez-Andres J, Beltran E, Suzuki T, Mai A*, et al* (2015). Chronic stress and antidepressant induced changes in Hdac5 and Sirt2 affect synaptic plasticity. *European neuropsychopharmacology : the journal of the European College of Neuropsychopharmacology* **25**(11): 2036-2048.

Erlejman AG, De Leo SA, Mazaira GI, Molinari AM, Camisay MF, Fontana V*, et al* (2014). NF-kappaB transcriptional activity is modulated by FK506-binding proteins FKBP51 and FKBP52: a role for peptidyl-prolyl isomerase activity. *The Journal of biological chemistry* **289**(38): 26263-26276.

Fang CY, Ross EA, Pathak HB, Godwin AK, Tseng M (2014). Acculturative stress and inflammation among Chinese immigrant women. *Psychosomatic medicine* **76**(5): 320-326.

Felitti VJ, Anda RF, Nordenberg D, Williamson DF, Spitz AM, Edwards V*, et al* (1998). Relationship of childhood abuse and household dysfunction to many of the leading causes of death in adults. The Adverse Childhood Experiences (ACE) Study. *American journal of preventive medicine* **14**(4): 245-258.

Florath I, Butterbach K, Muller H, Bewerunge-Hudler M, Brenner H (2014). Cross-sectional and longitudinal changes in DNA methylation with age: an epigenome-wide analysis revealing over 60 novel age-associated CpG sites. *Human molecular genetics* **23**(5): 1186-1201.

Fortin JP, Fertig E, Hansen K (2014a). shinyMethyl: interactive quality control of Illumina 450k DNA methylation arrays in R. *F1000Research* **3**: 175.

Fortin JP, Labbe A, Lemire M, Zanke BW, Hudson TJ, Fertig EJ*, et al* (2014b). Functional normalization of 450k methylation array data improves replication in large cancer studies. *Genome biology* **15**(12): 503.

Fraga MF, Ballestar E, Paz MF, Ropero S, Setien F, Ballestar ML*, et al* (2005). Epigenetic differences arise during the lifetime of monozygotic twins. *Proceedings of the National Academy of Sciences of the United States of America* **102**(30): 10604-10609.

Franceschi C, Campisi J (2014). Chronic inflammation (inflammaging) and its potential contribution to age-associated diseases. *The journals of gerontology Series A, Biological sciences and medical sciences* **69 Suppl 1**: S4-9.

Gaali S, Kirschner A, Cuboni S, Hartmann J, Kozany C, Balsevich G*, et al* (2015). Selective inhibitors of the FK506-binding protein 51 by induced fit. **11**(1): 33-37.

Gassen NC, Chrousos GP, Binder EB, Zannas AS (2016). Life stress, glucocorticoid signaling, and the aging epigenome: Implications for aging-related diseases. *Neurosci Biobehav Rev*.

Gassen NC, Fries GR, Zannas AS, Hartmann J, Zschocke J, Hafner K*, et al* (2015). Chaperoning epigenetics: FKBP51 decreases the activity of DNMT1 and mediates epigenetic effects of the antidepressant paroxetine. *Sci Signal* **8**(404): ra119.

Gassen NC, Hartmann J, Zschocke J, Stepan J, Hafner K, Zellner A*, et al* (2014). Association of FKBP51 with priming of autophagy pathways and mediation of antidepressant treatment response: evidence in cells, mice, and humans. *PLoS medicine* **11**(11): e1001755.

Gassen NC, Hartmann J, Zannas AS, Zschocke J, Maccarrone G, Hafner K, Zellner A, Wagner KV, Mehta D, Kloiber S, Turck CW, Lucae S, Chrousos GP, Holsboer F, Binder EB, Ising M, Schmidt MV, Rein T (2015). FKBP51 inhibits GSK3β and augments the effects of distinct psychotropic medications. *Molecular psychiatry* **In press**.

Gillespie CF, Bradley B, Mercer K, Smith AK, Conneely K, Gapen M*, et al* (2009). Trauma exposure and stress-related disorders in inner city primary care patients. *General hospital psychiatry* **31**(6): 505-514.

Giordano A, Avellino R, Ferraro P, Romano S, Corcione N, Romano MF (2006). Rapamycin antagonizes NF-kappaB nuclear translocation activated by TNF-alpha in primary vascular smooth muscle cells and enhances apoptosis. *American journal of physiology Heart and circulatory physiology* **290**(6): H2459-2465.

Gronniger E, Weber B, Heil O, Peters N, Stab F, Wenck H*, et al* (2010). Aging and chronic sun exposure cause distinct epigenetic changes in human skin. *PLoS genetics* **6**(5): e1000971.

Hafner S, Emeny RT, Lacruz ME, Baumert J, Herder C, Koenig W*, et al* (2011). Association between social isolation and inflammatory markers in depressed and non-depressed individuals: results from the MONICA/KORA study. *Brain, behavior, and immunity* **25**(8): 1701-1707.

Hampf M, Gossen M (2006). A protocol for combined Photinus and Renilla luciferase quantification compatible with protein assays. *Analytical biochemistry* **356**(1): 94-99.

Hannon E, Lunnon K, Schalkwyk L, Mill J (2015). Interindividual methylomic variation across blood, cortex, and cerebellum: implications for epigenetic studies of neurological and neuropsychiatric phenotypes. *Epigenetics : official journal of the DNA Methylation Society* **10**(11): 1024-1032.

Hannum G, Guinney J, Zhao L, Zhang L, Hughes G, Sadda S*, et al* (2013). Genome-wide methylation profiles reveal quantitative views of human aging rates. *Molecular cell* **49**(2): 359-367.

Hanzelmann S, Beier F, Gusmao EG, Koch CM, Hummel S, Charapitsa I*, et al* (2015). Replicative senescence is associated with nuclear reorganization and with DNA methylation at specific transcription factor binding sites. *Clinical epigenetics* **7**(1): 19.

Heck A, Lieb R, Ellgas A, Pfister H, Lucae S, Roeske D*, et al* (2009). Investigation of 17 candidate genes for personality traits confirms effects of the HTR2A gene on novelty seeking. *Genes, brain, and behavior* **8**(4): 464-472.

Heim C, Newport DJ, Mletzko T, Miller AH, Nemeroff CB (2008). The link between childhood trauma and depression: insights from HPA axis studies in humans. *Psychoneuroendocrinology* **33**(6): 693-710.

Herbstman JB, Wang S, Perera FP, Lederman SA, Vishnevetsky J, Rundle AG*, et al* (2013). Predictors and consequences of global DNA methylation in cord blood and at three years. *PloS one* **8**(9): e72824.

Hernandez DG, Nalls MA, Gibbs JR, Arepalli S, van der Brug M, Chong S*, et al* (2011). Distinct DNA methylation changes highly correlated with chronological age in the human brain. *Human molecular genetics* **20**(6): 1164-1172.

Heyn H, Li N, Ferreira HJ, Moran S, Pisano DG, Gomez A*, et al* (2012). Distinct DNA methylomes of newborns and centenarians. *Proceedings of the National Academy of Sciences of the United States of America* **109**(26): 10522-10527.

Holle R, Happich M, Lowel H, Wichmann HE (2005). KORA--a research platform for population based health research. *Gesundheitswesen (Bundesverband der Arzte des Offentlichen Gesundheitsdienstes (Germany))* **67 Suppl 1**: S19-25.

Horvath S (2013). DNA methylation age of human tissues and cell types. *Genome biology* **14**(10): R115.

Horvath S, Erhart W, Brosch M, Ammerpohl O, von Schonfels W, Ahrens M*, et al* (2014). Obesity accelerates epigenetic aging of human liver. *Proceedings of the National Academy of Sciences of the United States of America* **111**(43): 15538-15543.

Horvath S, Ritz BR (2015). Increased epigenetic age and granulocyte counts in the blood of Parkinson's disease patients. *Aging*.

Horvath S, Zhang Y, Langfelder P, Kahn RS, Boks MP, van Eijk K*, et al* (2012). Aging effects on DNA methylation modules in human brain and blood tissue. *Genome biology* **13**(10): R97.

Houseman EA, Accomando WP, Koestler DC, Christensen BC, Marsit CJ, Nelson HH*, et al* (2012). DNA methylation arrays as surrogate measures of cell mixture distribution. *BMC bioinformatics* **13**: 86.

Houtepen LC, Vinkers CH, Carrillo-Roa T, Hiemstra M, van Lier PA, Meeus W*, et al* (2016). Genome-wide DNA methylation levels and altered cortisol stress reactivity following childhood trauma in humans. *Nature communications* **7**: 10967.

Howcroft TK, Campisi J, Louis GB, Smith MT, Wise B, Wyss-Coray T*, et al* (2013). The role of inflammation in age-related disease. *Aging* **5**(1): 84-93.

Huber W, von Heydebreck A, Sultmann H, Poustka A, Vingron M (2002). Variance stabilization applied to microarray data calibration and to the quantification of differential expression. *Bioinformatics* **18 Suppl 1**: S96-104.

Issa JP (2014). Aging and epigenetic drift: a vicious cycle. *The Journal of clinical investigation* **124**(1): 24-29.

Jankord R, Solomon MB, Albertz J, Flak JN, Zhang R, Herman JP (2011). Stress vulnerability during adolescent development in rats. *Endocrinology* **152**(2): 629-638.

Johnson WE, Li C, Rabinovic A (2007). Adjusting batch effects in microarray expression data using empirical Bayes methods. *Biostatistics (Oxford, England)* **8**(1): 118-127.

Jones PA, Baylin SB (2007). The epigenomics of cancer. *Cell* **128**(4): 683-692.

Kaminsky Z, Wilcox HC, Eaton WW, Van Eck K, Kilaru V, Jovanovic T*, et al* (2015). Epigenetic and genetic variation at SKA2 predict suicidal behavior and post-traumatic stress disorder. *Translational psychiatry* **5**: e627.

Kananen L, Surakka I, Pirkola S, Suvisaari J, Lonnqvist J, Peltonen L*, et al* (2010). Childhood adversities are associated with shorter telomere length at adult age both in individuals with an anxiety disorder and controls. *PloS one* **5**(5): e10826.

Kao GS, Cheng LY, Chen LH, Tzeng WY, Cherng CG, Su CC*, et al* (2012). Neonatal isolation decreases cued fear conditioning and frontal cortical histone 3 lysine 9 methylation in adult female rats. *European journal of pharmacology* **697**(1-3): 65-72.

Kellogg SH, McHugh PF, Bell K, Schluger JH, Schluger RP, LaForge KS*, et al* (2003). The Kreek-McHugh-Schluger-Kellogg scale: a new, rapid method for quantifying substance abuse and its possible applications. *Drug and alcohol dependence* **69**(2): 137-150.

Kim YS, Kim YJ, Lee JM, Kim EK, Park YJ, Choe SK*, et al* (2012). Functional changes in myeloid-derived suppressor cells (MDSCs) during tumor growth: FKBP51 contributes to the regulation of the immunosuppressive function of MDSCs. *Journal of immunology (Baltimore, Md : 1950)* **188**(9): 4226-4234.

Klengel T, Mehta D, Anacker C, Rex-Haffner M, Pruessner JC, Pariante CM*, et al* (2013). Allele-specific FKBP5 DNA demethylation mediates gene-childhood trauma interactions. *Nature neuroscience* **16**(1): 33-41.

Ko JY, Chuang PC, Ke HJ, Chen YS, Sun YC, Wang FS (2015). MicroRNA-29a mitigates glucocorticoid induction of bone loss and fatty marrow by rescuing Runx2 acetylation. *Bone* **81**: 80-88.

Kobayashi Y (2008). The role of chemokines in neutrophil biology. *Frontiers in bioscience : a journal and virtual library* **13**: 2400-2407.

Koch CM, Wagner W (2011). Epigenetic-aging-signature to determine age in different tissues. *Aging* **3**(10): 1018-1027.

Kohli MA, Lucae S, Saemann PG, Schmidt MV, Demirkan A, Hek K*, et al* (2011). The neuronal transporter gene SLC6A15 confers risk to major depression. *Neuron* **70**(2): 252-265.

Ladwig KH, Marten-Mittag B, Baumert J, Lowel H, Doring A (2004). Case-finding for depressive and exhausted mood in the general population: reliability and validity of a symptom-driven diagnostic scale. Results from the prospective MONICA/KORA Augsburg Study. *Annals of epidemiology* **14**(5): 332-338.

Lam LL, Emberly E, Fraser HB, Neumann SM, Chen E, Miller GE*, et al* (2012). Factors underlying variable DNA methylation in a human community cohort. *Proceedings of the National Academy of Sciences of the United States of America* **109 Suppl 2**: 17253-17260.

Langevin SM, Pinney SM, Leung YK, Ho SM (2014). Does epigenetic drift contribute to age-related increases in breast cancer risk? *Epigenomics* **6**(4): 367-369.

Le Francois B, Soo J, Millar AM, Daigle M, Le Guisquet AM, Leman S*, et al* (2015). Chronic mild stress and antidepressant treatment alter 5-HT1A receptor expression by modifying DNA methylation of a conserved Sp4 site. *Neurobiology of disease* **82**: 332-341.

Lee RS, Tamashiro KL, Yang X, Purcell RH, Harvey A, Willour VL*, et al* (2010). Chronic corticosterone exposure increases expression and decreases deoxyribonucleic acid methylation of Fkbp5 in mice. *Endocrinology* **151**(9): 4332-4343.

Lee RS, Tamashiro KL, Yang X, Purcell RH, Huo Y, Rongione M*, et al* (2011). A measure of glucocorticoid load provided by DNA methylation of Fkbp5 in mice. *Psychopharmacology* **218**(1): 303-312.

Levine ME, Hosgood HD, Chen B, Absher D, Assimes T, Horvath S (2015a). DNA methylation age of blood predicts future onset of lung cancer in the women's health initiative. *Aging* **7**(9): 690-700.

Levine ME, Lu AT, Bennett DA, Horvath S (2015b). Epigenetic age of the pre-frontal cortex is associated with neuritic plaques, amyloid load, and Alzheimer's disease related cognitive functioning. *Aging*.

Levine ME, Lu AT, Chen BH, Hernandez DG, Singleton AB, Ferrucci L*, et al* (2016). Menopause accelerates biological aging. *Proceedings of the National Academy of Sciences of the United States of America* **113**(33): 9327-9332.

Li TK, Baksh S, Cristillo AD, Bierer BE (2002). Calcium- and FK506-independent interaction between the immunophilin FKBP51 and calcineurin. *Journal of cellular biochemistry* **84**(3): 460-471.

Li Y, Liu Y, Strickland FM, Richardson B (2010). Age-dependent decreases in DNA methyltransferase levels and low transmethylation micronutrient levels synergize to promote overexpression of genes implicated in autoimmunity and acute coronary syndromes. *Experimental gerontology* **45**(4): 312-322.

Lightman SL (2008). The neuroendocrinology of stress: a never ending story. *Journal of neuroendocrinology* **20**(6): 880-884.

Litzelman K, Witt WP, Gangnon RE, Nieto FJ, Engelman CD, Mailick MR*, et al* (2014). Association between informal caregiving and cellular aging in the survey of the health of wisconsin: the role of caregiving characteristics, stress, and strain. *American journal of epidemiology* **179**(11): 1340-1352.

Lopez-Otin C, Blasco MA, Partridge L, Serrano M, Kroemer G (2013). The hallmarks of aging. *Cell* **153**(6): 1194-1217.

Lu AT, Hannon E, Levine ME, Hao K, Crimmins EM, Lunnon K*, et al* (2016). Genetic variants near MLST8 and DHX57 affect the epigenetic age of the cerebellum. *Nature communications* **7**: 10561.

Lucae S, Salyakina D, Barden N, Harvey M, Gagne B, Labbe M*, et al* (2006). P2RX7, a gene coding for a purinergic ligand-gated ion channel, is associated with major depressive disorder. *Human molecular genetics* **15**(16): 2438-2445.

Maiaru M, Tochiki KK, Cox MB, Annan LV, Bell CG, Feng X*, et al* (2016). The stress regulator FKBP51 drives chronic pain by modulating spinal glucocorticoid signaling. *Science translational medicine* **8**(325): 325ra319.

Marioni RE, Harris SE, Shah S, McRae AF, von Zglinicki T, Martin-Ruiz C*, et al* (2016). The epigenetic clock and telomere length are independently associated with chronological age and mortality. *International journal of epidemiology*.

Marioni RE, Shah S, McRae AF, Chen BH, Colicino E, Harris SE*, et al* (2015a). DNA methylation age of blood predicts all-cause mortality in later life. *Genome biology* **16**(1): 25.

Marioni RE, Shah S, McRae AF, Ritchie SJ, Muniz-Terrera G, Harris SE*, et al* (2015b). The epigenetic clock is correlated with physical and cognitive fitness in the Lothian Birth Cohort 1936. *International journal of epidemiology*.

McGowan PO, Sasaki A, D'Alessio AC, Dymov S, Labonte B, Szyf M*, et al* (2009). Epigenetic regulation of the glucocorticoid receptor in human brain associates with childhood abuse. *Nature neuroscience* **12**(3): 342-348.

Mehta D, Klengel T, Conneely KN, Smith AK, Altmann A, Pace TW*, et al* (2013). Childhood maltreatment is associated with distinct genomic and epigenetic profiles in posttraumatic stress disorder. *Proceedings of the National Academy of Sciences of the United States of America* **110**(20): 8302-8307.

Menke A, Arloth J, Putz B, Weber P, Klengel T, Mehta D*, et al* (2012). Dexamethasone stimulated gene expression in peripheral blood is a sensitive marker for glucocorticoid receptor resistance in depressed patients. *Neuropsychopharmacology : official publication of the American College of Neuropsychopharmacology* **37**(6): 1455-1464.

Montagud-Romero S, Montesinos J, Pascual M, Aguilar MA, Roger-Sanchez C, Guerri C*, et al* (2016). `Up-regulation of histone acetylation induced by social defeat mediates the conditioned rewarding effects of cocaine. *Progress in neuro-psychopharmacology & biological psychiatry* **70**: 39-48.

Monteleone MC, Adrover E, Pallares ME, Antonelli MC, Frasch AC, Brocco MA (2014). Prenatal stress changes the glycoprotein GPM6A gene expression and induces epigenetic changes in rat offspring brain. *Epigenetics : official journal of the DNA Methylation Society* **9**(1): 152-160.

Murgatroyd C, Patchev AV, Wu Y, Micale V, Bockmuhl Y, Fischer D*, et al* (2009). Dynamic DNA methylation programs persistent adverse effects of early-life stress. *Nature neuroscience* **12**(12): 1559-1566.

Mychasiuk R, Schmold N, Ilnytskyy S, Kovalchuk O, Kolb B, Gibb R (2011). Prenatal bystander stress alters brain, behavior, and the epigenome of developing rat offspring. *Developmental neuroscience* **33**(2): 159-169.

Nasca C, Zelli D, Bigio B, Piccinin S, Scaccianoce S, Nistico R*, et al* (2015). Stress dynamically regulates behavior and glutamatergic gene expression in hippocampus by opening a window of epigenetic plasticity. *Proceedings of the National Academy of Sciences of the United States of America* **112**(48): 14960-14965.

Niccoli T, Partridge L (2012). Ageing as a risk factor for disease. *Current biology : CB* **22**(17): R741-752.

Niwa M, Jaaro-Peled H, Tankou S, Seshadri S, Hikida T, Matsumoto Y*, et al* (2013). Adolescent stress-induced epigenetic control of dopaminergic neurons via glucocorticoids. *Science (New York, NY)* **339**(6117): 335-339.

Ouellet-Morin I, Wong CC, Danese A, Pariante CM, Papadopoulos AS, Mill J*, et al* (2013). Increased serotonin transporter gene (SERT) DNA methylation is associated with bullying victimization and blunted cortisol response to stress in childhood: a longitudinal study of discordant monozygotic twins. *Psychological medicine* **43**(9): 1813-1823.

Palacios-Garcia I, Lara-Vasquez A, Montiel JF, Diaz-Veliz GF, Sepulveda H, Utreras E*, et al* (2015). Prenatal stress down-regulates Reelin expression by methylation of its promoter and induces adult behavioral impairments in rats. *PloS one* **10**(2): e0117680.

Palma-Gudiel H, Cordova-Palomera A, Eixarch E, Deuschle M, Fananas L (2015). Maternal psychosocial stress during pregnancy alters the epigenetic signature of the glucocorticoid receptor gene promoter in their offspring: a meta-analysis. *Epigenetics : official journal of the DNA Methylation Society* **10**(10): 893-902.

Park J, Kim M, Na G, Jeon I, Kwon YK, Kim JH*, et al* (2007). Glucocorticoids modulate NF-kappaB-dependent gene expression by up-regulating FKBP51 expression in Newcastle disease virus-infected chickens. *Molecular and cellular endocrinology* **278**(1-2): 7-17.

Parks CG, Miller DB, McCanlies EC, Cawthon RM, Andrew ME, DeRoo LA*, et al* (2009). Telomere length, current perceived stress, and urinary stress hormones in women. *Cancer epidemiology, biomarkers &*

prevention : a publication of the American Association for Cancer Research, cosponsored by the American Society of Preventive Oncology **18**(2): 551-560.

Peavy GM, Salmon DP, Jacobson MW, Hervey A, Gamst AC, Wolfson T*, et al* (2009). Effects of chronic stress on memory decline in cognitively normal and mildly impaired older adults. *The American journal of psychiatry* **166**(12): 1384-1391.

Pereira MJ, Palming J, Svensson MK, Rizell M, Dalenback J, Hammar M*, et al* (2014). FKBP5 expression in human adipose tissue increases following dexamethasone exposure and is associated with insulin resistance. *Metabolism: clinical and experimental* **63**(9): 1198-1208.

Perna L, Zhang Y, Mons U, Holleczek B, Saum KU, Brenner H (2016). Epigenetic age acceleration predicts cancer, cardiovascular, and all-cause mortality in a German case cohort. *Clinical epigenetics* **8**: 64.

Perroud N, Paoloni-Giacobino A, Prada P, Olie E, Salzmann A, Nicastro R*, et al* (2011). Increased methylation of glucocorticoid receptor gene (NR3C1) in adults with a history of childhood maltreatment: a link with the severity and type of trauma. *Translational psychiatry* **1**: e59.

Pidsley R, CC YW, Volta M, Lunnon K, Mill J, Schalkwyk LC (2013). A data-driven approach to preprocessing Illumina 450K methylation array data. *BMC genomics* **14**: 293.

Poulsen P, Esteller M, Vaag A, Fraga MF (2007). The epigenetic basis of twin discordance in age-related diseases. *Pediatric research* **61**(5 Pt 2): 38r-42r.

Powell ND, Allen RG, Hufnagle AR, Sheridan JF, Bailey MT (2011). Stressor-induced alterations of adaptive immunity to vaccination and viral pathogens. *Immunology and allergy clinics of North America* **31**(1): 69-79.

Powell ND, Tarr AJ, Sheridan JF (2013). Psychosocial stress and inflammation in cancer. *Brain, behavior, and immunity* **30 Suppl**: S41-47.

Prevention CfDCa (2013). The State of Aging and Health in America 2013. Atlanta, GA.

Puterman E, Lin J, Blackburn E, O'Donovan A, Adler N, Epel E (2010). The power of exercise: buffering the effect of chronic stress on telomere length. *PloS one* **5**(5): e10837.

Rakyan VK, Down TA, Maslau S, Andrew T, Yang TP, Beyan H*, et al* (2010). Human aging-associated DNA hypermethylation occurs preferentially at bivalent chromatin domains. *Genome research* **20**(4): 434-439.

Renthal W, Maze I, Krishnan V, Covington HE, 3rd, Xiao G, Kumar A*, et al* (2007). Histone deacetylase 5 epigenetically controls behavioral adaptations to chronic emotional stimuli. *Neuron* **56**(3): 517-529.

Rodgers AB, Morgan CP, Bronson SL, Revello S, Bale TL (2013). Paternal stress exposure alters sperm microRNA content and reprograms offspring HPA stress axis regulation. *The Journal of neuroscience : the official journal of the Society for Neuroscience* **33**(21): 9003-9012.

Rodgers AB, Morgan CP, Leu NA, Bale TL (2015). Transgenerational epigenetic programming via sperm microRNA recapitulates effects of paternal stress. *Proceedings of the National Academy of Sciences of the United States of America* **112**(44): 13699-13704.

Roebuck KA (1999). Regulation of interleukin-8 gene expression. *Journal of interferon & cytokine research : the official journal of the International Society for Interferon and Cytokine Research* **19**(5): 429-438.

Romano MF, Avellino R, Petrella A, Bisogni R, Romano S, Venuta S (2004). Rapamycin inhibits doxorubicin-induced NF-kappaB/Rel nuclear activity and enhances the apoptosis of melanoma cells. *European journal of cancer (Oxford, England : 1990)* **40**(18): 2829-2836.

Romano S, D'Angelillo A, Pacelli R, Staibano S, De Luna E, Bisogni R*, et al* (2010). Role of FK506-binding protein 51 in the control of apoptosis of irradiated melanoma cells. *Cell death and differentiation* **17**(1): 145-157.

Romano S, Xiao Y, Nakaya M, D'Angelillo A, Chang M, Jin J*, et al* (2015). FKBP51 employs both scaffold and isomerase functions to promote NF-kappaB activation in melanoma. *Nucleic acids research* **43**(14): 6983-6993.

Roth TL, Lubin FD, Funk AJ, Sweatt JD (2009). Lasting epigenetic influence of early-life adversity on the BDNF gene. *Biological psychiatry* **65**(9): 760-769.

Roth TL, Zoladz PR, Sweatt JD, Diamond DM (2011). Epigenetic modification of hippocampal Bdnf DNA in adult rats in an animal model of post-traumatic stress disorder. *Journal of psychiatric research* **45**(7): 919-926.

Rozanski A, Blumenthal JA, Kaplan J (1999). Impact of psychological factors on the pathogenesis of cardiovascular disease and implications for therapy. *Circulation* **99**(16): 2192-2217.

Ruo B, Rumsfeld JS, Hlatky MA, Liu H, Browner WS, Whooley MA (2003). Depressive symptoms and health-related quality of life: the Heart and Soul Study. *JAMA : the journal of the American Medical Association* **290**(2): 215-221.

Russo SJ, Murrough JW, Han MH, Charney DS, Nestler EJ (2012). Neurobiology of resilience. *Nature neuroscience* **15**(11): 1475-1484.

Savolainen K, Eriksson JG, Kananen L, Kajantie E, Pesonen AK, Heinonen K*, et al* (2014). Associations between early life stress, self-reported traumatic experiences across the lifespan and leukocyte telomere length in elderly adults. *Biological psychology* **97**: 35-42.

Sawamura T, Klengel T, Armario A, Jovanovic T, Norrholm SD, Ressler KJ*, et al* (2015). Dexamethasone Treatment Leads to Enhanced Fear Extinction and Dynamic Fkbp5 Regulation in Amygdala. *Neuropsychopharmacology : official publication of the American College of Neuropsychopharmacology*.

Schafer J, Strimmer K (2005). An empirical Bayes approach to inferring large-scale gene association networks. *Bioinformatics* **21**(6): 754-764.

Schiene-Fischer C, Yu C (2001). Receptor accessory folding helper enzymes: the functional role of peptidyl prolyl cis/trans isomerases. *FEBS letters* **495**(1-2): 1-6.

Schraut KG, Jakob SB, Weidner MT, Schmitt AG, Scholz CJ, Strekalova T*, et al* (2014). Prenatal stress-induced programming of genome-wide promoter DNA methylation in 5-HTT-deficient mice. *Translational psychiatry* **4**: e473.

Sinclair D, Fillman SG, Webster MJ, Weickert CS (2013). Dysregulation of glucocorticoid receptor co-factors FKBP5, BAG1 and PTGES3 in prefrontal cortex in psychotic illness. *Scientific reports* **3**: 3539.

Smith AK, Conneely KN, Kilaru V, Mercer KB, Weiss TE, Bradley B*, et al* (2011). Differential immune system DNA methylation and cytokine regulation in post-traumatic stress disorder. *American journal of medical genetics Part B, Neuropsychiatric genetics : the official publication of the International Society of Psychiatric Genetics* **156B**(6): 700-708.

Srivastava SK, Bhardwaj A, Arora S, Tyagi N, Singh AP, Carter JE*, et al* (2015). Interleukin-8 is a key mediator of FKBP51-induced melanoma growth, angiogenesis and metastasis. *British journal of cancer* **112**(11): 1772-1781.

Statistics OfN (2012). *National Population Projections, 2012-based Statistical Bulletin*: Newport, UK.

Sun H, Damez-Werno DM, Scobie KN, Shao NY, Dias C, Rabkin J*, et al* (2015). ACF chromatin-remodeling complex mediates stress-induced depressive-like behavior. *Nature medicine* **21**(10): 1146-1153.

Talens RP, Christensen K, Putter H, Willemsen G, Christiansen L, Kremer D*, et al* (2012). Epigenetic variation during the adult lifespan: cross-sectional and longitudinal data on monozygotic twin pairs. *Aging cell* **11**(4): 694-703.

Team RC (2014). A Language and Environment for Statistical Computing. *R Foundation for Statistical Computing, Vienna, Austria*.

Telese F, Gamliel A, Skowronska-Krawczyk D, Garcia-Bassets I, Rosenfeld MG (2013). "Seq-ing" insights into the epigenetics of neuronal gene regulation. *Neuron* **77**(4): 606-623.

Teschendorff AE, Marabita F, Lechner M, Bartlett T, Tegner J, Gomez-Cabrero D*, et al* (2013). A beta-mixture quantile normalization method for correcting probe design bias in Illumina Infinium 450 k DNA methylation data. *Bioinformatics* **29**(2): 189-196.

Thomassin H, Flavin M, Espinas ML, Grange T (2001). Glucocorticoid-induced DNA demethylation and gene memory during development. *The EMBO journal* **20**(8): 1974-1983.

Tran L, Chaloner A, Sawalha AH, Greenwood Van-Meerveld B (2013). Importance of epigenetic mechanisms in visceral pain induced by chronic water avoidance stress. *Psychoneuroendocrinology* **38**(6): 898-906.

Tsigos C, Chrousos GP (2002). Hypothalamic-pituitary-adrenal axis, neuroendocrine factors and stress. *Journal of psychosomatic research* **53**(4): 865-871.

Tyrka AR, Price LH, Marsit C, Walters OC, Carpenter LL (2012). Childhood adversity and epigenetic modulation of the leukocyte glucocorticoid receptor: preliminary findings in healthy adults. *PloS one* **7**(1): e30148.

Tyrka AR, Ridout KK, Parade SH, Paquette A, Marsit CJ, Seifer R (2015). Childhood maltreatment and methylation of FK506 binding protein 5 gene (FKBP5). *Development and psychopathology* **27**(4 Pt 2): 1637-1645.

Uchida S, Hara K, Kobayashi A, Otsuki K, Yamagata H, Hobara T*, et al* (2011). Epigenetic status of Gdnf in the ventral striatum determines susceptibility and adaptation to daily stressful events. *Neuron* **69**(2): 359-372.

Uchoa ET, Aguilera G, Herman JP, Fiedler JL, Deak T, de Sousa MB (2014). Novel aspects of glucocorticoid actions. *Journal of neuroendocrinology* **26**(9): 557-572.

Unternaehrer E, Luers P, Mill J, Dempster E, Meyer AH, Staehli S*, et al* (2012). Dynamic changes in DNA methylation of stress-associated genes (OXTR, BDNF) after acute psychosocial stress. *Translational psychiatry* **2**: e150.

Ursini G, Bollati V, Fazio L, Porcelli A, Iacovelli L, Catalani A*, et al* (2011). Stress-related methylation of the catechol-O-methyltransferase Val 158 allele predicts human prefrontal cognition and activity. *J Neurosci* **31**(18): 6692-6698.

Vaccarino V, Goldberg J, Rooks C, Shah AJ, Veledar E, Faber TL*, et al* (2013). Post-traumatic stress disorder and incidence of coronary heart disease: a twin study. *Journal of the American College of Cardiology* **62**(11): 970-978.

van der Knaap LJ, Riese H, Hudziak JJ, Verbiest MM, Verhulst FC, Oldehinkel AJ*, et al* (2014). Glucocorticoid receptor gene (NR3C1) methylation following stressful events between birth and adolescence. The TRAILS study. *Translational psychiatry* **4**: e381.

van der Knaap LJ, Riese H, Hudziak JJ, Verbiest MM, Verhulst FC, Oldehinkel AJ*, et al* (2015). Adverse life events and allele-specific methylation of the serotonin transporter gene (SLC6A4) in adolescents: the TRAILS study. *Psychosomatic medicine* **77**(3): 246-255.

Vidal-Bralo L, Lopez-Golan Y, Mera-Varela A, Rego-Perez I, Horvath S, Zhang Y*, et al* (2016). Specific premature epigenetic aging of cartilage in osteoarthritis. *Aging* **8**(9): 2222-2231.

Vockley CM, D'Ippolito AM, McDowell IC, Majoros WH, Safi A, Song L*, et al* (2016). Direct GR Binding Sites Potentiate Clusters of TF Binding across the Human Genome. *Cell* **166**(5): 1269-1281.e1219.

Volk N, Pape JC, Engel M, Zannas AS, Cattane N, Cattaneo A*, et al* (2016). Amygdalar MicroRNA-15a Is Essential for Coping with Chronic Stress. *Cell reports* **17**(7): 1882-1891.

Volk N, Paul ED, Haramati S, Eitan C, Fields BK, Zwang R*, et al* (2014). MicroRNA-19b associates with Ago2 in the amygdala following chronic stress and regulates the adrenergic receptor beta 1. *The Journal of neuroscience : the official journal of the Society for Neuroscience* **34**(45): 15070-15082.

Wang J, Duncan D, Shi Z, Zhang B (2013). WEB-based GEne SeT AnaLysis Toolkit (WebGestalt): update 2013. *Nucleic acids research* **41**(Web Server issue): W77-83.

Weaver IC, Cervoni N, Champagne FA, D'Alessio AC, Sharma S, Seckl JR*, et al* (2004). Epigenetic programming by maternal behavior. *Nature neuroscience* **7**(8): 847-854.

Weaver IC, Champagne FA, Brown SE, Dymov S, Sharma S, Meaney MJ*, et al* (2005). Reversal of maternal programming of stress responses in adult offspring through methyl supplementation: altering epigenetic marking later in life. *The Journal of neuroscience : the official journal of the Society for Neuroscience* **25**(47): 11045-11054.

Weaver IC, Meaney MJ, Szyf M (2006). Maternal care effects on the hippocampal transcriptome and anxiety-mediated behaviors in the offspring that are reversible in adulthood. *Proceedings of the National Academy of Sciences of the United States of America* **103**(9): 3480-3485.

Weidner CI, Lin Q, Koch CM, Eisele L, Beier F, Ziegler P*, et al* (2014). Aging of blood can be tracked by DNA methylation changes at just three CpG sites. *Genome biology* **15**(2): R24.

Weiwad M, Edlich F, Kilka S, Erdmann F, Jarczowski F, Dorn M*, et al* (2006). Comparative analysis of calcineurin inhibition by complexes of immunosuppressive drugs with human FK506 binding proteins. *Biochemistry* **45**(51): 15776-15784.

Wiederrecht G, Hung S, Chan HK, Marcy A, Martin M, Calaycay J*, et al* (1992). Characterization of high molecular weight FK-506 binding activities reveals a novel FK-506-binding protein as well as a protein complex. *The Journal of biological chemistry* **267**(30): 21753-21760.

Wiench M, John S, Baek S, Johnson TA, Sung MH, Escobar T*, et al* (2011a). DNA methylation status predicts cell type-specific enhancer activity. *The EMBO journal* **30**(15): 3028-3039.

Wiench M, Miranda TB, Hager GL (2011b). Control of nuclear receptor function by local chromatin structure. *The FEBS journal* **278**(13): 2211-2230.

Winston JH, Li Q, Sarna SK (2014). Chronic prenatal stress epigenetically modifies spinal cord BDNF expression to induce sex-specific visceral hypersensitivity in offspring. *Neurogastroenterology and motility : the official journal of the European Gastrointestinal Motility Society* **26**(5): 715-730.

Witzmann SR, Turner JD, Meriaux SB, Meijer OC, Muller CP (2012). Epigenetic regulation of the glucocorticoid receptor promoter 1(7) in adult rats. *Epigenetics : official journal of the DNA Methylation Society* **7**(11): 1290-1301.

Wochnik GM, Ruegg J, Abel GA, Schmidt U, Holsboer F, Rein T (2005). FK506-binding proteins 51 and 52 differentially regulate dynein interaction and nuclear translocation of the glucocorticoid receptor in mammalian cells. *The Journal of biological chemistry* **280**(6): 4609-4616.

Wolf EJ, Logue MW, Hayes JP, Sadeh N, Schichman SA, Stone A*, et al* (2015). Accelerated DNA methylation age: Associations with PTSD and neural integrity. *Psychoneuroendocrinology* **63**: 155-162.

Xu L, Sun Y, Gao L, Cai YY, Shi SX (2014). Prenatal restraint stress is associated with demethylation of corticotrophin releasing hormone (CRH) promoter and enhances CRH transcriptional responses to stress in adolescent rats. *Neurochemical research* **39**(7): 1193-1198.

Yang X, Ewald ER, Huo Y, Tamashiro KL, Salvatori R, Sawa A*, et al* (2012). Glucocorticoid-induced loss of DNA methylation in non-neuronal cells and potential involvement of DNMT1 in epigenetic regulation of Fkbp5. *Biochemical and biophysical research communications* **420**(3): 570-575.

Yehuda R, Daskalakis NP, Bierer LM, Bader HN, Klengel T, Holsboer F*, et al* (2015). Holocaust Exposure Induced Intergenerational Effects on FKBP5 Methylation. *Biological psychiatry*.

Zannas AS (2016). Editorial Perspective: Psychological stress and epigenetic aging - what can we learn and how can we prevent? *J Child Psychol Psychiatry* **57**(6): 674-675.

Zannas AS, Arloth J, Carrillo-Roa T, Iurato S, Roh S, Ressler KJ*, et al* (2015a). Lifetime stress accelerates epigenetic aging in an urban, African American cohort: relevance of glucocorticoid signaling. *Genome biology* **16**(1): 266.

Zannas AS, Chrousos GP (2015b). Glucocorticoid signaling drives epigenetic and transcription factors to induce key regulators of human parturition. *Sci Signal* **8**(400): fs19.

Zannas AS, McQuoid DR, Steffens DC, Chrousos GP, Taylor WD (2012). Stressful life events, perceived stress, and 12-month course of geriatric depression: direct effects and moderation by the 5-HTTLPR and COMT Val158Met polymorphisms. *Stress* **15**(4): 425-434.

Zannas AS, West AE (2014). Epigenetics and the regulation of stress vulnerability and resilience. *Neuroscience* **264**: 157-170.

Zannas AS, Wiechmann T, Gassen NC, Binder EB (2016). Gene-Stress-Epigenetic Regulation of FKBP5: Clinical and Translational Implications. *Neuropsychopharmacology : official publication of the American College of Neuropsychopharmacology* **41**(1): 261-274.

Zhang B, Kirov S, Snoddy J (2005). WebGestalt: an integrated system for exploring gene sets in various biological contexts. *Nucleic acids research* **33**(Web Server issue): W741-748.

Zhang Y, Wang Y, Wang L, Bai M, Zhang X, Zhu X (2015). Dopamine Receptor D2 and Associated microRNAs Are Involved in Stress Susceptibility and Resistance to Escitalopram Treatment. *The international journal of neuropsychopharmacology / official scientific journal of the Collegium Internationale Neuropsychopharmacologicum (CINP)* **18**(8).

Zheng Y, Joyce BT, Colicino E, Liu L, Zhang W, Dai Q*, et al* (2016). Blood Epigenetic Age may Predict Cancer Incidence and Mortality. *EBioMedicine* **5**: 68-73.

Zucchi FC, Yao Y, Ward ID, Ilnytskyy Y, Olson DM, Benzies K*, et al* (2013). Maternal stress induces epigenetic signatures of psychiatric and neurological diseases in the offspring. *PloS one* **8**(2): e56967.

Acknowledgements

Over the last years, I have had the privilege to work with Elisabeth B. Binder, who has been a great supervisor and mentor. I would like to express my gratitude for her openness and willingness to explore new ideas, her genuine excitement for science that always inspires me, and her continuous mentorship and guidance.

I am indebted to Carsten T. Wotjak for his support and guidance as official advisor of this thesis, to Wolfgang Enard for his willingness to serve as second thesis reviewer, and to Michael Boshart and Benedikt Grothe for their willingness to examine this thesis. I greatly appreciate the time that Elisabeth Weiß and Mathias Schmidt spent on evaluating this thesis.

I am grateful to all current and former members of the Binder lab and the Department for Translational Research in Psychiatry at the Max Planck Institute of Psychiatry, as well as to all current and former collaborators for their invaluable support.

Curriculum Vitae

Anthony S. Zannas, MD, MSc
Max Planck Institute of Psychiatry, Kraepelinstr. 2-10, 80804, Munich, Germany
anthony_zannas@psych.mpg.de
anthony.zannas@duke.edu
aszannas@gmail.com

CURRENT APPOINTMENTS

Research Fellow (Marie Sklodowska-Curie) **2015 - present**
Department of Translational Research in Psychiatry
Max Planck Institute of Psychiatry, Munich, Germany

Adjunct Assistant Professor **2013 - present**
Department of Psychiatry and Behavioral Sciences
Duke University Medical Center, Durham, NC

EDUCATION

Ph.D. in Molecular Biology **2017 (expected)**
Faculty of Biology
Ludwig Maximilian University, Munich, Germany

EMBO Workshop **August 2016**
Molecular mechanisms of ageing and regeneration –
From pluripotency to senescence, Spetses, Greece

Advanced Statistical Course **2011 - 2012**
Clinical Research Training Program
Duke University School of Medicine

Master's Degree (M.Sc.) in the neurobiology of stress **2008 - 2010**
"Outstanding with honors" (summa cum laude)
Advisor: George P. Chrousos (Athens Medical School)

United States Medical Licensing Examinations (USMLE) **2008**
Step 1 score: 268; Step 2: 257; Step 3: 246

Doctor of Medicine (M.D.) **1998 - 2004**
National University of Athens Medical School, Athens, Greece

CLINICAL TRAINING AND EXPERIENCE

Psychiatry Residency **2009 - 2013**
Duke University Medical Center, Durham, NC, USA

Primary Care Physician **2007 - 2008**
Santorini (Thira), Greece

Military Service (mandatory in Greece) **2005 - 2006**

Served as primary care physician

Internship in Clinical and Translational Cardiology **2004 - 2005**
Alexandra Hospital, Athens Medical School, Greece

RESEARCH TRAINING AND EXPERIENCE

Research Fellow **2013 - present**
Max Planck Institute of Psychiatry, Munich, Germany
Advisor: Elisabeth B. Binder, Director

Visiting Research Fellow **2016 - present**
Max Planck Institute for Biology of Aging, Cologne, Germany
Advisor: Dario R. Valenzano, Principal Investigator

Research Fellow **2012 - 2013**
Duke Neurobiology, Durham, NC, USA
Advisor: Anne E. West, Associate Professor

Research Fellow **2009 - 2012**
Duke Psychiatry, Durham, NC, USA
Advisor: Warren D. Taylor, Associate Professor

Visiting Research Fellow **August 2008**
Weill Cornell Medical College, White Plains, NY, USA
Advisor: George S. Alexopoulos, Professor and Director

PEER-REVIEWED ARTICLES

(* indicates corresponding authorship)

1. **Zannas AS***, Gassen NC, Jia M, Baumert J, Hafner K, Haehle A, Iurato S, Carrillo-Roa S, Emeny RT, Lahti J, Räikkönen K, Waldenberger R, Wahl S, Kunze S, Lucae S, Bradley B, Gieger C, Hausch F, Smith AK, Ressler KJ, Ladwig KH, Müller-Myhsok B, Rein T, Binder EB. Stress-responsive FKBP5 is epigenetically upregulated by aging and stress-related phenotypes and contributes to NF-κB-driven inflammation and cardiovascular risk. Submitted
2. Rakesh G, Malik Z, **Zannas AS**, Marx C, Szabo ST. Resilience as a Clinical Endpoint in the Treatment of Mental Illness. Submitted
3. Rakesh G, Szabo ST, Alexopoulos GS, **Zannas AS***. Strategies for dementia prevention: latest evidence and implications. Submitted
4. Gassen NC, Muth D, Corman VM, Hafner K, Zellner A, **Zannas AS**, Müller-Myhsok B, Drosten C, Rein T. SKiPping viral infection: Treatment of MERS-CoV by triggering autophagy. Submitted
5. Emeny RT, Baumert J, **Zannas AS**, Peters A, Binder EB, Iurato S, Erhardt A, Weber P, Kunze S, Wahl S, Kretschmer A, Pfeiffer L, Kruse J, Strauch K, Gieger C, Waldenberger M, Peters A, Ladwig KH. Anxiety Associated Increased CpG Methylation in the Promoter of ASB1: evidence from the population-based KORA Study, a clinical study and murine model. Submitted
6. Balsevich G, Gassen NC, Häusl A, Meyer CW, Karamihalev S, Feng X, **Zannas AS**, Dournes C, Uribe A, Santarelli S, Hafner K, Jia M, Theodoropoulou M, Namendorf C, Uhr M, Paez-Pereda M, Hausch F, Chen A, Tschöp MH, Rein T, Schmidt MV. Loss or antagonism of FKBP51 protects against diet-induced metabolic dysfunction by shaping insulin signaling. Submitted
7. **Zannas AS***, Chrousos GP. Epigenetic programming by stress and glucocorticoids along the human life span. *Molecular Psychiatry*; In press

8. **Zannas AS***, Kim, JH, West AE. Regulation and function of the methyl-DNA binding protein MeCP2 in corticolimbic brain regions during U50488-induced conditioned place aversion. *Psychopharmacology*; doi: 10.1007/s00213-017-4527-7. In press
9. Koudoumas D, Terrovitis J, Glentis P, Ntalianis A, Tsolakis E, **Zannas AS**, Tseliou E, Papalois A, Drakos S, Nanas JN. Comparison of two biventricular infarct patterns with respect to the infarct burden required to induce cardiogenic shock: an experimental study. *Hellenic Journal of Cardiology*; pii: S1109-9666(16)30245-7. doi: 10.1016/j.hjc.2016.11.035. In press
10. Volk N, Pape JC, Engel M, **Zannas AS**, Cattane N, Cattaneo A, Binder EB, Chen A. Amygdalar microRNA-15a is essential for coping with chronic stress. *Cell Reports* 2016; 17(7):1882-1891. doi: 10.1016/j.celrep.2016.10.038
11. Gassen NC, Chrousos GP, Binder EB, **Zannas AS***. Life stress, glucocorticoid signaling, and the aging epigenome: implications for aging-related disease. *Neuroscience and Biobehavioral Reviews;* doi: 10.1016/j.neubiorev.2016.06.003. In press
12. **Zannas AS***, Balsevich G, Gassen NC. The emerging role of FKBP5 in the regulation of metabolism and body weight. *Surgery for Obesity and Related Diseases* 2016; 12(8):1560-1561. doi: 10.1016/j.soard.2016.05.016
13. **Zannas AS*.** Freud and the human connectome. *Acta Psychiatrica Scandinavica;* 134(3):275. doi: 10.1111/acps.12598
14. Whelan CD, Hibar DP, van Velzen LS, **Zannas AS**, Carrillo-Roa T, McMahon K, Prasad G, Kelly S, Faskowitz J, deZubicaray G, Iglesias JE, van Erp TG, Frodl T, Martin NG, Wright MJ, Jahanshad N, Schmaal L, Sämann PG, Thompson PM. Heritability and reliability of automatically segmented human hippocampal formation subregions. *Neuroimage* 2016; 128:125-37. doi: 10.1016/j.neuroimage.2015.12.039
15. **Zannas AS***. Psychological stress and epigenetic aging: what can we learn and how can we prevent? *Journal of Child Psychology and Psychiatry* 2016; 57(6):674-5. doi: 10.1111/jcpp.12535
16. Kao CY, He Z, **Zannas AS**, Hahn O, Kühne C, Reichel JM, Binder EB, Wotjak CT, Khaitovich P, Turck CW. Fluoxetine treatment prevents the inflammatory response in a mouse model of posttraumatic stress disorder. *Journal of Psychiatric Research* 2016; 76:74-83. doi: 10.1016/j.jpsychires.2016.02.003
17. **Zannas AS**, Chrousos GP. Glucocorticoid signaling drives epigenetic and transcription factors to induce key regulators of human parturition. *Science Signaling* 2015; 8(400):fs19. doi: 10.1126/scisignal.aad3022
18. **Zannas AS***, Arloth J, Carrillo-Roa T, Iurato S, Röh S, Ressler KJ, Nemeroff CB, Smith AK, Bradley B, Heim C, Lange JF, Brückl T, Ising M, Wray NR, Erhardt A, Binder EB, Mehta D. Lifetime stress accelerates epigenetic aging in an urban, African American cohort: relevance of glucocorticoid signaling. *Genome Biology* 2015; 16(1):266. doi: 10.1186/s13059-015-0828-5
19. Gassen NC, Fries GR, **Zannas AS**, Rüegg J, Hartmann J, Zschocke J, Hafner K, Pfaffeneder T, Zimmermann SN, Knop M, Weber F, Kloiber S, Lucae S, Chrousos GP, Carell T, Ising M, Binder EB, Schmidt MV, Rein T. Chaperoning epigenetics: FKBP51 regulates DNMT1 phosphorylation and activity, impacting BDNF and antidepressant action. *Science Signaling* 2015; 8(404):ra119. doi: 10.1126/scisignal.aac7695
20. **Zannas AS**, Wiechmann T, Gassen NC, Binder EB. Gene-stress-epigenetic regulation of FKBP5: clinical and translational implications. *Neuropsychopharmacology* 2016; 41(1):261-74. doi: 10.1038/npp.2015.235
21. **Zannas AS**, Provencal N, Binder EB. Epigenetics of posttraumatic stress disorder: current evidence, challenges, and future directions. *Biological Psychiatry* 2015; 78(5):327-35. doi: 10.1016/j.biopsych.2015.04.003
22. Gassen NC, Hartmann J, **Zannas AS**, Zschocke J, Maccarrone G, Hafner K, Zellner A, Wagner KV, Mehta D, Kloiber S, Turck CW, Lucae S, Chrousos GP, Holsboer F, Binder EB, Ising M, Schmidt MV, Rein T. FKBP51 inhibits GSK3β and augments the effects of distinct psychotropic medications. *Molecular Psychiatry* 2016; 21(2):277-89. doi: 10.1038/mp.2015.38

23. Gaali S, Kirschner A, Cuboni S, Hartmann J, Kozany C, Balsevich G, Namendorf C, Sippel C, **Zannas AS**, Draenert R, Binder EB, Fernandez-Vizarra P, Almeida OFX, Rühter G, Uhr M, Schmidt MV, Touma C, Bracher A, Hausch F. Selective inhibitors for the psychiatric risk factor FKBP51 enabled by an induced-fit mechanism. *Nature Chemical Biology* 2015; 11(1):33-7. doi: 10.1038/nchembio.1699
24. **Zannas AS***, McQuoid DR, Payne ME, MacFall JR, Ashley-Koch A, Steffens DC, Potter GG, Taylor WD. Gene variants of the renin-angiotensin system are associated with accelerated hippocampal volume loss and cognitive decline in old age. *American Journal of Psychiatry* 2014; 171(11):1214-21. doi: 10.1176/appi.ajp.2014.13111543. **European Psychiatric Association Research Prize 2015**
25. Wijayatunge R, Chen LF, Cha YM, **Zannas AS**, Frank C, West AE. The histone lysine demethylase Kdm6b is required for activity-dependent preconditioning of hippocampal neuronal survival. *Molecular and Cellular Neuroscience* 2014; 61C:187-200. doi: 10.1016/j.mcn.2014.06.008
26. Pelton GH, Andrews H, Roose SP, Marcus SM, D'Antonio K, Husn H, Petrella JR, **Zannas AS**, Doraiswamy PM, Devanand DP. Donepezil Treatment of Older Adults with Cognitive Impairment and Depression (DOTCODE study): clinical rationale and design. *Contemporary Clinical Trials* 2013; 37(2):200-8. pii: S1551-7144(13)00197-3. doi: 10.1016/j.cct.2013.11.015
27. **Zannas AS**, West AE. Epigenetics and the regulation of stress vulnerability and resilience. *Neuroscience* 2014; 264C:157-170. doi: 10.1016/j.neuroscience.2013.12.003
28. Taylor WD, McQuoid DR, Payne ME, **Zannas AS**, MacFall JR, Steffens DC. Hippocampus atrophy and the longitudinal course of late-life depression. *American Journal of Geriatric Psychiatry* 2014; 22(12):1504-12. doi: 10.1016/j.jagp.2013.11.004
29. **Zannas AS**, Binder EB. Gene-environment interactions at the FKBP5 locus: sensitive periods, mechanisms and pleiomorphism. *Genes Brain and Behavior* 2014; 13(1):25-37. doi: 10.1111/gbb.12104
30. **Zannas AS***, Okuno Y, Doraiswamy PM. Cholinesterase inhibitors and Pisa syndrome: a pharmacovigilance study. *Pharmacotherapy* 2014; 34(3):272-8; doi: 10.1002/phar.1359
31. **Zannas AS**, Doraiswamy PM, Shpanskaya KS, Murphy K, Petrella JR, Burke JR, Wong TZ. Impact of ^{18}F-florbetapir PET imaging of beta-amyloid neuritic plaque density on clinical decision making. *Neurocase* 2014; 20(4):466-73; doi: 10.1080/13554794.2013.791867
32. **Zannas AS**, McQuoid DR, Payne ME, Steffens DC, MacFall JR, Ashley-Koch A, Taylor WD. Negative life stress and longitudinal hippocampal volume changes in older adults with and without depression. *Journal of Psychiatric Research* 2013; 47(6):829-834. doi: 10.1016/j.jpsychires.2013.02.008
33. **Zannas AS**, Wong TZ, Doraiswamy PM. How much is a picture worth? Putting amyloid imaging to the test. *Dementia and Geriatric Cognitive Disorders Extra* 2012; 2:649-651. doi: 10.1159/000345982
34. **Zannas AS***, McQuoid DR, Steffens DC, Chrousos GP, Taylor WD. Stressful life events, perceived stress, and 12-month course off geriatric depression: direct effects and moderation by the 5-HTTLPR and COMT Val158Met polymorphisms. *Stress* 2012; 15(4):425-434. doi: 10.3109/10253890.2011.634263

OTHER ARTICLES AND BOOK CHAPTERS

1. **Zannas AS**, Binder EB, Mehta D. Genomics of posttraumatic stress disorder. In: Bremner JD (ed), *Posttraumatic stress disorder: from neurobiology to treatment.* Wiley-Blackwell, Hoboker, NJ, USA
2. Doraiswamy M, Kuriakose JR, **Zannas A.** The Global Threat of Alzheimer's Disease: Readying Nations for the Challenge. *The Huffington Post;* January 23, 2014
3. Diakos NA, Wever-Pinzon O, **Zannas AS**, Drakos SG. Mechanical unloading and heart remodeling features. In: Gabriel EA, Gabriel SA (eds), *Inflammatory response in cardiovascular surgery.* Springer, London, UK, 2013, pp 413-418

4. Kaltsas G, **Zannas AS**, Chrousos GP. Hypothalamic-pituitary-adrenal axis and cardiovascular disease. In: Hjemdahl P, Rosengren A, Steptoe A (eds), *Stress and cardiovascular Disease.* Springer, London, UK, 2012, pp 71-88
5. **Zannas AS.** LVADs, chronic stress, and mental illness. *International Society for Heart and Lung Transplantation (ISHLT) Newsletter* 2011; 3(5):14

PRESENTATIONS IN SCIENTIFIC CONFERENCES

2016

Keystone Symposium on Epigenetic and Metabolic Regulation of Aging and Aging-Related Diseases, Santa Fe, NM, USA (*poster presentation*)
Society of Biological Psychiatry, Atlanta, GA, USA (*oral presentation*)
Panhellenic Psychiatric Conference, Alexandroupoli, Greece (*oral presentation*)

2015

European Psychiatric Association Congress, Vienna, Austria (*poster presentation*)
Society of Biological Psychiatry, Toronto, Canada (*oral presentation*)
European College of Neuropsychopharmacology, Amsterdam, Netherlands (*poster presentation*)
Stress, Behavior, and the Heart, Erice, Italy (*oral presentation*)

2014

World Congress of Psychiatric Genetics, Copenhagen, Denmark (*poster presentation*)
European College of Neuropsychopharmacology, Berlin, Germany (*poster presentation*)
European College of Neuropsychopharmacology Workshop for Junior Scientists, Nice, France (*oral and poster presentation*)
Interact Life Sciences Meeting, Munich, Germany (*oral presentation*)

2013

Donders Discussions, Nijmegen, Netherlands (*oral presentation*)
Society of Biological Psychiatry, San Francisco, CA, USA (*poster presentation*)

2012

American Association for Geriatric Psychiatry, Washington DC, USA (*poster presentation*)

OTHER INVITED TALKS

Planned

World Congress of Biological Psychiatry, Copenhagen, Denmark, June 22nd, 2017
Duke Psychiatry Grand Rounds, Durham, NC, USA, April 13th, 2017
University of North Carolina Reproductive Mood Disorders Fellowship, Chapel Hill, NC, April 12th, 2017
Duke Psychiatry residency educational session, Durham, NC, USA, April 11th, 2017

Past

Duke Psychiatry Chair's Rounds, Durham, NC, USA, May 9th, 2016
Max Planck Institute for Biology of Aging, Cologne, Germany, October 21st, 2015
Max Planck Institute of Psychiatry, Chiemsee, Germany, October 27th, 2014
Duke Psychiatry residency educational session, Durham, NC, USA, May 1st, 2014
Duke Psychiatry residency educational session, Durham, NC, USA, July 18th, 2013
Duke Psychiatry residency educational session, Durham, NC, USA, May 9th, 2013

Duke University Med/Psych Conference, Durham, NC, USA, March 26th, 2013
National Institute of Mental Health, Washington, DC, USA, August 13th, 2012

AWARDS, STIPENDS, SCHOLARSHIPS, AND HONORARIA

Society of Biological Psychiatry **Early Career Investigator International Travel Fellowship Award**, 2016 ($2,000)
European College of Neuropsychopharmacology **Travel Award**, Amsterdam, 2015 (€500)
European Psychiatric Association **Research Prize** for best scientific paper 2015 (€2,500)
World Congress of Psychiatric Genetics **Travel Award**, Copenhagen 2014 ($1,000)
European College of Neuropsychopharmacology **Fellowship Award**, Berlin, 2014 (€1,500)
Max Planck Society Honorarium for the Conference on Personalized Medicine, Shanghai, 2014 (€1,100)
Stipend for the European College of Neuropsychopharmacology Workshop for Young Scientists, Nice, 2014 (€600)
Stipend for Donders Discussions, Nijmegen, 2013 (€500)
Duke Psychiatry **Resident Researcher Award** 2013
Duke Psychiatry Program **Travel Scholarship** 2012-2013 ($500)
Duke Psychiatry Program **Travel Scholarship** 2011-2012 ($1,000)
Duke Psychiatry Program **Travel Scholarship** 2010-2011 ($1,000)

GRANTS

NARSAD Young Investigator Grant/Award, "Neural Correlates of Epigenetic Aging", Jan 2017 – Jan 2019, $70,000

Marie Skolowska-Curie Individual Fellowship (H2020), "Molecular Mechanisms Linking Psychological Stress and Ageing-Related Disease", May 2015 - May 2017, €159,461

ORGANIZING ROLES IN SCIENTIFIC CONFERENCES

Symposium co-chair
World Congress of Biological Psychiatry, Copenhagen, Denmark, 2017

Session Chair
Stress, Behavior, and the Heart, Erice, Italy, 2015

Organizing Committee Member
World Congress of Psychiatric Genetics, Toronto, Canada, 2015

Steering Committee Fellow Member
Max Planck Conference on Personalized Medicine, Shanghai, 2014

ACADEMIC SERVICE

Teaching Faculty **2017 - 2019**
Master of Science Program "Social Psychiatry"
Faculty of Medicine, Demokritus University of Thrace, Greece

Teaching Faculty **2017 - 2018**
International Max Planck Research School in Translational Psychiatry

Chief Resident of Research and Education **2012 - 2013**
Duke Psychiatry

Residency Educational Curriculum Committee Co-Chair **2011 - 2012**
Duke Psychiatry

Grant proposal reviewer for the National Science Centre of Poland

Grant committee reviewer for Cohen Veterans Bioscience

Reviewer for Elsevier volumes "Medical Epigenetics" and "Handbook of Epigenetics"

Peer reviewer for the following scientific journals: American Journal of Psychiatry, Translational Psychiatry, Stress, Human Brain Mapping, Journal of Affective Disorders, Social Science & Medicine, Neuropsychiatric Genetics, Scientific Reports, Psychiatry Research, Acta Paediatrica, International Journal of Molecular Sciences, AGE, European Journal of Neurology, Medical Principles and Practice, Surgery for Obesity and Related Diseases, Molecular and Cellular Endocrinology, Neuroscience and Biobehavioral Reviews, Comprehensive Psychiatry, Aging, Development and Psychopathology, Neuroscience Letters, Journal of Psychiatric Research, World Journal of Biological Psychiatry, Neuropsychopharmacology, Biological Psychiatry

REFEREES

George S. Alexopoulos, Professor and Director, Institute of Geriatric Psychiatry, Weill Cornell Medical College, White Plains, NY, USA, gsalexop@med.cornell.edu

Elisabeth B. Binder, Director, Department of Translational Research in Psychiatry, Max Planck Institute of Psychiatry, Munich, Germany, binder@psych.mpg.de

George P. Chrousos, Chair, First Department of Pediatrics, National and Kapodistrian University of Athens, Athens, Greece, chrousos@gmail.com

Jane P. Gagliardi, Associate Professor, Department of Psychiatry and Behavioral Sciences, Duke University Medican Center, Durham, NC, USA, jane.gagliardi@duke.edu

David C. Steffens, Professors and Chair, Department of Psychiatry and Behavioral Sciences, University of Connecticut, steffens@uchc.edu

Warren D. Taylor, Associate Professor, Department of Psychiatry and Behavioral Sciences, Vanderbilt University, Nashville, TN, USA, warren.d.taylor@Vanderbilt.Edu

Anne E. West, Associate Professor, Department of Neurobiology, Duke University School of Medicine, Durham, NC, USA, west@neuro.duke.edu

Eidesstattliche Erklärung

Ich versichere hiermit an Eides statt, dass die vorgelegte Dissertation von mir selbständig und ohne unerlaubte Hilfe angefertigt ist.

München, den 21.2.2017 Antonios Zannas .....

(Unterschrift)

Erklärung

Hiermit erkläre ich, *

✓ dass die Dissertation nicht ganz oder in wesentlichen Teilen einer anderen Prüfungskommission vorgelegt worden ist.

✓ dass ich mich anderweitig einer Doktorprüfung ohne Erfolg nicht unterzogen habe.

München, den 21.2.2017 Antonios Zannas .....

(Unterschrift)

*) Nichtzutreffendes streichen

Declaration/Declaration of contribution as co-author

Publication I: **Zannas AS**, Arloth J, Carrillo-Roa T, Iurato S, Röh S, Ressler KJ, Nemeroff CB, Smith AK, Bradley B, Heim C, Lange JF, Brückl T, Ising M, Wray NR, Erhardt A, Binder EB, Mehta D. Lifetime stress accelerates epigenetic aging in an urban, African American cohort: relevance of glucocorticoid signaling. *Genome Biology* 2015; 16(1):266. doi: 10.1186/s13059-015-0828-5

Author contributions: ASZ conceived and designed the study, performed all statistical analyses, performed the disease enrichment analysis, and wrote the manuscript.

Other contributors: EBB and DM conceived and designed the study. TCR, JA, and SI were involved in the DNA methylation analyses. JA, SR, and AM analyzed the DEX-treated sample. JA and SR performed the GRE enrichment analysis. KJR, AKS, BB, JFL, MI, TB, AE, CBH, and CH contributed the clinical samples. JA, TCR, NRW, and DM contributed to the statistical analyses. JA, EBB, and DM contributed to the enrichment analysis. EBB and DM contributed to manuscript writing. All authors read and approved the final manuscript.

Publication II: Gassen NC, Fries GR, **Zannas AS**, Rüegg J, Hartmann J, Zschocke J, Hafner K, Pfaffeneder T, Zimmermann SN, Knop M, Weber F, Kloiber S, Lucae S, Chrousos GP, Carell T, Ising M, Binder EB, Schmidt MV, Rein T. Chaperoning epigenetics: FKBP51 regulates DNMT1 phosphorylation and activity, impacting BDNF and antidepressant action. *Science Signaling* 2015; 8(404):ra119. doi: 10.1126/scisignal.aac7695

Author contributions: ASZ performed the correlation analysis in the Grady sample, supervised all statistical analyses, and contributed to Western blot experiments.

Other contributors: NCG and GRF performed biochemical and molecular biology experiments and contributed to the study design and manuscript preparation. JH provided animal tissue and performed the in situ hybridization assays. JZ contributed to the study design. KH performed molecular biology and cell culture experiments. TC-R and MI performed statistical analyses. JS performed the global methylation analysis. SNP contributed to the DNMT1 activity assay. LH contributed to the in situ hybridization assays. MK and FW provided the BDNF ELISA kit. SK and SL contributed to the organization of the MARS sample. GPC contributed to manuscript

preparation. TC performed the global DNA methylation assays. EBB contributed to organizing the Grady sample collection. MVS provided animal tissue. JR performed the bisulfite sequencing, primer design, and pyrosequencing. TR contributed to the study design and manuscript preparation.

Manuscript I: **Zannas AS**, Gassen NC, Jia M, Baumert J, Hafner K, Ködel M, Haehle A, Iurato S, Carrillo-Roa T, Emeny RT, Lahti J, Räikkönen K, Waldenberger R, Wahl S, Kunze S, Lucae S, Bradley B, Gieger C, Hausch F, Smith AK, Ressler KJ, Ladwig KH, Müller-Myhsok B, Rein T, Binder EB. Stress-responsive FKBP5 is epigenetically upregulated by aging and stress-related phenotypes and contributes to NF-κB-driven inflammation and cardiovascular risk. *Submitted*
Author contributions: ASZ conceived and designed the study, was involved in the DNA methylation analyses, participated in the design and conduct of the protein experiments, designed and performed the ELISA experiments, designed and performed the reporter gene assays, designed and performed the pathway analyses, performed all statistical analyses, and wrote the manuscript.
Other contributors: EBB conceived and designed the study, was involved in data collection, and contributed to manuscript writing. JB, TCR, SI, RW, SW, SK, and AKS were involved in the DNA methylation analyses. KH and NCG designed and performed the protein experiments. MK performed the ELISA experiments. AH contributed to the design of the reporter gene assays. MJ and BM-M designed and performed the pathway analyses. JL, KR, SL, BB, CG, KJR, and KHL were involved in data collection. FH provided the FKBP5 antagonist.

München, den 21. Februar 2017

Antonios Zannas

PD Dr. Carsten T. Wotjak